AN ABSTRACT OF THE THESIS OF

John C. Hammond for the degree of Master of Science in Water Resources Science presented on July 14, 2014.

Title: Trends in Streamflow Above and Below Dams Across the Columbia River Basin from 1950 to 2012: Assessing Sub-basin Sensitivity

Abstract approved:

Julia A. Jones

Abstract

Climate change, combined with population growth, is expected to exacerbate water scarcity globally. In the Columbia River basin (CRB), streamflow is managed for multiple objectives with a network of dams and reservoirs distributed throughout the basin that may mitigate climate change effects on water scarcity. This study quantified trends in daily streamflow from 1950-2012 in 28 pairs of gages above and below dams in the CRB, including the U.S. and Canada. Each gage pair consisted of an above-dam gage that is primarily forested and has little apparent human disturbance and minimal flow regulation or diversions, combined with a below-dam gage immediately downstream of a major dam and reservoir. Monthly streamflow and precipitation for a total of 59 sites was correlated with monthly indices of the Pacific Decadal Oscillation (PDO), the Northern Pacific Index (NPI), the Pacific North America pattern (PNA), and the 700-millibar wind speeds (u700) using Pearson's r. Long-term trends and patterns in daily streamflow and climate data were estimated using linear regression, the Mann-Kendall test, and wavelet analysis. Streamflow was generally weakly correlated with NPI, PNA, and PDO, while positively correlated with upper elevation wind speed at low elevations during wet months. Fewer than half of above-dam gages in the CRB have experienced

increasing trends in springtime daily streamflow (mid-March to the beginning of May) over the period 1950 to 2012, whereas a majority has experienced decreasing summer and early autumn trends (mid- May to mid-October). These trends in above-dam basins are consistent with trends expected from climate change, but they also may be affected by legacies of past forest harvest or wildfire. Below dams, reservoir management appears to have overwritten the signal of earlier snowmelt, except in the Boise sub-basin, but long-term declines in late summer flows were evident at half of below-dam sites. Declining summer flows below dams were attributable to a variety of factors, including changes in reservoir management as well as reservoir management that propagates signals from above dam catchments, such as climate change or forest-harvest legacy effects on streamflow. There have been very few significant changes in annual flow volume throughout the basin, and these trends represent a small percentage of annual flow volume; thus, observed trends appear to be shifts in timing rather than shifts in the annual water balance. The magnitude of 60-yr declines in late-summer flow in above-dam catchments represents only a few percent of annual yield, and much less than the storage capacity of the dams, but these long-term changes may be quite important for water yield during the late-summer low-flow period. These findings are relevant for strategies to adaptively manage water resources in light of the ongoing review activities around possible renegotiation of the U.S.-Canada Columbia River Treaty.

Trends in Streamflow Above and Below Dams Across the Columbia River Basin from 1950 to 2012: Assessing Sub-basin Sensitivity

by John C. Hammond

A THESIS

submitted to

Oregon State University

in partial fulfillment of
the requirements for the
degree of

Master of Science

Presented July 14, 2014
Commencement June 2015

Master of Science thesis of John C. Hammond on July 14, 2014.

APPROVED:

Major Professor, representing Water Resources Science

Director of the Water Resources Graduate Program

Dean of the Graduate School

I understand that my thesis will become part of the permanent collection of Oregon State University libraries. My signature below authorizes release of my thesis to any reader upon request.

John C. Hammond, Author

ACKNOWLEDGEMENTS

I would like to thank my major advisor Julia Jones for her guidance and invaluable feedback throughout my time at Oregon State University. I would also like to thank Sean Fleming of Environment Canada for his continued assistance in accessing information in the Canadian component of the Columbia River basin and for methodological advice. I am grateful for the help I received from Jay Alder and Charlotte Wickham for their assistance with statistical calculations and coding in IDL and R. I am grateful to The H.J. Andrews Experimental Forest for providing continuous data at the Lookout Creek gage and to the USGS, Environment Canada and BC Hydro, for without access to this publically available streamflow data, this project would not have been possible. Special thanks to Mary Scullion, Michael Beus, and Gillian Kong for their consultation regarding reservoir management practices across the CRB. Thank you finally to my parents John and Rosemarie Hammond and partner Michelle Kim for their continued support and immeasurable inspiration.

TABLE OF CONTENTS

Page

LIST OF FIGURES

Figure Page

LIST OF TABLES

1. Introduction

Climate change and population growth are expected to exacerbate water scarcity globally (Vorosmarty et al., 2000). However, in North America, streamflow in large river basins is managed for multiple objectives, using large installations (dams and reservoirs) that are distributed throughout the basin (Graf, 1999), and this management may mitigate water shortages. In transboundary (international) basins, streamflow management involves multi-decade international treaties, which must to some degree anticipate effects of changes in climate, population, and stakeholder objectives. It remains unclear how these various factors might influence future water management in large river basins.

The Columbia River Basin (CRB, 668,000 km^2) exemplifies these issues. The CRB, which covers about 500,000 km^2 in the U.S., is the social, ecological, and economic heart of the Pacific Northwest. Additionally, although only 15% of the CRB land area lies within in Canada, the Canadian portion provides 25% of mean annual flow at the mouth of the CRB, and as much as 50% of the flow during extreme flood events or snowmelt. With more than 450 dams of various sizes that mostly produce hydroelectricity, the CRB is one of the most dammed systems in the world (CBT, 2014). Approximately six million people reside in the CRB, including stakeholders in parts of seven states, thirteen federally recognized Indian reservations, and one Canadian province. Reservoirs in the U.S. portion of the CRB tend to be located at the downstream edge of federally managed forests and upstream of privately managed forests and agriculture. Reservoirs in British Columbia are also surrounded by mostly public land,

which is primarily forested, and they drain mountainous areas with higher percentages of glaciated area than U.S. basins.

The U.S.-Canada Columbia River Treaty (CRT), ratified in 1964, governs reservoir management in the CRB, especially flood control and hydropower development (Ogren et al., 2013). In 2014, a comment period began to provide input to "a multi-year regional conversation to address a broad range of resource management issues related to the Columbia River," which may expire as early as 2024 (USACE, 2013). Given the changes in population, climate, and stakeholder objectives in the region, information about historical streamflow changes in this transboundary hydrologic system is very important to this review.

Minimum and maximum surface air temperatures have increased about 1°C since 1950 across the Western U.S. (Booth et al., 2012 and Lettenmaier, Wood et al., 1993) and regionally in the Columbia River Basin (Littell et al., 2011; Zhang et al., 2011). Luce et al. (2013) suggest that precipitation has not exhibited consistent region-wide trends at low-elevation climate stations, but also that mountain precipitation has declined, in the U.S. Pacific Northwest (PNW) from 1950 to 2012. However, the details of precipitation changes appear to have been spatially heterogeneous within the American portion of the PNW (Mote, 2003). Further, precipitation trend patterns shift northward into British Columbia, where precipitation has generally remained stable or increased in and near the Canadian portion of the expansive Columbia Basin, although again the trends exhibit substantial seasonal and geographic variation (e.g., Zhang et al., 2000; Taylor and Barton, 2004; Rodenhuis et al., 2007; Burford et al., 2009; Pike et al., 2010; Zhang et al., 2011). In contrast, snowpack (measured for example as snow water equivalent, SWE) has

clearly declined over much of western North America (e.g., Mote et al., 2006; Zhang et al., 2011). Similarly, the onset of springtime snowmelt and streamflow in western North America has clearly advanced by one to four weeks since 1948 (e.g., Stewart et al., 2005; Cayan et al., 2000; Pike et al., 2010).

Throughout North America, above-dam streams are displaying the effects of climate change (Jones et al., 2012). The Columbia Basin is no exception. In both the US and Canadian PNW, climate warming is expected to speed snowmelt, increase spring streamflows, and reduce late summer flows (e.g., Barnett et al., 2008; Schnorbus et al., 2012). In the US PNW, September streamflow declined and the proportion of March to annual streamflow increased at reference gages from 1958 to 2008 (Chang et al., 2012), and annual flow in dry years (the 25th percentile) declined significantly at headwater gages from 1948 to 2006 (Luce and Holden, 2009). In southern British Columbia, including the high-water-yield Canadian portion of the Columbia Basin, in general winter flow has increased, late-summer baseflow has decreased (especially at glacier-fed headwater locations), the melt freshet is occurring earlier, and annual water yield has remained unchanged or increased slightly (e.g., Zhang et al., 2001; Taylor and Barton, 2004; Stahl and Moore, 2006; Déry et al., 2009; Burford et al., 2009; Fleming, 2010; Pike et al., 2010; Fleming and Weber, 2012; Fleming and Dahlke, in press).

A number of factors may modify the signal of climate change on streamflow within the CRB. In above-dam catchments, by reducing evapotranspiration, or replacing old forest with younger forest, streamflow initially increases, but it can decline, especially in summer, as forest regenerates, and thereby mitigate or exacerbate streamflow responses to climate change (Jones and Post, 2004). Reservoir operation may

mitigate or reverse above-dam streamflow trends downstream of dams (Hatcher and Jones, 2013). Many other factors influence streamflow (Qian et al., 2009).

Despite these studies, relatively little is known about changes in daily streamflow, especially summer low flows, which are crucial for hydropower regulation, barge transportation, and minimum streamflow objectives in the CRB (Smerdon et al., 2004). No studies have examined streamflow and climate records from both the U.S. and Canadian portions of the CRB. Moreover, few analyses have examined streamflow trends below dams, and those studies (e.g., Hatcher and Jones, 2013) have been limited by the lack of above-dam streamflow records. Therefore, this study examines daily streamflow trends in 28 pairs of above and below-dam basins in all the major sub-basins of the CRB.

This study estimates trends in daily precipitation, temperature, and streamflow from 1950 to 2012 and compares trends in streamflow above and below dams to assess the potential for CRB reservoir management to mitigate climate change impacts on streamflow. We ask:

(1) How have spring and late summer streamflows changed in the CRB?

(2) How do streamflow changes differ above vs. below dams?

(3) How are changes in streamflow related to land use above dams and reservoir operation?

2. Study site selection

After collection of relevant spatial data (see 3.1 below), selected gages, dams and climate stations in the CRB were evaluated to identify pairs of stream gages above and below dams. Each pair consisted of a gage in an above-dam basin that (1) was primarily forested and had (2) no dams, (3) little apparent human disturbance, (4) minimal flow regulation or diversions upstream, (5) a record from approximately 1950 to 2012, and (6) could be matched with a downstream gage below an actively regulated dam with a record from approximately 1950 to 2012. Each pair of above and below-dam gages was matched with a climate station with daily records of precipitation, and maximum and minimum air temperature, from 1950 to 2012. Climate stations were located between 2 km and 60 km from streamflow gages.

A gage pair is a set of gages above/below a dam (Table 2.1). The study included 28 above- and below-dam pairs, but a total of 59 stream gages (25 below-dam and 34 above-dam gages) were included. Five above-dam gages are paired with two below-dam gages (Milltown Dam and Post Falls Dam), reducing the below-dam gage count to 25 (Tables 2.1 and 2.2). Six above-dam gages with no corresponding below-dam gage were included to assess streamflow trends in sub-basins that would have otherwise been excluded, raising the above-dam gage count to 34 (Tables 2.1 and 2.3). The 59 stream gages occupy eleven United States Geological Survey (USGS) hydrologic unit code (HUC)-6 sub-basins. Gage pairs are distributed throughout 15 of 17 HUC-6 sub-basins of the CRB (see e.g., the Willamette sub-basin, Figure 2.1, 2.2). The Middle Snake and Yakima sub-basins were omitted.

Sub-basins range in size from 18 to 48,830 km^2 (Table 2.1, Figure 2.1, 2.3). Above-dam gages range from 627 m to 2,486 m elevation, with mean annual precipitation from 416 mm to 2,987 mm and mean annual temperature from 0.6 °C to 11.2 °C (Table 2.2, Figure 2.4, Figure 2.5, Figure 2.6). Study sites are mostly in temperate forest, but some are in temperate wet forest, boreal forest, or savanna biomes (Figure 2.7). Land cover in the sub-basins is primarily forest with lesser areas of shubland, rangeland, grassland and cultivated areas.

Streamflow gage and climate records span the period 1950-2012 (Figure 2.8). Seventeen streamflow records have gaps in the record due to missing data. Of these, six are missing ~ six years (ten percent of the study length) and eleven are missing over ten years. Dams were constructed between 1904 and 1950 in 15 of 28 cases, and in thirteen cases dams were constructed between 1950 and 1975 (Figure 2.8).

The USGS "reference/non-reference" classification was used in selecting above-dam gages for study (Falcone, 2011). This classification includes some basins with disturbances: for example, the gage for Lookout Creek (14161500) is defined by USGS as a reference gage despite >100km of forest roads and 25% clear-cutting mostly from 1950-1970. Above-dam basins in this study included some "reference" sites as well as some additional basins with small water withdrawals for agriculture, water diversions, forest roads, and active forestry (Table A-4).

All of the above-dam gages in this study in the Canadian component of the CRB are classified as reference gages according to the Water Survey of Canada's Reference Hydrometric Basin Network (RHBN) (https://www.ec.gc.ca/rhc-wsc/default.asp?lang=En&n=E228B6E8-1).

The current study used different above-dam gages from those in two previous studies of streamflow trends and timing (Figure 2.9). Luce et al. (2013) and Chang (2012) used only "reference" gages defined by the USGS Gages II (Falcone, 2011), and they also included gages outside of the CRB.

Table 2.1. Station numbers, drainage area and record length for streamflow and climate data from the US and Canada portions of the Columbia River basin used in this study.

Gage	Station Name	Above / Below	Drainage Area (sq km)	Proximal Climate Station	Record	
12301933	Kootenai River below Libby Dam, MT	Below	23271	245015	1950 to 2012	B1
12340500	Clark Fork above Missoula, MT	Below	15592	247286	1950 to 2012	B2
12372000	Flathead River near Polson, MT	Below	16726	247286	1950 to 2012	B3
12419000	Spokane River near Post Falls, ID	Below	10162	101956	1950 to 2012	B4
12452500	Chelan River at Chelan, WA	Below	2415	459012	1950 to 2012	B5
13011000	Snake River near Moran, WY	Below	1964	486440	1950 to 2012	B6
13032500	Snake River near Irwin, ID	Below	13424	480140	1950 to 2012	B7
13081500	Snake River near Minidoka, ID	Below	48830	104140	1950 to 2012	B8
13148500	Little Wood River near Carey, ID	Below	802	104845	1950 to 2012	B9
13190500	South fork Boise River at Anderson Ranch Dam, ID	Below	2533	100448	1950 to 2012	B10
13202000	Boise River near Boise, ID	Below	6959	100448	1954 to 2012	B11
13341050	Clearwater River near Peck, ID	Below	20665	102845	1964 to 2012	B12
14054000	Deschutes River below Crane Prairie La Pine, OR	Below	671	350694	1950 to 1991	B13
14092500	Deschutes River near Madras, OR	Below	20857	350694	1950 to 2012	B14
14097100	Warm Springs River near Kahneeta hot springs, OR	Below	1362	352440	1972 to 2012	B15
14140000	Bull Run River near Bull Run, OR	Below	278	353770	1950 to 2012	B16
14142500	Sandy River below Bull Run River, OR	Below	1118	353770	1950 to 2012	B17
14153500	Coast fork Willamette River below Cottage Grove Dam, OR	Below	275	351897	1950 to 2012	B18
14158850	McKenzie River below Trail Bridge Dam, OR	Below	480	355362	1950 to 2012	B19

14159500	South fork McKenzie river near Rainbow, OR	Below	540	355362	1950 to 2012	B20
14162200	Blue River at Blue River, OR	Below	228	355362	1966 to 2012	B21
14181500	North Santiam River at Niagara, OR	Below	1171	351433	1950 to 2012	B22
08NH118	Duncan River below Lardeau River, BC	Below	4080	1143900	1963 to 2012	B23
08NM050	Okanagan River at Penticton, BC	Below	5980	1126150	1950 to 2011	B24
Mica Outflow	Mica Dam on the Columbia River, BC	Below	11790	1160899	1976 to 2012	B25
12332000	Middle fork Rock Creek near Philipsburg, MT	Above	315	246472	1950 to 2012	A1
12358500	Middle fork Flathead River near West Glacier, MT	Above	2939	244558	1950 to 2012	A2
12370000	Swan River near Bigfork, MT	Above	1715	244558	1950 to 2012	A3
12413000	North fork Coeur d'Alene River at Enaville, ID	Above	2325	104831	1950 to 2012	A4
12414500	St. Joe River at Calder, ID	Above	2679	104831	1950 to 2012	A5
12414900	St. Maries River near Santa, ID	Above	706	104831	1965 to 2012	A6
12451000	Stehekin River at Stehekin, WA	Above	831	458059	1950 to 2012	A7
13011500	Pacific Creek at Moran, WY	Above	404	486440	1950 to 2012	A8
13022500	Snake River above reservoir near Alpine, WY	Above	8867	480140	1950 to 2012	A9
13078000	Raft River above Onemile Creek near Malta, ID	Above	1060	106542	1950 to 2012	A10
13147900	Little Wood River above High Five Creek near Carey, ID	Above	646	104845	1958 to 2012	A11
13185000	Boise River near Twin Springs, ID	Above	2154	100448	1950 to 2012	A12
13186000	South fork Boise River near Featherville, ID	Above	1660	100448	1950 to 2012	A13
13313000	Johnson Creek at Yellow Pine, ID	Above	562	101408	1950 to 2012	A14
13330000	Lostine River near Lostine, OR	Above	185	358997	1950 to 2012	A15
13337000	Lochsa River near Lowell, ID	Above	3053	103143	1950 to 2012	A16

13340600	North fork Clearwater River near Canyon Ranger Station, ID	Above	3355	102845	1967 to 2012	A17
14020000	Umatilla River above Meacham Creek near Gibbon, OR	Above	341	355593	1950 to 2012	A18
14037500	Strawberry Creek above Slide Creek near Prairie City, OR	Above	18	355162	1950 to 1991	A19
14050500	Cultus River above Cultus Creek near La Pine, OR	Above	39	350694	1950 to 1991	A20
14091500	Metolius River near Grandview, OR	Above	818	350694	1950 to 2012	A21
14095500	Warm Springs River near Simnasho, OR	Above	277	352440	1950 to 2009	A22
14107000	Klickitat River above West fork near Glenwood, WA	Above	394	453222	1950 to 2012	A23
14138800	Blazed Alder Creek near Rhododendron, OR	Above	21	353770	1963 to 2012	A24
14141500	Little Sandy River near Bull Run, OR	Above	60	353770	1950 to 2012	A25
14152500	Coast fork Willamette River at London, OR	Above	185	351897	1950 to 2012	A26
14158500	McKenzie River at outlet of Clear Lake, OR	Above	237	355362	1950 to 2012	A27
14159200	South fork McKenzie River near Rainbow, OR	Above	414	355362	1957 to 2012	A28
14161500	Lookout Creek near Blue River, OR	Above	62	355362	1950 to 2012	A29
14179000	Breitenbush River above French Creek near Detroit, OR	Above	273	351433	1950 to 2012	A30
08NC004	Canoe River below Kimmel Creek, BC	Above	298	1171393	1971 to 2011	A31
08NF001	Kootenay River at Kootenay Crossing, BC	Above	420	1173210	1950 to 2011	A32
08NH119	Duncan River below BB Creek, BC	Above	1330	1143900	1912 to 2012	A33
08NM174	Whiteman Creek above Bouleau Creek, BC	Above	112	1128582	1900 to 2012	A34

Table 2.2. Gage pairs sharing the same below-dam gage.

Above Dam Gage	Below Dam Gage	Sub Basin	Dam
12332000	12340500	Flathead	Milltown Dam
12358500	12340500	Flathead	Milltown Dam
12413000	12419000	Coeur D'Alene	Post Falls Dam
12414500	12419000	Coeur D'Alene	Post Falls Dam
12414900	12419000	Coeur D'Alene	Post Falls Dam

Table 2.3. Above-dam streamflow gages without corresponding below-dam gages.

Gage	Name and location	Gage Record	Sub-basin Name
13313000	Johnson Creek at Yellow Pine, ID	1950 to 2012	Salmon
13330000	Lostine River near Lostine, OR	1950 to 2012	Lower Snake
13337000	Lochsa River near Lowell, ID	1950 to 2012	Clearwater
14020000	Umatilla River above Meacham Creek near Gibbon, OR	1950 to 2012	Middle Columbia
14037500	Strawberry Creek above Slide Creek near Prairie City, OR	1950 to 1991	John Day
14107000	Klickitat River above West fork near Glenwood, WA	1950 to 2012	Middle Columbia

Table 2.4. Topographic and climatic characteristics of study basins above dams in the Columbia River Basin. Averages are for the period of available record (see Table 1)**.**

Gage	Mean Basin Elevation (m)	Gage Elevation (m)	Precipitation (mm)	Tave (C)	Tmax (C)	Tmin (C)	Sub-basin Name	Abbreviation
12332000	2170	1661	767	1.7	8.1	-4.1	Clark Fork	CLF
12358500	1724	957	1271	2.6	7.8	-2.9	Flathead	FLA
12370000	1530	936	1095	4.0	9.8	-1.6	Flathead	FLA
12413000	1168	677	1206	6.3	11.0	-0.1	Coeur d'Alene	CDA
12414500	1381	667	1277	5.7	10.5	-0.3	Coeur dAlene	CDA
12414900	1095	788	1122	6.2	12.4	-0.1	Coeur d'Alene	CDA
12451000	1534	355	1732	5.2	8.1	-1.5	Lake Chelan	LKC
13011500	2471	2055	957	1.5	8.2	-6.0	Snake Headwaters	SHW
13022500	2486	1772	876	0.6	8.2	-6.1	Snake Headwaters	SHW
13078000	1934	1524	416	6.4	13.1	-0.2	Upper Snake	UPS
13147900	2184	1614	554	4.4	11.0	-3.4	Upper Snake	UPS
13185000	1955	996	928	4.6	11.5	-2.0	Boise	BOI
13186000	2141	1288	876	4.0	10.6	-2.8	Boise	BOI
13313000	2180	1439	1120	2.5	8.7	-5.2	Salmon	SAL
13330000	2101	1121	1201	2.4	8.2	-3.5	Lower Snake	LOW
13337000	1584	449	1298	4.0	10.0	-1.5	Clearwater	CLW
13340600	1443	512	1432	4.6	10.7	-0.7	Clearwater	CLW
14020000	1209	578	1058	7.1	12.2	0.9	Middle Columbia	MID

14037500	2097	1496	815	5.1	9.8	-2.3	John Day	JDY
14050500	1554	1357	1372	5.4	11.5	-1.2	Deschutes	DES
14091500	1268	606	1281	6.7	12.8	0.2	Deschutes	DES
14095500	1134	778	1122	7.0	12.2	0.8	Deschutes	DES
14107000	1429	830	984	5.1	9.4	-0.8	Middle Columbia	MID
14138800	1000	781	2987	7.3	11.1	2.3	Sandy	SAN
14141500	725	301	2732	9.5	13.0	3.3	Sandy	SAN
14152500	627	265	1700	11.2	15.9	4.9	Willamette	WIL
14158500	1254	948	2185	6.9	12.3	0.4	Willamette	WIL
14159200	1281	534	1817	7.5	12.5	1.2	Willamette	WIL
14161500	983	435	2272	8.5	15.1	2.4	Willamette	WIL
14179000	1150	525	2054	7.4	12.3	1.3	Willamette	WIL
08NC004	2050	972	1639	2.6	3.4	-4.8	Upper Columbia	UPC
08NF001	1861	1169	1032	4.9	5.5	-4.7	Kootenay River	KOO
08NH119	2015	600	1446	7.6	4.3	-3.8	Duncan River	KOO
08NM174	1532	633	825	8.2	8.4	-1.4	Upper Columbia	UPC

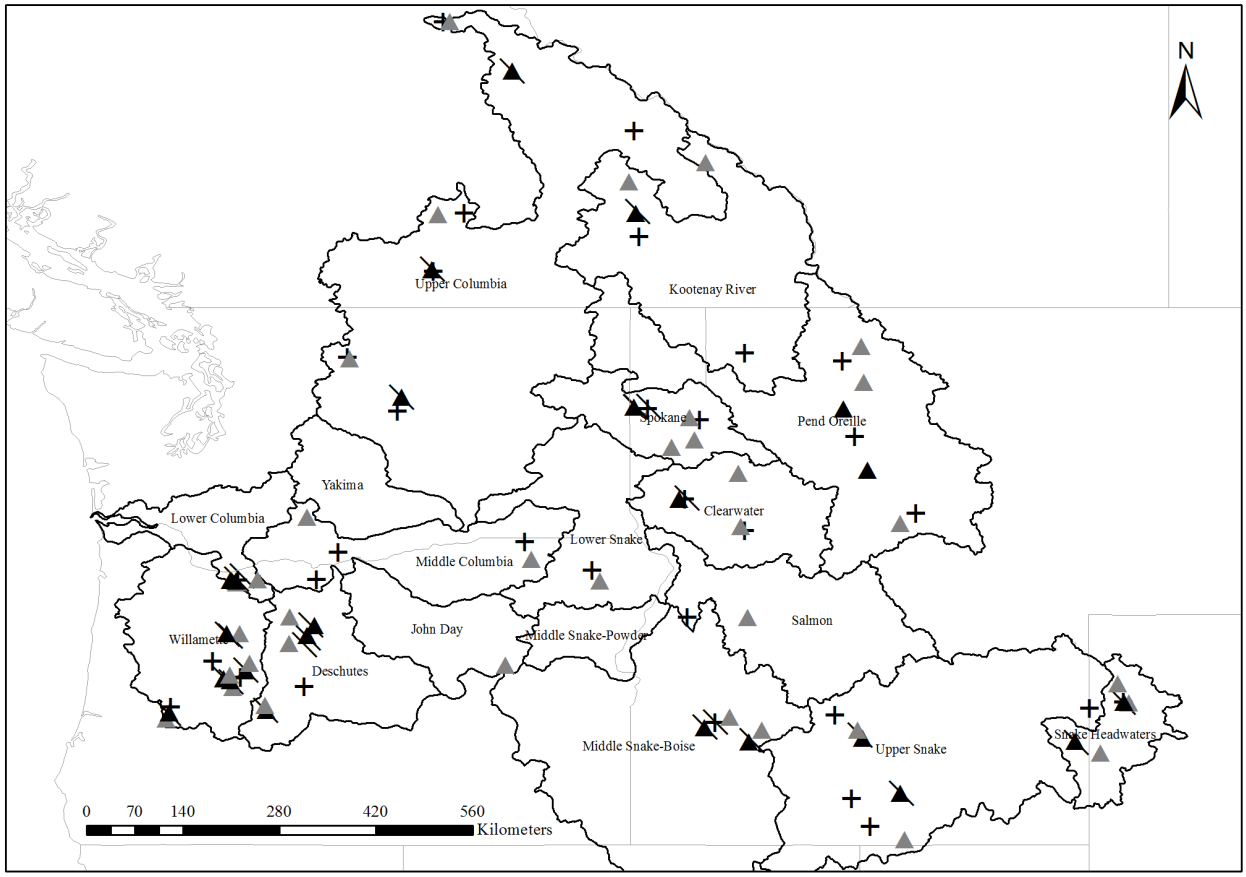

Figure 2.1. Streamflow gages (triangles, above-dam grey, below-dam black), dams (black slash), and climate stations (plus sign) included in this study along with the HUC-6 sub-basins of the Columbia River Basin.

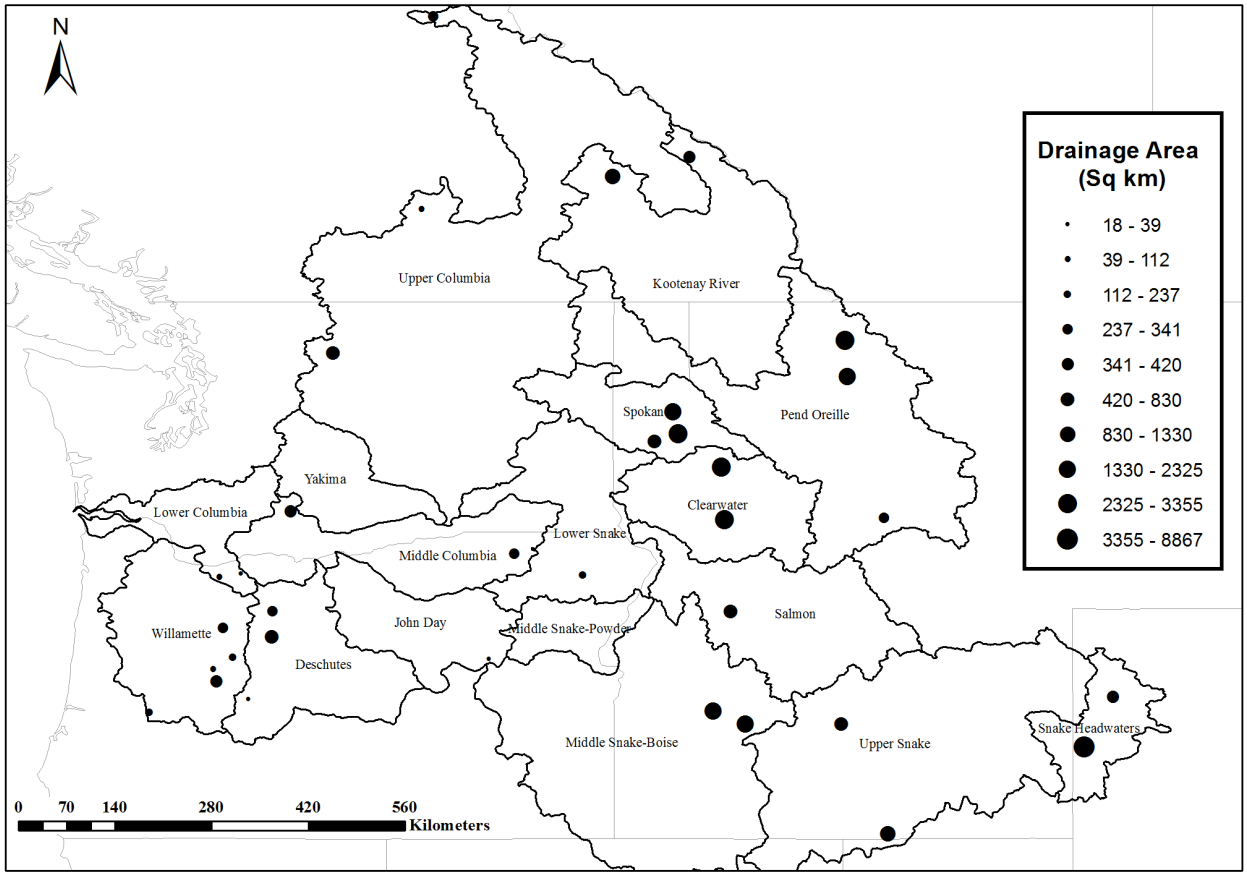

Figure 2.2. Drainage areas of sub-basins in the Columbia River Basin with streamflow gage records used in this study.

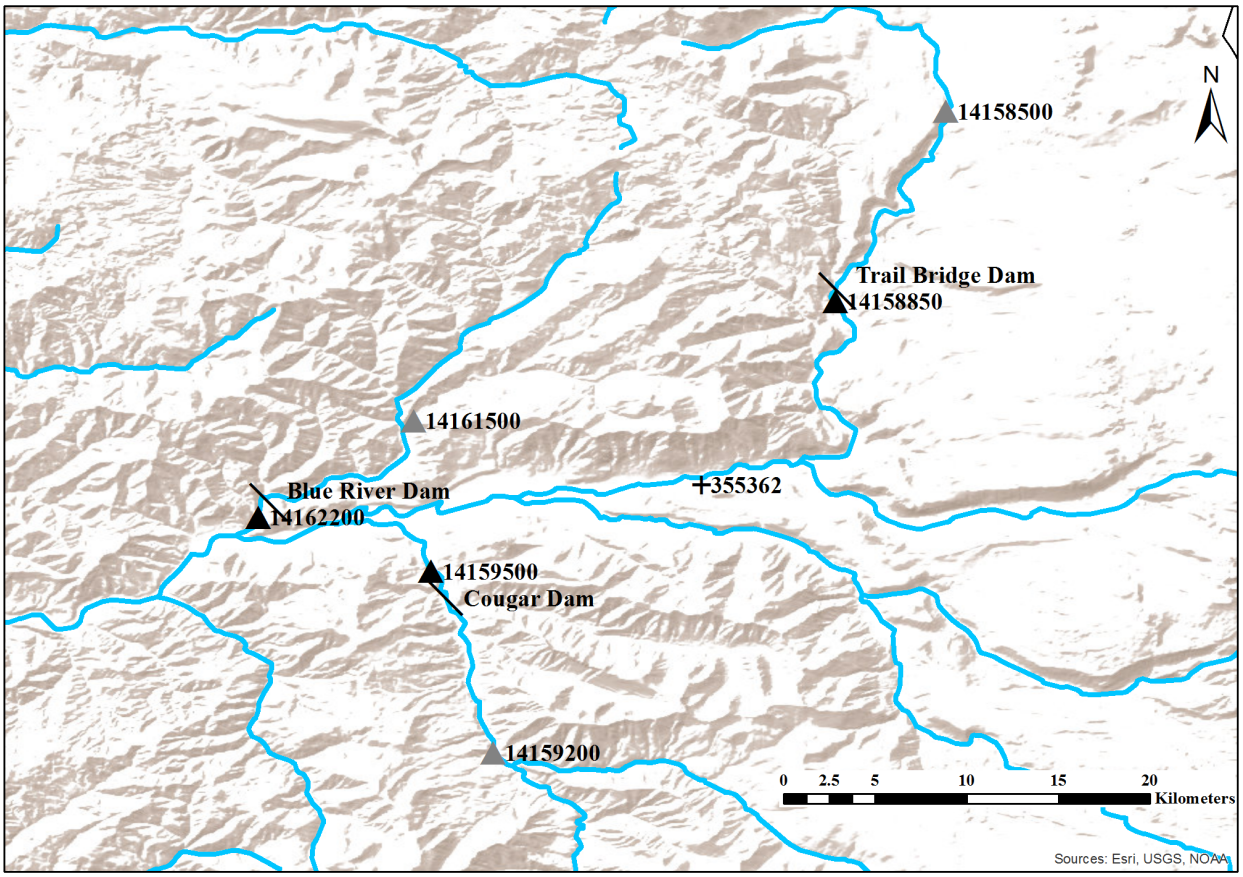

Figure 2.3. Example of spatial arrangement of stream and climate gages for two above- and below-dam pairs in the Willamette River sub-basin. Grey triangle = above-dam streamflow gage, black triangle = below-dam streamflow gage, black slash = dam, and plus sign = climate station.

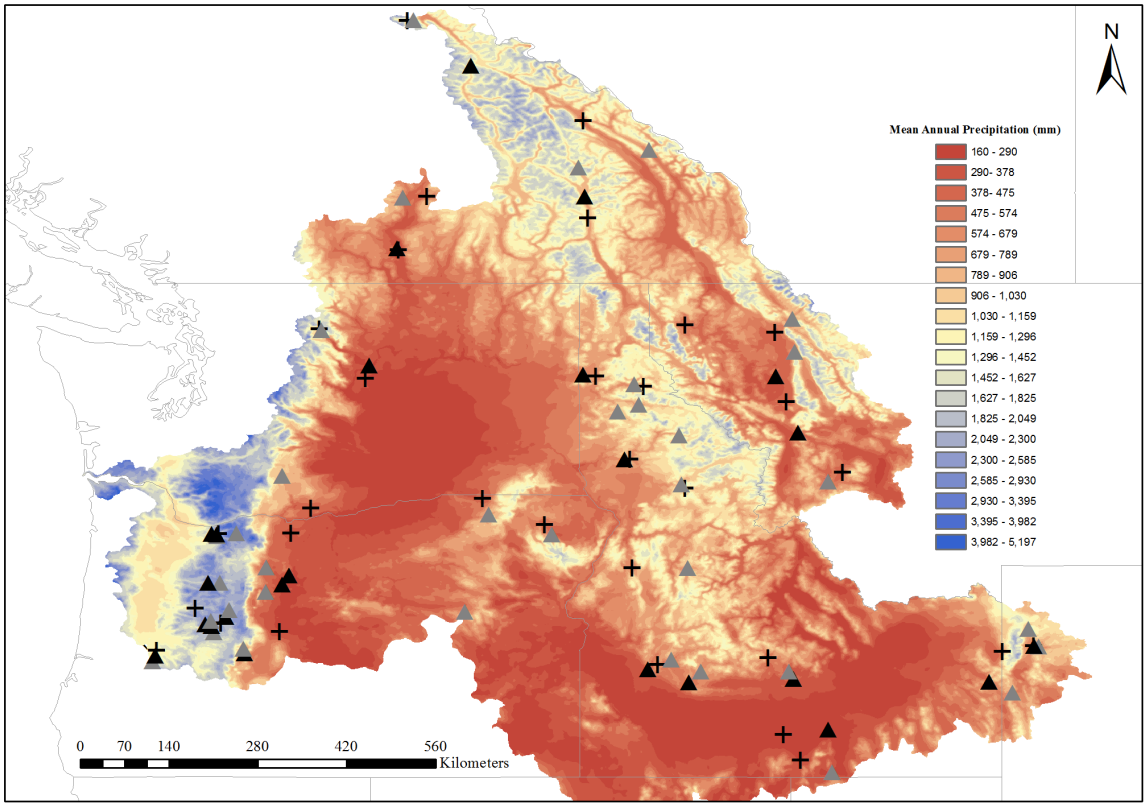

Figure 2.4. Mean annual precipitation across the CRB obtained from Parameter-elevation Relationships on Independent Slopes Model (PRISM, http://www.prism.oregonstate.edu/) datasets.

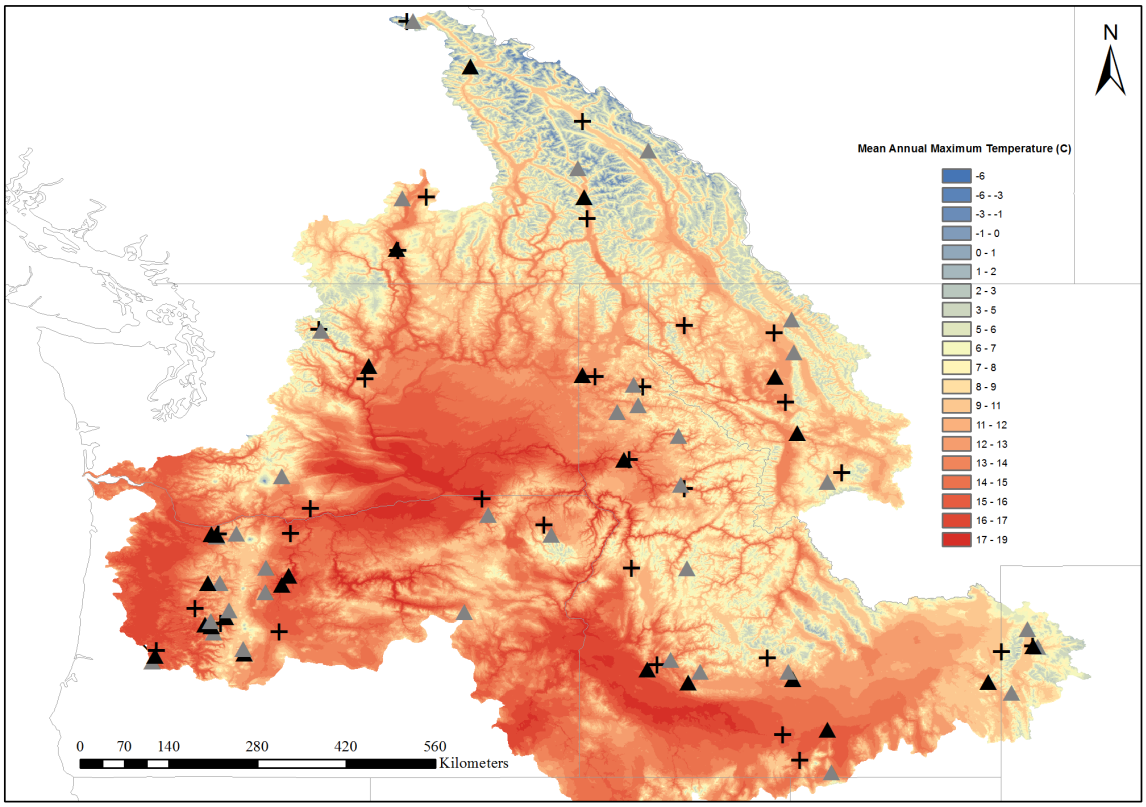

Figure 2.5. Mean annual maximum temperature across the CRB obtained from Parameter-elevation Relationships on Independent Slopes Model (PRISM, http://www.prism.oregonstate.edu/) datasets.

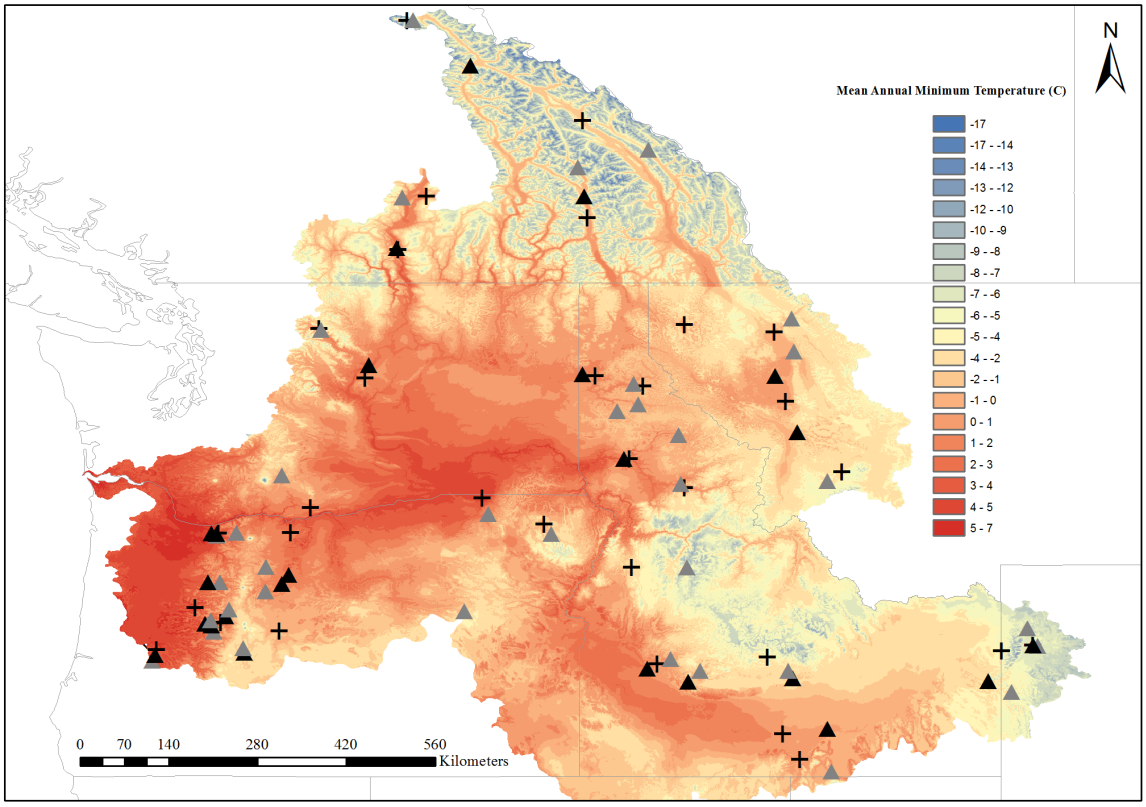

Figure 2.6. Mean annual minimum temperature across the CRB obtained from Parameter-elevation Relationships on Independent Slopes Model (PRISM, http://www.prism.oregonstate.edu/) datasets.

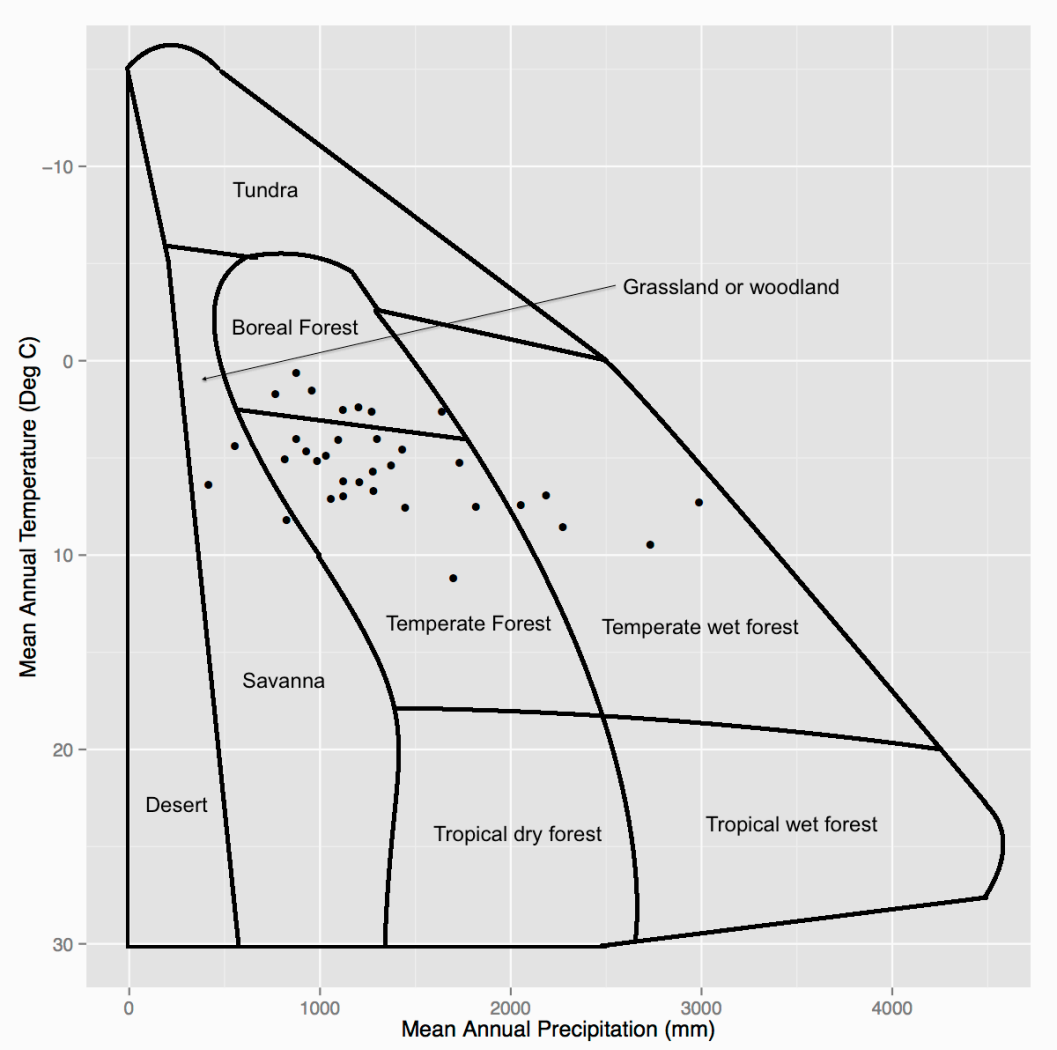

Figure 2.7. Mean annual temperature and mean annual precipitation from climate stations in the Columbia River basin used in this study (see Table 2.2), superimposed on Whittaker biomes.

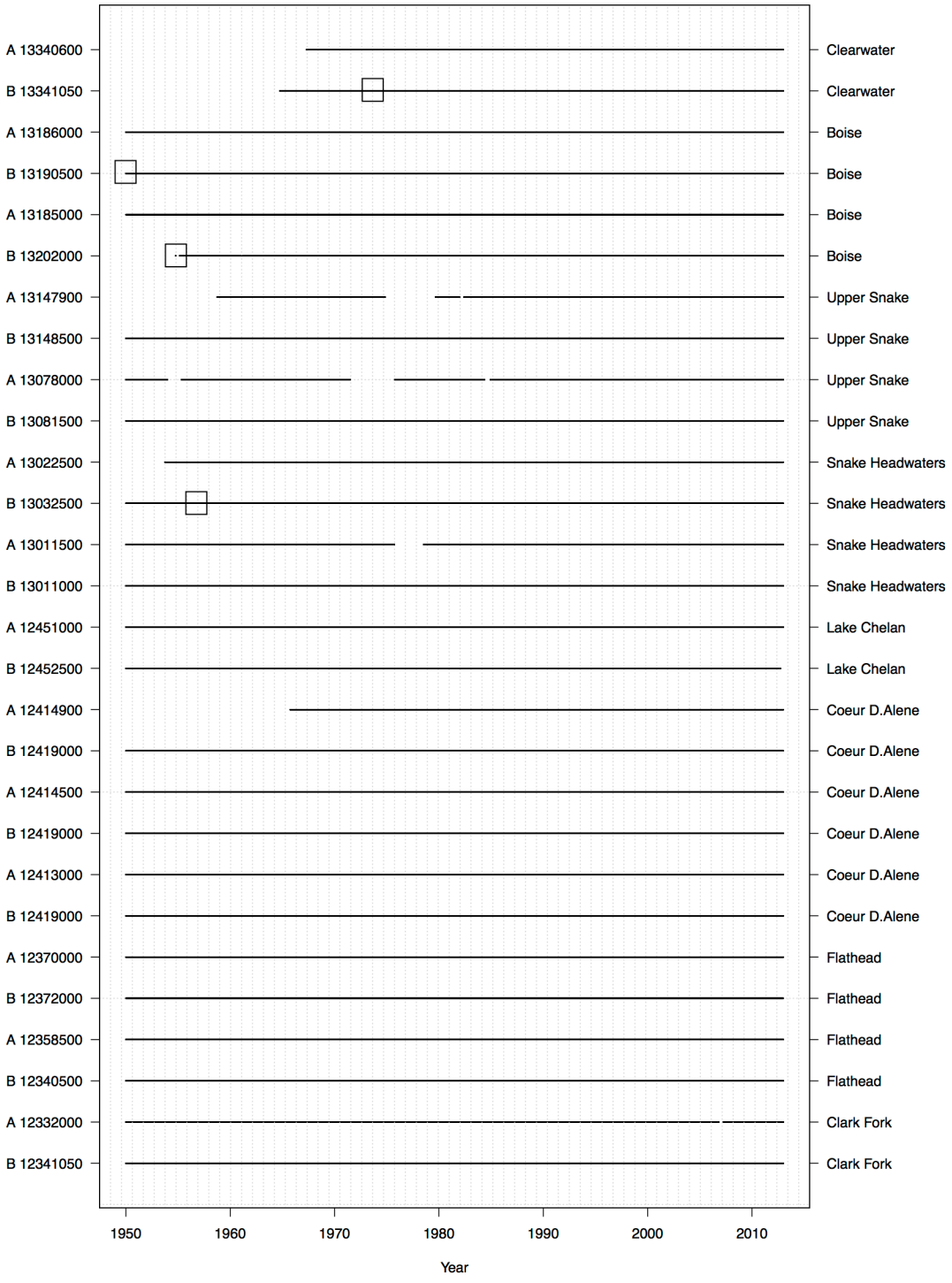

Figure 2.8a. Timeline of gage records for each study site. Squares indicate dam construction date if the dam was built after 1950.

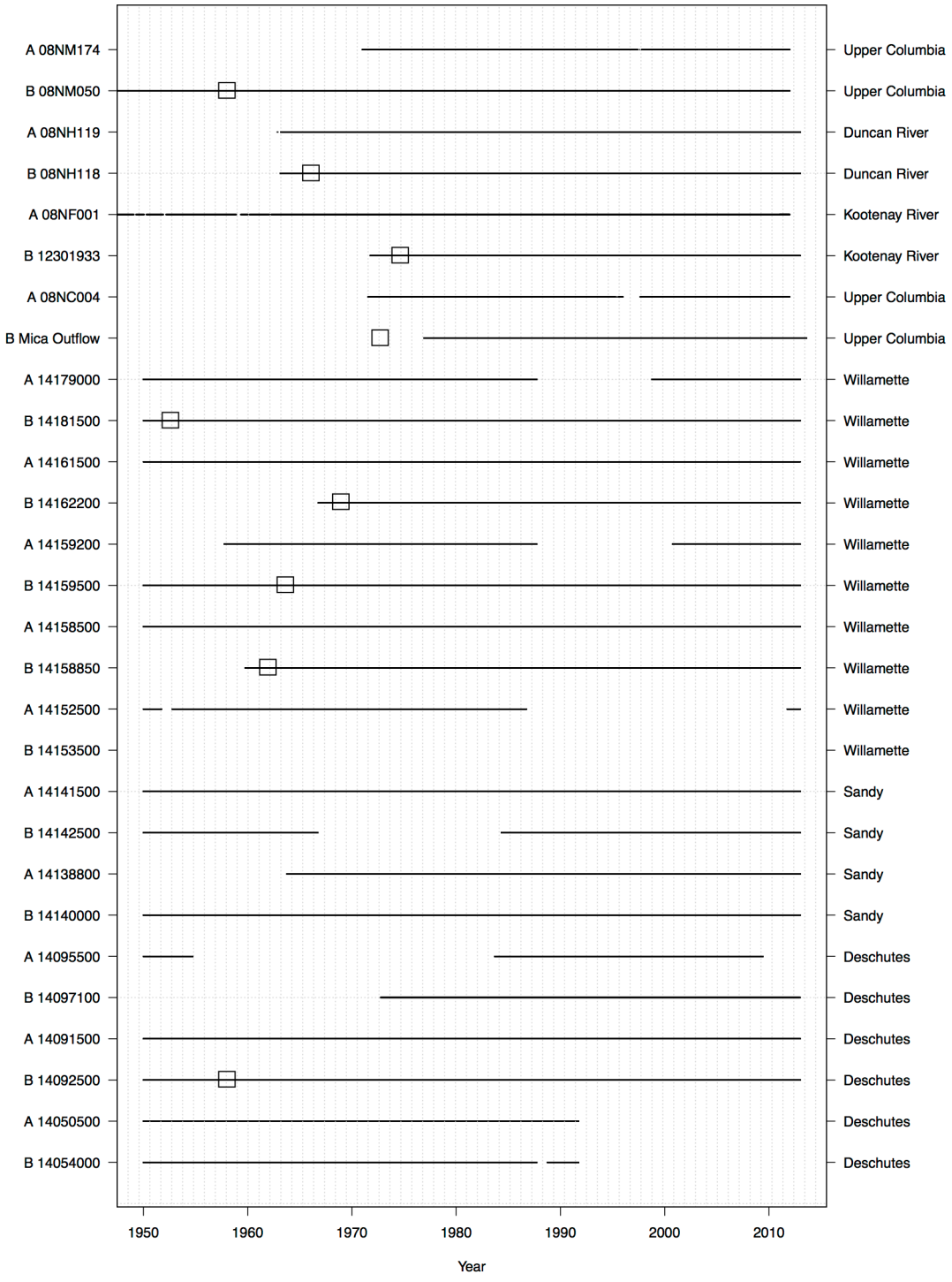

Figure 2.8b. Timeline of gage records for each study site. Squares indicate dam construction date if the dam was built after 1950.

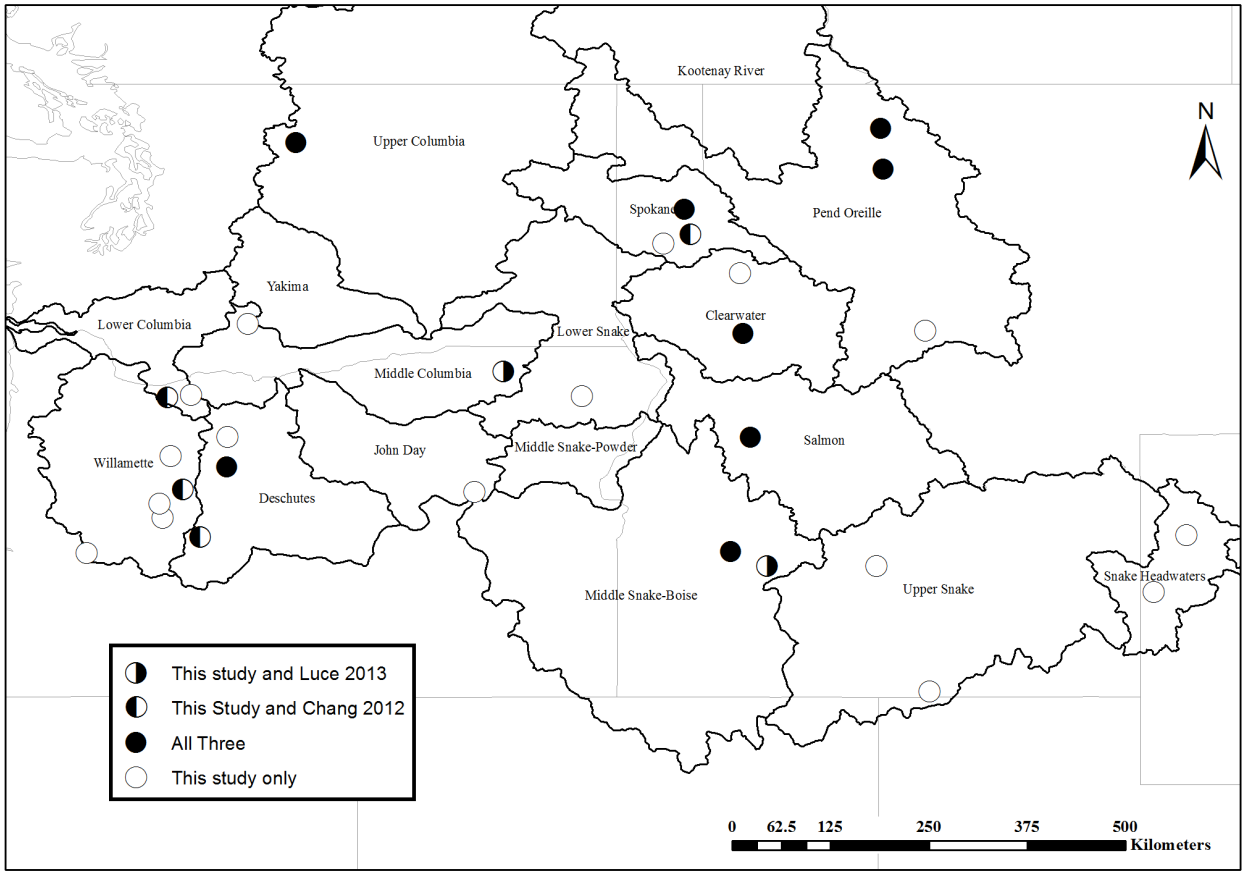

Figure 2.9. Comparison of the above-dam gages used in this study and in Chang (2012) and Luce et al. (2013). Chang (2012) and Luce et al. (2013) did not include British Columbia.

3. Methods

This analysis tested three hypotheses:

(1) interannual variability of streamflow in the CRB is associated with climate mechanisms including upper-atmosphere wind speed (u700 wind speed), fluctuations in the strength and location of the East Asian jet stream (Pacific North American pattern [PNA]), sea-level pressure over the northern Pacific (Northern Pacific Index [NPI]) and northern Pacific Ocean sea surface temperature (Pacific Decadal Oscillation [PDO]);

(2) over the period 1950-2012, streamflow in the CRB increased in spring and declined in late summer and

(3) over the study period, the magnitude and direction and timing of seasonal streamflow trends differ below dams compared to above dams.

Hypothesis (1) was tested by calculating and interpreting correlations (Pearson's r) of streamflow with climate indices (u700 wind speed, NPI, and PDO) for each month of the year. Hypothesis (2) was tested by checking data stationarity using wavelet analysis and then calculating trends over the period 1950-2012 in daily air temperature, daily precipitation, daily streamflow, annual streamflow, the date of center of timing in each year, and March and September monthly streamflow, for 28 sites (59 streamflow gage records, 34 above dams and 25 below dams), and counting the numbers of sites at which trends were positive. Hypothesis (3) was tested by comparing streamflow trends above and below dams in each of the 28 pairs of above- and below-dam pairs of sites, by sub-basin, and for the whole CRB.

3.1. Data sources

Data for this study were of four types: (1) spatial data, (2) historic climate and streamflow records, (3) ancillary information on reservoir operation and dam construction, and (4) climate indices. Data were obtained from existing records. The entire daily record of streamflow and climate variables was downloaded for each gaging and climate station. These data were then subset to only include the period from January 1, 1950 to December 31, 2012.

Spatial data and data sources included: (1) HUC 6 sub-basin boundaries obtained from the National Atlas (http://www.nationalatlas.gov/maplayers.html); (2) streamflow gage locations in the U.S. obtained from the USGS Gages project (http://water.usgs.gov/GIS/metadata/usgswrd/XML/gagesII_Sept2011.xml); and (3) streamflow gage locations in British Columbia (http://www.geobase.ca/geobase/en/data/nhn/index.html).

Climate data that had been adjusted and homogenized were obtained from (1) the U.S. historic climate data network (USHCN) (http://cdiac.ornl.gov/epubs/ndp/ushcn/ushcn_map_interface.html); and (2) Adjusted and Homogenized Canadian Climate Data (AHCCD) (http://www.ec.gc.ca/dccha-ahccd/). USHCN and AHCCD climate data are adjusted and homogenized to remove effects such as changes due to relocations of stations or changes in station instrumentation. During homogenization, climate stations are compared to a reference time series from neighboring stations.

Daily records of streamflow for the gages in the United States were obtained from the United States Geological Survey (USGS

http://waterdata.usgs.gov/nwis/dv/?referred_module=sw) online distribution center, supplemented by data available from the HJ Andrews Experimental Forest to fill in gaps in the USGS record for Lookout Creek (14161500, http://andrewsforest.oregonstate.edu/lter/about/weather/hja.cfm). Daily records of streamflow for gages in British Columbia were obtained from the Environment Canada Water Survey of Canada (WSC http://www.ec.gc.ca/rhc-wsc/default.asp?lang=En&n=4EED50F1-1) online distribution center. An additional record, for the outflow of Mica Dam, was obtained from BC Hydro.

Information on reservoir operation and dam construction for dams in the U.S. was obtained from (1) the National Inventory of Dams (http://geo.usace.army.mil/pgis/f?p=397:12) and (2) the USGS (http://water.usgs.gov/GIS/metadata/usgswrd/XML/reservoir.xml), and supplemented by additional research on each dam and reservoir from USACE and USBR websites. Information on reservoir operation and dam construction for dams in British Columbia was obtained from Data BC (https://apps.gov.bc.ca/pub/geometadata/metadataDetail.do?recordUID=49718&recordSet=ISO19115).

Climate indices included (1) U700 windspeed, (2) the Pacific Decadal Oscillation (PDO), (3) the Northern Pacific Index (NPI), and (4) the Pacific North America pattern (PNA). U700 winds, which are westerly lower tropospheric winds at 700 hPa, were obtained from the NCEP/NCAR Reanalysis 1 (http://www.esrl.noaa.gov/psd/data/gridded/data.ncep.reanalysis.html). Gridded data for the entire globe was downloaded and then a mask was created to extract data for the

Columbia River Basin. The thirteen gridded points falling within the CRB were then combined to one value for each monthly time step using an average value weighted by latitude due to the decreasing area represented by each 2.5 degree grid cell as one moves toward the pole, yielding a monthly time series of 700 hPa winds for the CRB. The monthly PDO index was obtained from University of Washington (http://jisao.washington.edu/pdo/PDO.latest) while the monthly NPI index was obtained from the University Corporation for Atmospheric Research (https://climatedataguide.ucar.edu/sites/default/files/climate_index_files/npindex_monthly_0.txt). The PNA index was obtained from the National Oceanic and Atmospheric Administration's Climate Prediction Center (ftp://ftp.cpc.ncep.noaa.gov/cwlinks/).

3.2. Data Analysis

3.2.1. Streamflow metrics

Most of the analyses in this study were performed on daily data, but two annual metrics were additionally derived and analyzed. Annual flow volume, a measure of total water supply availability, was calculated by summing daily records of streamflow by calendar year. The annual hydrograph centroid date on a water year basis (which can be used to monitor overall hydrograph timing shifts) was defined as:

$$CT = \Sigma (t_i q_i)/\Sigma q_i$$

where CT is the day of the water year at which half of the water year flow has passed, t_i is the day of the water year and q_i is the mean flow on that day of year.

3.2.2 Correlations of streamflow with winds and climate indices

Monthly streamflow and precipitation for all gages was correlated with monthly indices of PDO, NPI, PNA, and u700 wind speeds using Pearson's r, for each month of the year.

3.2.3. Trend analysis

For daily data, both parametric (linear regression) and non-parametric (Mann-Kendall) tests were performed. Anomalies were calculated as departures from the day-of-year mean for the 62-year period of record, for daily precipitation, maximum and minimum temperature, and streamflow. Prior to analysis of the daily data, below-dam records were trimmed to remove the record prior to dam operation in order to exclude the influence of dam construction and the influence of changes in reservoir management. Trend analysis was also performed using the Mann-Kendall test for annual streamflow, March and September monthly streamflow, and centroid date.

In linear regression tests of daily data, the daily anomalies were regressed against year, and the significance of the corresponding relationships was determined at $p = 0.05$. Prior to linear regression analysis, daily streamflow and precipitation data values of 0 were replaced by 0.0001, and data were then log-transformed to produce normally distributed data as required by the parametric test. Zero values in precipitation occur commonly because of days with no rain, whereas zeroes in streamflow data occur when flow falls below the measurement resolution of the gage. In either case, zeros are meaningful and should be included in the analysis. Assigning a very small real number, such as 0.0001, permits a natural logarithm to be calculated and also allows the data to be included in the analysis. The units of slope for these linear regression tests are degrees

Celsius for the maximum and minimum temperatures, and the natural logarithm of precipitation (mm) and streamflow (m^3/s), per year.

In Mann-Kendall tests of daily data, the daily anomalies of precipitation, maximum and minimum temperature, and streamflow were ranked and correlated against year. Significant increases and decreases in daily streamflow in this case were determined by evaluating whether tau of the Mann-Kendall test for each day was positive or negative at $p < 0.05$. The Mann-Kendall test assumes monotonicity but not linearity, and it requires no distributional assumptions. Thus, data were not transformed prior to analysis using this method.

In daily analyses, for each day of the year, the Excel countif function was used to count the number of gages (stations) with significant increases or decreases from 1950 to 2012 in the following: (1) streamflow; (2) maximum temperature; (3) minimum temperature and (4) precipitation. Numbers of sites with streamflow changes were counted (a) across the entire CRB, (b) by sub-basin, (c) for above-dam basins, (d) for basins below dams, and (e) for below-dam basins by primary reservoir management objective (flood control, hydropower, irrigation, or water supply). Numbers of sites with precipitation changes were counted for the entire CRB and by sub-basin. Daily tests were also examined to determine, for each gage, whether three or more consecutive days between March 1 and May 1 experienced a significant increase or decrease, and whether five or more consecutive days and ten or more total days between May 1 to November 1 experienced a significant increase or decrease. The results from this definition of trend are summarized in Tables 4.5 to 4.8 and Figures 4.34 and 4.35.

Changes in reservoir management were identified through consultation with reservoir management and water operations officials at selected examples of dams throughout the CRB. The managers consulted were Michael Beus of the U.S. Bureau of Reclamation - Water Operations Manager, Mary Karen Scullion of the U.S. Army Corps of Engineers – Dam Manager, and Gillian Kong of BC Hydro – Generation Resource Management.

3.2.4. Wavelet analysis

Wavelet analysis was conducted for streamflow, precipitation and maximum air temperature using the Biwavelet package for R and anomaly-corrected time series of daily variables as described in Gouheir and Grinsted (2014) (selected examples in Appendix C). Bias-corrected wavelet power was plotted versus day of record and the period of cycle. Wavelet power was also computed and plotted over time at time scales of interest, including fifteen days, 90 days, one year and four years. These plots were interpreted to determine how cyclical patterns in streamflow may have influenced trend estimation.

3.2.5 Magnitude of streamflow changes

The magnitude of streamflow increase in spring was estimated for the period from March 1 to May 1, and the magnitude of streamflow decrease in summer was estimated for the period between and including May 1 to November 1. The daily anomalies for all days March 1 to May 1 with trend > 0 and $p < 0.05$ were summed to obtain a total spring anomaly value for each year. The daily anomalies for all days May 1 to November 1 with trend > 0 and $p < 0.05$ were summed to obtain a total summer anomaly value for each year. These daily anomalies were converted to units of millions of cubic meters per year.

4. Results

4.1. CRB streamflow and precipitation correlations with upper-elevation winds and climate indices

NPI, PDO and PNA climate oscillations along with u700 winds would be expected to influence streamflow and precipitation patterns across the CRB. Each influence likely has varying relationships with the two variables of interest.

4.1.1. u700 correlations

The u700 winds were positively correlated with precipitation in October through March, with the strongest correlations below 1,000 m (Figures 4.1 to 4.6). Correlations were weak to moderately negative during the summer months. Positive precipitation and u700 wind correlations in November, December and January are distributed throughout the CRB (Figures 4.7, 4.8 and 4.9).

Above-dam streamflow and u700 winds were generally positively correlated during wet months and negatively correlated during dry months. Correlations were moderate to strongly positive from October to January, especially at low elevations and low latitudes, but u700 winds were not correlated with streamflow in October to January at high elevation in Oregon, or north of the Canadian border (Figures 4.1 to 4.6). From February to May correlations of u700 winds and streamflow were weak to moderately negative at high latitude and some high elevation sites. In January to March, u700 winds are negatively related to streamflow, but positively related to precipitation, at high elevation and northern latitude. Strong positive correlations in winter months between u700 winds and streamflow are clustered adjacent to the Cascade Range of Oregon and in northern Idaho. (Figures 4.10, 4.11, and 4.12). Below-dam streamflow and u700 winds

were positively correlated at low elevation and low latitude sites, but correlations were lower than above dams.

4.1.2. Correlations of NPI, PDO, and NPA

Correlations between precipitation and NPI are weakly positive from September to January, and weakly negative from February to August. Precipitation is positively correlated with PDO from April to July, but the rest of year displayed a mixed or weak negative relationship. Correlations between precipitation and PNA were weakly negative from October to January; the rest of the year displayed mixed results.

Correlations between above-dam streamflow and NPI were mostly negative from February to August, with the strongest relationships in April at high latitudes. Above-dam streamflow and PDO were negatively correlated especially south of the Canadian border and below 1000 m (in April and May) and throughout the CRB (in June and July). Above-dam streamflow and PNA were weakly to moderately negatively correlated in July, November, December, and January.

Correlations of below-dam streamflow and NPI, PDO, PNA were generally weak and mixed; some strong correlations resemble above-dam streamflow correlations with these indices.

4.2. Changes in climate and streamflow in the CRB

4.2.1. Trends in daily air temperature and precipitation

Linear trends from regression analyses show that precipitation by day of year across the Columbia River Basin for the most part has not changed at the stations analyzed in this study (Figure 4.13). However, Boise and John Day sub-basins are dominated by negative daily trends in precipitation on multiple days throughout the year.

Many sub-basins in this study including the Boise, Kootenay, Lake Chelan, Lower Columbia, Lower Snake and Salmon show more daily significant increases than decreases in maximum surface air temperature (Figure 4.14). Twenty to sixty percent of stations show occasional increases on a few days in January, March, and June through November. In contrast, daily minimum surface air temperature increased significantly in many of the sub-basins (Figure 4.15). Minimum temperature increased on a majority of days in January and March through November at 20% of more of the climate stations.

4.2.2. Trends in daily streamflow

Sub-basins of the Columbia River have experienced both significant increases and decreases in daily streamflow trends above dams. Across the CRB, increasing daily trends occur most markedly from mid-March to the beginning of May, with corresponding decreasing trends from the middle of May to the middle of October (Figure 4.16). There is a general increase in the proportion of gages displaying decreasing trends in daily discharge as time progresses from May 1 to November 1, with a peak of nearly 60% of gages displaying decreasing trends in the middle of October.

Below dams, the daily proportion of gages displaying significant increases or decreases in streamflow does not match the pattern at above-dam gages (Figure 4.17). Streamflow both increases and decreases at 10 to 20% of below-dam sites in most months.

Plots over time of daily streamflow anomalies on days with significant trends only display the magnitude of increasing spring and declining summer streamflow as a percent of annual flow for examples of above-dam gages [12370000, 12413000, 12414500, 12451000, 08NC004, OHNH119, 13078000, 13147900] (Figure 4.18). In three-quarters

of cases, the magnitude of the red bars is much greater than the blue bars, indicating that flow decreases from May 1 to November 1 (five months of decreasing flows) are much greater than flow increases from March 1 to May 1 (two months of increases) (Figure 4.18). The magnitude of declining trends in summer flows is less than 10% of annual flow in most years, but for at least one site, it is as much as 30% of annual flow in some years (Figure 4.19). The running-mean magnitude of increases in spring flows and decreases in summer flows is less than five percent of annual flow (Figure 4.20 and Figure 4.21, sites listed in Appendix F).

4.2.3. Changes in annual flow and centroid timing.

There were few apparent trends in annual flow volume across the CRB over the period 1950 to 2012 based on the Mann-Kendall test at $p < 0.05$. These changes were scattered across the CRB both above and below dams. The only positive trends occurred in the Upper Columbia and Deschutes sub-basins draining areas with large seasonal snow zones and glaciers (Figure 4.22).

The centroid of timing of streamflow shifted both earlier and later over the period 1950 to 2012 in the CRB. Shifts toward later water year centroid timing, marked by blue arrows, only occurred below dams, whereas shifts toward earlier centroid timing, marked by red arrows, occurred above and below dams. The most concentrated changes were in the Canadian component of the CRB, where five of seven gages showed earlier centroid timing (Figure 4.23).

4.2.4. Changes in March and September monthly flows above and below dams

March streamflow increased significantly at nine of 34 gages above dams (Figure 4.24), but at only one of 25 gages below dams (Figure 4.25). September streamflow

decreased significantly at 16 of 34 gages above dams (Figure 4.26), but at only six gages below dams (Figure 4.27).

4.2.5. Multi-annual cycles above and below dams

Multi-annual cycles (non-stationarity) in climate and streamflow could affect detection of trends; wavelet analysis was used to assess stationarity in the records. Wavelet power of streamflow did not change over the period of record at the Flathead, Sandy and Willamette sub-basins (Appendix C). Wavelet power declined at multiple scales in streamflow after 1996 below the dam in the Upper Columbia, and after 1956 in the Snake headwaters. However, streamflow trends were not affected by the period of record (1950 to 2012 vs. 1957 to 2012) in the Snake headwaters. In the Kootenay sub-basin, wavelet power did not change before vs. after dam construction, but wavelet variance in below-dam streamflow was lower than in above-dam streamflow throughout the record. Wavelet power in below-dam streamflow at the Boise sub-basin declined after 1967 at 15, 90-day, and three-year time scales, but streamflow trends were not affected by the period of record (1950 to 2012 vs. 1968 to 2012). In general, wavelet power was different in below-dam vs above-dam streamflow for the Upper Columbia, Snake Headwater, Kootenay, Boise, and Sandy sub-basins. Wavelet power below dams resembled wavelet power above dams at the 15-day, 90-day, and three-year time scales in the Flathead basin and at the three-year time scale in the Willamette basin (Figure C-9).

Wavelet power in streamflow at the three to twelve year time scale was high at the beginning and low at the end of the records for the Boise, Flathead, Sandy, Snake Headwaters and Upper Columbia basins, and low at beginning and high at the end of the

records for the Kootenay basin. Extreme flows occurred above the dam in the Boise sub-basin early in the record, and in 2006 in the Flathead sub-basin.

4.3. Changes in streamflow related to land use and water withdrawals above dams and reservoir operation below dams

Streamflow increased significantly on three or more consecutive spring days (March 1- May 1) at fourteen of 34 above-dam gages but at only six below-dam gages. Streamflow (March 1 to May 1) decreased significantly on three or more consecutive days at one above-dam gage and two below-dam gages. Streamflow decreased significantly on five or more consecutive days and ten additional days in summer (May 1 to November 1) at 28 of 34 above-dam gages but at only six below-dam gages. Changes in daily streamflow at above-dam gages occur at all latitudes and elevations for the March 1 to May 1 period (Figure 4.28, Tables 4.1, 4.2) and the May 1 to November 1 period (Figure 4.29).

Daily streamflow both increased and decreased on various days over the period May 1 to November 1 at eight below-dam USGS gages (12301933, 12372000, 12452500, 13011000, 13341050, 14153500, 14159500 and 14162200). Daily streamflow increased on days in late summer to early fall at all but one of these eight USGS gages (12452500). Daily streamflow also increased during late spring at three below-dam gages (USGS 12452500, 13011000, and 14153500). Three below-dam gages showed spring increases at the same time as their above-dam counterparts, USGS 13190500, 13202000, and 12301933.

4.3.1. Changes in streamflow related to land use and water withdrawals above dams

Wildfire is spatially distributed across the forested, rural CRB and temporally distributed almost evenly from 1980 to 2010 (Figures 4.30 and 4.31). Forest harvest and wildfire affect much of the forested area in many of the basin studies (Table 4.3).

Spring streamflow increased at eleven (of 34) above-dam gages; eight of these have experienced timber harvest, and five have experienced wildfire. Summer streamflow decreased at 25 (of 34) above-dam gages; 18 of these have experienced timber harvest, and ten have experienced fire. Summer streamflow also has decreased at above-dam gages where there has been no timber harvest.

4.3.2. Changes in streamflow related to reservoir operation below dams

In almost all cases involving flood control dams, the below-dam streamflow changes differed from changes above dams (Figure 4.32, 4.33). Spring streamflow increased both above and below dams at only three sites, and summer streamflow decreased both above and below dams at only five sites (Table 4.2, 4.4, Figures 4.32, 4.33).

4.3.3. Summary of trends in daily streamflow at paired above- and below-dam sites

Based on the definition of -,+, or 0 trend in section 3.2.3, fourteen of the 28 above- and below-dam gage pairs experienced the same trend in streamflow from March 1 to May 1 above and below the dam, over the period 1950 to 2012, and fourteen pairs experienced a different trend below- vs above-dams. A signal of increasing spring streamflow was observed at eleven of 28 pairs, but this signal was matched below the dam at only three pairs (Table 4.5, Figure 4.34).

Based on the definition of -,+, or 0 trend in section 3.2.3, nine of the 28 above- and below-dam gage pairs experienced the same trend in streamflow from May 1 to November 1 above and below the dam, over the period 1950 to 2012, and ten pairs experienced a different trend below- vs above-dams. These do not sum to the total of 28 pairs due to the presence of groups of days with both positive and negative trends during the summer period at some below-dam gages. A signal of declining May 1 to November 1 streamflow was observed at 18 of 28 pairs, and this signal was matched below the dam at nine pairs (Table 4.6, Figure 4.35).

Table 4.1. Summary of trends in streamflow at 34 gages above dams in the Columbia River basin, by season: spring (March 1 to May 1) and summer (May 1 to November 1). Summary is based on trends in daily streamflow.

Above Dam Spring Change	Above Dam Summer Change	Above Dam Gauge	Gage Name	Sub Basin
+	-	12332000	Middle fork Rock Creek near Philipsburg, MT	Clark Fork
+	-	12358500	Middle fork Flathead River near West Glacier, MT	Flathead
+	-	12370000	Swan River near Bigfork, MT	Flathead
+	-	12413000	North fork Coeur d'Alene River at Enaville, ID	Coeur D'Alene
+	-	12414500	St. Joe River at Calder, ID	Coeur D'Alene
0	0	12414900	St. Maries River near Santa, ID	Coeur D'Alene
+	-	12451000	Stehekin River at Stehekin, WA	Lake Chelan
+	-	13011500	Pacific Creek at Moran, WY	Snake Headwaters
0	+,-	13022500	Snake River above reservoir near Alpine, WY	Snake Headwaters
0	-	13078000	Raft River above Onemile Creek near Malta, ID	Upper Snake
0	-	13147900	Little Wood River above High Five Creek near Carey, ID	Upper Snake
+	-	13185000	Boise River near Twin Springs, ID	Boise
+	-	13186000	South fork Boise River near Featherville, ID	Boise
0	-	13340600	North fork Clearwater River near Canyon Ranger Station, ID	Clearwater
-	-	14050500	Cultus River above Cultus Creek near La Pine, OR	Deschutes
0	-	14091500	Metolius River near Grandview, OR	Deschutes
0	-	14095500	Warm Springs River near Simnasho, OR	Deschutes
0	-	14138800	Blazed Alder Creek near Rhododendron, OR	Sandy
0	-	14141500	Little Sandy River near Bull Run, OR	Sandy
0	0	14152500	Coast fork Willamette River at London, OR	Willamette
0	-	14158500	McKenzie River at outlet of Clear Lake, OR	Willamette
0	0	14159200	South fork McKenzie River near Rainbow, OR	Willamette
0	-	14161500	Lookout Creek near Blue River, OR	Willamette
0	-	14179000	Breitenbush River above French Creek near Detroit, OR	Willamette
0	-	08NC004	Canoe River below Kimmel Creek, BC	Upper Columbia
+	-	08NF001	Kootenay River at Kootenay Crossing, BC	Kootenay River
0	-	08NH119	Duncan River below BB Creek, BC	Duncan River
+	-	08NM174	Whiteman Creek above Bouleau Creek, BC	Upper Columbia

Table 4.2. Summary of trends in streamflow at 25 gages below dams in the Columbia River basin, by season: spring (March 1 to May 1) and summer (May 1 to November 1). Summary is based on trends in daily streamflow.

Below Dam Spring Change	Below Dam Summer Change	Below Dam Gauge	Gage Name	Sub Basin
0	-	12340500	Clark Fork above Missoula, MT	Clark Fork
0	-	12340500	Clark Fork above Missoula, MT	Flathead
0	+,-	12372000	Flathead River near Polson, MT	Flathead
0	+	12419000	Spokane River near Post Falls, ID	Coeur D'Alene
0	+	12419000	Spokane River near Post Falls, ID	Coeur D'Alene
0	+	12419000	Spokane River near Post Falls, ID	Coeur D'Alene
-	+,-	12452500	Chelan River at Chelan, WA	Lake Chelan
0	+,-	13011000	Snake River near Moran, WY	Snake Headwaters
0	+	13032500	Snake River near Irwin, ID	Snake Headwaters
-	+	13081500	Snake River near Minidoka, ID	Upper Snake
0	-	13148500	Little Wood River near Carey, ID	Upper Snake
+	-	13202000	Boise River near Boise, ID	Boise
+	+	13190500	South fork Boise River at Anderson Ranch Dam, ID	Boise
+	+,-	13341050	Clearwater River near Peck, ID	Clearwater
0	0	14054000	Deschutes River below Crane Prairie La Pine, OR	Deschutes
0	+	14092500	Deschutes River near Madras, OR	Deschutes
0	0	14097100	Warm Springs River near Kahneeta hot springs, OR	Deschutes
0	-	14140000	Bull Run River near Bull Run, OR	Sandy
0	-	14142500	Sandy River below Bull Run River, OR	Sandy
0	+,-	14153500	Coast fork Willamette River below Cottage Grove Dam, OR	Willamette
+	0	14158850	McKenzie River below Trail Bridge Dam, OR	Willamette
+	+,-	14159500	South fork McKenzie river near Rainbow, OR	Willamette
0	+,-	14162200	Blue River at Blue River, OR	Willamette
0	-	14181500	North Santiam River at Niagara, OR	Willamette

0	-	Mica Outflow	Mica Dam on the Columbia River, BC	Upper Columbia
+	+,-	12301933	Kootenai River below Libby Dam, MT	Kootenay River
+	-	08NH118	Duncan River below Lardeau River, BC	Duncan River
0	0	08NM050	Okanagan River at Penticton, BC	Upper Columbia

Table 4.3. Summary information for above-dam basin disturbance and reservoir management. Areas affected by timber harvest were visually estimated by looking at satellite imagery for each catchment.

Above Dam Gauge	Large Fire Events 1980 to 2010	Timber Harvest	Timber Harvest Area	USGS, ECWRS Ref	USGS Comments
12332000	-	Yes	10%	Ref	Mostly roadless, small diversions near gage
12358500	83 sq km 2003, 179 sq km 2007	No		Ref	Mostly roadless, some local irrigation
12370000	-	Yes	50%	Non-ref	Diversions for irrigation
12413000	-	Yes	25%	Ref	Some small local irrigation
12414500	-	Yes	> 50 %	Ref	Proximal logging, wilderness HW
12414900	-	Yes	> 50 %	Non-ref	Forested and logging, irrigated pasture
12451000	-	No		Ref	Mostly wilderness, Glacer Peak Wilderness
13011500	-	No		Ref	Wilderness, Yellowstone National Park
13022500	92 sq km 2006, 39 sq km 2011	No		Non-ref	Upstrm reservoir, Jackson Lake
13078000	-	No		Non-ref	Upstrm irrigated agriculture and diversions
13147900	-	No		Non-ref	Proximal irrigated agriculture on main trib
13185000	118 sq km 1994, 107 sq km 2003	Yes	< 5 %	Ref	Mostly roadless
13186000	153 sq km 2008	Yes	< 5 %	Non-ref	Mostly roadless
13340600	-	Yes	25%	Ref	Wilderness area
14050500	-	Yes	10%	Non-ref	Spring
14091500	45 sq km 2003, 47 sq km 2007	Yes	50%	Non-ref	Spring
14095500	-	Yes	> 75 %	Ref	Many forest roads and logging
14138800	-	Yes	50%	Ref	Some forest roads
14141500	-	Yes	> 50 %	Ref	Some forest roads
14152500	-	Yes	75%	Ref	Agriculture in basin, logging in HW

14158500	323 sq km 2003	Yes	50%	Ref	Natural lake outlet
14159200	-	Yes	50%	Ref	Mostly roadless, some wilderness
14161500	-	Yes	25%	Ref	Some forest roads
14179000	-	Yes	50%	Ref	Many forest roads and logging
08NC004	1 sq km 2007	No		Ref	No forest roads or logging
08NF001	2 sq km 2006	Yes	50%	Ref	National Park with one paved road
08NH119	1 sq km each decade	Yes	< 5 %	Ref	One paved road, little to no forestry
08NM174	2009	Yes	> 50 %	Ref	Some roads and logging

Table 4.4. Comparison of trends in streamflow above and below dams at 28 pairs of gages in the Columbia River basin, by season: spring (March 1 to May 1) and summer (May 1 to November 1). Results from Tables 4.2 and 4.3.

Above Dam Spring Change	Above Dam Summer Change	Above Dam Gauge	Below Dam Spring Change	Below Dam Summer Change	Below Dam Gauge	Sub Basin
+	-	12332000	0	-	12340500	Clark Fork
+	-	12358500	0	-	12340500	Flathead
+	-	12370000	0	+,-	12372000	Flathead
+	-	12413000	0	+	12419000	Coeur D'Alene
+	-	12414500	0	+	12419000	Coeur D'Alene
0	0	12414900	0	+	12419000	Coeur D'Alene
+	-	12451000	-	+,-	12452500	Lake Chelan
+	-	13011500	0	+,-	13011000	Snake Headwaters
0	+,-	13022500	0	+	13032500	Snake Headwaters
0	-	13078000	-	+	13081500	Upper Snake
0	-	13147900	0	-	13148500	Upper Snake
+	-	13185000	+	-	13202000	Boise
+	-	13186000	+	+	13190500	Boise
0	-	13340600	+	+,-	13341050	Clearwater
-	-	14050500	0	0	14054000	Deschutes
0	-	14091500	0	+	14092500	Deschutes
0	-	14095500	0	0	14097100	Deschutes
0	-	14138800	0	-	14140000	Sandy
0	-	14141500	0	-	14142500	Sandy
0	0	14152500	0	+,-	14153500	Willamette

0	-	14158500	+	0	14158850	Willamette
0	0	14159200	+	+,-	14159500	Willamette
0	-	14161500	0	+,-	14162200	Willamette
0	-	14179000	0	-	14181500	Willamette
0	-	08NC004	0	-	Mica Outflow	Upper Columbia
+	-	08NF001	+	+,-	12301933	Kootenay River
0	-	08NH119	+	-	08NH118	Duncan River
+	-	08NM174	0	0	08NM050	Upper Columbia

Table 4.5. Numbers of pairs of above- and below-dam trends in March 1 to May 1 daily streamflow over the period 1950 to 2012 in the Columbia River basin. Each above- and below-dam gage had a +, 0, or – signal, corresponding to three or more consecutive days with declining (-), increasing (+), or no trend in streamflow. If the signals agree (diagonal cells of the table, shaded in grey), the above-dam signal was propagated through, or mimicked by the reservoir operations. If the signals differ (off-diagonal cells of the table), the signal was obscured or mitigated by reservoir operations. Footnotes indicate the dams that had each effect. Several above-dam gages shared the same dam and below-dam gage, in which case the dam was only listed once.

March 1 to May 1 Trends

		Below Dam			
		-	**0**	**+**	
Above Dam	**-**	0[a]	1[b]	0[c]	1
	0	1[d]	11[e]	4[f]	16
	+	1[g]	7[h]	3[i]	11
					28

[b] Craine Prairie; [d] Minidoka, [e] Post Falls, Palisades, Little Wood River, Pelton, Warm Springs, Bull Run, Cottage Grove, Blue River, Detroit, Mica; [f] Dworshak, Trail Bridge, Cougar, Duncan; [g] Chelan; [h] Milltown, Kerr, Post Falls, Jackson Lake, Okanagan Lake; [i] Luck Peak, Anderson Ranch, Libby.

Table 4.6. Numbers of pairs of above- and below-dam trends in May 1 to November 1 daily streamflow over the period 1950 to 2012 in the Columbia River basin. Each above- and below-dam gage had a +, 0, or – signal, corresponding to five or more consecutive days and ten or more tota days with declining (-), increasing (+), or no trend in streamflow. If the signals agree (diagonal cells of the table, shaded in grey), the above-dam signal was propagated through, or mimicked by the reservoir operations. If the signals differ (off-diagonal cells of the table), the signal was obscure or mitigated by reservoir operations. Numbers in parentheses include below-dam gages where there was both an increase as well as a decrease during this period. Footnotes indicate the dams that had each effect. Several above-dam gages shared the same dam and below-dam gage, in which case the dam was only listed once.

May 1 to November 1 Trends

		Below Dam			
		-	**0**	**+**	
Above Dam	**-**	9[a] (15)	4[b]	5[c] (12)	18
	0	0[d] (2)	0[e]	1[f] (3)	1
	+	0[g]	0[h]	0[i] (1)	0
					28

[a] Milltown, Little Wood River, Lucky Peak, Bull Run, Detroit, Mica, Duncan; [b] Craine Prairie, Warm Springs, Trail Bridge, Okanagan Lake; [c] Post Falls, Minidoka, Anderson Ranch, Pelton; [f] Post Falls.

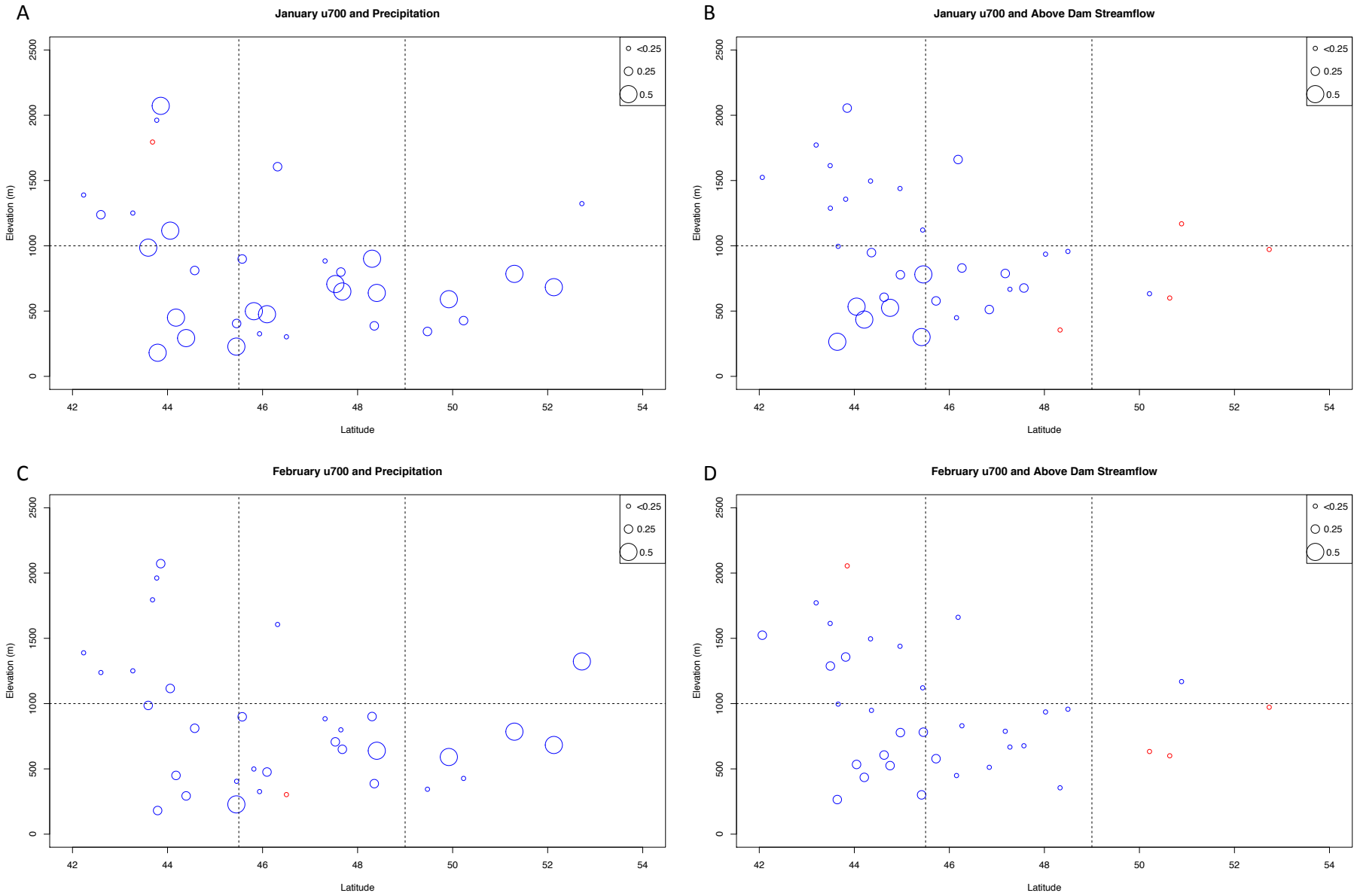

Figure 4.1. January and February monthly correlations between precipitation and u700 winds (A,C) and streamflow and u700 winds (B,D). Positive correlations are shown by blue circles whereas negative correlations are shown by red. Vertical dashed lines indicate the latitude of Portland, on the Oregon-Washington border (45.5°N) and the US-Canada border (49°N).

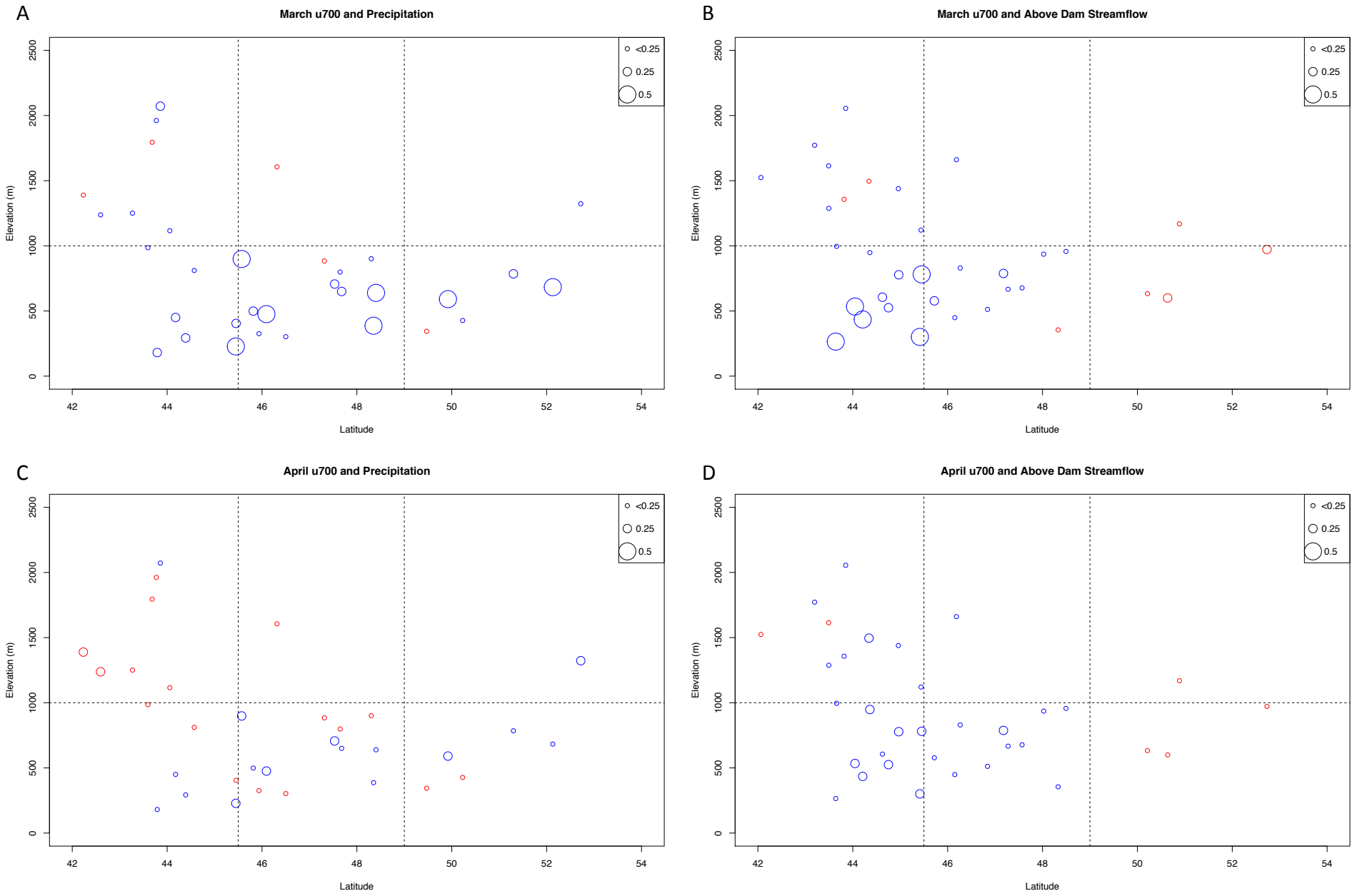

Figure 4.2. March and April monthly correlations between precipitation and u700 winds (A,C) and streamflow and u700 winds (B,D). Positive correlations are shown by blue circles whereas negative correlations are shown by red.

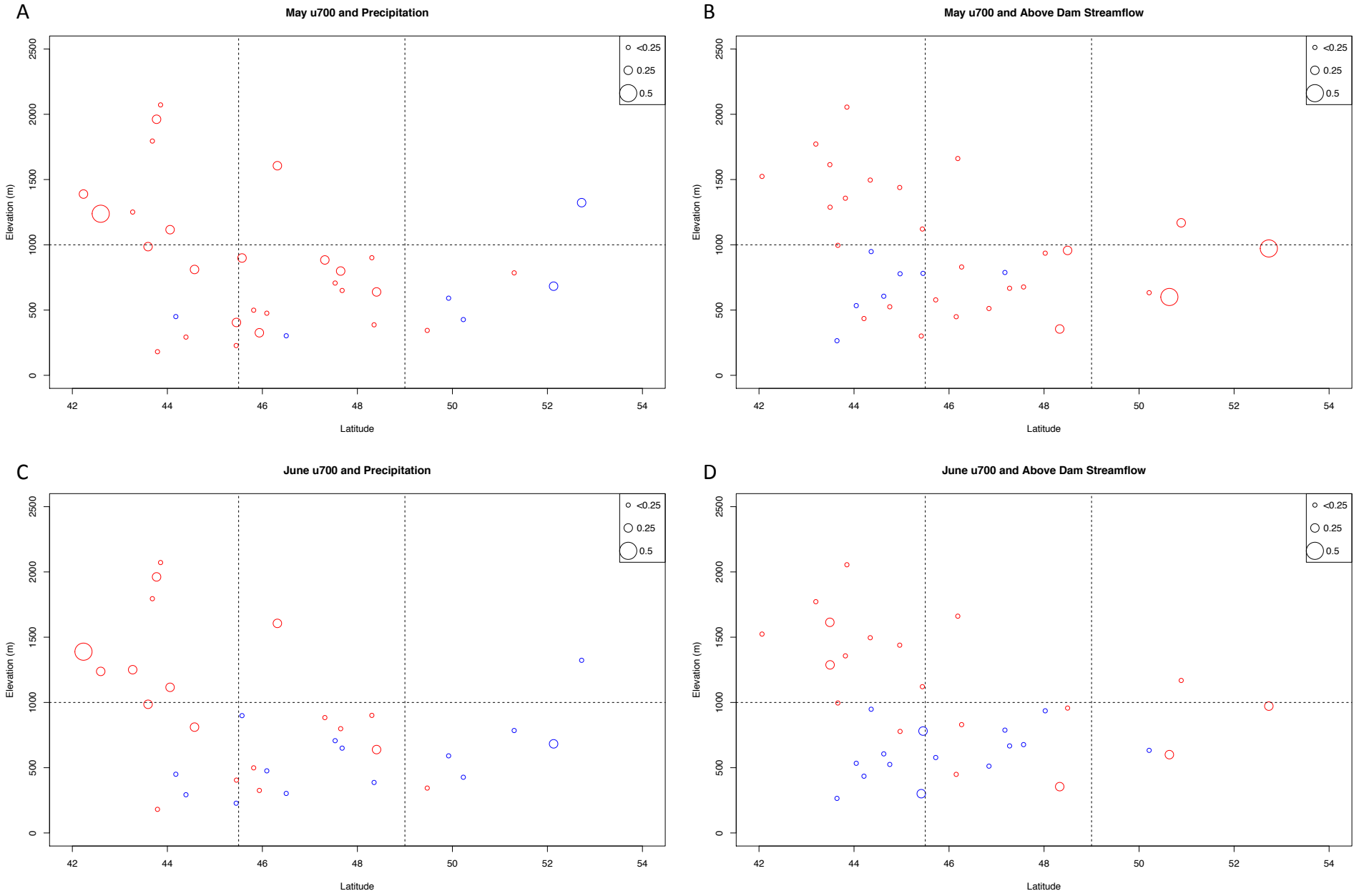

Figure 4.3. May and June monthly correlations between precipitation and u700 winds (A,C) and streamflow and u700 winds (B,D). Positive correlations are shown by blue circles whereas negative correlations are shown by red.

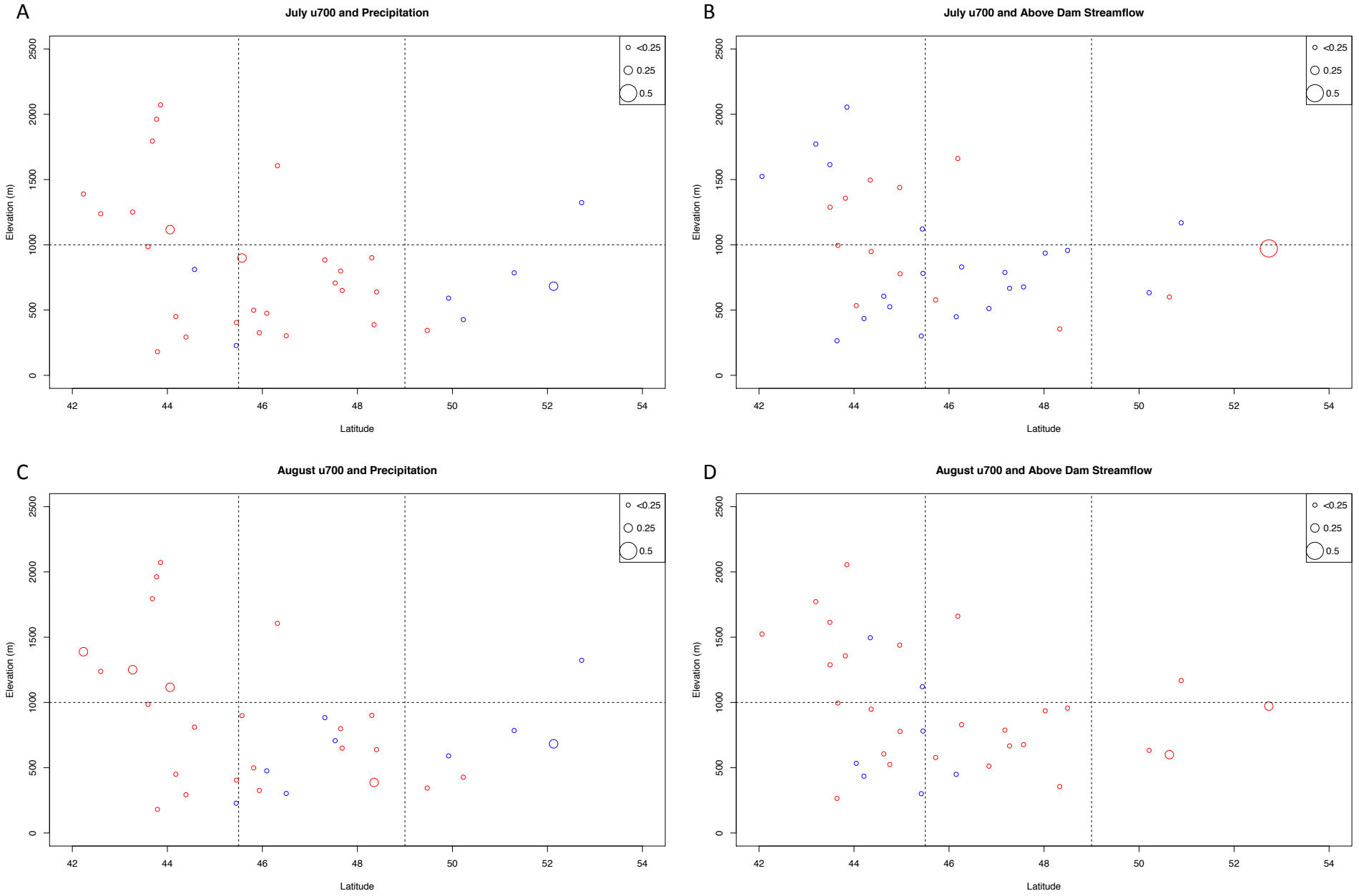

Figure 4.4. July and August monthly correlations between precipitation and u700 winds (A,C) and streamflow and u700 winds (B,D). Positive correlations are shown by blue circles whereas negative correlations are shown by red.

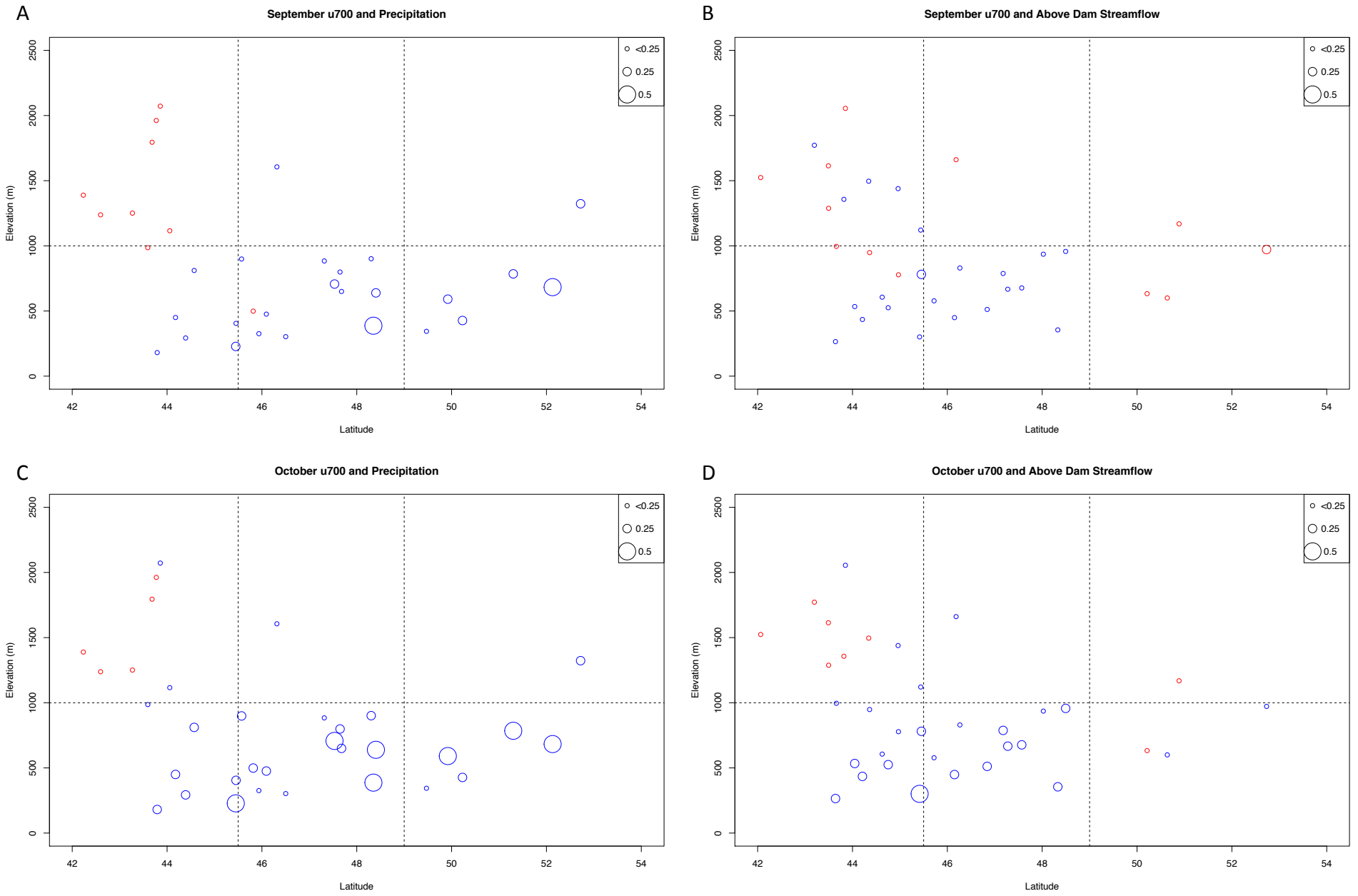

Figure 4.5. September and October monthly correlations between precipitation and u700 winds (A,C) and streamflow and u700 winds (B,D). Positiv correlations are shown by blue circles whereas negative correlations are shown by red.

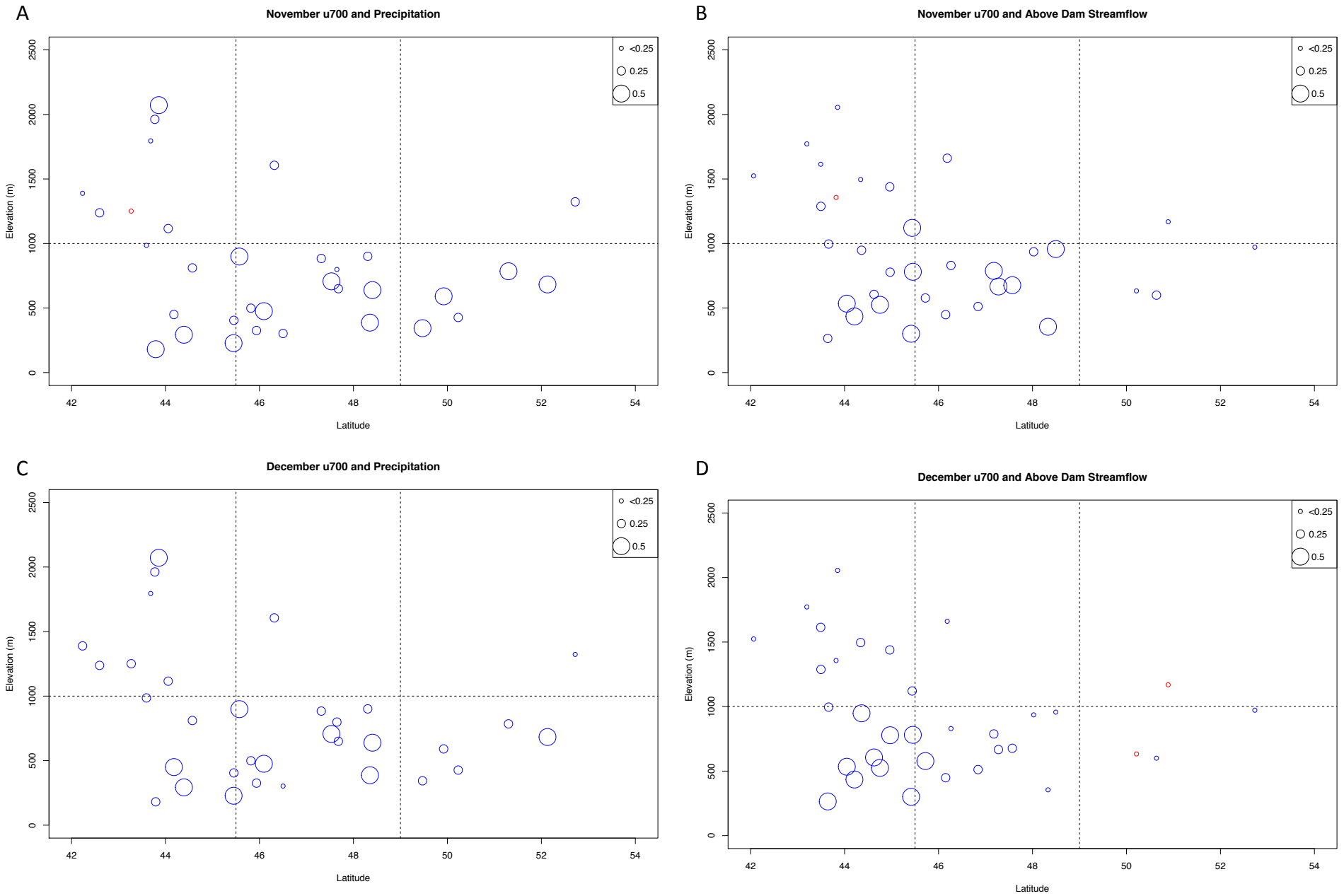

Figure 4.6. November and December monthly correlations between precipitation and u700 winds (A,C) and streamflow and u700 winds (B,D). Positive correlations are shown by blue circles whereas negative correlations are shown by red.

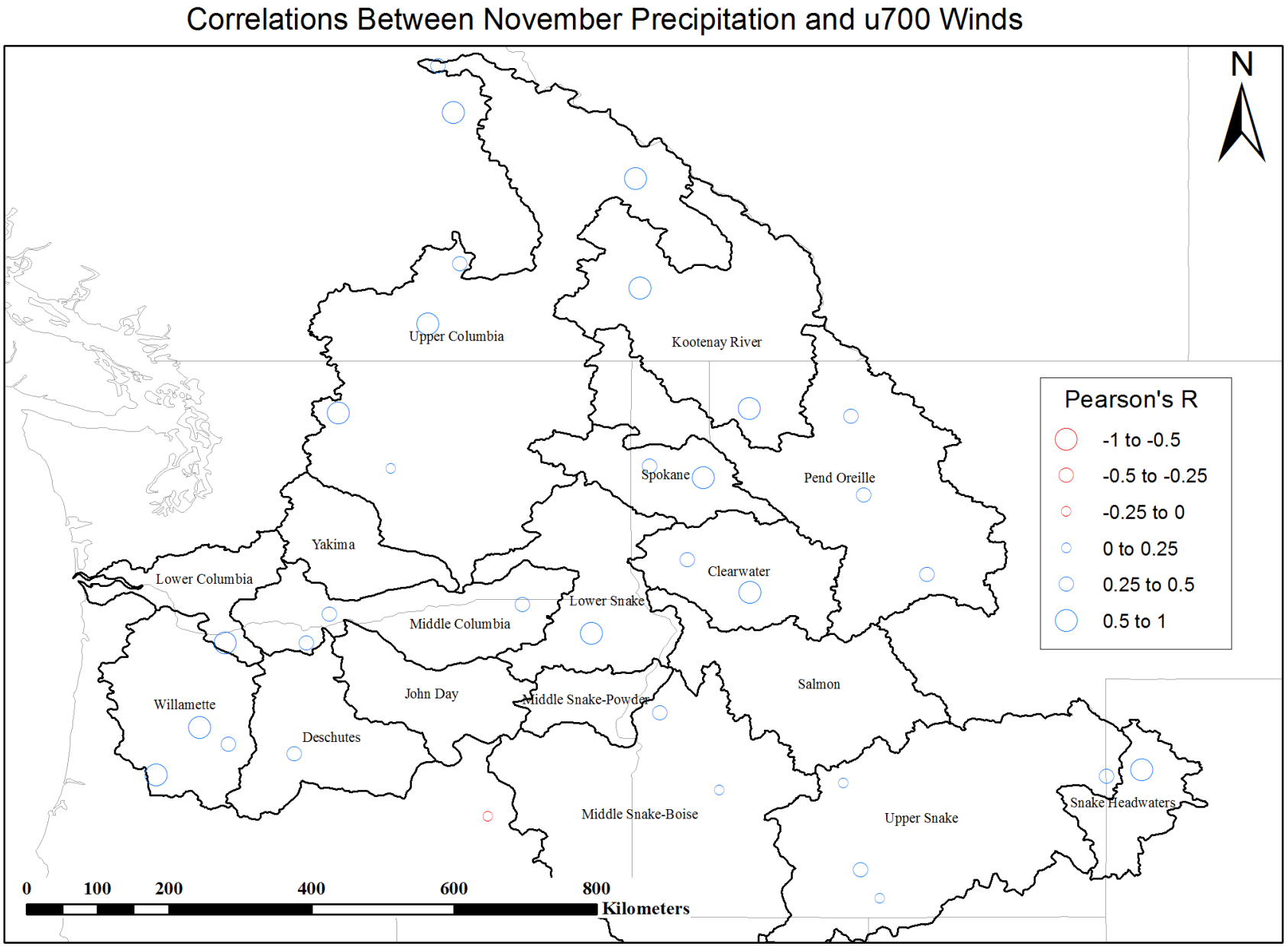

Figure 4.7. November monthly correlations between precipitation and u700 winds. Positive correlations are shown by blue circles whereas negative correlations are shown by red.

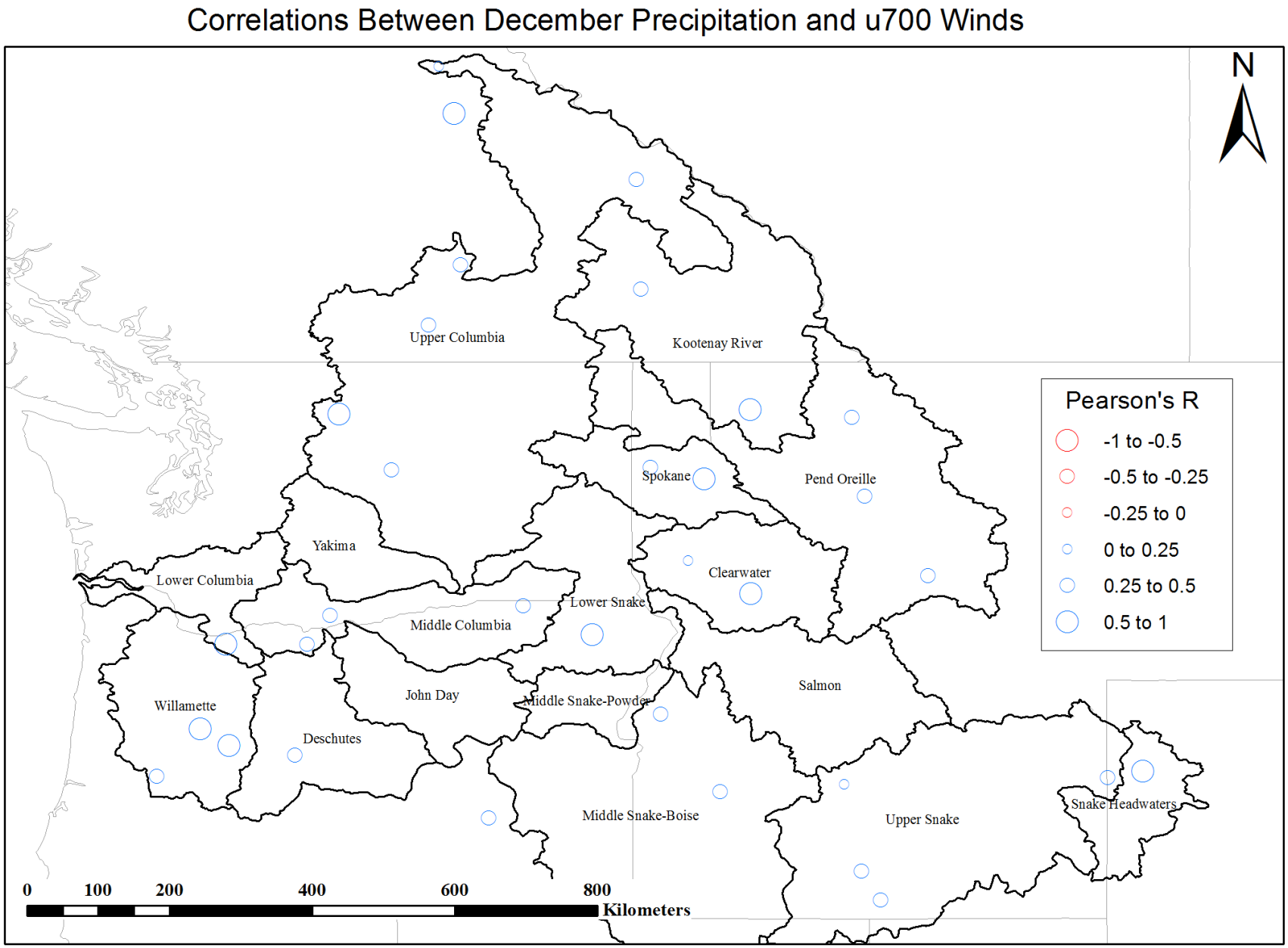

Figure 4.8. December monthly correlations between precipitation and u700 winds. Positive correlations are shown by blue circles whereas negative correlations are shown by red.

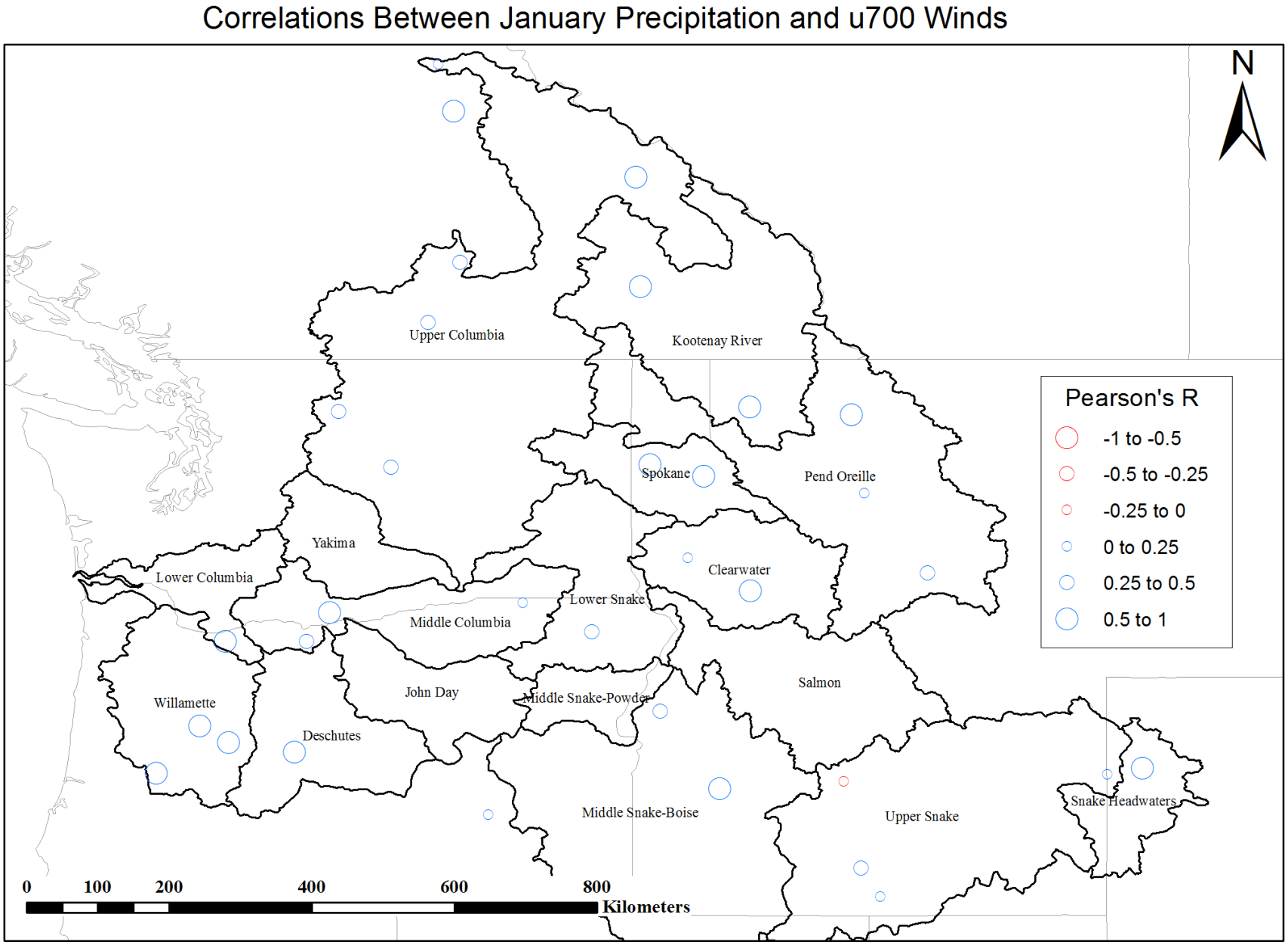

Figure 4.9. January monthly correlations between precipitation and u700 winds. Positive correlations are shown by blue circles whereas negative correlations are shown by red.

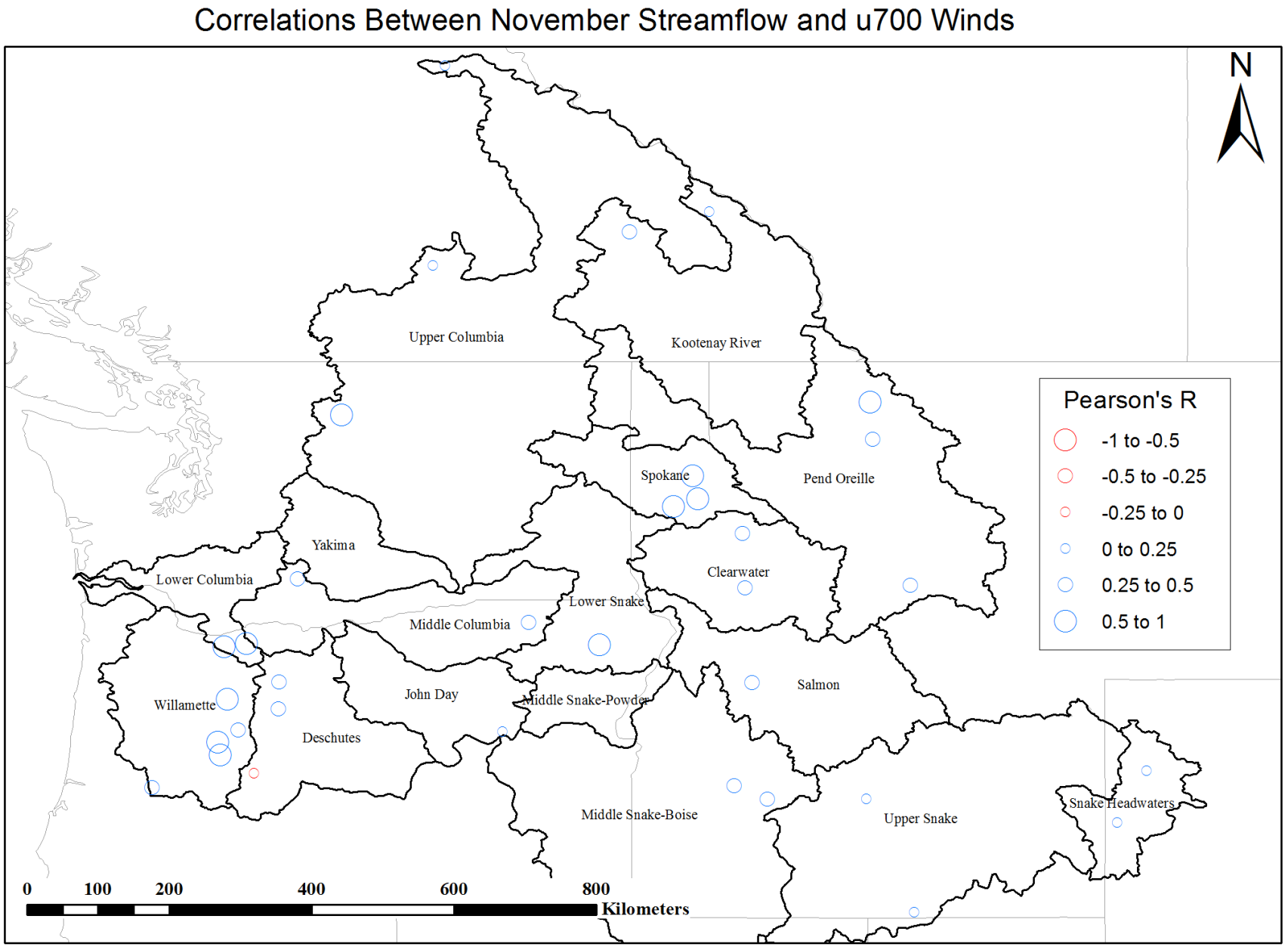

Figure 4.10. November monthly correlations between above-dam streamflow and u700 winds. Positive correlations are shown by blue circles whereas negative correlations are shown by red.

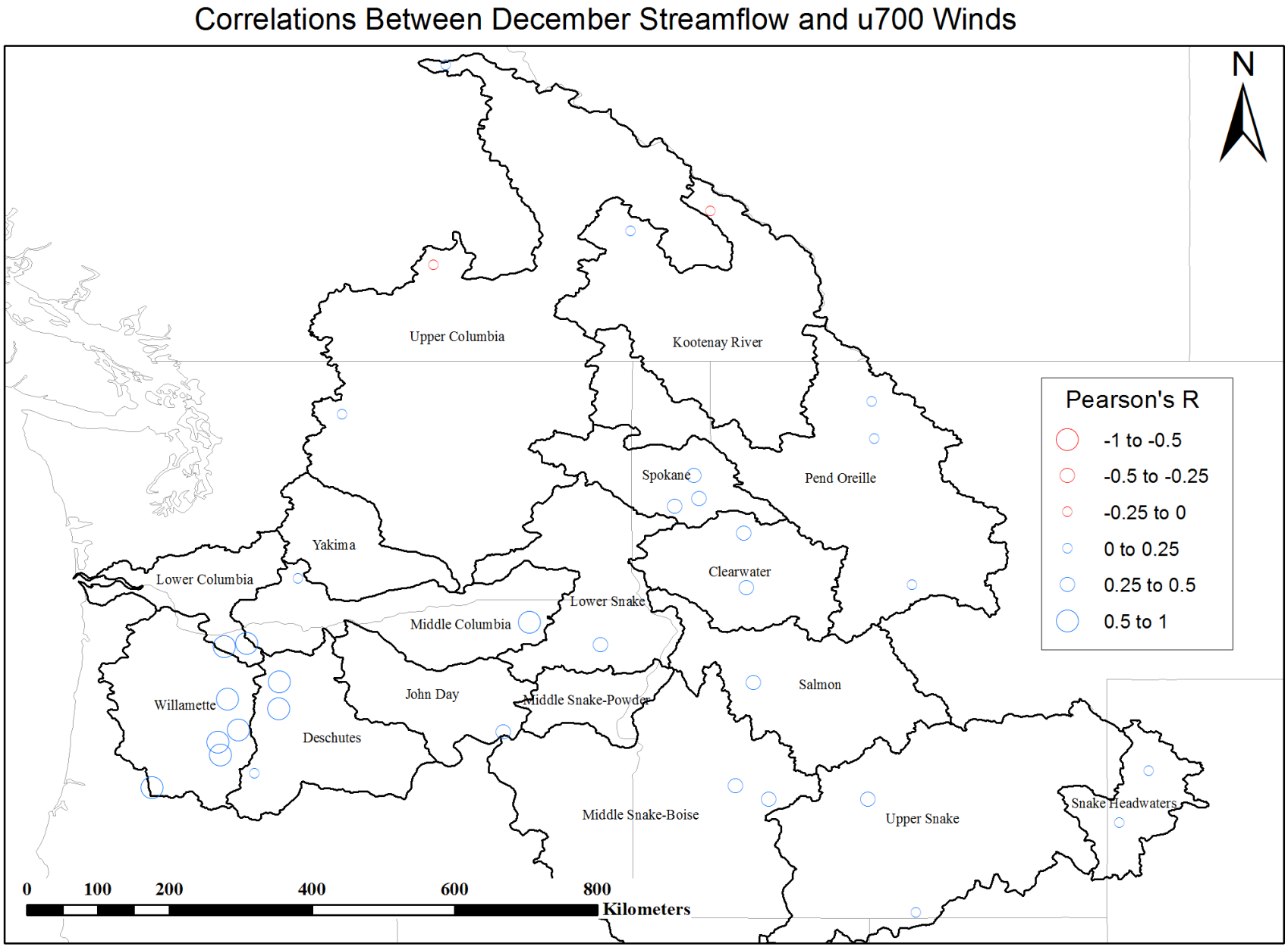

Figure 4.11. December monthly correlations between above-dam streamflow and u700 winds. Positive correlations are shown by blue circles whereas negative correlations are shown by red.

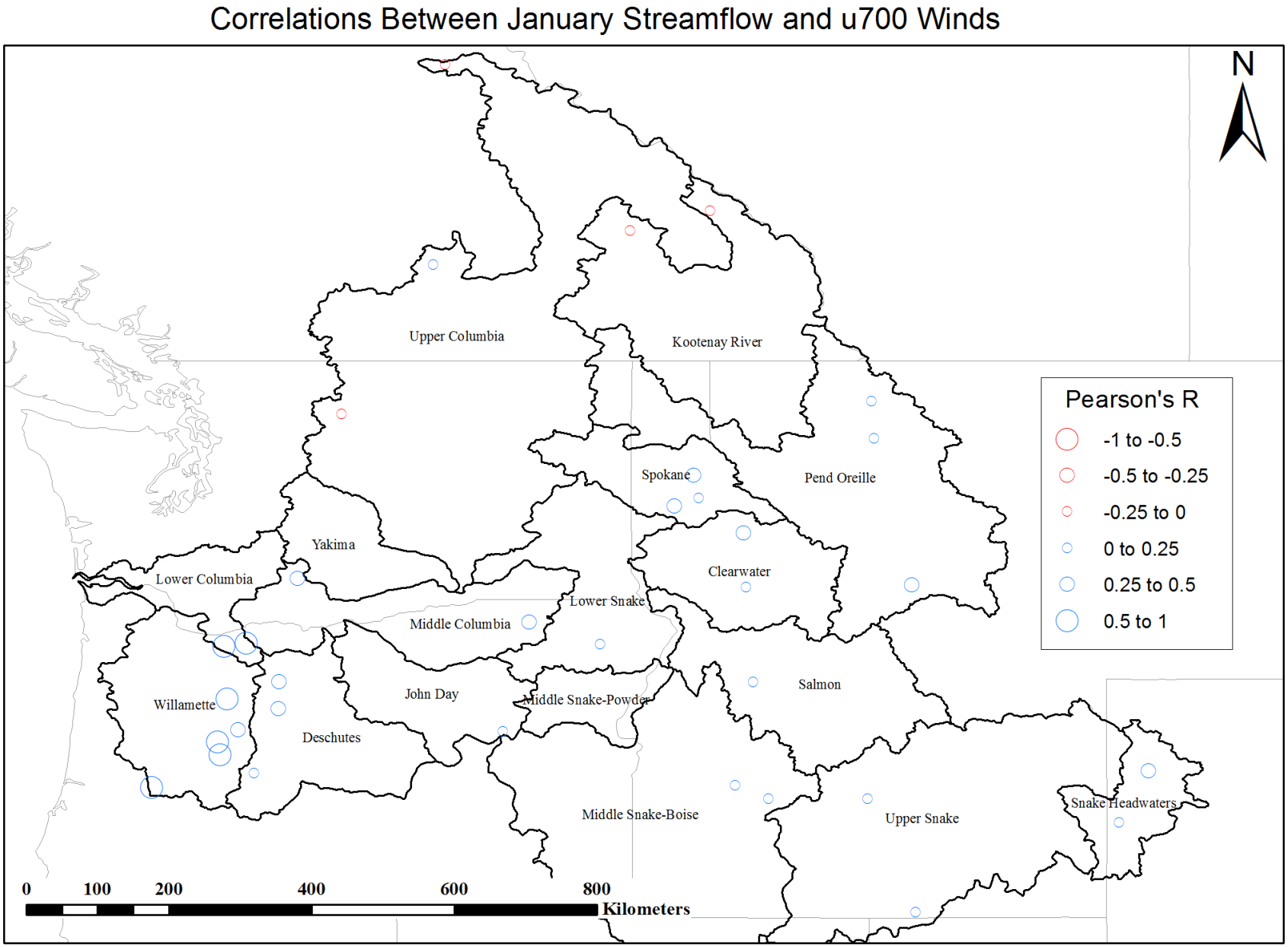

Figure 4.12. January monthly correlations between above-dam streamflow and u700 winds. Positive correlations are shown by blue circles whereas negative correlations are shown by red.

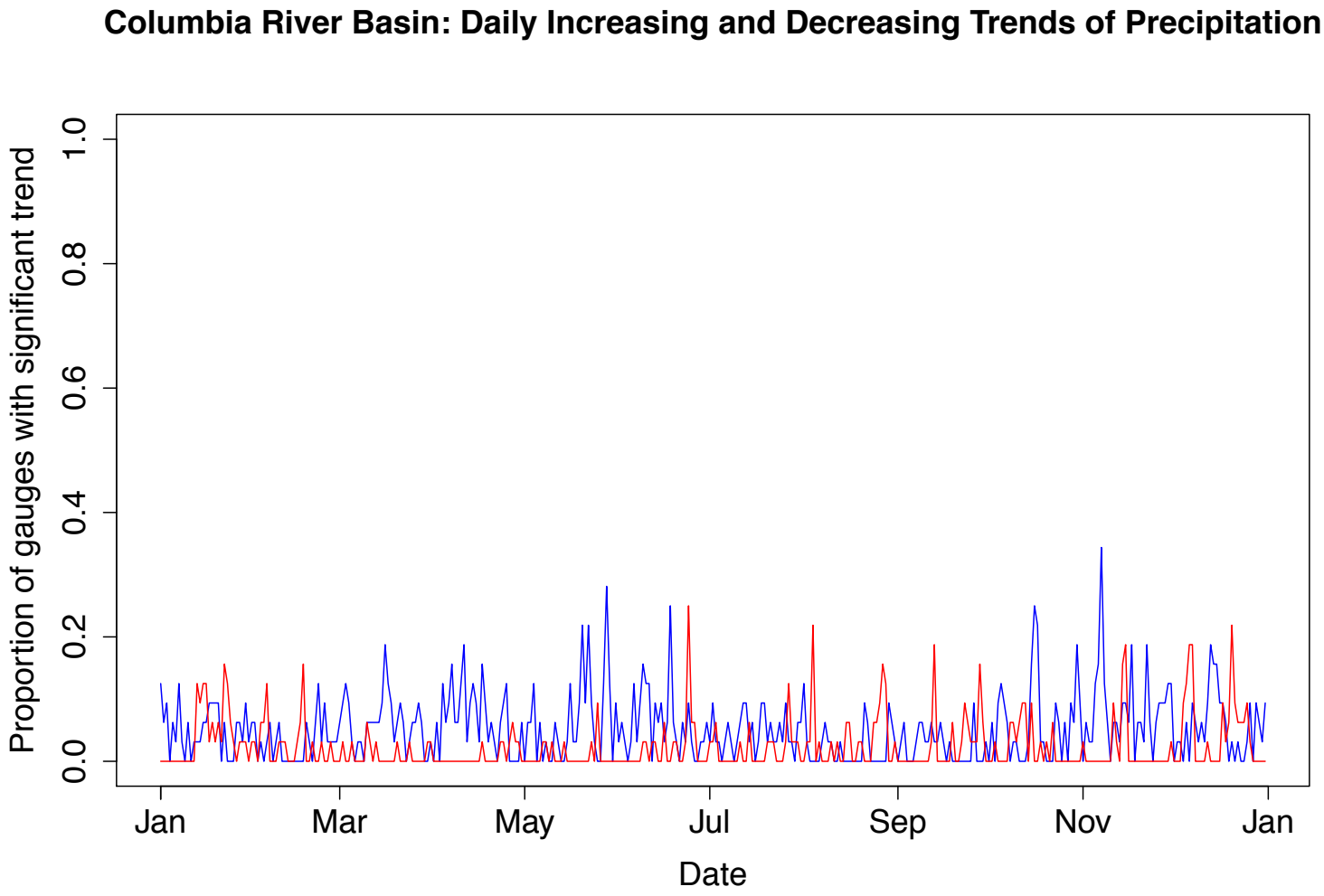

Figure 4.13. The proportion of climate stations (n=33) across the CRB showing significant increases (blue) or decreases (red) in daily precipitation.

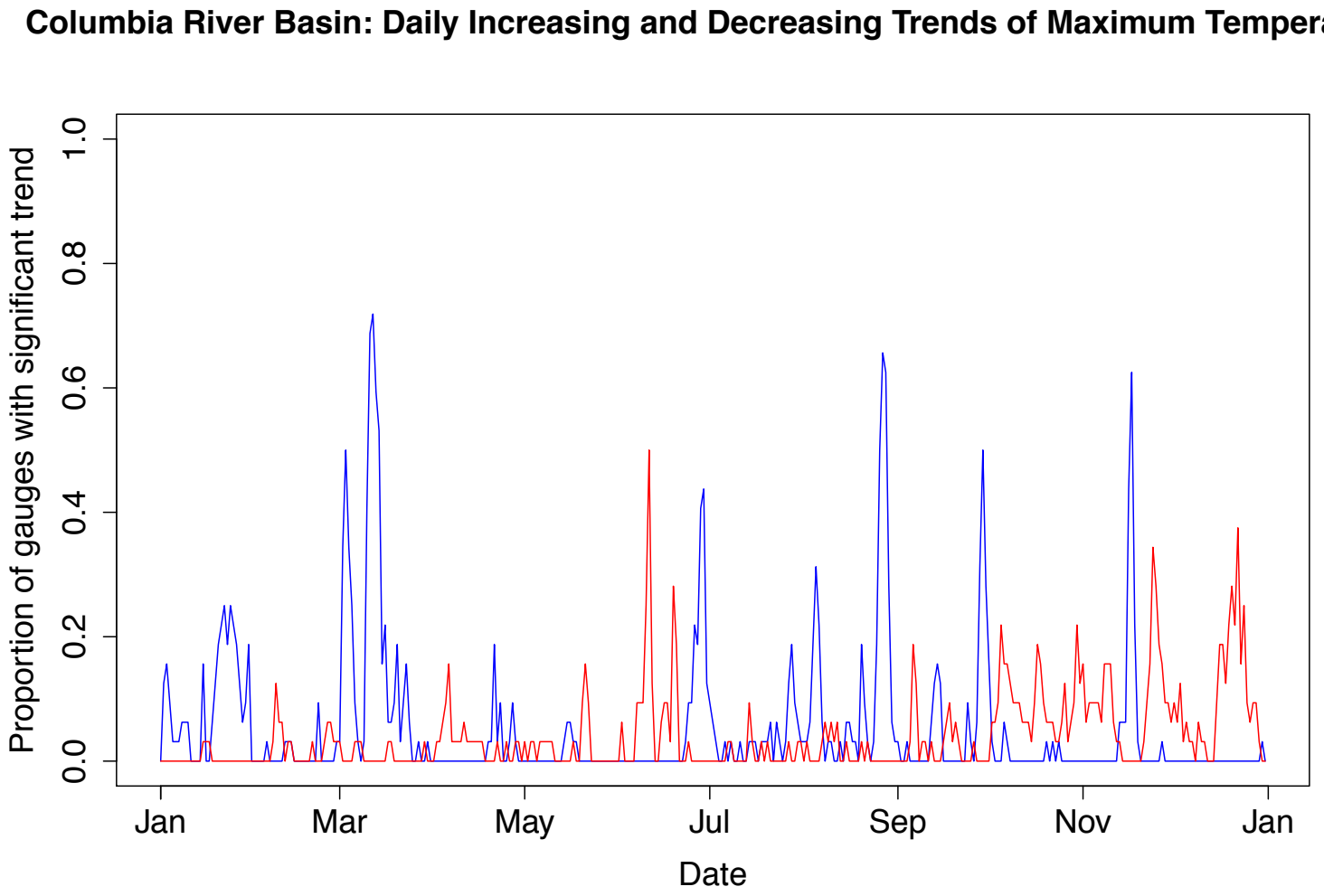

Figure 4.14. The proportion of climate stations (n=33) across the CRB showing significant increases (blue) or decreases (red) in daily maximum air temperature.

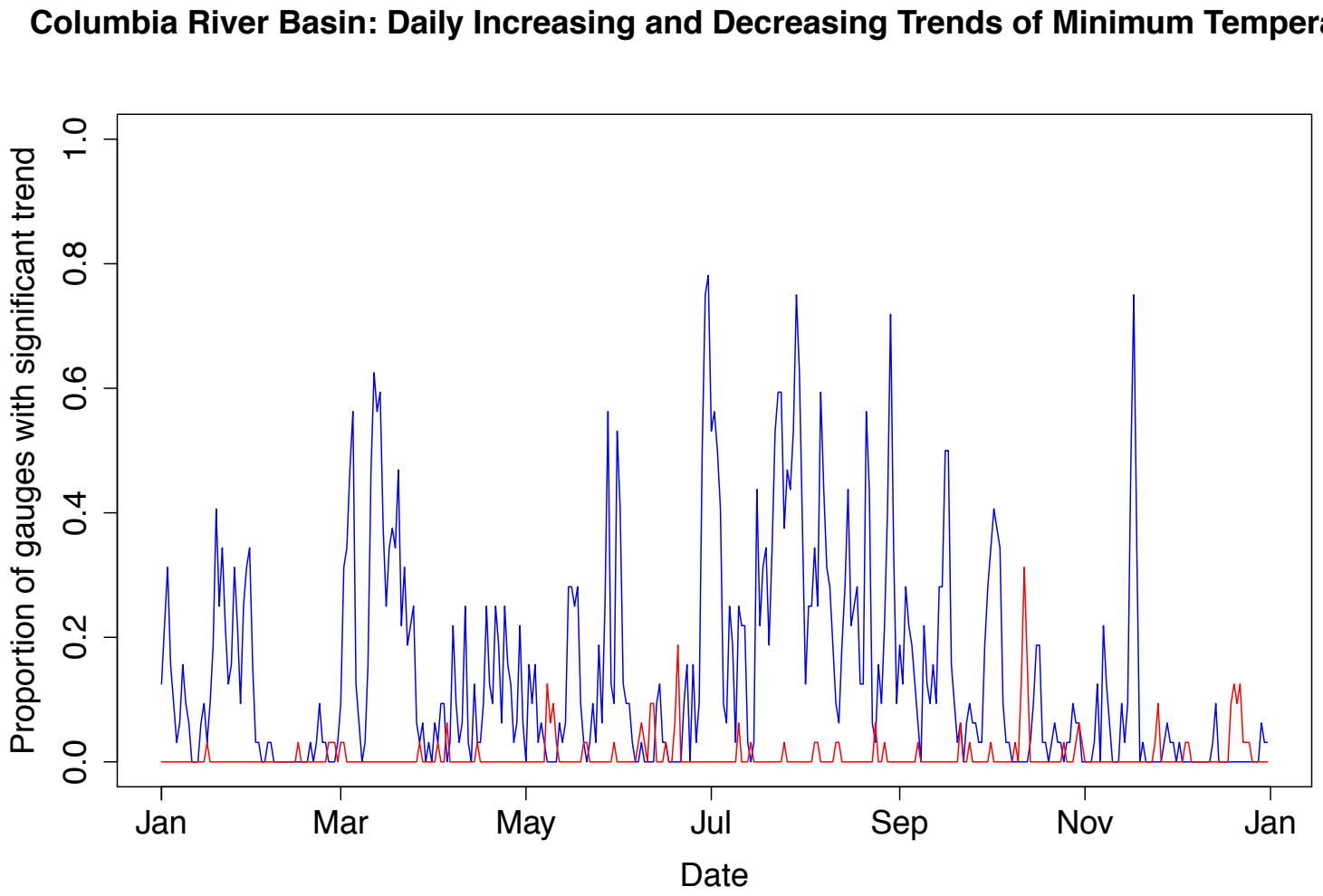

Figure 4.15. The proportion of climate stations (n=33) across the CRB showing significant increases (blue) or decreases (red) in daily minimum air temperature.

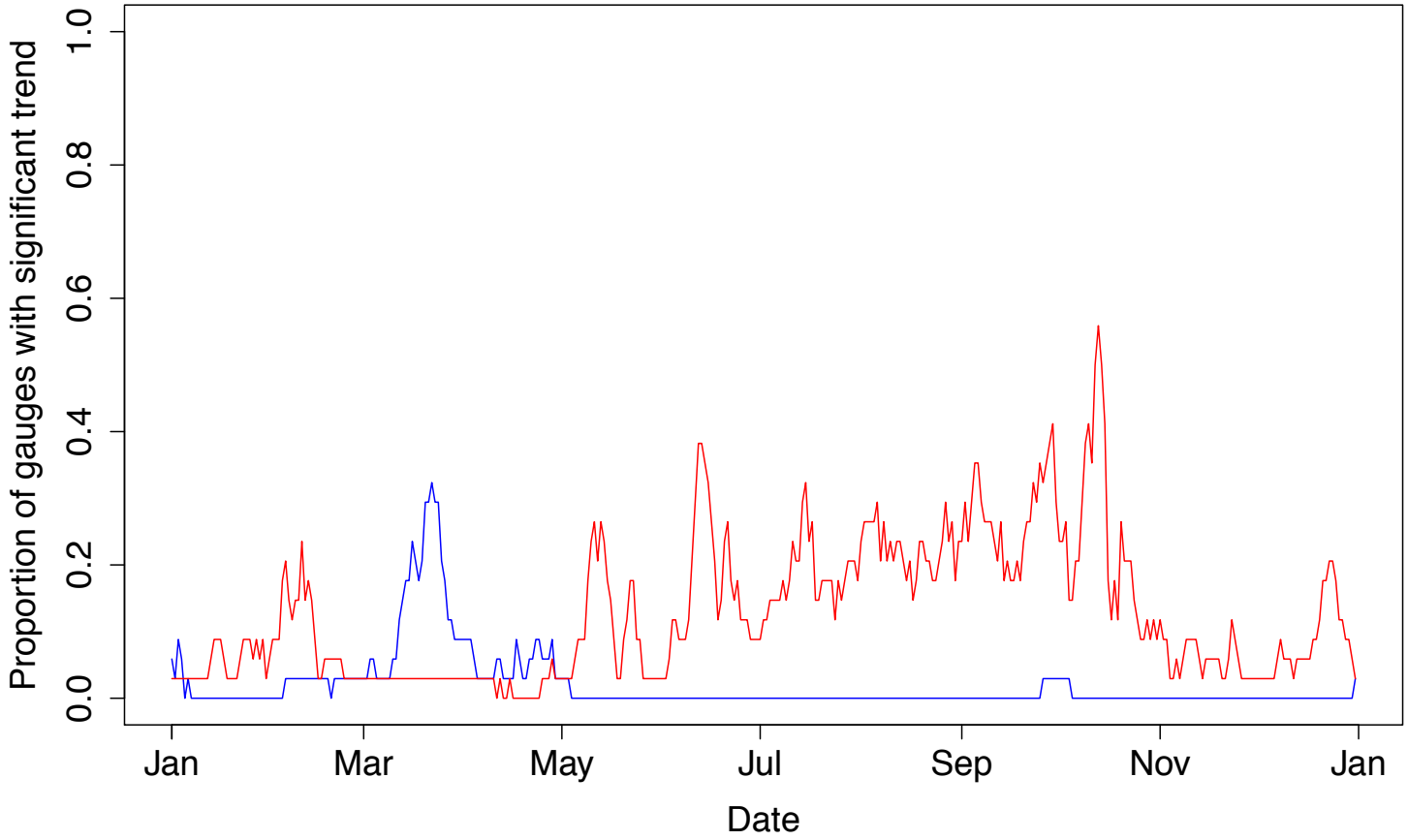

Figure 4.16. Proportion of gages (n=34) showing significant increasing (blue) and decreasing (red) trends in daily streamflow above dams.

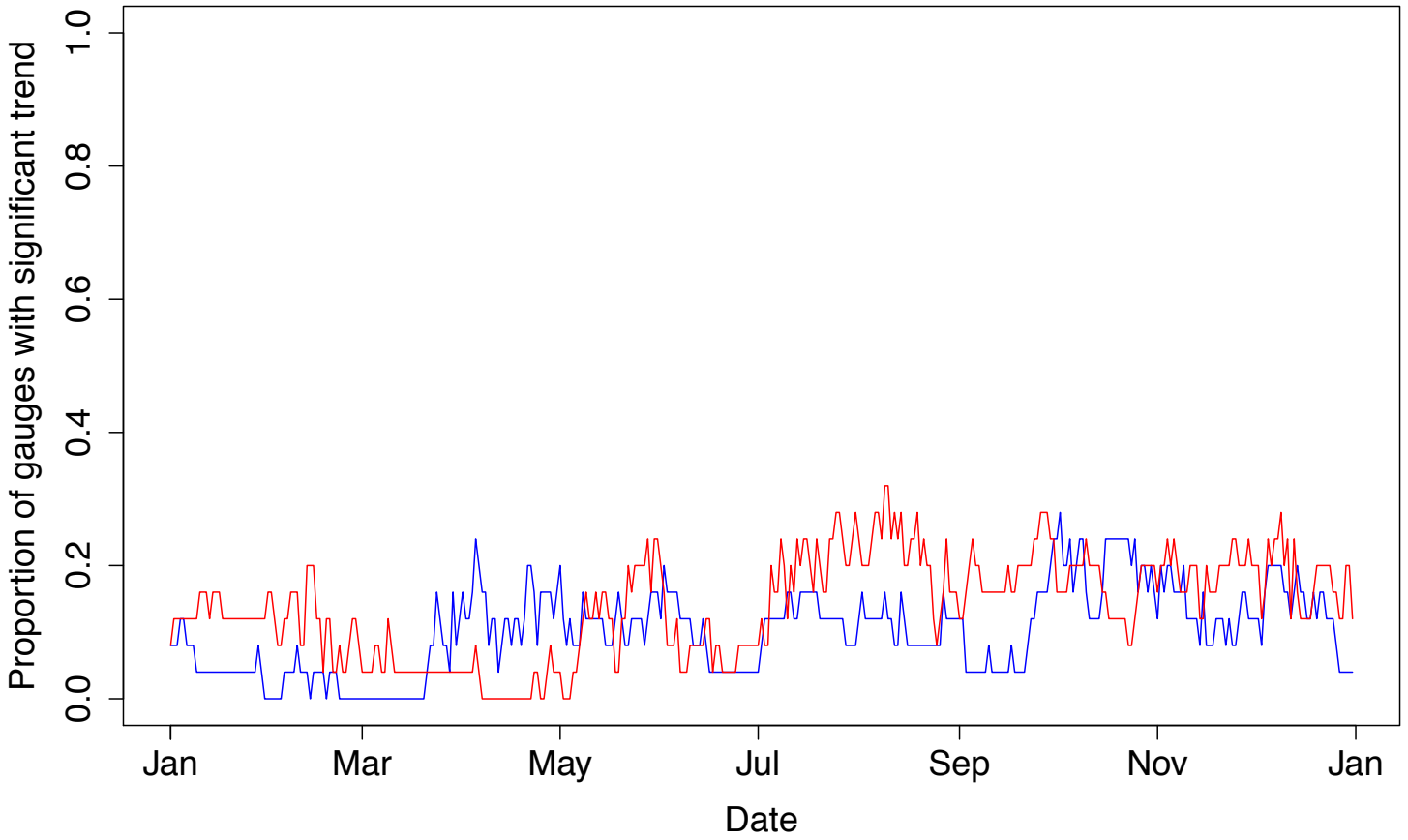

Figure 4.17. Proportion of gages (n=25) showing significant increasing (blue) and decreasing (red) trends in daily streamflow below dams.

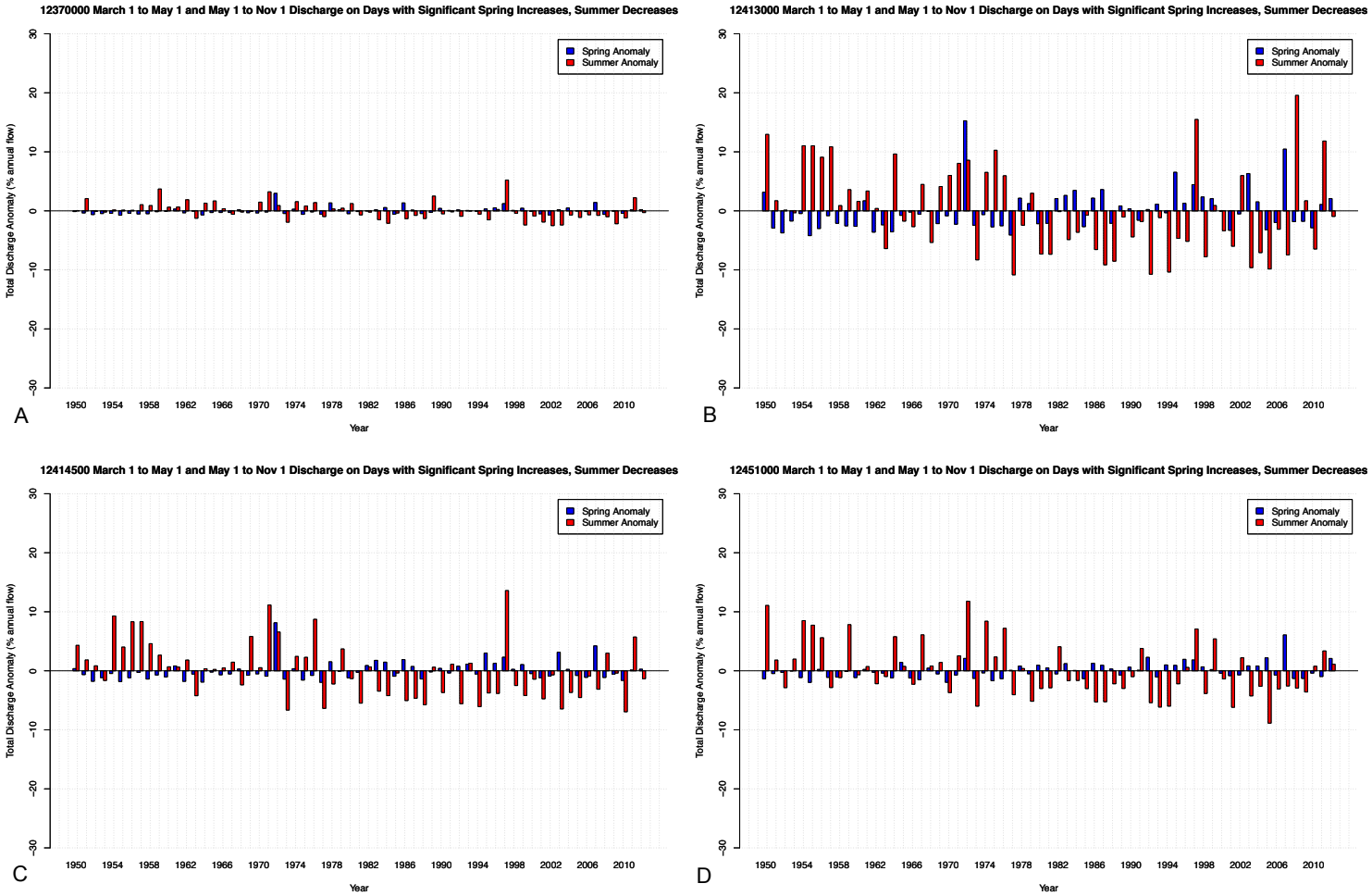

Figure 4.18. Sum of above-dam anomalous daily flows over the period from March 1 to May 1 (spring) and May 1 to November 1 (summer) expressed as percent of annual flow. Remaining figures for above-dam changes can be found in Appendix F. A= Swan R., MT, B= Coeur D'Alene R., ID, C= St. Joe R., ID, D= Stehekin R., WA.

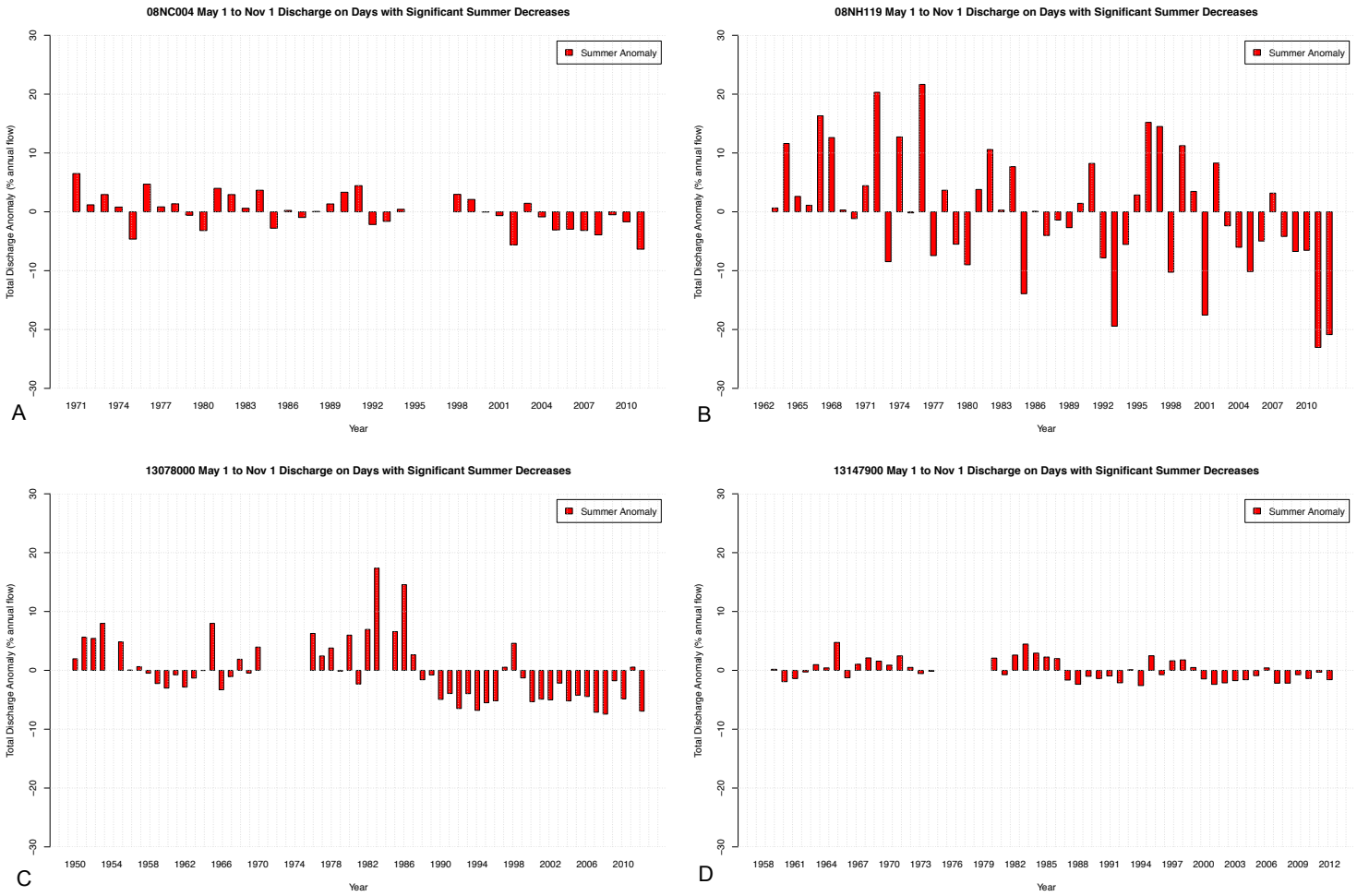

Figure 4.19. Sum of above-dam anomalous daily flows over the period May 1 to November 1 (summer) expressed as percent of annual flow. Remaining figures for above-dam changes can be found in Appendix F. Remaining figures for below-dam changes can be found in Appendix F. A= Canoe R., BC, B= Duncan R., BC, C= Raft R., ID, D= Little Wood R., ID.

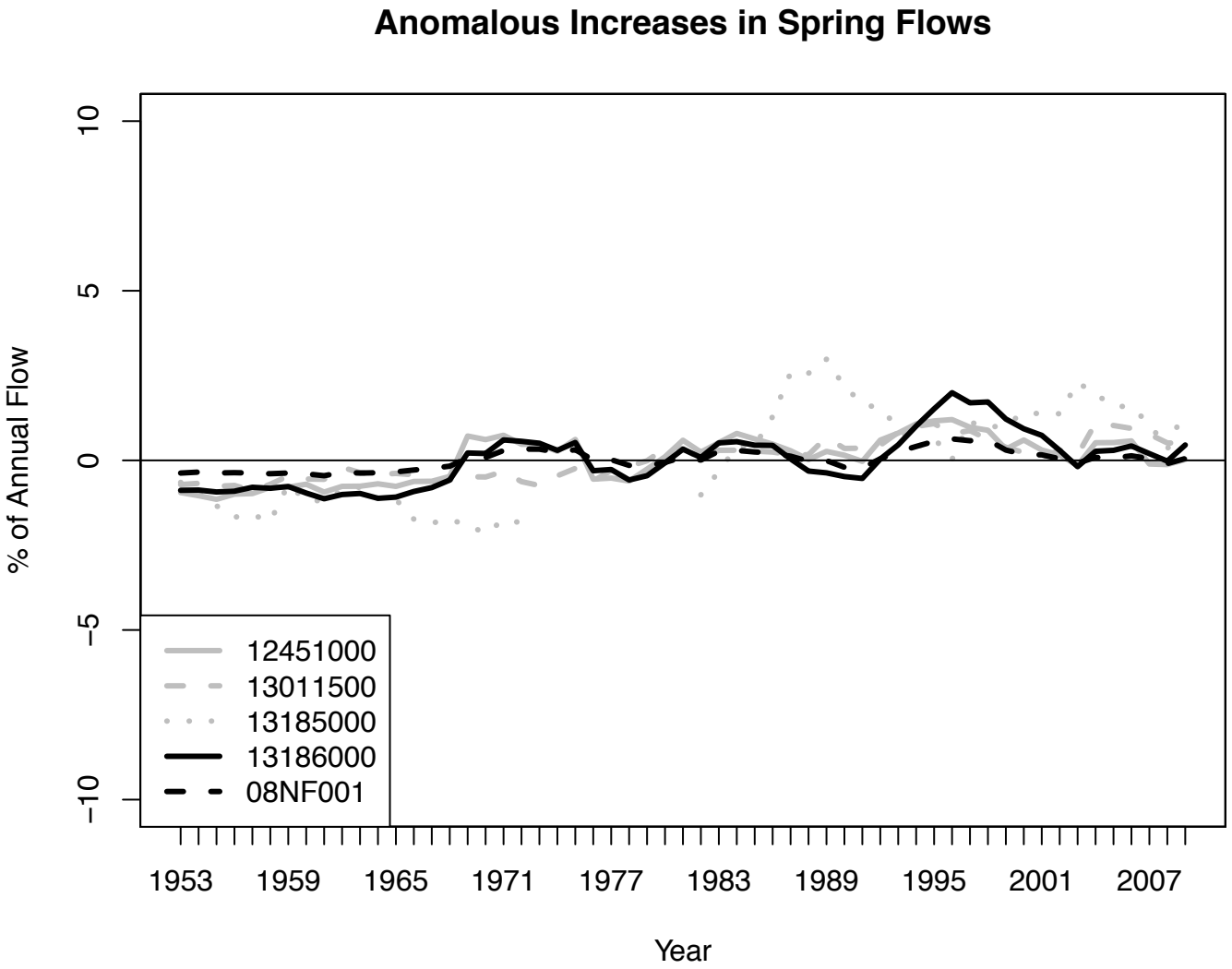

Figure 4.20. Smoothed anomalies of streamflow on days from March 1 to May 1 that had significant trends in flow over the period 1950-2012, as a percent of annual streamflow above dams shown in figure 4.18.

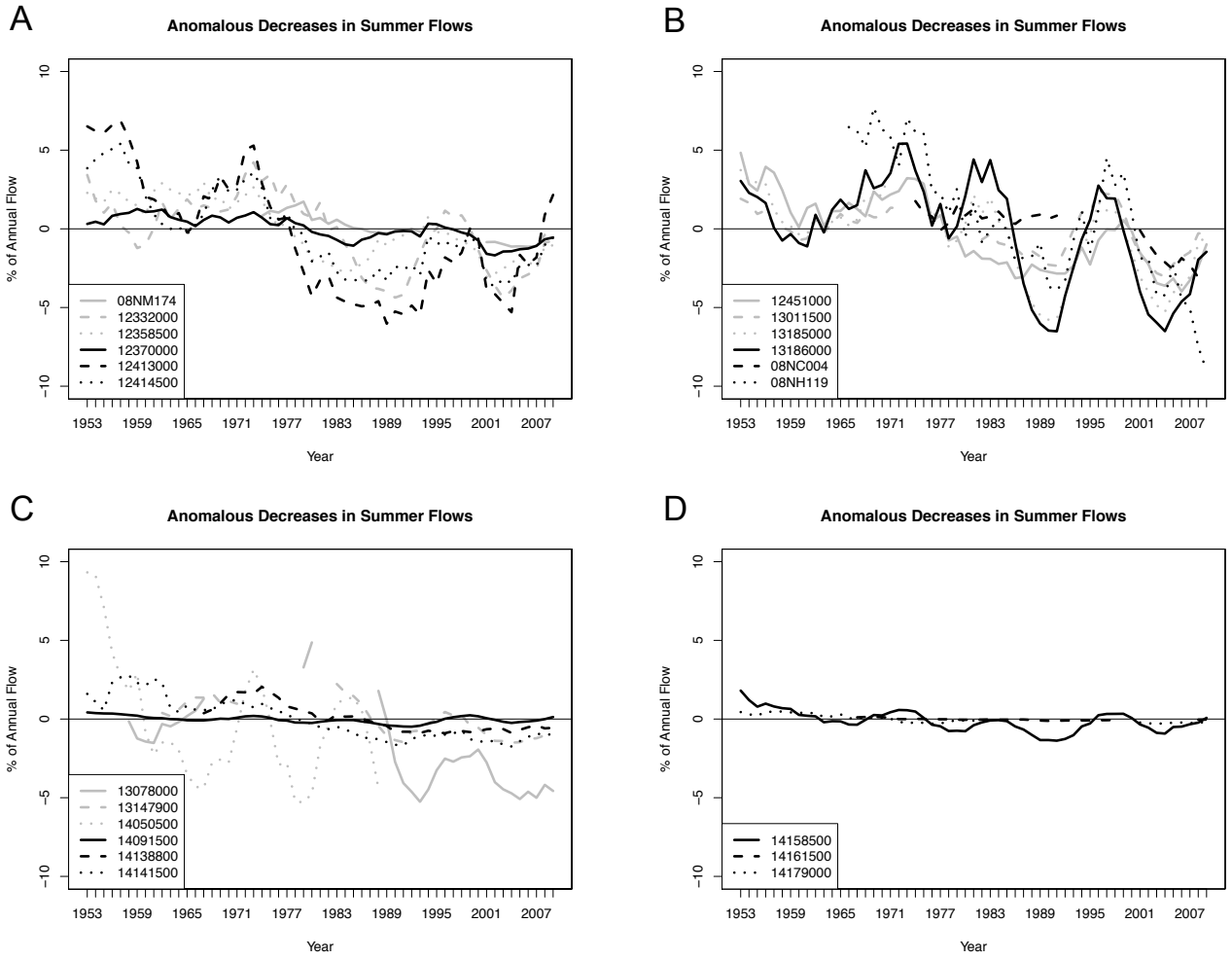

Figure 4.21. Smoothed anomalies of streamflow on days from May 1 to November 1 that had significant trends in flow over the period 1950-2012, as a percent of annual streamflow above dams shown in figures 4.18 and 4.19. Lines show the annual sum of flow on days with significant increasing flow, for the following gages: 12451000, 13011500, 13185000, 13186000, 08NF001.

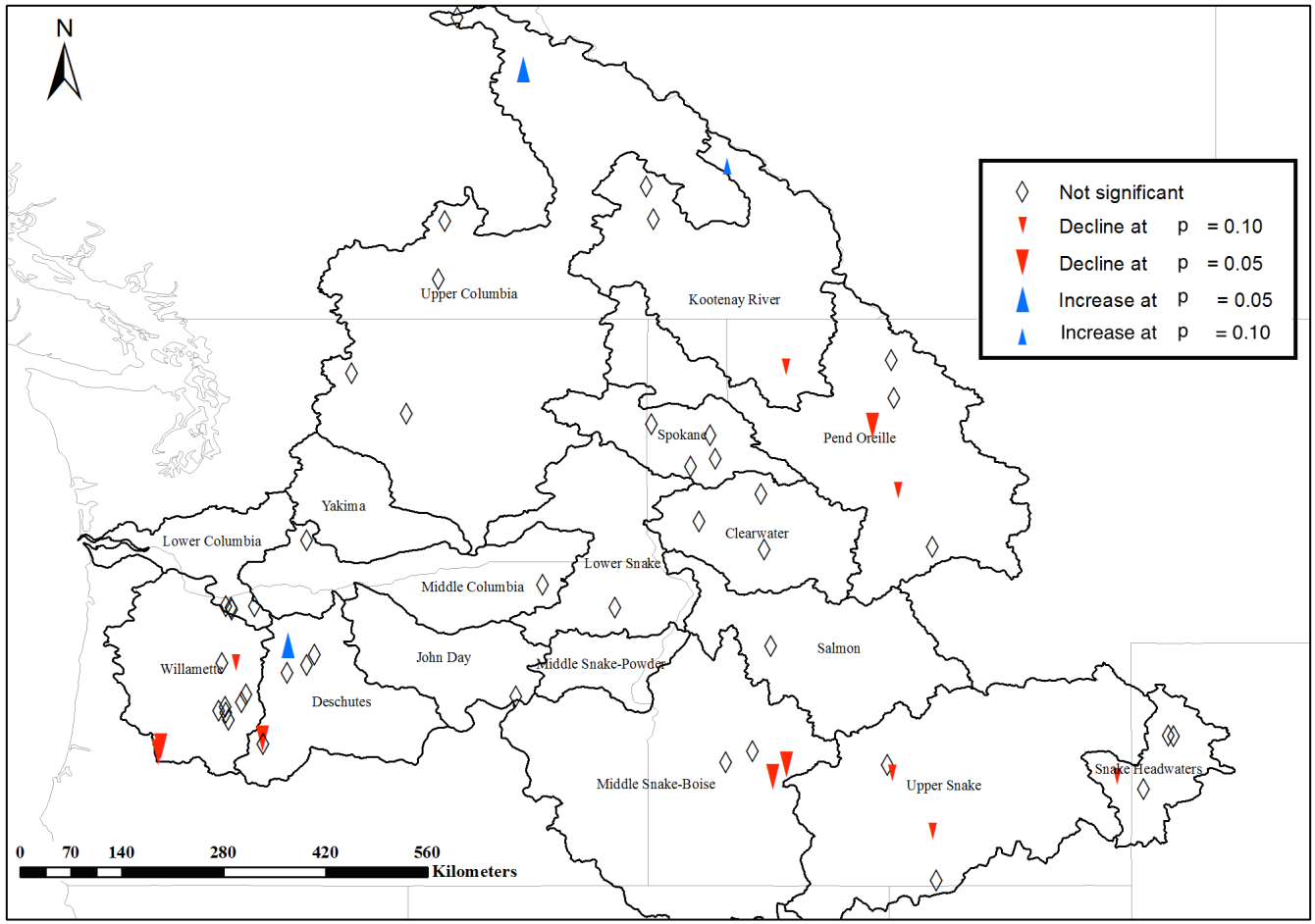

Figure 4.22. Result of a Mann-Kendall testing for the significance of a trend in annual flow volume above and below dams using thresholds of p <= 0.05 and 0.10. Lines show the annual sum of flow on days with significant declining flow, for the following gages: A) 08NM174, 12332000, 12358500, 12370000, 12413000, 12414500, B) 12451000, 13011500, 13185000, 13186000, 08NC004, 08NH119, C) 13078000, 13147900, 14050500, 14091500, 14138800, 14141500, D) 14158500, 14161500, 14179000.

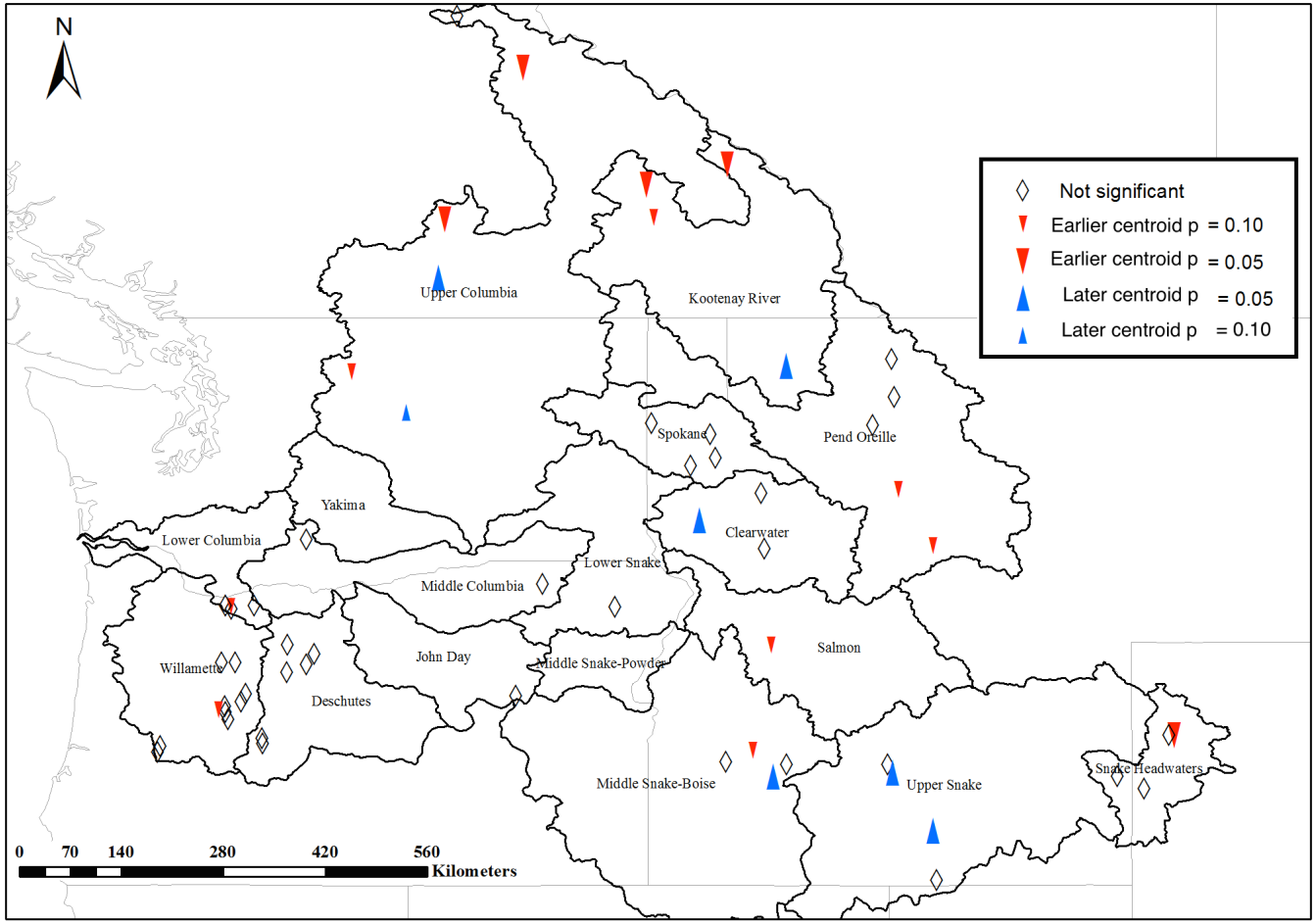

Figure 4.23. Result of a Mann-Kendall testing for the significance of a trend in centroid timing above and below dams using thresholds of p <= 0.05 and 0.10. Centroid timing is defined as the the day of year on which 50% of water year flow occurred.

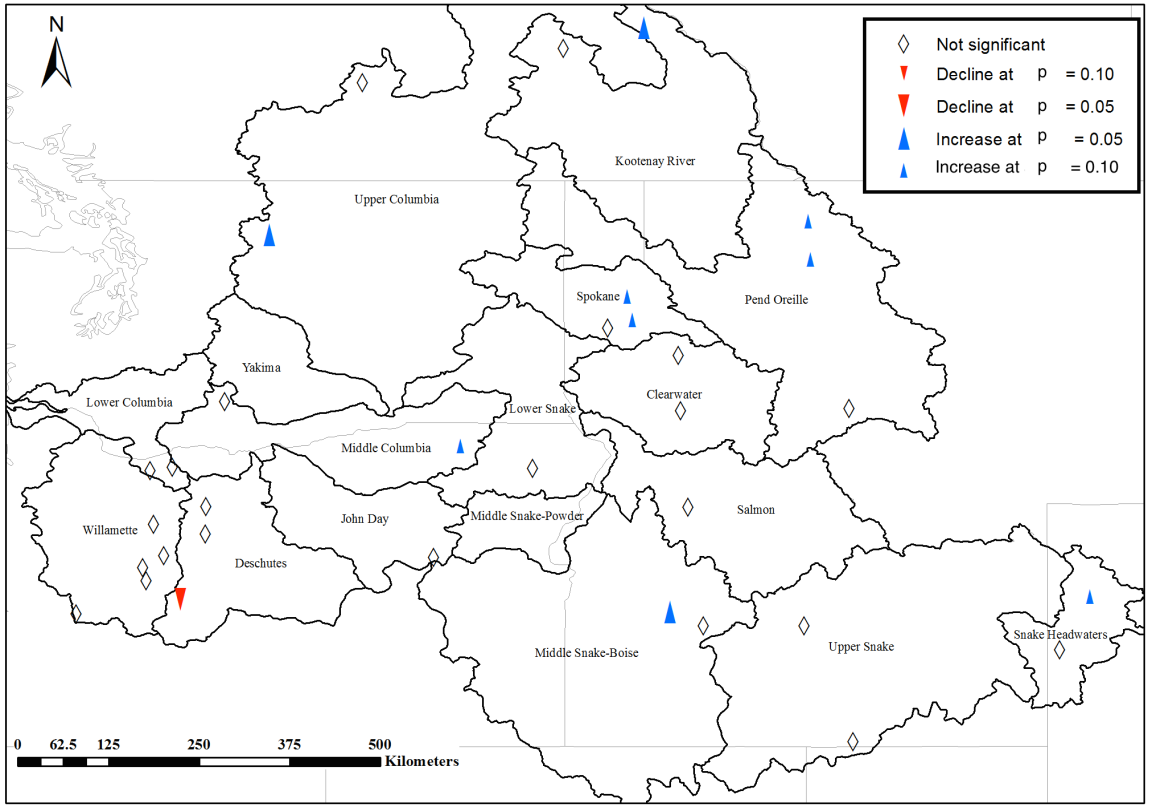

Figure 4.24. Result of a Mann-Kendall testing for the significance of a trend in March streamflow above dams using thresholds of p <= 0.05 and 0.10.

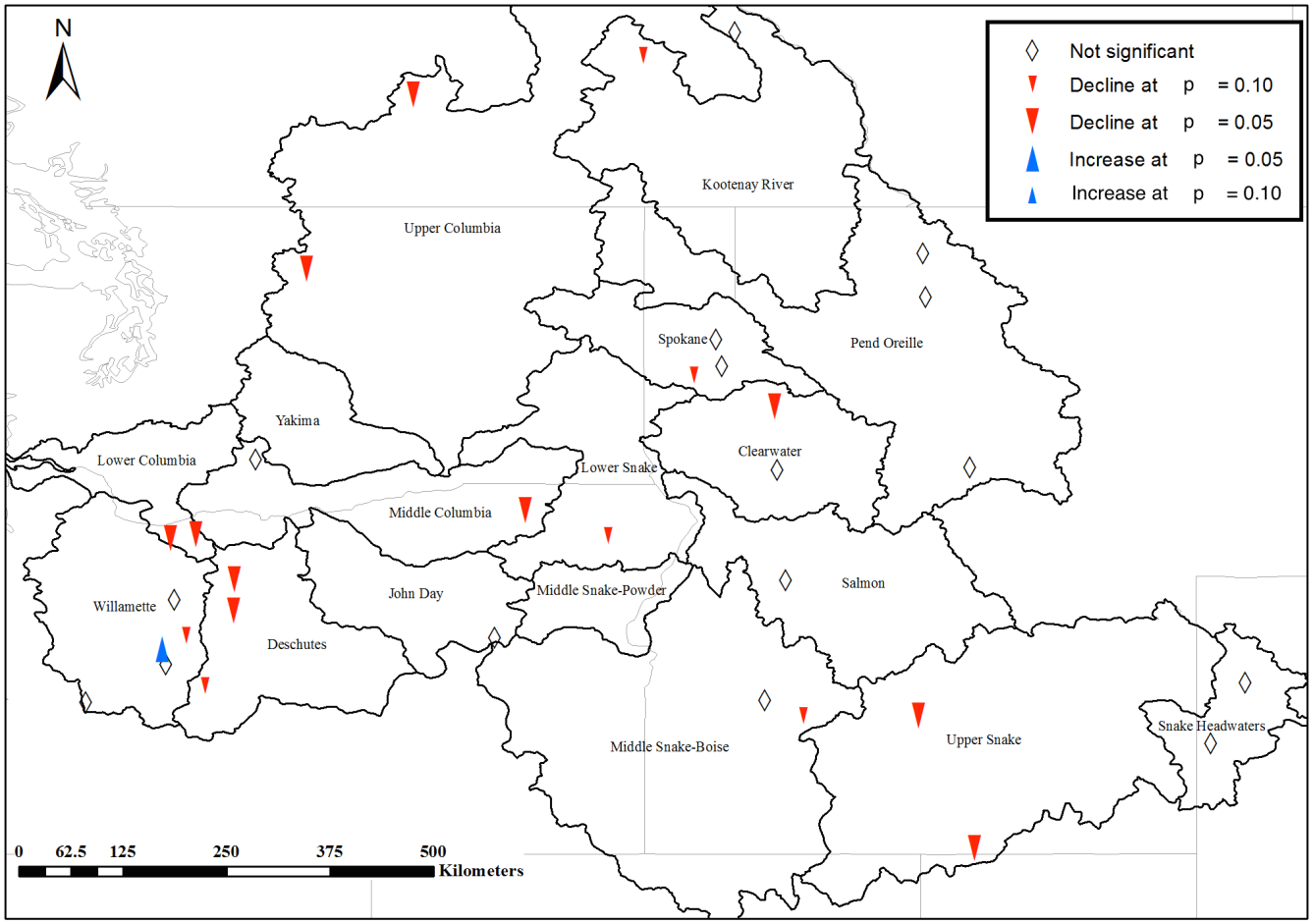

Figure 4.25. Result of a Mann-Kendall testing for the significance of a trend in September streamflow above dams using thresholds of p <= 0.05 and 0.10.

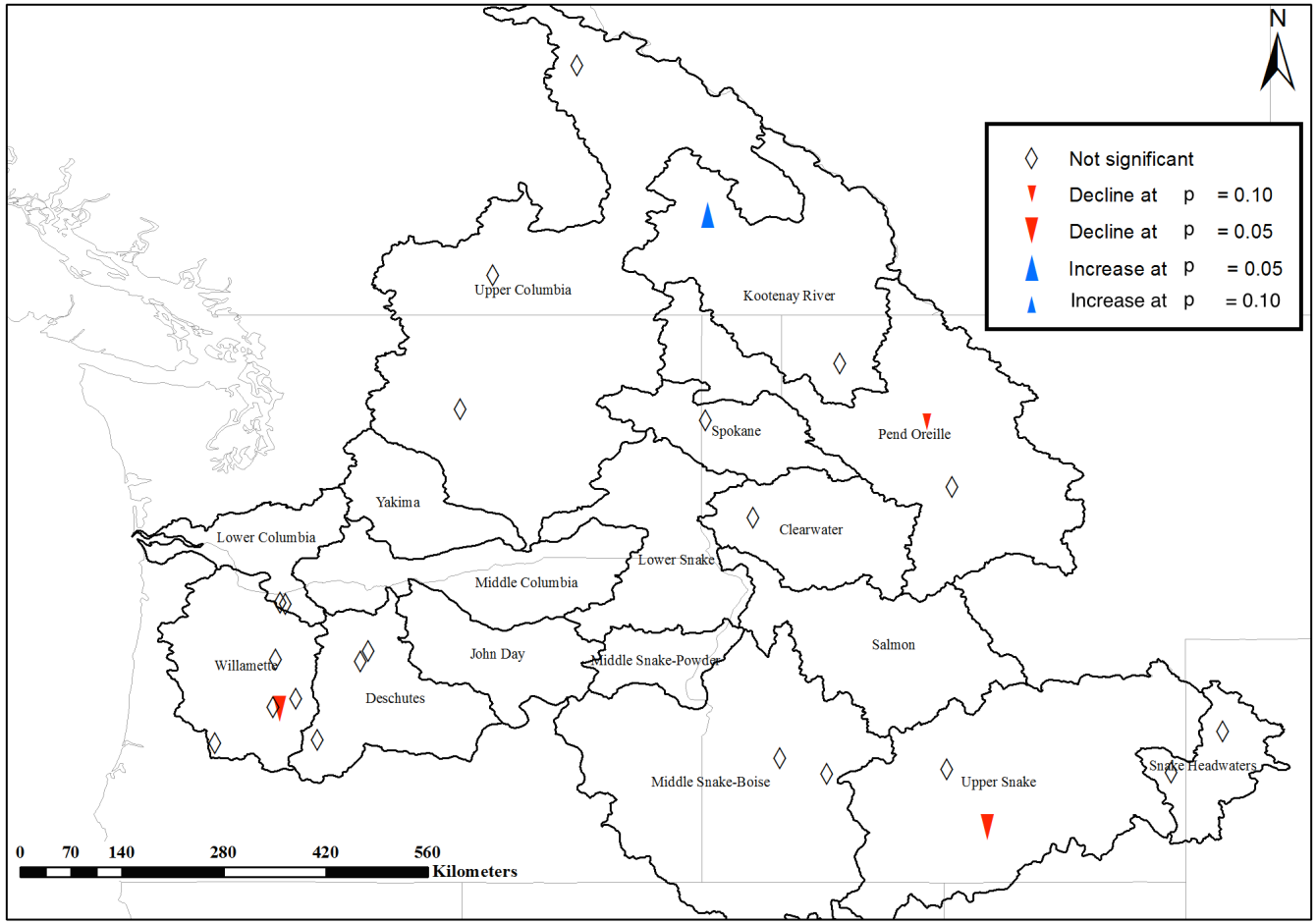

Figure 4.26. Result of a Mann-Kendall testing for the significance of a trend in March streamflow below dams using thresholds of p <= 0.05 and 0.10.

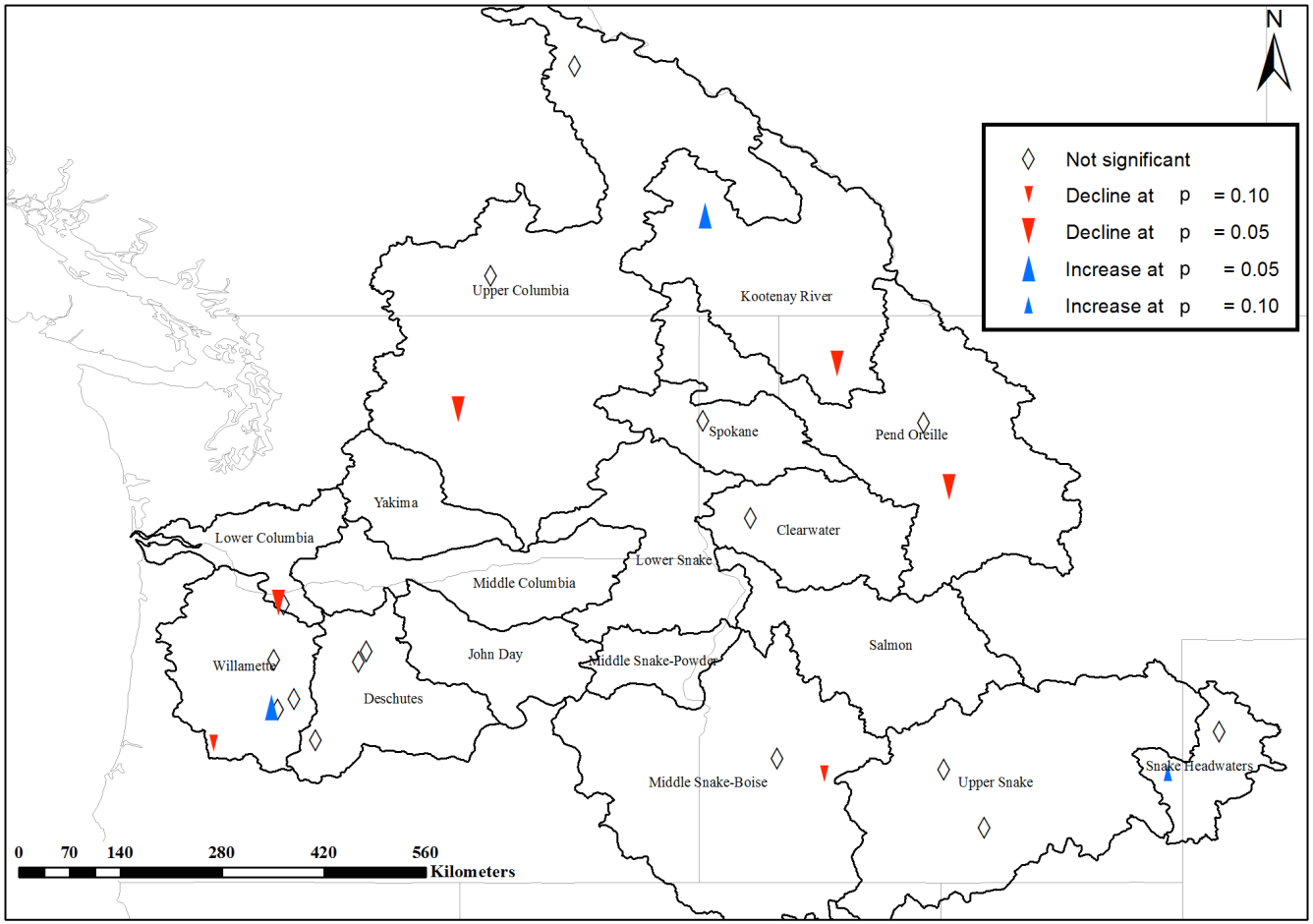

Figure 4.27. Result of a Mann-Kendall testing for the significance of a trend in September streamflow below dams using thresholds of p <= 0.05 and 0.10.

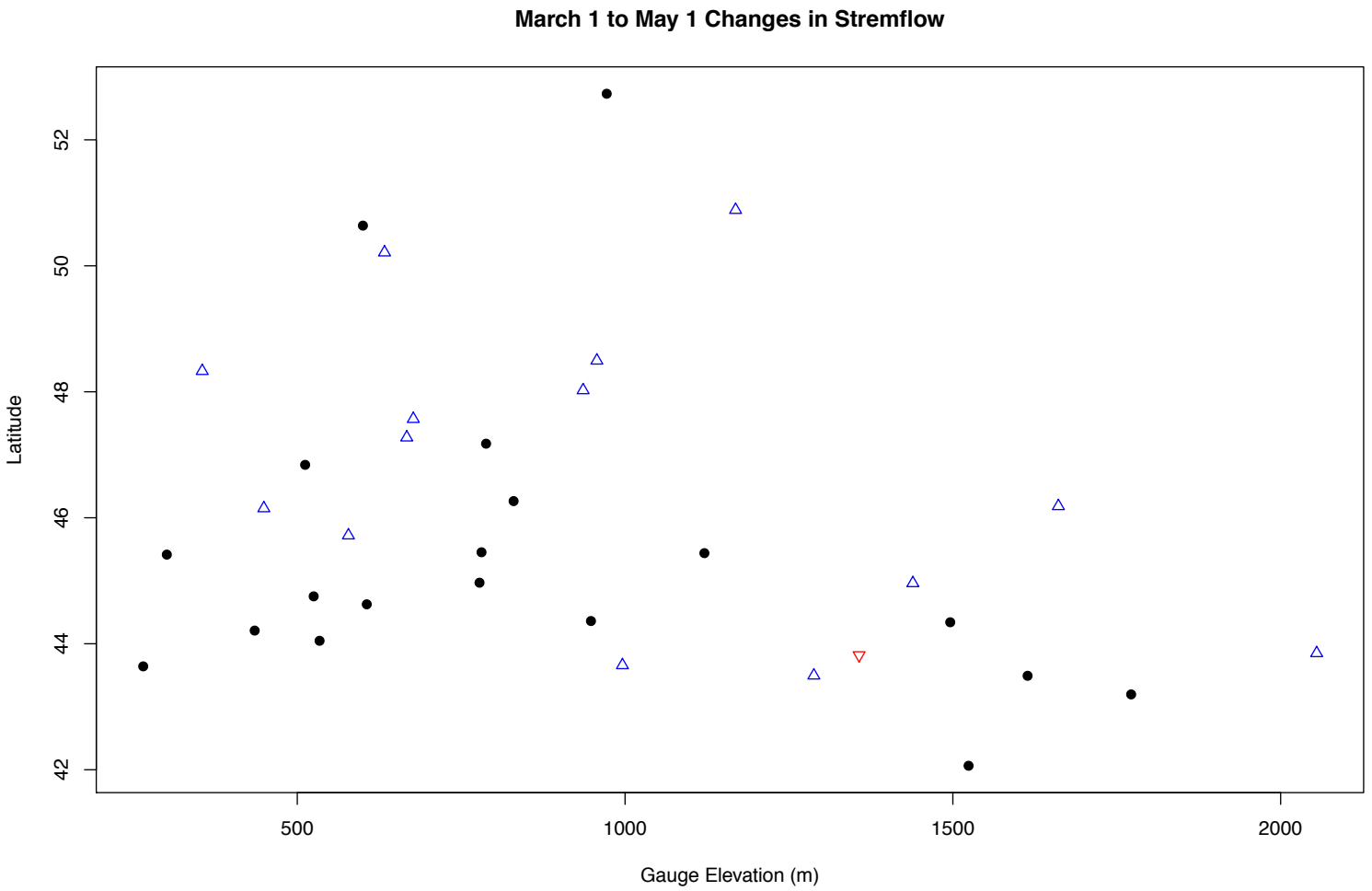

Figure 4.28. Significant changes in spring above-dam daily flows by elevation and latitude. Black dots show no change, blue triangles show increases and red triangles show decreases.

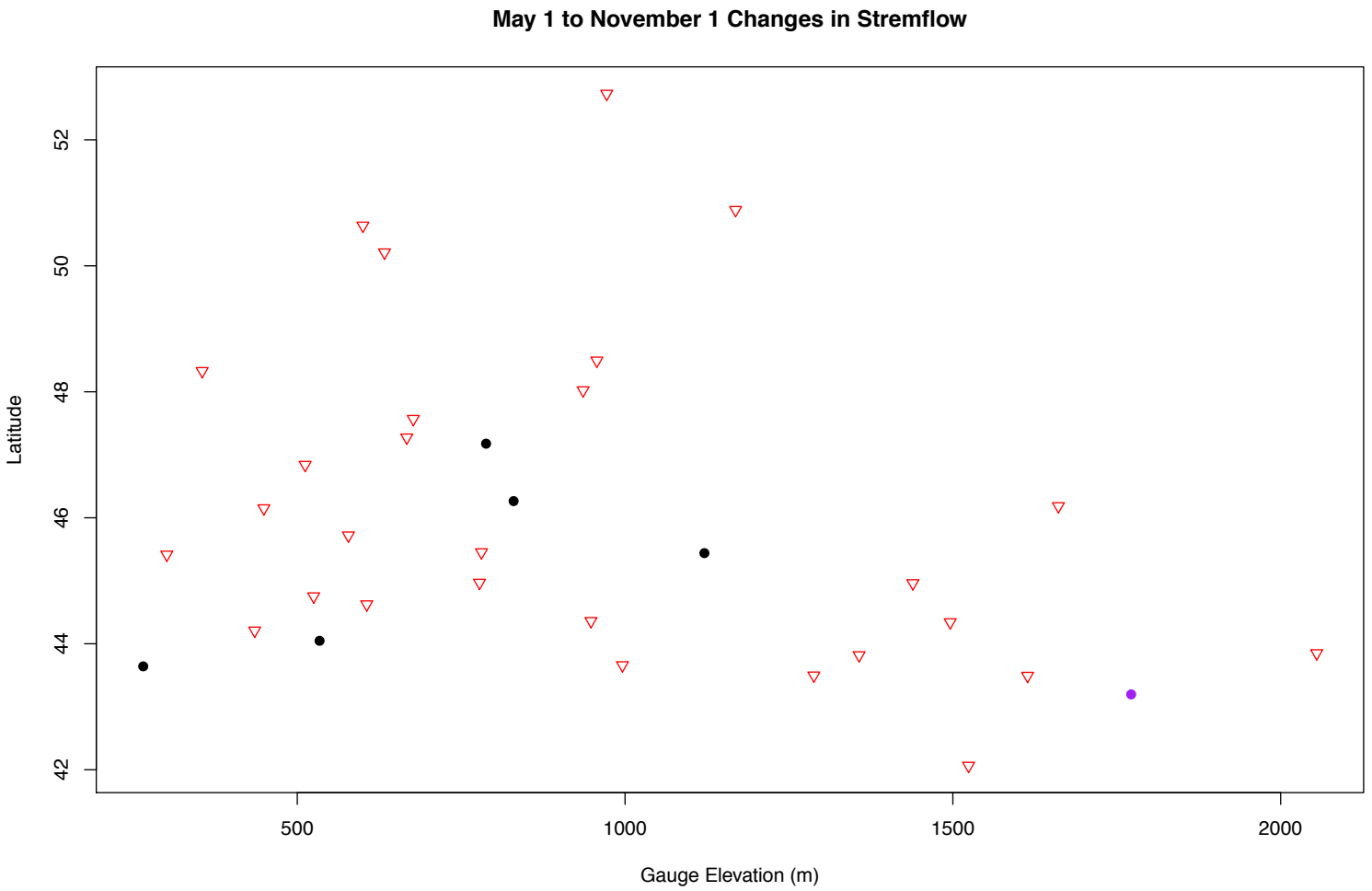

Figure 4.29. Significant changes in summer above-dam daily flows by elevation and latitude. Black dots show no change, blue triangles show increases and red triangles show decreases.

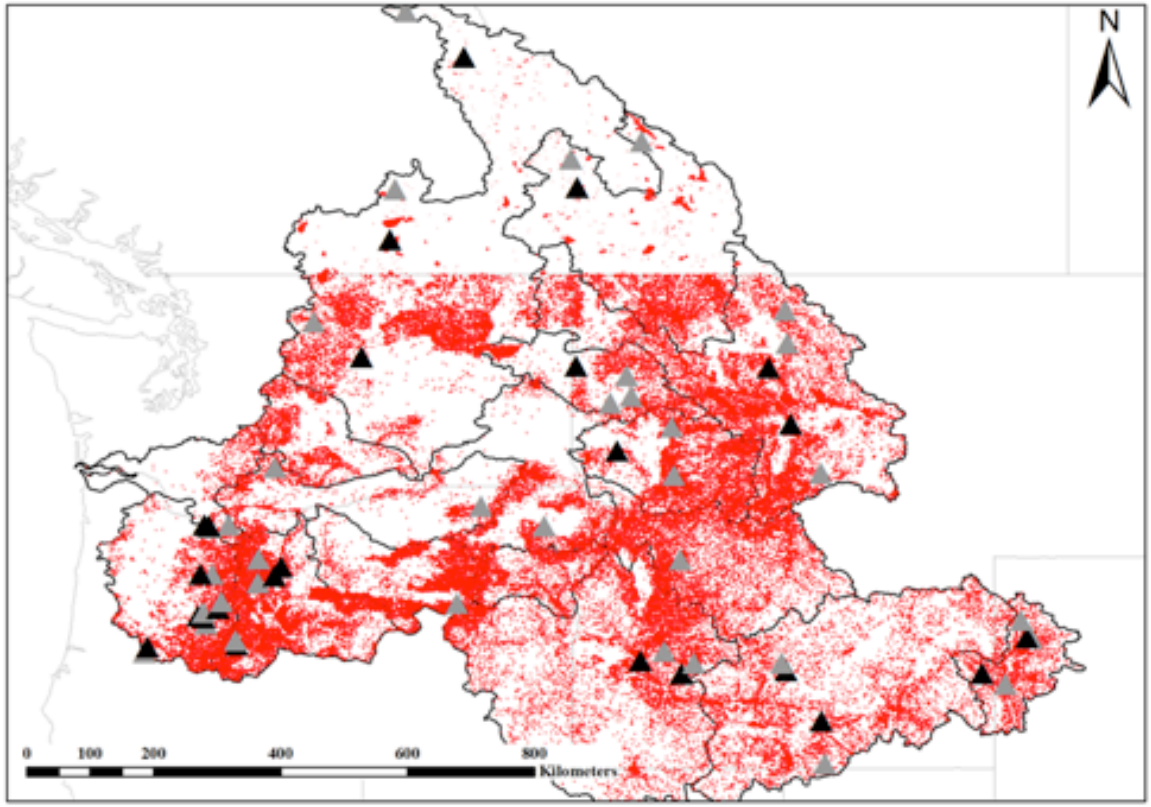

Figure 4.30. Occurrence of wildfire from 1980 to 2010. Federal Wildland Fire Occurrence, USGS. Historical Fire Perimeters, Ministry of Forests, Lands and Natural Resource Operations. Red polygons and points show the location and extent of wildfire events. Differences across the international border are due to reporting procedures and techniques. Black triangles are below-dam gages while grey triangles are above-dam gages.

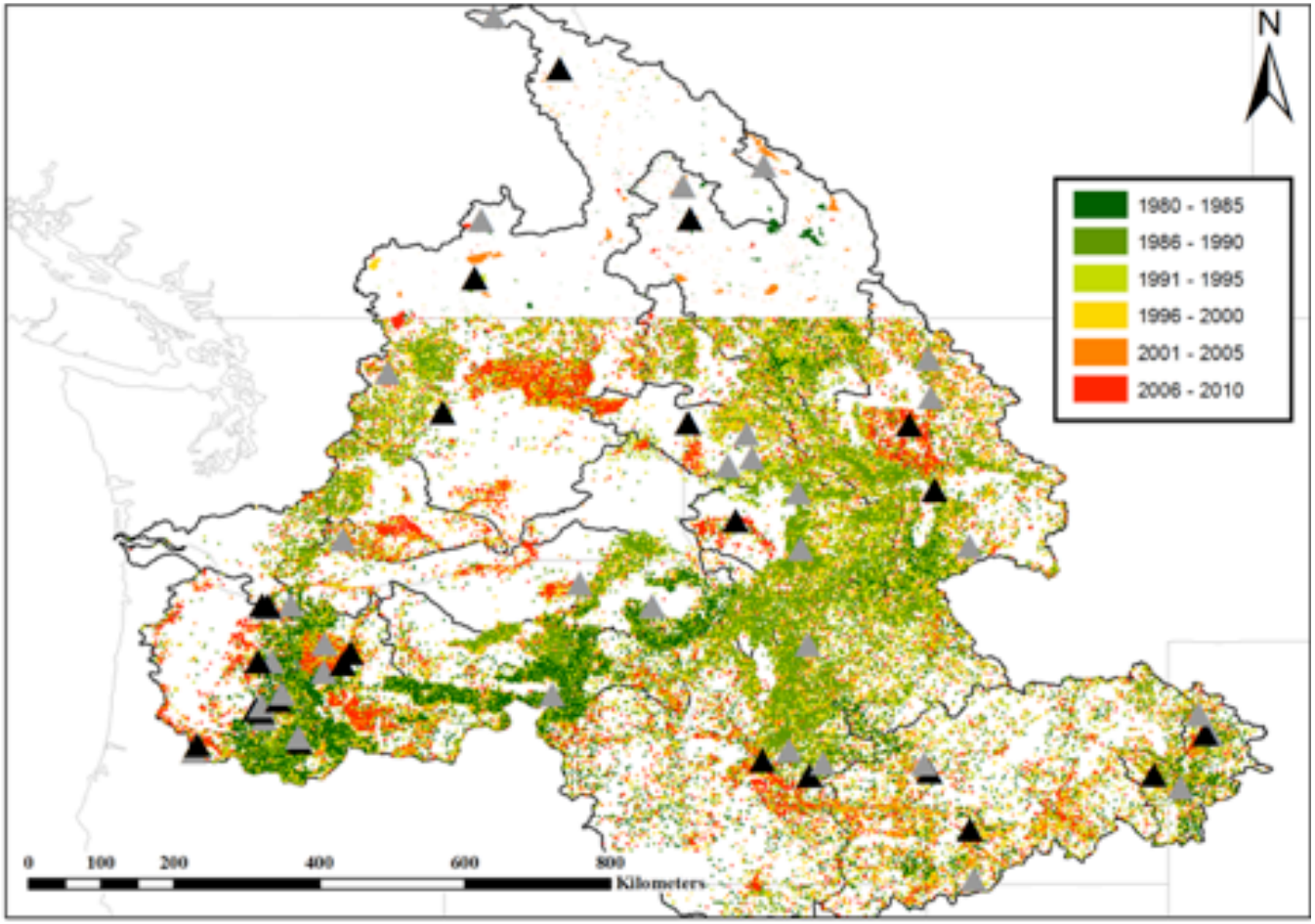

Figure 4.31. Occurrence of wildfire from 1980 to 2010. Federal Wildland Fire Occurrence, USGS. Historical Fire Perimeters, Ministry of Forests, Lands and Natural Resource Operations.. Colored polygons and points show the location and timing of wildfire events. Differences across the international border are due to reporting procedures and techniques. Black triangles are below-dam gages while grey triangles are above-dam gages.

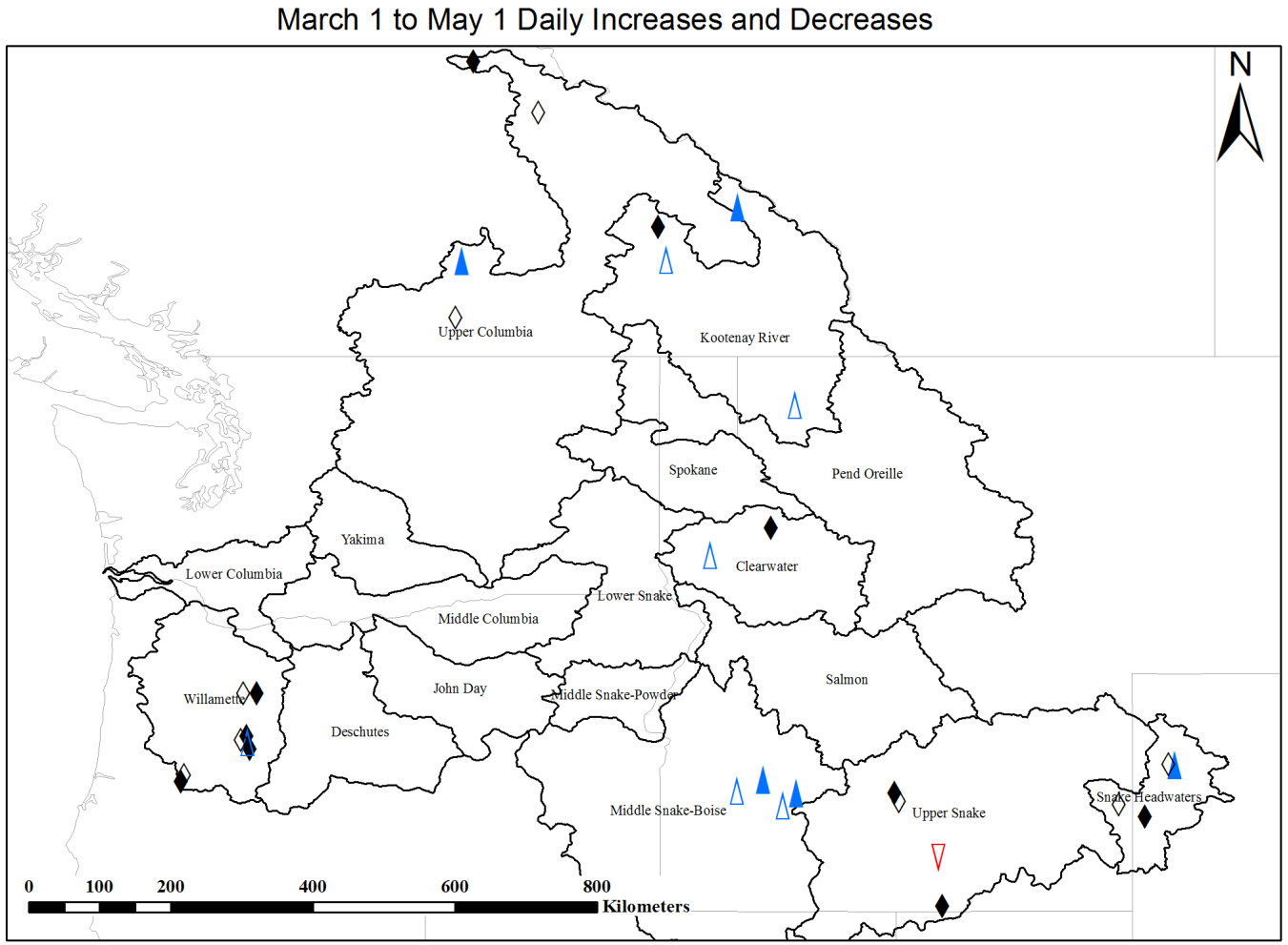

Figure 4.32. Significant changes in spring flows with three or more consecutive days with a significant change between March 1 and May 1 in flood control systems. Changes above and below dams are not necessarily on the same days.

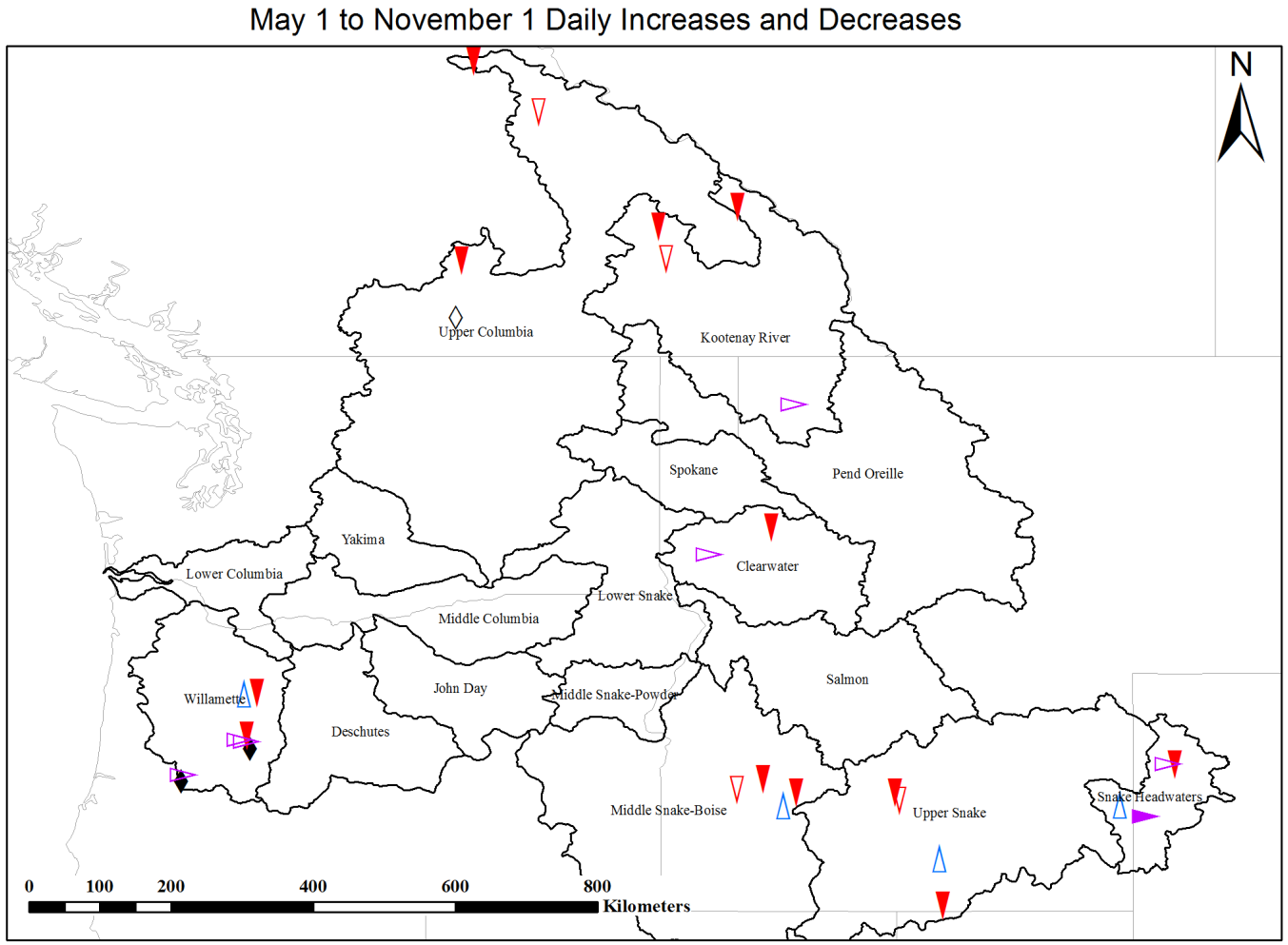

Figure 4.33. Significant changes in summer flows with five or more consecutive days and ten or more total days between in May 1 to November 1 in flood control systems. Changes above and below dams are not necessarily on the same days.

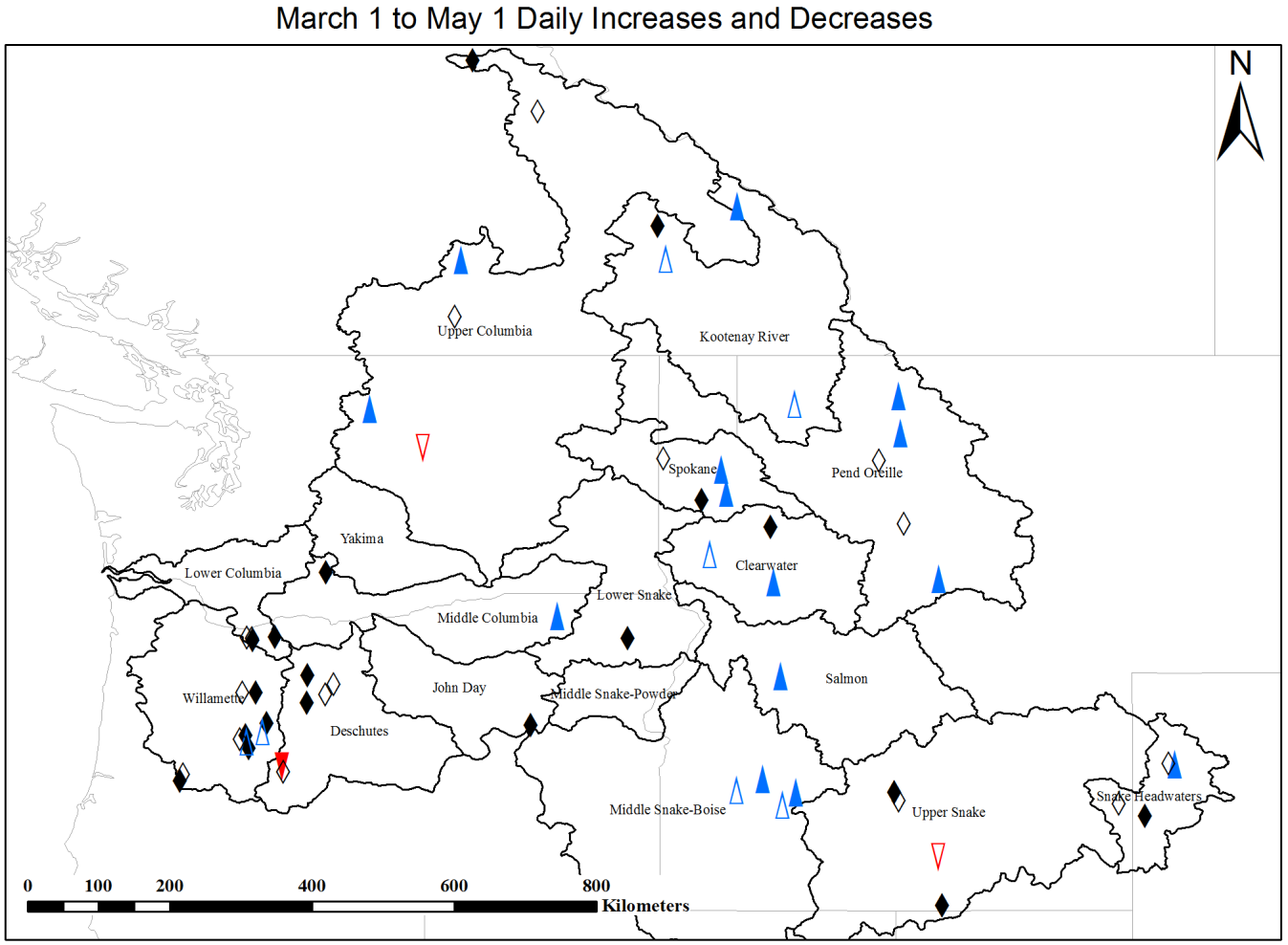

Figure 4.34. Significant changes in spring flows with three or more consecutive days with a significant change between March 1 and May 1.

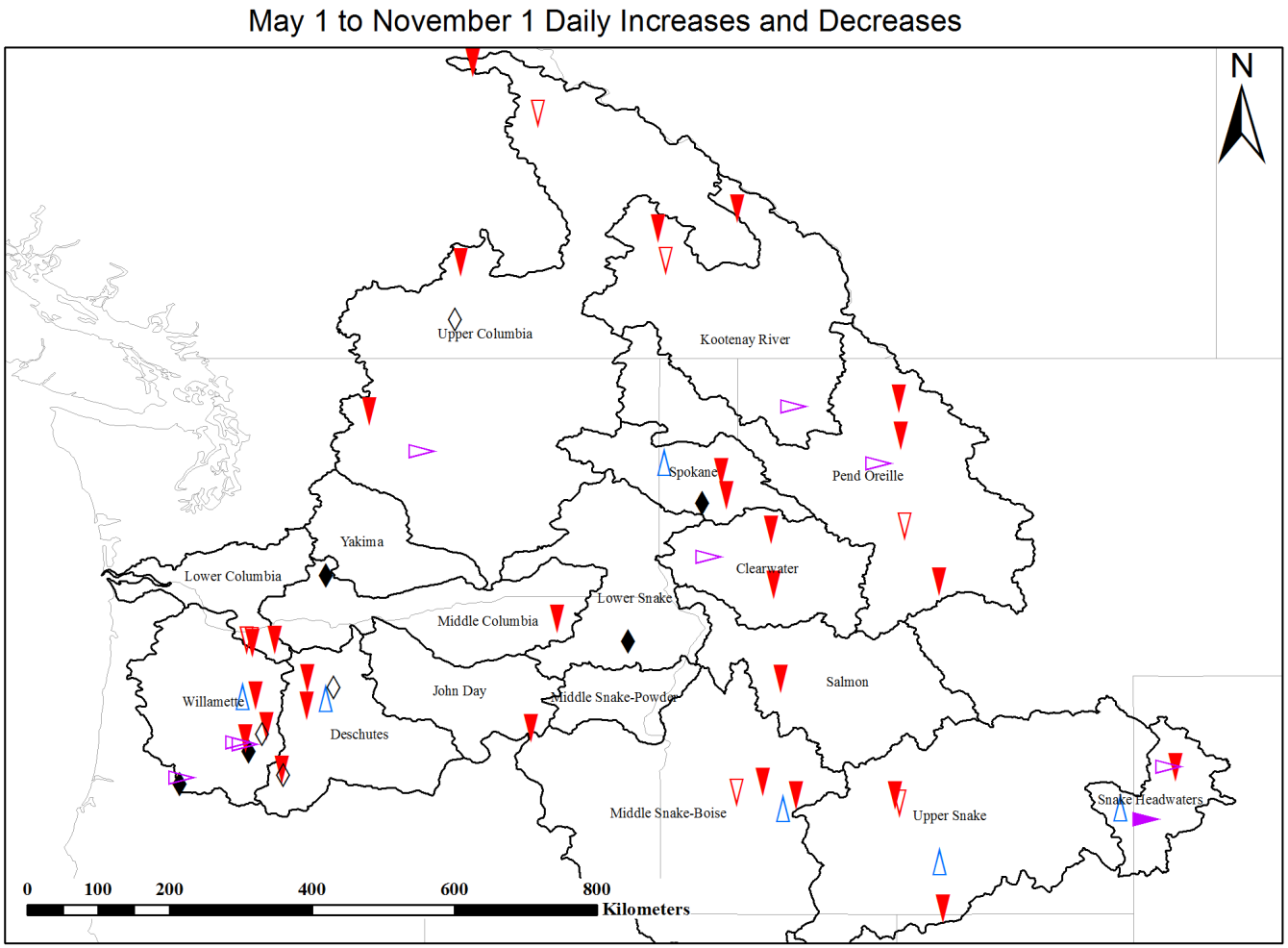

Figure 4.35. Significant changes in summer flows with five or more consecutive days and ten or more total days between in May 1 to November 1.

5. Discussion

Since 1950 in the CRB, daily air temperature has warmed, streamflow has increased during the onset of seasonal snowmelt (March-April), and late summer flows have declined (May-October); these changes are consistent with climate change, but also could be the result of legacies of past forest harvest or wildfire above dams. The signal of changing snowmelt freshet timing above dams is not generally visible below dams; thus, reservoir management appears to have obscured the signal of changing snowmelt freshet timing above dams except in the Boise sub-basin. The magnitude of late summer flow declines above dams is somewhat larger than increases in spring snowmelt above dams, but most changes are less than +/- five percent of annual flow, explaining why no trends in annual streamflow were observed, and suggesting that many streamflow trends within the CRB may reflect changes in timing rather than annual water yield. Analysis of daily flow by the methods used in this study permits identification of changes in streamflow timing and magnitude that may not be detected using monthly or annual data, but are important indicators of climate and land use change, and may be useful for adapting reservoir operations. Multiple aspects of reservoir management have contributed to this "engineering resilience" in the Columbia River Basin.

5.1. Uncertainties in data and analysis

Because the relationship between year vs. day-of-year streamflow is not necessarily linear, standard regression may not accurately identify trends; this possibility was investigated using wavelet analysis to detect the strength and timing of streamflow variability at multiple time scales and by comparing linear regressions to the non-parametric Mann-Kendall test. Non-stationarity in climate or streamflow may have

obscured trends that were actually present or detected trends that are truly long term (Mengistu et al., 2013, Chen and Grasby, 2009). However, Fleming and Weber (2012) demonstrated that removing the PDO signal prior to trend analysis was found to have little effect. Additionally, our ca. 1950-2012 datasets span several PDO regime shifts and many realizations of higher-frequency climatic oscillations, mitigating the potential for spurious monotonic trend detections that can occur if a climatic cycle occurs with a period similar to or longer than the record length. Our analysis (Appendix C) indicates that changes in streamflow variability over the periods of record may have affected trends detected in the Flathead, Sandy, Snake Headwater and Kootenay sub-basins, but not in the Boise, Upper Columbia, and Willamette sub-basins. However, analyses of shorter periods of record produced similar trends, suggesting that the trend patterns identified here are robust to record length.

Although the Mann-Kendall test is recommended for streamflow trend analysis (Lins and Slack, 1999), it may not be necessary for trends in daily flow: Mann-Kendall daily trend results showed the same distribution and similar magnitude of trend rates through time for streamflow and agreed with linear regression trend identification at 54 out of 59 stream gages. Hatcher and Jones (2013) and Fleming and Weber (2012) also found a lack of sensitivity to methodological choices for trend analysis.

5.2 Changes in streamflow and climate above dams

Above dams in the Columbia River basin, streamflow increased in March 1 to May 1 daily flows, and decreased in May 1 to November 1 daily flows, from 1950 to 2012. Increases in spring streamflow are relatively small and occur in a short season, whereas those in flow are larger and occur from early May to late October. These

findings suggest that annual streamflow has declined, but no trends were detected in annual flow. However, high variability in spring flows may have obscured increasing trends in this period. Overall these changes are small: increases in spring streamflow have amounted to about three percent of annual flow volume or less over the past sixty-three years, whereas summer decreases in daily flows in many basins have amounted to about five percent of annual flow volume (Figures 4.20 and 4.21).

Results from statistical analyses of climate variables in this study are consistent with the wide body of literature of climatic trends across the western United States and southern British Columbia, generally showing increases in minimum and maximum daily air temperatures since 1950 and few changes in precipitation timing. This study confirmed declining precipitation in the Boise sub-basin, consistent with Luce and Holden (2009) and Luce et al. (2013), but did not find any evidence for declining precipitation in the rest of the Columbia River Basin, loosely consistent with other studies discussed in the introductory section of this thesis.. Moreover, while u700 winds were correlated with precipitation during the winter months as suggested by Luce et al (2013), these correlations were weak at high elevation stations in the Columbia River basin, counter to the findings of Luce et al (2013). Positive correlations of PDO with April to July precipitation but negative correlations of PDO with April to July streamflow, especially south of the Canadian border and below 1000 m, are suggestive of enhancement of precipitation by warm North Pacific Ocean conditions, and evapotranspiration losses that reduce streamflow.

Climate indices (PNA, NPI, and PDO) do not provide much explanatory power for precipitation or streamflow in the Columbia River basin. Nevertheless, correlations of

climate indices (PDO, NPI, PNA) and u700 wind speeds with precipitation and streamflow differed in most months between high-elevation and high-latitude sites, versus sites below 1,500 m and south of the Canadian border (49 °N). These two portions of the Columbia River basin appear to differ in their coupling to regional climate drivers; this finding deserves further exploration.

Increased spring streamflow and declining summer flow in the Columbia River Basin observed in this study may reflect declining snowpack, melting glaciers, and earlier snowmelt noted in many studies for the western US (e.g., Hidalgo, 2009; Stewart et al. 2004, 2005) and the Pacific Northwest (e.g., Chang et al, 2012; Fleming and Weber 2012; Hatcher and Jones 2013). This study corroborates these findings by identifying specific days when streamflow has increased or decreased above dams. Compared to trends reported by Hatcher and Jones (2013), this study found more widespread trends of increasing spring flows (at 14 of 34 above-dam gages, compared to only 2 of 7 gages), and more widespread trends of declining summer flows (at 16 of 34 gages compared to 0 of gages). However, the trends detected in this study represented only a small percent (less than 5%) of annual flow, and only 20 to 40% of stations experienced significant trends on any given day. No trends in annual flow were detected, consistent with Fleming and Weber (2012) for the Canadian Columbia Basin, but counter to trends inferred by Luce and Holden (2009) for the US PNW.

5.3 Transmission of above-dam streamflow changes to below dams

Reservoir operations can obscure, mimic, or propagate upstream climate change effects on streamflow. Six different cases are possible. Changes in reservoir management for environmental flows (case 1) or irrigation (case 2) may mitigate or obscure upstream

climate signals. Reservoir management may propagate a climate signal (case 3). Upstream disturbances (wildfire (case 4), forest harvest (case 5)) and their legacies may produce signals that mimic climate change. Changes in reservoir objectives (case 6) also may mimic climate change signals on streamflow.

Reservoir operations may obscure or mitigate an upstream climate signal in two ways. These include: through (1) changes in reservoir operations for environmental flows/minimum flows/temperature for fish or (2) reservoir operations for irrigation increase late summer flows below dams.

In several cases, streamflow trends can be attributed to changes in reservoir management to meet environmental flow requirements. For example, significant increases in late summer flow below Blue River Dam do not correspond to above-dam trends; these increases are likely due to increased releases from Blue River to compensate for reduced streamflow when nearby Cougar Dam was offline for construction of a temperature regulating tower during the early 2000's. Below Detroit Dam, late September and early October streamflow has increased, and mid-February streamflow has decreased; the September/October trends may be due to increased early fall releases to meet in-stream flow requirements for endangered fish specified by the Endangered Species Act (Scullion, 2014 and Anderson, 2001). Dworshak reservoir historically attained full pool at the start of summer, but now reaches full pool infrequently because in-stream minimum flow requirements are more important than recreational use objectives. Below Palisade Dam, increasing early October streamflow may be attributed to altered reservoir operations to maintain in-stream flows for native cutthroat trout.

A pattern of increasing summer flows also may arise from reservoir operations to store winter flows and spring snowmelt for late summer irrigation. Above Okanagan Lake Dam, flows show a very strong signal of declining summer low flow whereas below the dam there have been no significant changes in flows during summer months. Below the dam it appears that reservoir releases for irrigation in late summer obscure the climate signal from above the dam. Below Dworshak Dam, which is also managed for irrigation, there have been significant declines in September and early October flows as well as a consistent increase in flows from the middle of July to the middle of September. This summer increasing signal is contrary to observed above-dam climate signals and might be the result of groundwater pumping for irrigation of agricultural land in the basin, or a change in management for environmental flows linked to other dams along the Clearwater River. Summer flows below Okanagan Lake dam appear to be controlled by irrigation operations similar to those below Dworshak Dam.

Synchronous patterns of summer declines in flow may indicate the propagation of a climate signal through a dam (case 3). Streamflow has declined in July and August daily flows on the same days above and below Mica Dam. A Water Use Plan (WUP) for the Columbia in 2007 included Mica reservoir management, but to date no changes to operations have been made and it continues to operate as needed to satisfy system requirements. As there have been no major, systematic changes, it is likely that reservoir operations at Mica Dam are propagating the climate signal from above the dam. In the gage pair flanking Lucky Peak Dam, both above and below-dam gages show increases in mid March daily flows and daily declines in flow on multiple days throughout the summer months. Reservoir operations for flood control at Mica and Lucky Peak dams

might propagate the signal from above to below the dam by releasing water during rainstorm events in the early winter that would have historically fallen as snow and remained until spring melt. The matching above- and below-dam streamflow changes at Mica and Lucky Peak dams are consistent with expected effects of climate change. Declines in August flows may be associated with glacier retreat (Nolin et al., 2010; Stahl and Moore, 2006; Jost et al., 2012; Fleming and Dahlke, in press), an earlier transition to late-summer baseflow due to earlier snowmelt timing or a cold-season shift from snow to rain, less summertime precipitation, or any combination of these factors.

Reservoir management or upstream land use changes may mimic climate signals when (4) wildfire or insect outbreaks increase spring streamflow or (5) post-harvest forest succession reduces summer flows. Twenty-one (of 34) study basins above dams had some evidence of forest harvest, and more than 50% of basin area in 16 basins had been subjected to forest harvest at some time during the study period. In contrast, wildfire has affected much smaller portions of study basins. Wildfire may mimic or accentuate increases in spring streamflow due to climate warming. In the first few years after wildfire in forested ecosystems, snow accumulation increases and snowmelt occurs earlier (e.g., Pomeroy et al., 2002; Veatch et al. 2009; Gleason et al. 2013). Mountain pine beetle infestations have reduced forest canopy cover over large areas of British Columbia and are believed to have affected snow accumulation and evapotranspiration over large areas (Maness et al. 2013, Pugh and Gordon 2013). Forest harvest and regeneration may mimic or accentuate decreases in summer streamflow due to climate warming. Streamflow has decreased from July to September both above and below Blue River dam. Long-term records from small reference catchments in Lookout Creek (the

H.J. Andrews Experimental Forest) above Blue River Dam do not show declines in late summer streamflow (Moore, 2010). Instead, above-dam declines in late summer streamflow are likely due to young forest plantations, which transpire more water during late summer (Hicks et al., 1991; Jones and Post, 2004; Moore and Wondzell, 2005; Perry, 2007). More work is needed to better understand the legacies of disturbances and their effects on streamflow trends above dams (e.g., Zhang and Wei, 2012).

Changes in reservoir management to balance multiple objectives (6) may also produce a pattern of increasing spring flows and declining summer flows (Knowles et al., 2007). For example, below Jackson Lake Dam increases in spring flows and decreases in summer flows mimic changes due to climate. However, dam managers suggested that this shift reflects efforts to appease diverse recreation interests on the river between Jackson Lake and Palisades Reservoir. In particular, since the late 1980s spring releases have been increased to accommodate whitewater recreation users, and summer releases have been reduced and stabilized to accommodate fishing groups downstream of Jackson Dam. In another example, since 2007 fall and winter releases have been increased for fish habitat at Duncan Dam, resulting in lower spring and summer flows below this dam.

5.4 Consequences and Implications

This study provides evidence of widespread, but not large, changes in streamflow in the Columbia River basin over the period from 1950 to 2012. These findings are relevant for strategies to adaptively manage water resources in light of the ongoing planning for possible renegotiation of the U.S.-Canada Columbia River Treaty. Above dams, streamflow increased significantly at 20% of the 28 gages on multiple days in spring (March 1 to May 1), and decreased significantly at 20 to 60% of gages on many

days in summer (May 1 to November 1). Documented climate change and the legacy of fire and forestry practices are plausible explanations for observed changes. Decreases in summer streamflow were five to ten times larger than increases in spring streamflow. However, overall streamflow changes represent less than 5% of annual streamflow and appear to be shifts in timing rather than declines in annual water yield.

Fewer changes in streamflow were observed below dams, indicating that diverse and (in some cases) changing reservoir operations in the Columbia River basin are insulating downstream water users from climate change and other effects on streamflow above dams. This "engineered resilience" of water systems (Hatcher and Jones 2013) may continue, or it may cease to dominate climate signals from above dams in the Columbia River basin, depending on reservoir management goals, changes in above-dam flows, and reservoir capacity. Dams whose effective storage capacity is small relative to inflows (e.g., Blue River Dam, Cougar Dam, Anderson Ranch Dam and Lucky Peak Dam, or "run of the river" dams managed for hydroelectricity) may be most sensitive to climate change effects on streamflow. Further work is needed to explore the capacity of reservoir operations to adjust to climate change and other drivers of streamflow change in the Columbia River basin.

6 Conclusions and further research

Increases in minimum surface air temperature from 1950 to 2012 were associated with increases in spring streamflow, and declining streamflow in late spring, summer, and early fall, above dams in in the CRB. These trends are consistent with earlier and accelerated melting of mountain snowpacks as well as shifts towards more precipitation falling as rain rather than snow. Reservoir management seems to have overwritten the signal of earlier snowmelt timing above dams except in the Boise sub-basin. However, reservoir management, particularly at flood control dams, appear to propagate the above-dam signal of declining late-summer flows downstream.

There is no single primary management goal for most dams in the Columbia River basin. Instead, dams are typically managed for a variety of goals during the fall and winter months such as flood control, with other values such as recreation and irrigation becoming more actively used during spring and summer months. Trends in daily spring and summer flows were mainly observed below dams managed for flood control and not below dams that were not managed for flood control. Flood control management typically take place between the middle of October and the beginning of June with the greatest downstream flow impact of Columbia flood control operations between spring and summer, overprinting the above-dam climate signal due to warming, but potentially propagating late-summer trends from above dams.

Depending on the combination of multiple management objectives within the water year, dams sometimes overwhelm, but in other cases propagate, above-dam trends downstream. Combinations of management including irrigation overwrite above-dam

signals during spring and summer months, whereas those including flood control could overwrite signals during the fall and winter months.

In mixed rain-snow systems, once there is a shift to a certain proportion of precipitation that falls as rain, a climate signal will propagate , first during rain storm events, and then again during summer months when all water uses cannot be supported due to the decreased summer flows. Changes will reflect uses or management goals that cannot be provided. In snow-dominated systems, predominantly on the east side of the Cascades, reservoirs with large capacity and high elevation headwaters may be able to adapt to changes in precipitation falling as rain rather than snow for parts of the snowpack accumulation season, but summer low flows would likely still decline and certain management goals such as recreation may not be met. Streamflow in mid-elevation zones is most sensitive to changes in maximum and minimum daily temperatures, which affectsnowpack melting and the phase of falling precipitation. In most areas, reservoirs appear to have had the capacity to address these changes, but future changes may overwhelm this capacity.

Above dams, areas that are dominated by snowfall are the most sensitive to increasing temperatures and have showed the most significant changes in spring and summer daily flows. These areas would be expected to show additional changes as warming continues throughout the century. This supply of water is utilized for many competing demands and small changes in the distribution of flows throughout the year are likely to disrupt current water management systems above dams. Below dams, areas dominated by snowfall and with small reservoir capacity are strongly sensitive to increasing temperatures and are expected to continue to display the most significant

changes in spring and summer daily flows. Places where the combination of reservoir management goals has thus far overwhelmed above-dam signals may continue to overwrite above-dam signals depending on the magnitude of future changes.

Future research, including analysis of daily streamflow trends using more above-dam gages, could improve the spatial resolution of changes in streamflow timing in the Columbia River Basin and elsewhere. More detailed studies including quantification of human and natural disturbances affecting land cover would provide greater mechanistic understanding about causes of observed trends in streamfow and climate variables. Hydrologic changes predicted by models suggest increased competition for reservoir storage between firm hydropower and instream flow targets. Modeled alternative reservoir operating strategies combining earlier reservoir refill and greater storage allocations for instream flow targets mitigated some of the negative impacts to flow, but only with significant losses to firm hydropower, yet these revenue changes were less than five percent for all scenarios (Payne et al., 2004 and Barnett et al., 2005). The present study identified various below-dam responses to above-dam signals and reservoir management at dams not included in previous studies. In addition, a comparison between individual dam responses to above-dam changes in this empirical study versus model-based studies could serve as a validation of modeled representations of reservoir management strategies.

It is vitally important to note daily streamflow trends and to understand the sensitivity of these flows to changes in climate and land cover in order to aid reservoir managers in developing strategies to manage water resources and adapt management plans for the coming decades and further into the future. The results of this research are

important to all surface water users in the Columbia River Basin because daily trends and timing of streamflow greatly affect water management decisions and the livelihoods of everyone within the basin. Increased understanding of these influences is necessary to be able to sustain and optimally manage agricultural productivity, hydroelectric power generation, recreational uses, and the natural ecosystems of the CRB in the face of continuing climatic change.

7 Literature cited

Anderson, J. (2001). History of the Flow Survival Relationship and Flow Augmentation Policy in the Columbia River Basin, (June), 1–12.

Barnett, Tim P., Adam, J.C., Lettenmaier, D.P. (2005). Potential impacts of a warming climate on water availability in snow-dominated regions. *Nature, 438,* 303-309. doi:10.1038/nature04141

Barnett, Tim P., Pierce, D. W., Hidalgo, H. G., Bonfils, C., Benjamin, D., Das, T., … Cayan, R. (2014). Human-Induced Changes in the Hydrology of the Western United States, *319*(5866), 1080–1083.

Beus, Michael W. (2014). [Water Operations Manager at the US Bureau of Reclamation] 3 June 2014.

Booth, E. L. J., Byrne, J. M., & Johnson, D. L. (2012). Climatic changes in western North America, 1950-2005. *International Journal of Climatology*, *32*(15), 2283–2300. doi:10.1002/joc.3401

Burford JE, Dery SJ, Holmes RD. 2009. Some aspects of the hydroclimatology of the Quesnel River Basin, British Columbia, Canada. *Hydrological Processes*, 23, 1529-1536.

Cayan, D. (2001). Changes in the onset of spring in the western United States. *Bulletin of the …*, *82*(3), 399–415.

Chang, H., & Jung, I. (2012). Spatial patterns of March and September streamflow trends in Pacific Northwest streams, 1958–2008. *Geographical Analysis*, *44*(3), 177–201. doi:10.1111/j.1538-4632.2012.00847.x

Chen, Z., Grasby, S.E. (2009). Impact of decadal and century-scale oscillations on hydroclimate trend analyses. *Journal of Hydrology*, 365, 122–133.

Columbia Basin Trust (CBT). (2014). *Water in the Columbia Basin* (pp. 1–5).

Cuo, L., & Lettenmaier, D. (2009). Effects of a century of land cover and climate change on the hydrology of the Puget Sound basin. *Hydrological Processes 933*(January), 907–933. doi:10.1002/hyp

Déry SJ, Stahl K, Moore RD, Whitfield PH, Menounos B, Burford JE. 2009. Detection of runoff timing changes in pluvial, nival, and glacial rivers of western Canada. *Water Resources Research*, 45, W04426, doi:10.1029/2008WR006975.

Falcone, James. (2011). GAGES-II: Geospatial Attributes of Gages for Evaluating Streamflow. *U.S. Geological Survey.*

Fleming SW. 2010. Signal-to-noise ratios of geophysical and environmental time series. *Environmental and Engineering Geoscience*, 16, 389-399.

Fleming SW, Dahlke HE. In press. Modulation of linear and nonlinear hydroclimatic dynamics by mountain glaciers in Canada and Norway: results from information-theoretic polynomial selection. *Canadian Water Resources Journal*.

Fleming, S., & Weber, F. (2012). Detection of long-term change in hydroelectric reservoir inflows: Bridging theory and practice. *Journal of Hydrology*, *470-471*, 36–54. doi:10.1016/j.jhydrol.2012.08.008

Graf, W. L. (1999). Dam nation: A geographic census of American dams and their large-scale hydrologic impacts. *Water Resources Research*, *35*(4), 1305–1311. doi:10.1029/1999WR900016

Gleason, K. E., Nolin, A. W., & Roth, T. R. (2013). Charred forests increase snowmelt: Effects of burned woody debris and incoming solar radiation on snow ablation. *Geophysical Research Letters*, *40*(17), 4654–4661. doi:10.1002/grl.50896

Gouhier, A. T. C., & Grinsted, A. (2014). Package Biwavelet.

Hamlet, A. F., Mote, P. W., Clark, M. P., & Lettenmaier, D. P. (2005). Effects of Temperature and Precipitation Variability on Snowpack Trends in the Western United States*. *Journal of Climate*, *18*(21), 4545–4561. doi:10.1175/JCLI3538.1

Hamlet, A. F., Mote, P. W., Clark, M. P., & Lettenmaier, D. P. (2007). Twentieth-Century Trends in Runoff, Evapotranspiration, and Soil Moisture in the Western United States*. *Journal of Climate*, *20*(8), 1468–1486. doi:10.1175/JCLI4051.1

Hatcher, K. L., & Jones, J. a. (2013). Climate and Streamflow Trends in the Columbia River Basin: Evidence for Ecological and Engineering Resilience to Climate Change. *Atmosphere-Ocean*, *51*(4), 436–455. doi:10.1080/07055900.2013.808167

Helsel, D. R., & Hirsch, R. M. (Eds.). (1992). Statistical methods in water resources. New York: Elsevier.

Helvey, J. (1980). Effects of a north central Washington wildfire on runoff and sediment production. *Water Resources Bulletin*, *16*(4), 627–634.

Hibbert, A. (1967). Forest Treatment Effects on Water Yield. In *International Symposium For Hydrology* (pp. 527–543).

Hicks, B., Beschta, R., & Harr, R. (1991). Long-term changes in streamflow following logging in western Oregon and associated fisheries implications. *JAWRA Journal of the …*, *27*(2), 217–226.

Hidalgo, H. G., Das, T., Dettinger, M. D., Cayan, D. R., Pierce, D. W., Barnett, T. P., … Nozawa, T. (2009). Detection and Attribution of Streamflow Timing Changes to Climate Change in the Western United States. *Journal of Climate*, *22*(13), 3838–3855. doi:10.1175/2009JCLI2470.1

Hubbart, J., Link, T., Gravelle, J., & Elliot, W. (2007). Timber harvest impacts on water yield in the continental/maritime hydroclimatic region of the United States. *Forest Science*, *53*(2), 169–180.

Jones, J. A. (2011). Hydrologic responses to climate change: considering geographic context and alternative hypotheses. *Hydrological Processes*, *25*(12), 1996–2000. doi:10.1002/hyp.8004

Jones, J. A., Creed, I. F., Hatcher, K. L., Warren, R. J., Adams, M. B., Melinda, H., … Clifford, N. (2012). Ecosystem Processes and Human Influences Regulate Streamflow Response to Climate Change at Long-Term Ecological Research Sites. *BioScience*, *62*(4), 390–404. doi:10.1525/bio.2012.62.4.10

Jones, J. A., & Post, D. A. (2004). Seasonal and successional streamflow response to forest cutting and regrowth in the northwest and eastern United States. *Water Resources Research*, *40*(5), 1–19. doi:10.1029/2003WR002952

Jost G, Moore RD, Menounos B, Wheate R. 2012. Quantifying the contribution of glacier runoff to streamflow in the upper Columbia River Basin, Canada. Hydrol. and Earth Syst. Sci., 16, 849-860.

Knowles, N., M. Dettinger, and D. Cayan. (2007). Trends in Snowfall Versus Rainfall for the Western United States, 1949–2001. *California Energy Commission, PIER Energy-Related Environmental Research Program*. CEC-500-2007-032.

Kong, Gillian. (2014). [Engineer and Program Manager at British Columbia Hydro] Interview. 10 June 2014.

Lettenmaier, D., Wood, E., & Wallis, J. (1994). Hydro-climatological trends in the continental united states. *Journal of Climate*, *7*, 586–607.

Lins, H., & Slack, J. (1999). Streamflow trends in the United States. *Geophysical Research letters*, *26*(2), 227–230.

Littell, J., Elsner, M., & Mauger, G. (2011). Regional Climate and Hydrologic Change in the Northern US Rockies and Pacific Northwest: Internally Consistent Projections of Future Climate for Resource Management, (April), 1–109.

Luce, C. H., Abatzoglou, J. T., & Holden, Z. a. (2013). The missing mountain water: slower westerlies decrease orographic enhancement in the Pacific Northwest USA. *Science (New York, N.Y.)*, *342*(6164), 1360–4. doi:10.1126/science.1242335

Luce, C., & Holden, Z. (2009). Declining annual streamflow distributions in the Pacific Northwest United States, 1948–2006. *Geophysical Research Letters*, *36*(16), 1–6. doi:10.1029/2009GL039407

Maness, H., Kushner, P. J., & Fung, I. (2012). Summertime climate response to mountain pine beetle disturbance in British Columbia. *Nature Geoscience*, *6*(1), 65–70. doi:10.1038/ngeo1642

Matheussen, B. (2000). Effects of land cover change on streamflow in the interior Columbia River Basin (USA and Canada). *Hydrological Processes*, *14*, 867–885.

Mengistu, S., Creed, I., Kulperger, R., & Quick, C. (2012). nesting dolls effect–Using wavelet analysis to reveal non-stationary and nested stationary signals in water yield from catchments on a northern forested landscape. *Hydrological Processes*. doi:10.1002/hyp

Moore, J., Arrigoni, A., & Wilcox, A. (2012). Impacts of Dams on Flow Regimes in Three Headwater Subbasins of the Columbia River Basin, United States. *Journal of the American Water Resources Association*, *48*(5), 925–938.

Moore, K. (2010). Trends in streamflow from old growth forested watersheds in the western Cascades. *Oregon State University, Geosciences Department*, 1–220.

Moore RD, Wondzell S.M. (2005). Physical hydrology and the effects of forest harvesting in the Pacific Northwest: a review. *Journal of the American Water Resources Association*, 41, 763-784.

Mote, P.W. 2003. Trends in snow water equivalent in the Pacific Northwest and their climatic causes. *Geophysical Research Letters*, 30, doi:10.1029/2003GL017258.

Mote, P. (2006). Climate-Driven Variability and Trends in Mountain Snowpack in Western North America*. *Journal of Climate*, (1134), 6209–6220.

Naik, P. K., & Jay, D. a. (2011). Distinguishing human and climate influences on the Columbia River: Changes in mean flow and sediment transport. *Journal of Hydrology*, *404*(3-4), 259–277. doi:10.1016/j.jhydrol.2011.04.035

Ogren, K. L., Schuetz, S. R., Preppernau, C. A., Brooke, E., Arnold, N. D., Darbyshire, J. E., … Heitmeyer, L. D. (2013). *Atlas of the Columbia River Basin* (pp. 1–33). Corvallis, Oregon.

Payne, J., Wood, A., & Hamlet, A. (2004). Mitigating the effects of climate change on the water resources of the Columbia River basin. *Climatic Change*, *62*, 233–256.

Perry, T. D. (2007). *Do Vigorous Young Forests Reduce Streamflow? Results from up to 54 Years of Streamflow Records in Eight Paired-watershed Experiments in the H. J. Andrews and South Umpqua Experimental Forests*.

Pike, R.G., K.E. Bennett, T.E. Redding, A.T. Werner, D.L. Spittlehouse, R.D. Moore, T.Q. Murdock, J. Beckers, B.D. Smerdon, K.D. Bladon, V.N. Foord, D.A. Campbell, and P.J. Tschaplinski. 2010. Climate Change Effects on Watershed Processes in British Columbia (Chapter 19). In: Pike, R.G., T.E. Redding, R.D. Moore, R.D. Winkler, and K.D. Bladon (editors). 2010. Compendium of forest hydrology and geomorphology in British Columbia. B.C. Min. For. Range, *For. Sci. Prog., Victoria, B.C. and FORREX Forum for Research and Extension in Natural Resources*, Kamloops, B.C. Land Manag. Handb. 66. Pp. 699-747. www.for.gov.bc.ca/hfd/pubs/Docs/Lmh/Lmh66.htm

Pomeroy, J. W., Gray, D. M., Hedstrom, N. R., & Janowicz, J. R. (2002). Prediction of seasonal snow accumulation in cold climate forests. *Hydrological Processes*, *16*(18), 3543–3558. doi:10.1002/hyp.1228

Pugh, E., and Gordon, E. (2013). A conceptual model of water yield effects from beetle-induced tree death in snow-dominated lodgepole pine forests. *Hydrological Processes*, 1–13. doi:10.1002/hyp

Qian, Y., Gustafson, W. I., Leung, L. R., & Ghan, S. J. (2009). Effects of soot-induced snow albedo change on snowpack and hydrological cycle in western United States based on Weather Research and Forecasting chemistry and regional climate simulations. *Journal of Geophysical Research*, *114*(D3), D03108. doi:10.1029/2008JD011039

Rodenhuis, D.R., Bennett, K.E., Werner, A.T., Murdock, T.Q., Bronaugh, D., 2007. Hydro-Climatology and Future Climate Impacts in British Columbia. *University of Victoria, Victoria, BC, Pacific Climate Impacts Consortium*.

Schnorbus M, Werner A, Bennett K. 2012. Impacts of climate change in three hydrologic regimes in British Columbia, Canada. *Hydrological Processes*, DOI: 10.1002/hyp.9661.

Scullion, Mary K. (2014). [Dam Manager with U.S. Army Corps of Engineers] Interview. 29 May 2014.

Smerdon, E. T., Adams, R. M., Chapman, D. W., Fontane, D., & Giorgi, A. E. (2004). *Managing the Columbia River: instream flows, water withdrawals, and salmon survival* (pp. 1–159).

Stahl, K., and Moore, R.D. (2006). Influence of watershed glacial coverage on summer streamflow in British Columbia, Canada. *Water Resources Research, 42,* doi:10.1029/2006WR005022

Stewart, I., Cayan, D., & Dettinger, M. (2005). Changes toward earlier streamflow timing across western North America. *Journal of climate*, *18*, 1136–1155.

Taylor, B., and M. Barton. 2004. Climate. In: Expanding the Dialogue on Climate Change & Water Management in the Okanagan Basin, British Columbia (S. Cohen, D. Neilsen, R. Welbourn eds.). *Environment Canada, Agriculture and Agri-Food Canada*, and University of British Columbia, Vancouver, BC, pp. 25-45.

U.S. Army Corps of Engineers (USACE) (2013). Columbia River Treaty 2014-2024 Review. Retrieved August 22, 2013, from http://www.crt2014-2024review.gov/

VanShaar, J. R., Haddeland, I., & Lettenmaier, D. P. (2002). Effects of land-cover changes on the hydrological response of interior Columbia River basin forested catchments. *Hydrological Processes*, *16*(13), 2499–2520. doi:10.1002/hyp.1017

Veatch, W., & Brooks, P. (2009). Quantifying the effects of forest canopy cover on net snow accumulation at a continental , mid-latitude site. *Ecohydrology*, *128*(February), 115–128. doi:10.1002/eco

Vörösmarty, C., Green, P., Salisbury, J., & Lammers, R. (2000). Global Water Resources: Vulnerability from climate chnage and population growth. *Science*, *289*(5477), 284–288.

Zhang, M., & Wei, X. (2012). The effects of cumulative forest disturbance on streamflow in a large watershed in the central interior of British Columbia, Canada. *Hydrology and Earth System Sciences*, *16*(7), 2021–2034. doi:10.5194/hess-16-2021-2012.

Zhang X, Brown R, Vincent L, Skinner W, Feng Y, Mekis E. 2011. Canadian climate trends, 1950-2007. *Canadian Biodiversity: Ecosystem Status and Trends 2010, Technical Thematic Report No. 5*. Canadian Councils of Resource Ministers. Ottawa, ON. iv + 21 p. http://www.biodivcanada.ca/default.asp?lang=En&n=137E1147-0

Zhang, X., & Harvey, K. (2001). Trends in Canadian streamflow. *Water Resources Research*, *37*(4), 987–998.

Zhang X, Vincent LA, Hogg WD, Niitsoo A. 2000. Temperature and precipitation trends in Canada during the 20th century. *Atmosphere-Ocean*, 38, 395-429.

LIST OF APPENDICES

Appendices

Appendix A

Additional Basic information for streamflow gauges used in this study and GIS data sources

Table A-1. Below dam streamflow gauges with dam information from the USGS "Summary of selected characteristics of large reservoirs" dataset.

Gauge	Dam	Management Objectives	Date Dam Constructed	Gauge Record
12340500	Milltown Dam	Hydropower	1908	1950 to 2012
12372000	Kerr Dam	Hydropower, Recreation	1938	1950 to 2012
12419000	Post Falls Dam	Irrigation, Hydropower	1908	1950 to 2012
12452500	Chelan Dam	Hydropower, Recreation	1927	1950 to 2012
13011000	Jackson Lake Dam	Irrigation, Flood Control, Recreaiton	1916	1950 to 2012
13032500	Palisades Dam	Irrigation, Hydropower, Flood Control, Recreation	1957	1950 to 2012
13081500	Minidoka Dam	Irrigation, Hydropower, Flood Control, Recreation	1906	1950 to 2012
13148500	Little Wood River Dam	Irrigation, Recreation, Flood Control	1939	1950 to 2012
13190500	Anderson Ranch Dam	Irrigation, Flood Control, Recreation, Hydropower	1950	1950 to 2012
13202000	Lucky Peak Dam	Flood Control, Recreation, Irrigation	1955	1954 to 2012
13341050	Dworshak Dam	Hydropower, Flood Control, Recreation	1973	1964 to 2012
14054000	Crane Prairie Dam	Irrigation, Recreation	1940	1950 to 2012
14092500	Pelton Dam	Hydropower	1958	1950 to 2012
14097100	Warm Springs Dam	Hydropower	1919	1972 to 2012
14140000	Bull Run Dam 2	Metropolitan Water Supply	1928	1950 to 2012
14153500	Cottage Grove Dam	Flood Control, Irrigation, Recreation	1942	1950 to 2012
14158850	Trail Bridge Dam	Hydropower	1963	1950 to 2012
14159500	Cougar Dam	Hydropower, Flood Control	1964	1950 to 2012
14162200	Blue River Dam	Flood Control, Recreation	1968	1966 to 2012
14181500	Detroit Dam	Hydropower, Flood Control, Recreation	1953	1950 to 2012
08NH118	Duncan Dam	Flood Control, Regulating flow for hydropower downstream	1967	1963 to 2012
08NM050	Okanagan Lake Dam	Flood Control, Water Supply, Recreation	1958	1950 to 2011
Mica Outflow	Mica Dam	Hydropower, Flood Control	1973	1976 to 2012

Table A-2. Above dam streamflow gauges with elevation and general climate information.

Gauge	Mean Catchment Elevation (m)	Gauge Elevation (m)	Precipitation (mm)	Tave (C)	Tmax (C)	Tmin (C)	Sub-basin	Site Abreviation
12332000	2170	1661	767	1.7	8.1	-4.1	Clark Fork	CLF
12358500	1724	957	1271	2.6	7.8	-2.9	Flathead	FLA
12370000	1530	936	1095	4.0	9.8	-1.6	Flathead	FLA
12413000	1168	677	1206	6.3	11.0	-0.1	Coeur D'Alene	CDA
12414500	1381	667	1277	5.7	10.5	-0.3	Coeur D'Alene	CDA
12414900	1095	788	1122	6.2	12.4	-0.1	Coeur D'Alene	CDA
12451000	1534	355	1732	5.2	8.1	-1.5	Lake Chelan	LKC
13011500	2471	2055	957	1.5	8.2	-6.0	Snake Headwaters	SHW
13022500	2486	1772	876	0.6	8.2	-6.1	Snake Headwaters	SHW
13078000	1934	1524	416	6.4	13.1	-0.2	Upper Snake	UPP
13147900	2184	1614	554	4.4	11.0	-3.4	Upper Snake	UPP
13185000	1955	996	928	4.6	11.5	-2.0	Boise	BOI
13186000	2141	1288	876	4.0	10.6	-2.8	Boise	BOI
13313000	2180	1439	1120	2.5	8.7	-5.2	Salmon	SAL
13330000	2101	1121	1201	2.4	8.2	-3.5	Lower Snake	LOW
13337000	1584	449	1298	4.0	10.0	-1.5	Clearwater	CLW
13340600	1443	512	1432	4.6	10.7	-0.7	Clearwater	CLW
14020000	1209	578	1058	7.1	12.2	0.9	Middle Columbia	MID
14037500	2097	1496	815	5.1	9.8	-2.3	John Day	JDY
14050500	1554	1357	1372	5.4	11.5	-1.2	Deschutes	DES
14091500	1268	606	1281	6.7	12.8	0.2	Deschutes	DES
14095500	1134	778	1122	7.0	12.2	0.8	Deschutes	DES
14107000	1429	830	984	5.1	9.4	-0.8	Middle Columbia	MID
14138800	1000	781	2987	7.3	11.1	2.3	Sandy	SAN
14141500	725	301	2732	9.5	13.0	3.3	Sandy	SAN
14152500	627	265	1700	11.2	15.9	4.9	Willamette	WIL
14158500	1254	948	2185	6.9	12.3	0.4	Willamette	WIL
14159200	1281	534	1817	7.5	12.5	1.2	Willamette	WIL
14161500	983	435	2272	8.5	15.1	2.4	Willamette	WIL
14179000	1150	525	2054	7.4	12.3	1.3	Willamette	WIL
08NC004	2050	972	1639	2.6	3.4	-4.8	Upper Columbia	UPP
08NF001	1861	1169	1032	4.9	5.5	-4.7	Kootenay River	KOO
08NH119	2015	600	1446	7.6	4.3	-3.8	Duncan River	KOO
08NM174	1532	633	825	8.2	8.4	-1.4	Upper Columbia	UPP

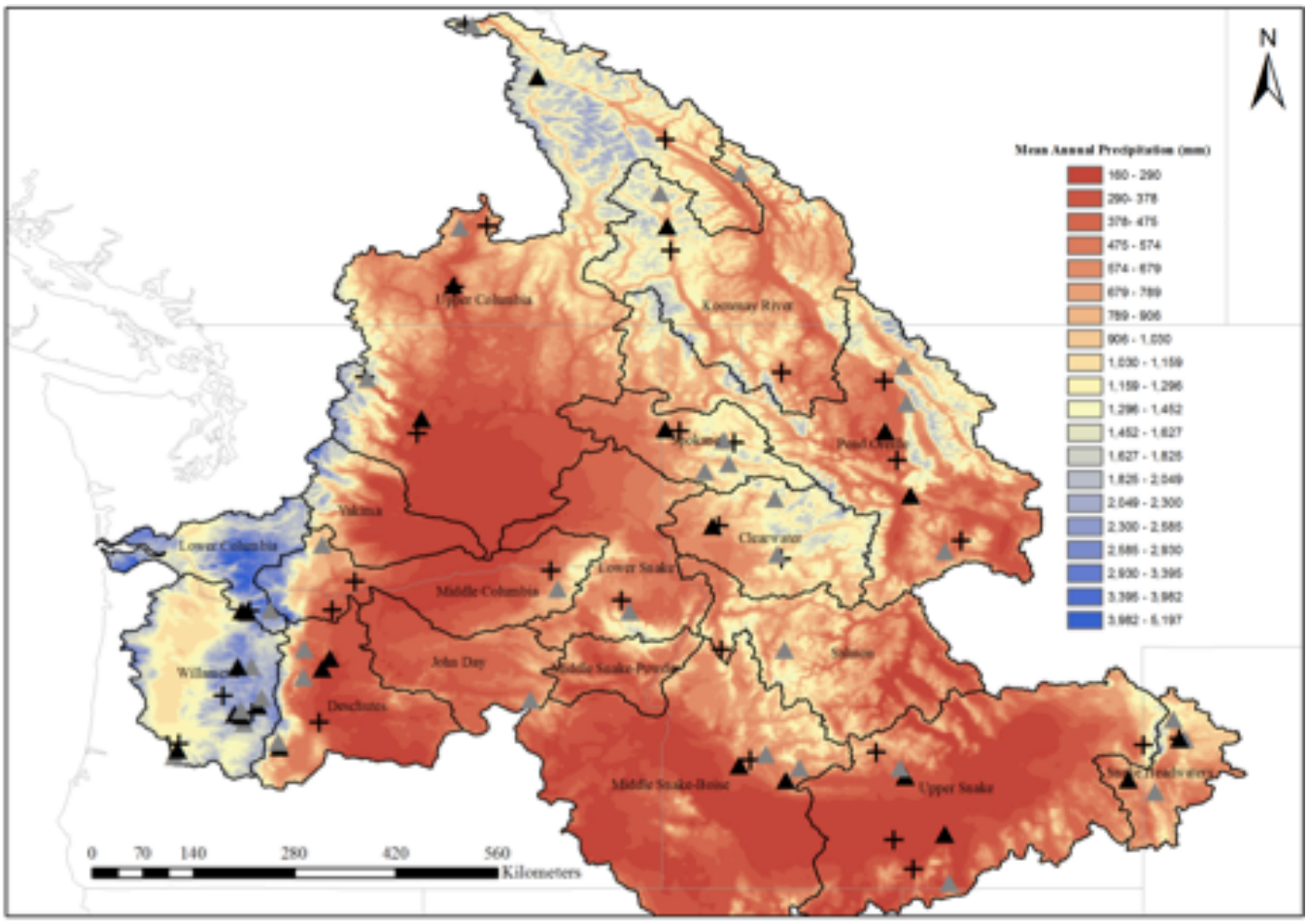

Figure A-3. Streamflow gauges and climate stations included in this study plotted over the PRISM mean annual precipitation climate normal for 1971 to 2000.

Table A-3. Normal storage capacity of dams studied obtained from the National Inventory of Dams.

Dam Name	State	Normal Storage (km^3)
Anderson Ranch Dam	ID	0.61
Arrowrock Dam	ID	0.35
Big Cliff Dam	OR	0.00
Blue River Dam	OR	0.10
Bull Run Dam 1	OR	0.03
Bull Run Dam 2	OR	0.03
Chelan Dam	WA	0.83
Cottage Grove Dam	OR	0.04
Cougar Dam	OR	0.26
Crane Prairie Dam	OR	0.07
Detroit Dam	OR	0.19
Duncan Dam	BC	1.80
Dworshak Dam	ID	4.28
Jackson Lake Dam	WY	1.04
Kerr Dam	MT	1.50
Libby Dam	MT	7.43
Little Wood River Dam	ID	0.04
Lucky Peak Dam	ID	0.36
Mica Dam	BC	24.76
Minidoka Dam	ID	0.26
Okanagan Lake Dam	BC	24.60
Palisades Dam	ID	1.73
Pelton Dam	OR	0.05
Post Falls Dam	ID	0.28
Post Falls Dam	ID	0.28
Post Falls Dam	ID	0.28
Round Butte Dam	OR	0.66
Trail Bridge Dam	OR	0.00

Table A-4. Above dam streamflow gauges with reference category and disturbance comments from the USGS Gauges II project.

Gauge	Reference	WR Report Remarks	Screening Comments
12332000	Ref	Minor local irrigation diversions	Mostly roadless, small diversions near gage
12358500	Ref	-	Mostly roadless, some local irrigation
12370000	Non-ref	Diversions for irrigation of about 360 acres upstream	Outlet of large natural lake (Swan Lake)
12413000	Ref	-	Some small local irrigation
12414500	Ref	-	Proximal logging, wilderness HW
12414900	Non-ref	-	Forested and logging, irrigated pasture & lt development
12451000	Ref	No known regulation or diversion	Mostly wilderness, Glacer Peak Wilderness
13011500	Ref	No diversion or regulation	Wilderness, Yellowstone Natoinal Park
13022500	Non-ref	-	Upstrm reservoir, Jackson Lake
13078000	Non-ref	Diversions above station for irrigation of about 16,000 acres	Upstrm irrigated agriculture and diiversions
13147900	Non-ref	Diversions above station for irrigation of about 1,300 acres	Proximal irrigated agriculture on main trib
13185000	Ref	-	Mostly roadless
13186000	Non-ref	No regulation. Diversions above station for irrigation of about 450 acres (1966 determination).	Mostly roadless
13313000	Ref	Small diversion from Johnson Creek to Deadwood River until September 20, 1988	Some roads
13330000	Non-ref	Diversions for irrigation upstream from station	Proximal off-channel impoundment & upstrm diversion, undelveloped basin
13337000	Ref	-	Some roads and logging
13340600	Ref	No regulation or diversion upstream from station	Wilderness area
14020000	Ref	No regulation or diversion upstream from station	Roads and logging in HW
14037500	Ref	Flow affected by natural storage in Strawberry Lake. No diversions upstream from station.	Stawberry Mountain Wilderness
14050500	Non-ref	No regulation or diversion upstream from station.	Spring
14091500	Non-ref	No regulation. Many small diversions for irrigation upstream	Spring
14095500	Ref	No regulation or diversion upstream from station.	Many forest roads and logging
14107000	Ref	No regulation or diversion upstream from station.	Little developemnt, roadless hw
14138800	Ref	No regulation or diversion upstream	Some forest roads
14141500	Ref	No regulation or diversion upstream	Some forest roads
14152500	Ref	No regulation. Diversions for irrigation upstream from station.	Agriculture in basin, logging in HW
14158500	Ref	Flow regulated by natural storage in lake.	Natural lake outlet
14159200	Ref	No regulation or diversion upstream	Mostly roadless, some wilderness
14161500	Ref	No regulation or diversion	Some forest roads
14179000	Ref	No regulation or diversion upstream from station	Many forest roads and logging
08NC004	Ref	-	No forest roads or logging
08NF001	Ref	-	National Park with one paved road and several trails
08NH119	Ref	-	One paved road, little to no forestry
08NM174	Ref	-	Some roads and logging

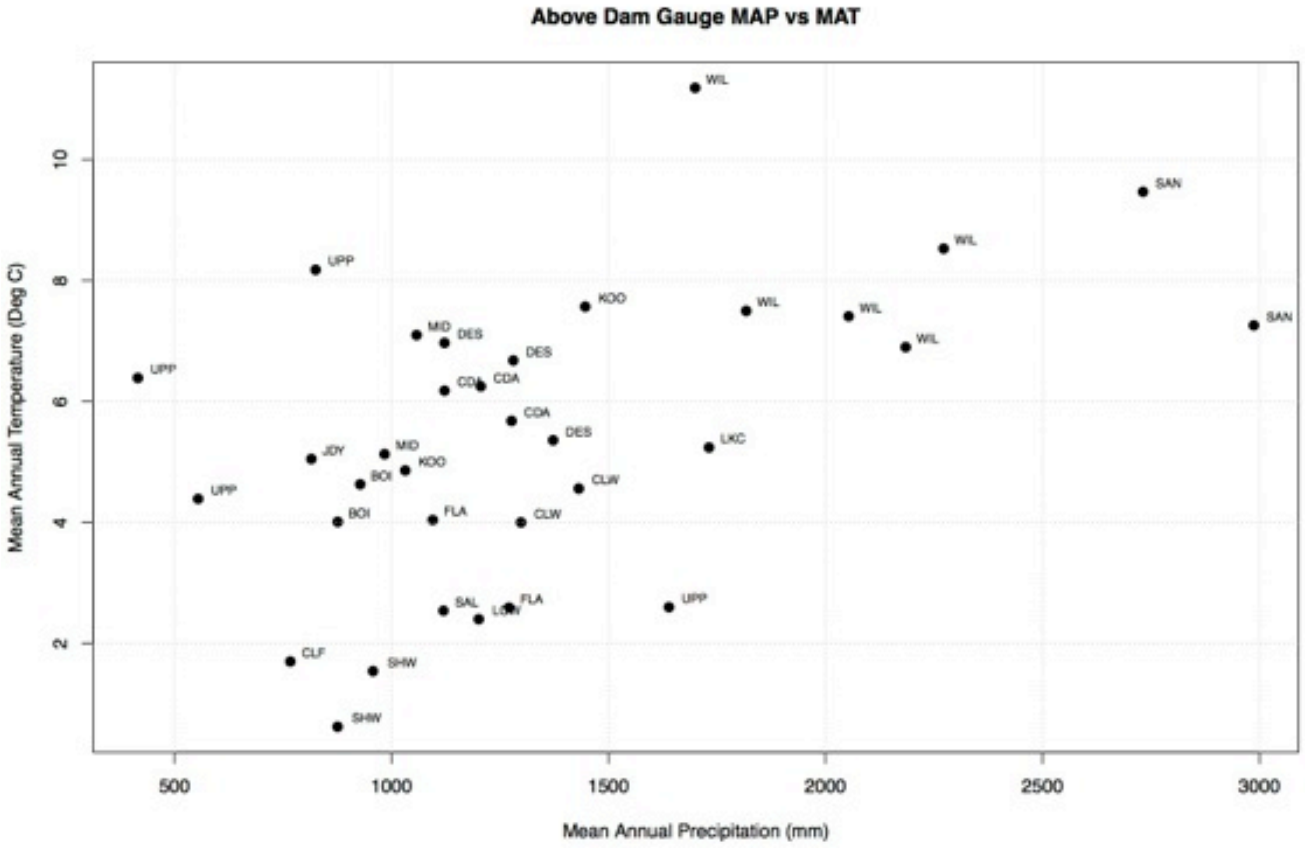

Figure A-5. Mean annual precipitation vs. mean annual temperature for all study sites.

Table A-6. Mean annual flow volume for above dam catchments.

Gauge	Mean annual flow (million cubic meters)	Mean annual flow (cubic km)
12332000	105.59	0.10559
12358500	2628.58	2.62858
12370000	1063.07	1.06307
12413000	1717.9	1.7179
12414500	2129.41	2.12941
12414900	312.72	0.31272
12451000	1300.18	1.30018
13011500	239.18	0.23918
13022500	3954.74	3.95474
13078000	16.22	0.01622
13147900	126.98	0.12698
13185000	1107.48	1.10748
13186000	670.99	0.67099
13313000	316.54	0.31654
13330000	165.79	0.16579
13337000	2585.38	2.58538
13340600	3062.71	3.06271
14020000	206.27	0.20627
14037500	11.67	0.01167
14050500	56.46	0.05646
14091500	1383.77	1.38377
14095500	139.58	0.13958
14107000	224.54	0.22454
14138800	51.01	0.05101
14141500	130.76	0.13076
14152500	186.36	0.18636
14158500	409.06	0.40906
14159200	565.61	0.56561
14161500	110.7	0.1107
14179000	525.76	0.52576
08NC004	453.58	0.45358
08NF001	154.68	0.15468
08NH119	1966.99	1.96699
08NM174	20.66	0.02066

GIS data for HUC 6 sub-basins obtained from the National Atlas (http://www.nationalatlas.gov/maplayers.html)

GIS data for streamflow gauges in the US was obtained from the USGS Gauges project (http://water.usgs.gov/GIS/metadata/usgswrd/XML/gagesII_Sept2011.xml).

GIS data for BC streamflow gauges (http://www.geobase.ca/geobase/en/)

GIS data for US and BC dams, National Inventory of Dams (http://geo.usace.army.mil/pgis/f?p=397:12)

GIS data for reservoirs in the US was obtained from the USGS (http://water.usgs.gov/GIS/metadata/usgswrd/XML/reservoir.xml)

GIS data for US climate stations

(http://cdiac.ornl.gov/epubs/ndp/ushcn/ushcn_map_interface.html)

GIS data for BC climate stations

(http://geobc.gov.bc.ca/)

Appendix B

Linear trend results by individual streamflow gauge and climate station

Climate

As patterns and changes in climate, along with other variables, are physical determinants of trends in discharge, analyses of climate were performed prior to those of streamflow. Linear trend from daily linear regression analyses as well as cyclical or edge patterning results from wavelet analyses of bias corrected power are displayed in the following climate results sections.

Linear trends results from individual climate stations for the variables of precipitation, maximum surface air temperature and minimum surface air temperature, are displayed in figures B-1 through B-16. At the study site scale, significant increases and decreases in precipitation do not display coherent trends. Significant increases and decreases appear to be randomly spaced throughout the year occurring in close proximity to one another. Maximum surface air temperatures at the study sites display mostly significant increases throughout the calendar year, though sites in the Clearwater, Clark Fork, Coeur D'Alene, John Day and other sub-basins additionally display many days with significant decreases in maximum temperature. Minimum surface air temperatures at each site display the most frequent significant trends of the three climate variables analyzed. Nearly all climate stations show predominantly daily significant increases in minimum temperature throughout the year.

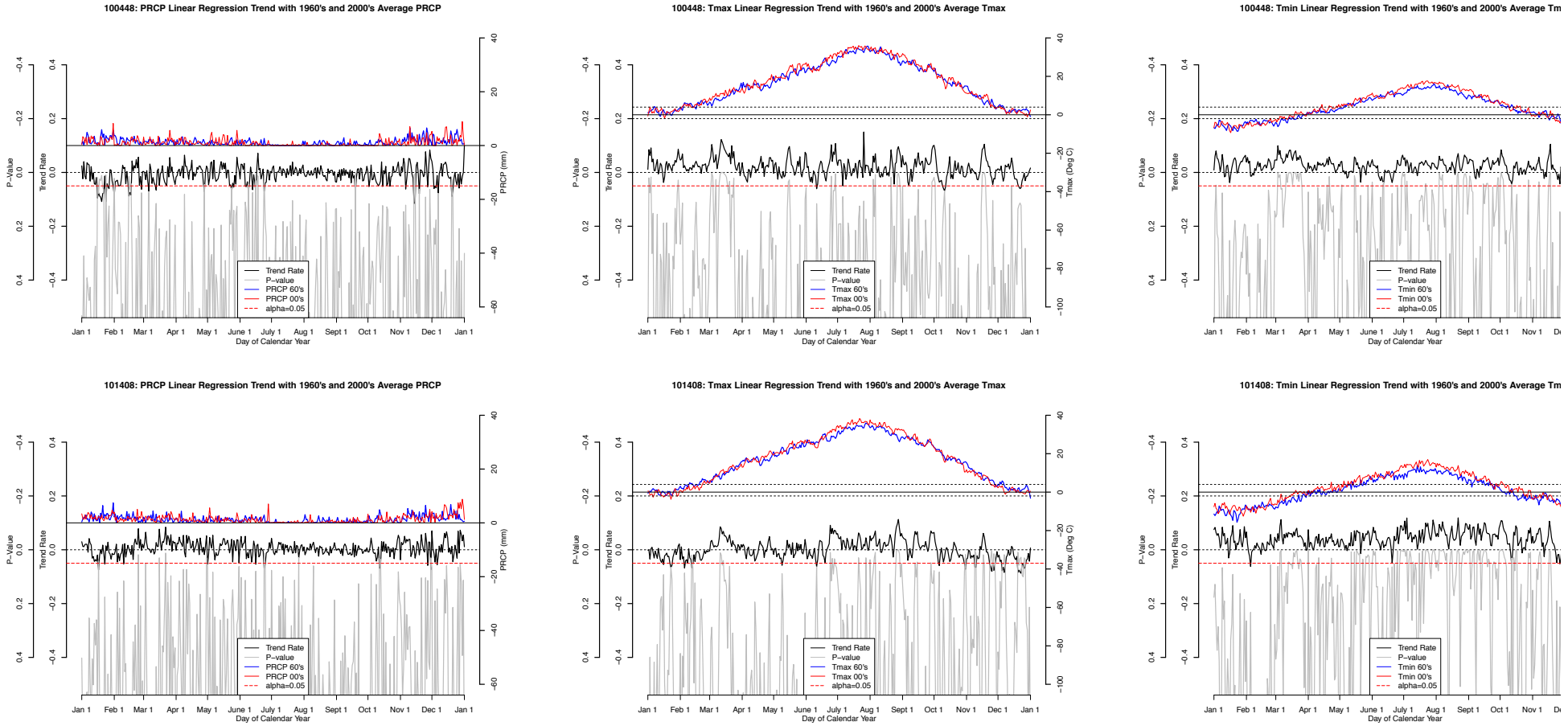

Figure B-1. Daily significant increases and decreases in precipitation, maximum temperature and minimum temperature along with 1960's and 2000's mean precipitation and temperatures. Trend rate units are log(mm)/year for precipitation and Deg C/year for temperatures. Temperature plots have dotted lines at -2 and 4 degrees C representing the rain to snow transition zone.

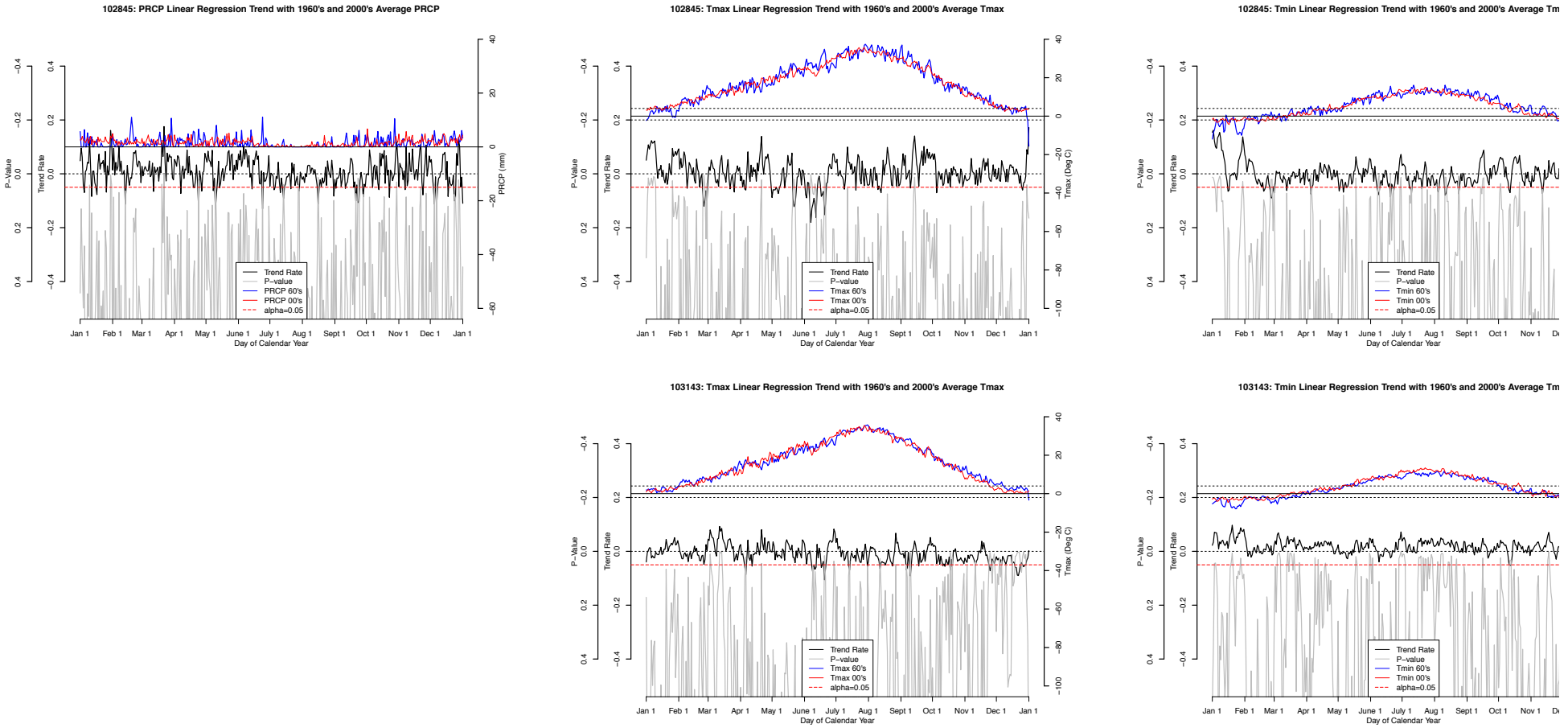

Figure B-2. Daily significant increases and decreases in precipitation, maximum temperature and minimum temperature along with 1960's and 2000's mean precipitation and temperatures. Trend rate units are log(mm)/year for precipitation and Deg C/year for temperatures. Temperature plots have dotted lines at -2 and 4 degrees C representing the rain to snow transition zone.

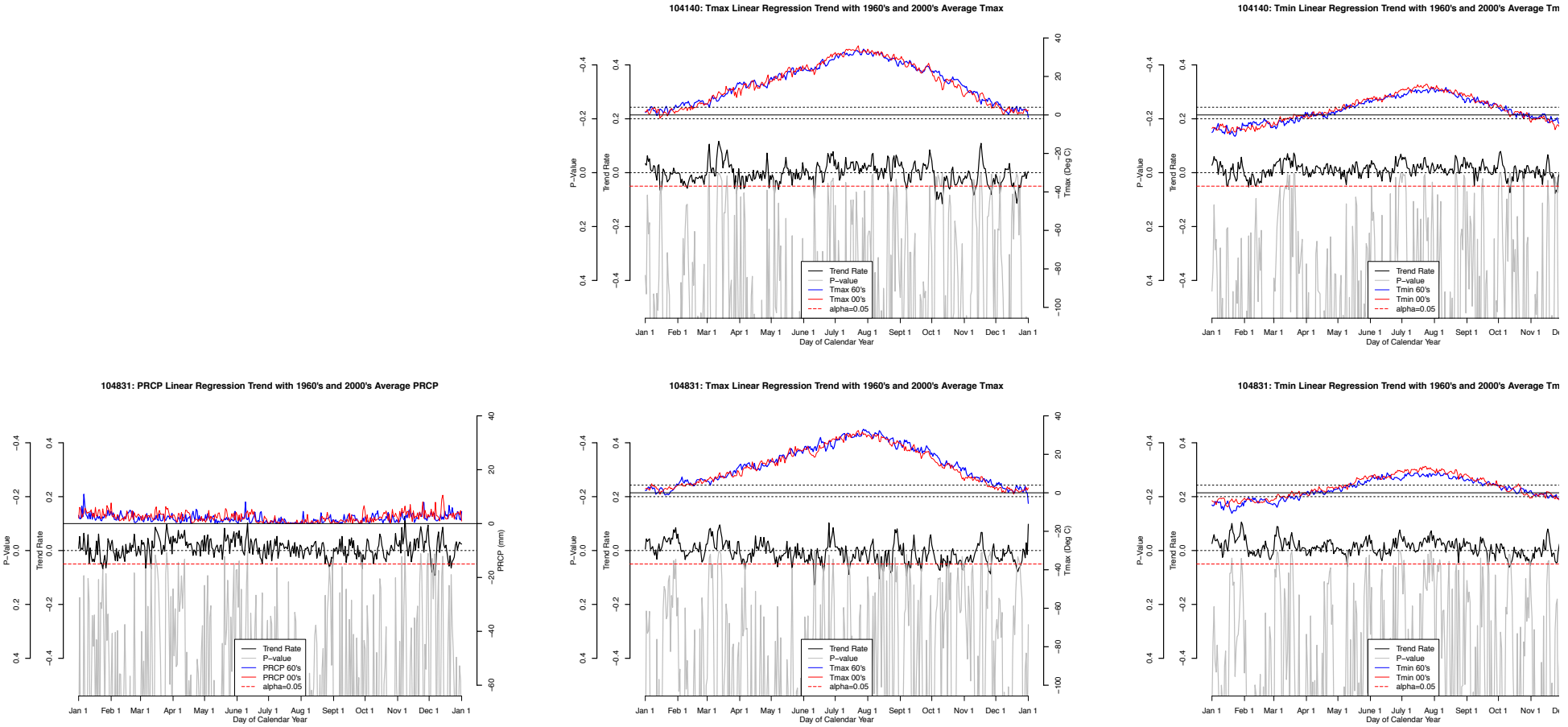

Figure B-3. Daily significant increases and decreases in precipitation, maximum temperature and minimum temperature along with 1960's and 2000's mean precipitation and temperatures. Trend rate units are log(mm)/year for precipitation and Deg C/year for temperatures. Temperature plots have dotted lines at -2 and 4 degrees C representing the rain to snow transition zone.

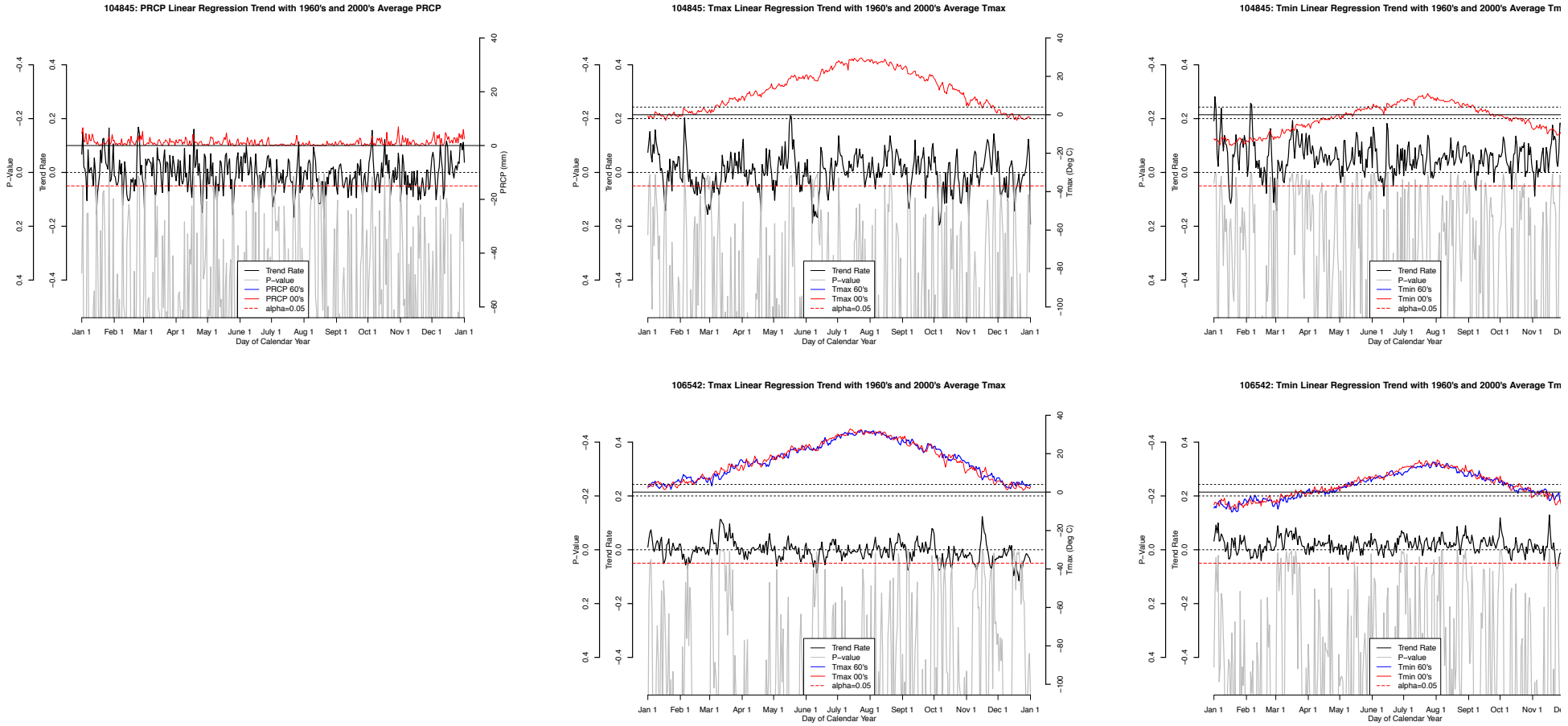

Figure B-4. Daily significant increases and decreases in precipitation, maximum temperature and minimum temperature along with 1960's and 2000's mean precipitation and temperatures. Trend rate units are log(mm)/year for precipitation and Deg C/year for temperatures. Temperature plots have dotted lines at -2 and 4 degrees C representing the rain to snow transition zone.

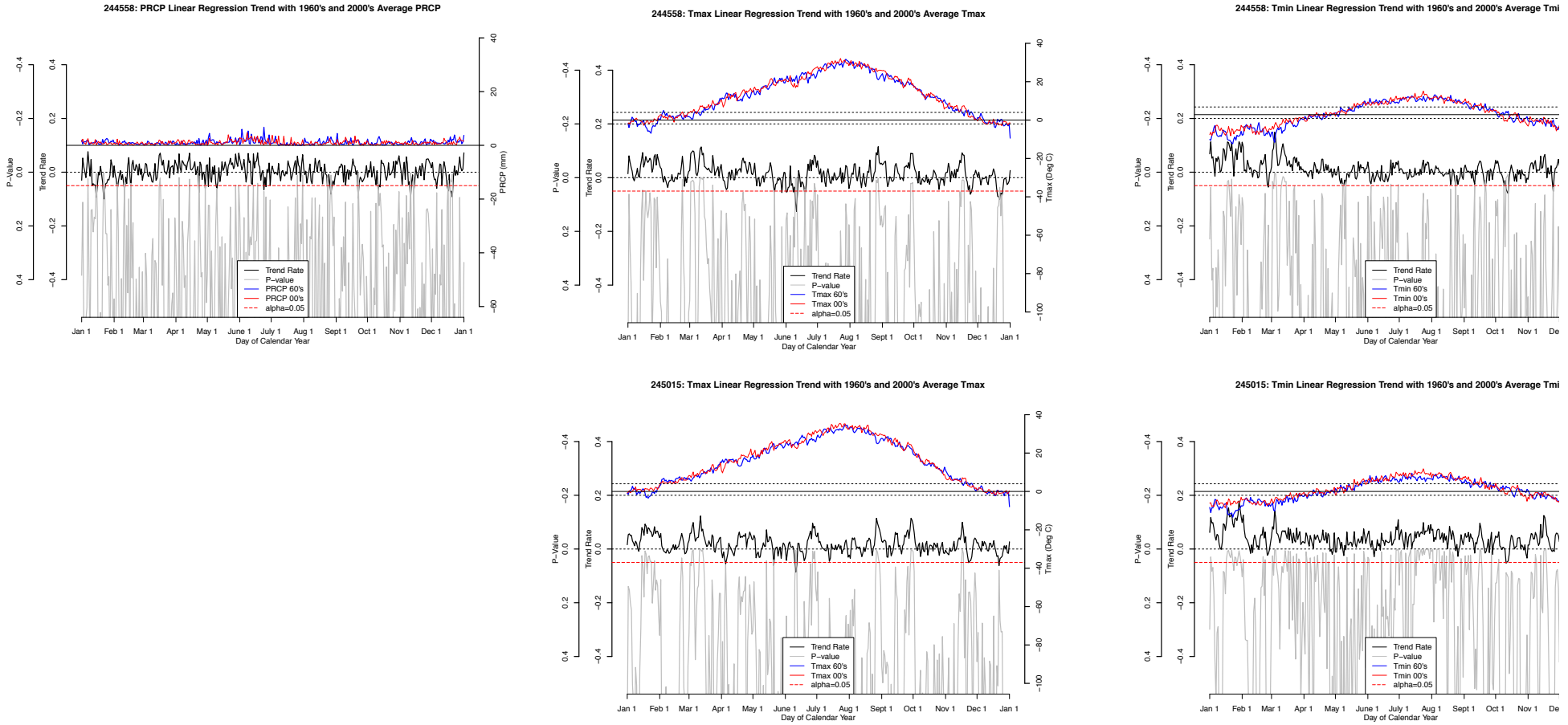

Figure B-5. Daily significant increases and decreases in precipitation, maximum temperature and minimum temperature along with 1960's and 2000's mean precipitation and temperatures. Trend rate units are log(mm)/year for precipitation and Deg C/year for temperatures. Temperature plots have dotted lines at -2 and 4 degrees C representing the rain to snow transition zone.

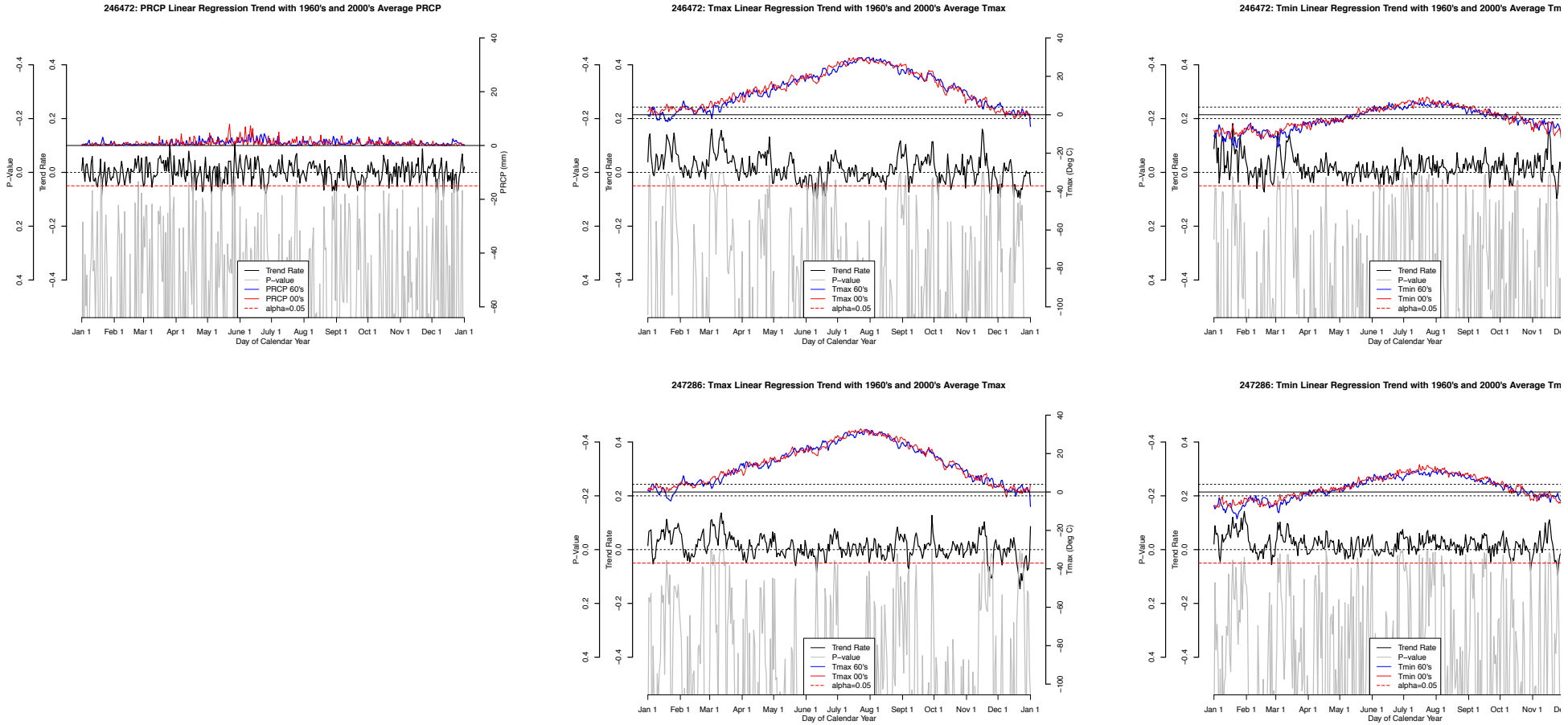

Figure B-6. Daily significant increases and decreases in precipitation, maximum temperature and minimum temperature along with 1960's and 2000's mean precipitation and temperatures. Trend rate units are log(mm)/year for precipitation and Deg C/year for temperatures. Temperature plots have dotted lines at -2 and 4 degrees C representing the rain to snow transition zone.

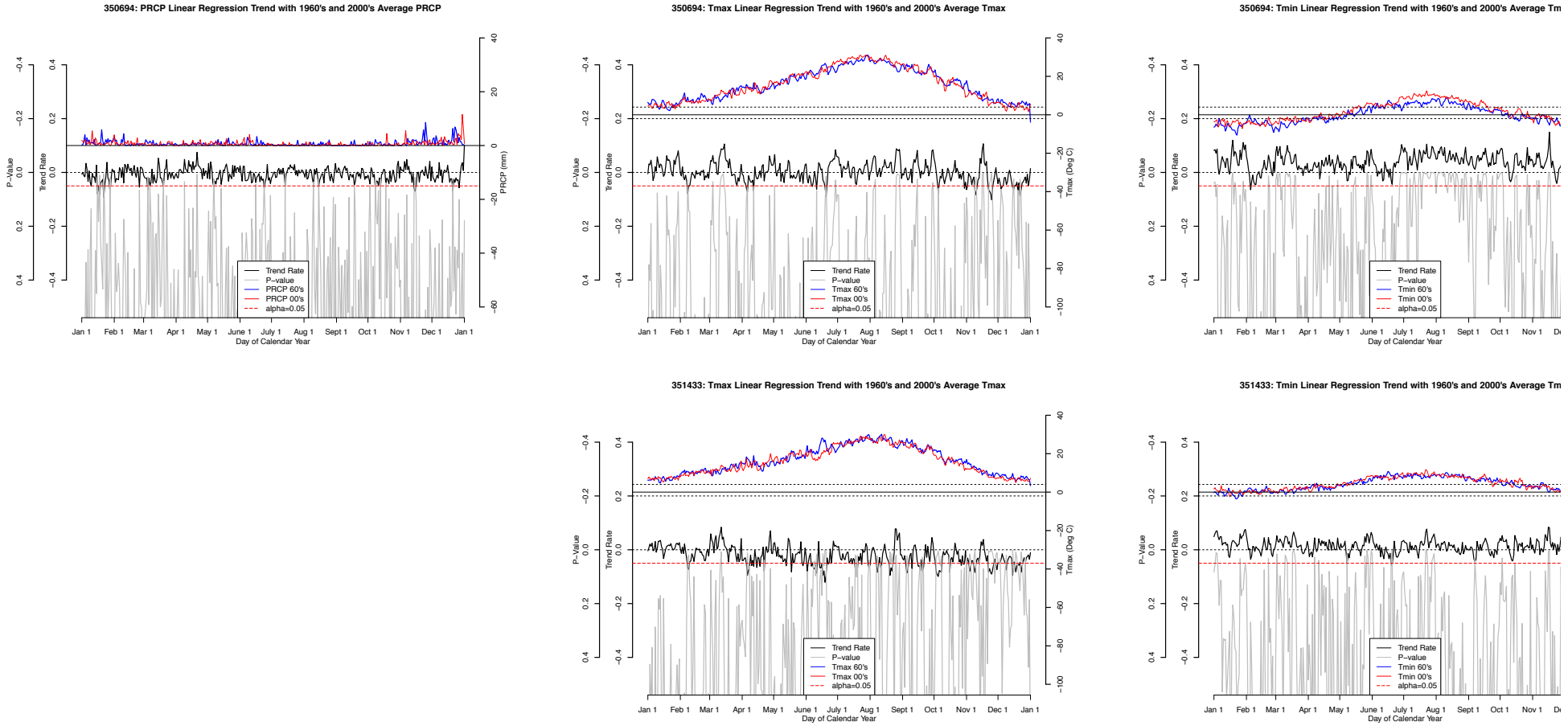

Figure B-7. Daily significant increases and decreases in precipitation, maximum temperature and minimum temperature along with 1960's and 2000's mean precipitation and temperatures. Trend rate units are log(mm)/year for precipitation and Deg C/year for temperatures. Temperature plots have dotted lines at -2 and 4 degrees C representing the rain to snow transition zone.

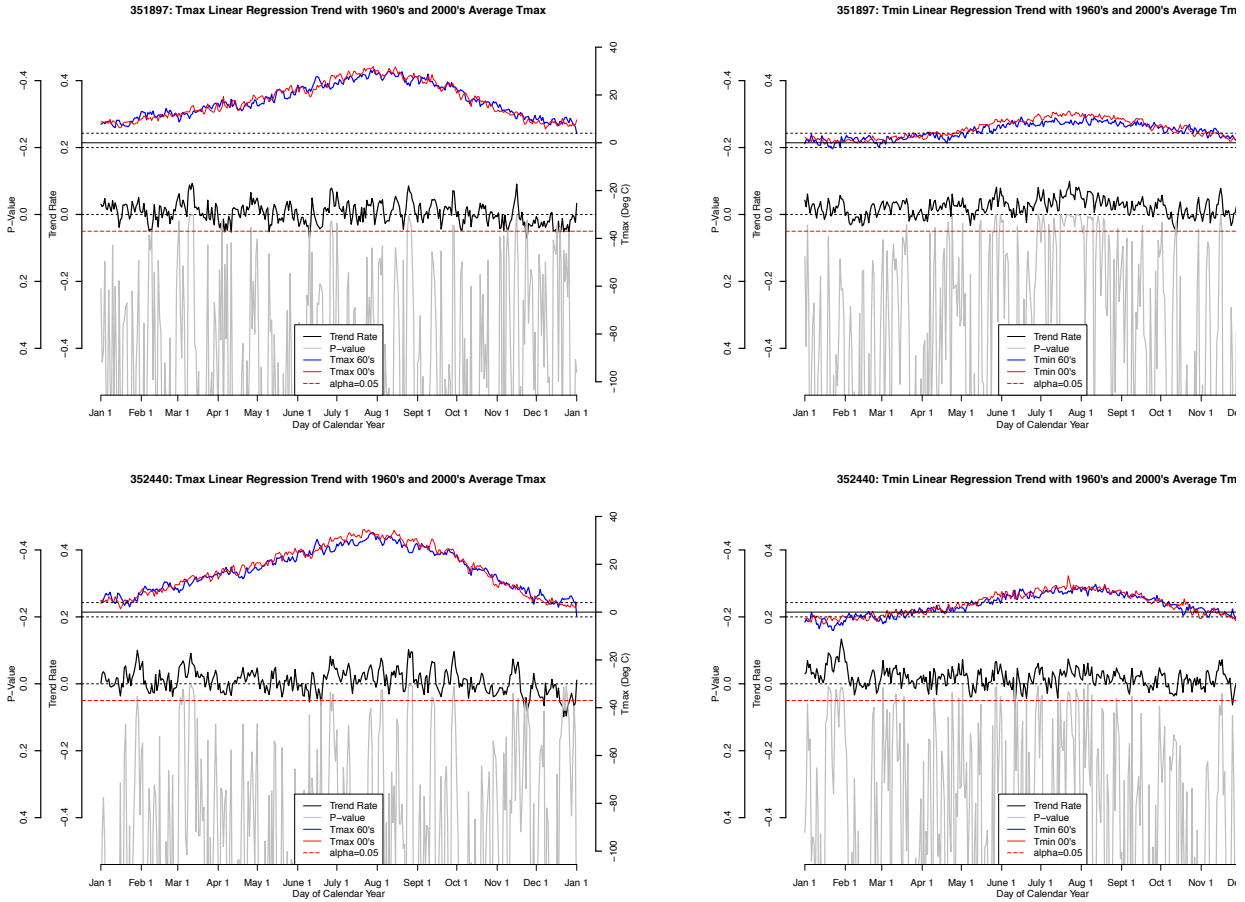

Figure B-8. Daily significant increases and decreases in precipitation, maximum temperature and minimum temperature along with 1960's and 2000's mean precipitation and temperatures. Trend rate units are log(mm)/year for precipitation and Deg C/year for temperatures. Temperature plots have dotted lines at -2 and 4 degrees C representing the rain to snow transition zone.

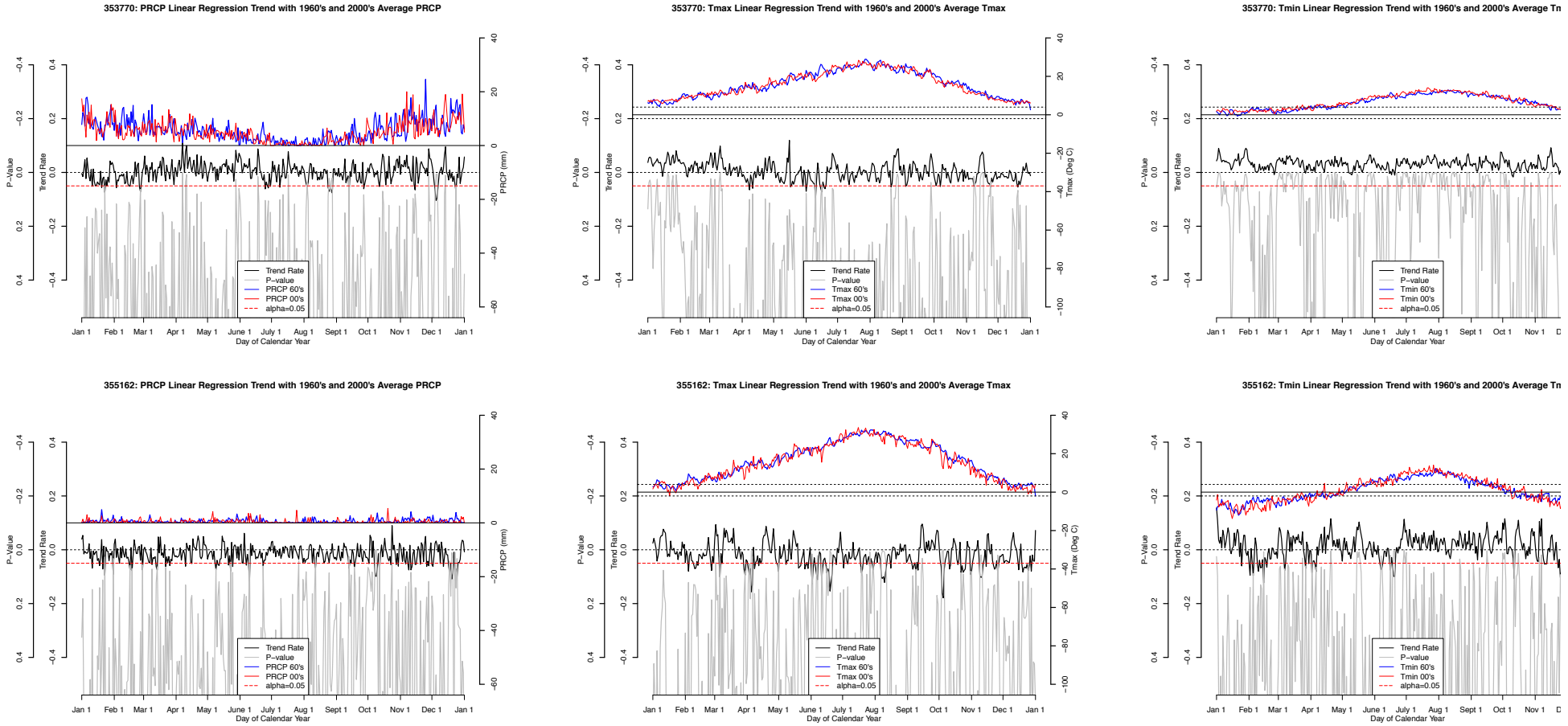

Figure B-9. Daily significant increases and decreases in precipitation, maximum temperature and minimum temperature along with 1960's and 2000's mean precipitation and temperatures. Trend rate units are log(mm)/year for precipitation and Deg C/year for temperatures. Temperature plots have dotted lines at -2 and 4 degrees C representing the rain to snow transition zone.

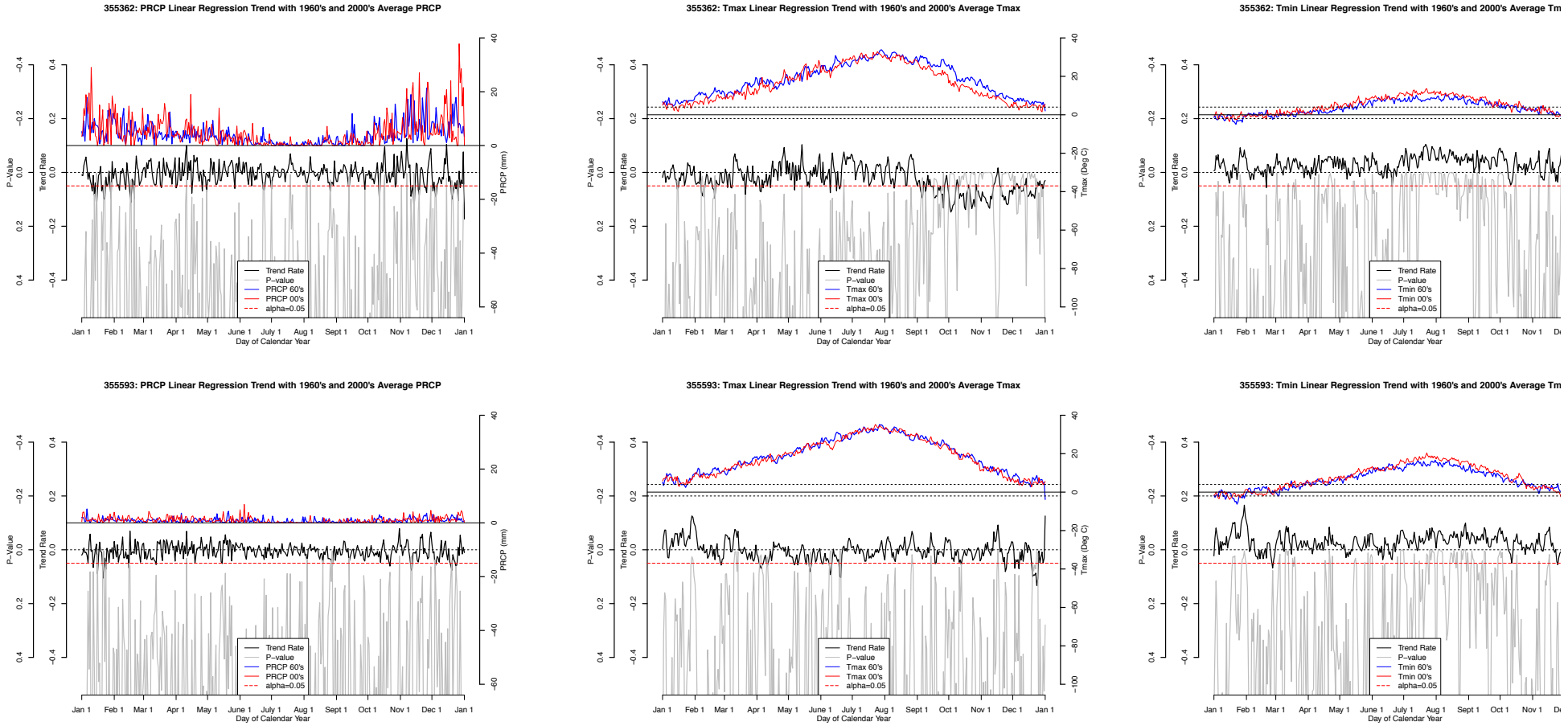

Figure B-10. Daily significant increases and decreases in precipitation, maximum temperature and minimum temperature along with 1960's and 2000's mean precipitation and temperatures. Trend rate units are log(mm)/year for precipitation and Deg C/year for temperatures. Temperature plots have dotted lines at -2 and 4 degrees C representing the rain to snow transition zone.

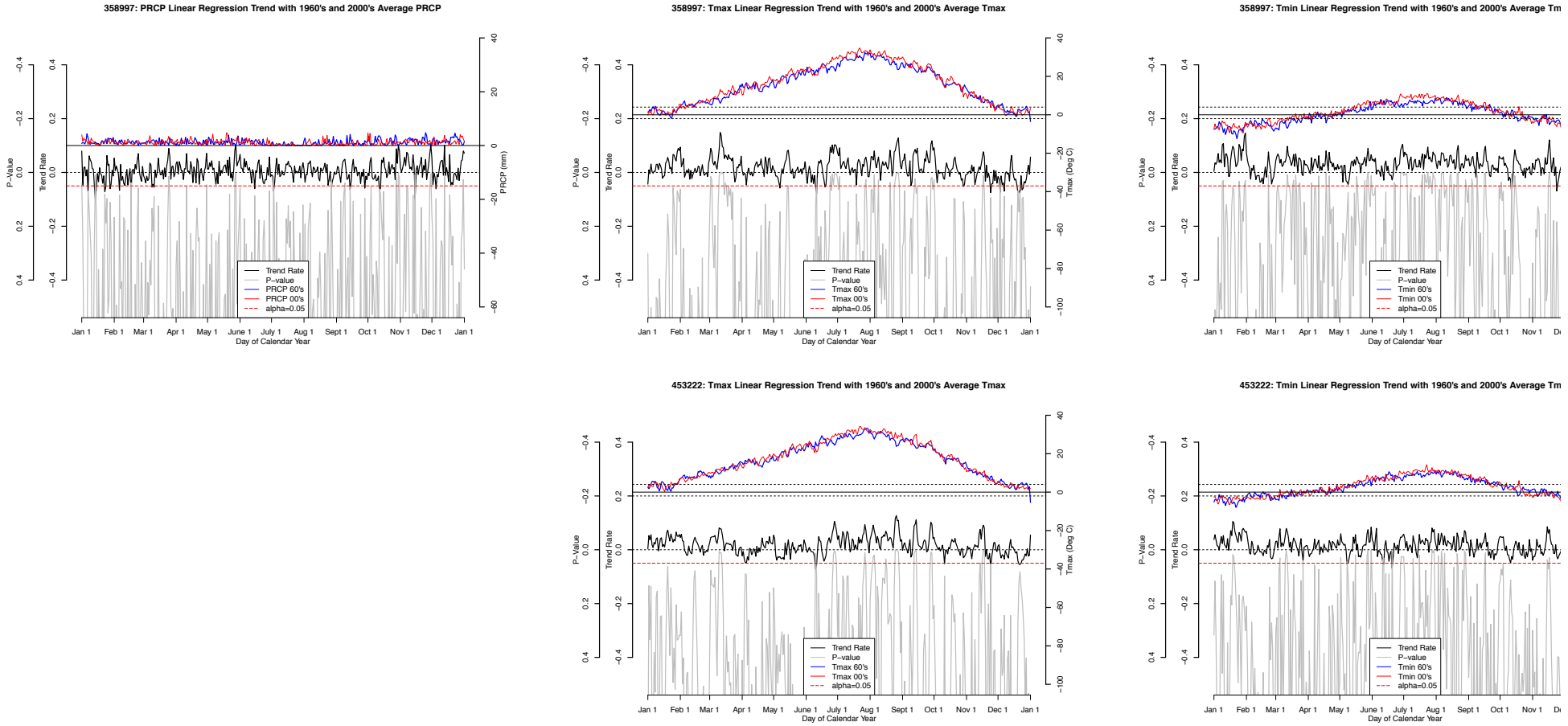

Figure B-11. Daily significant increases and decreases in precipitation, maximum temperature and minimum temperature along with 1960's and 2000's mean precipitation and temperatures. Trend rate units are log(mm)/year for precipitation and Deg C/year for temperatures. Temperature plots have dotted lines at -2 and 4 degrees C representing the rain to snow transition zone.

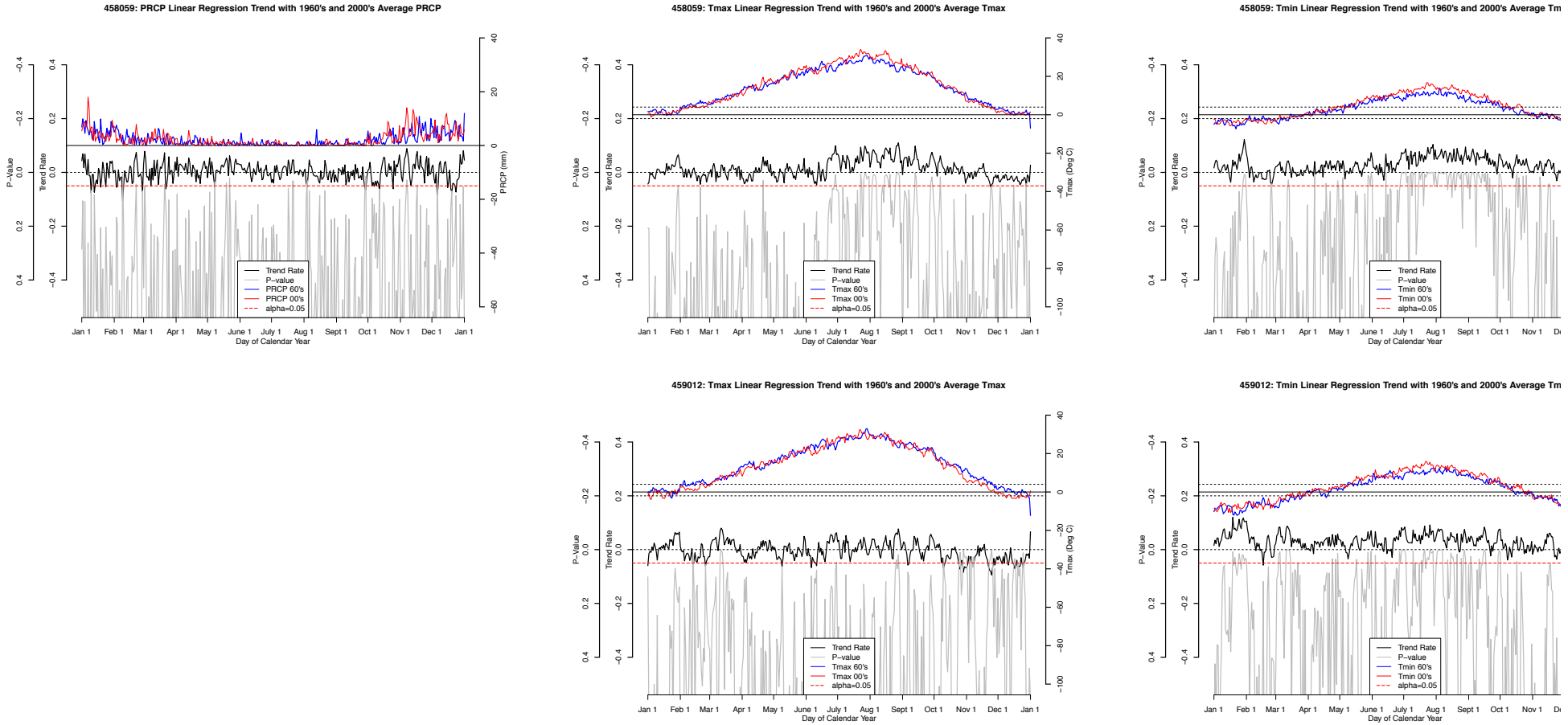

Figure B-12. Daily significant increases and decreases in precipitation, maximum temperature and minimum temperature along with 1960's and 2000's mean precipitation and temperatures. Trend rate units are log(mm)/year for precipitation and Deg C/year for temperatures. Temperature plots have dotted lines at -2 and 4 degrees C representing the rain to snow transition zone.

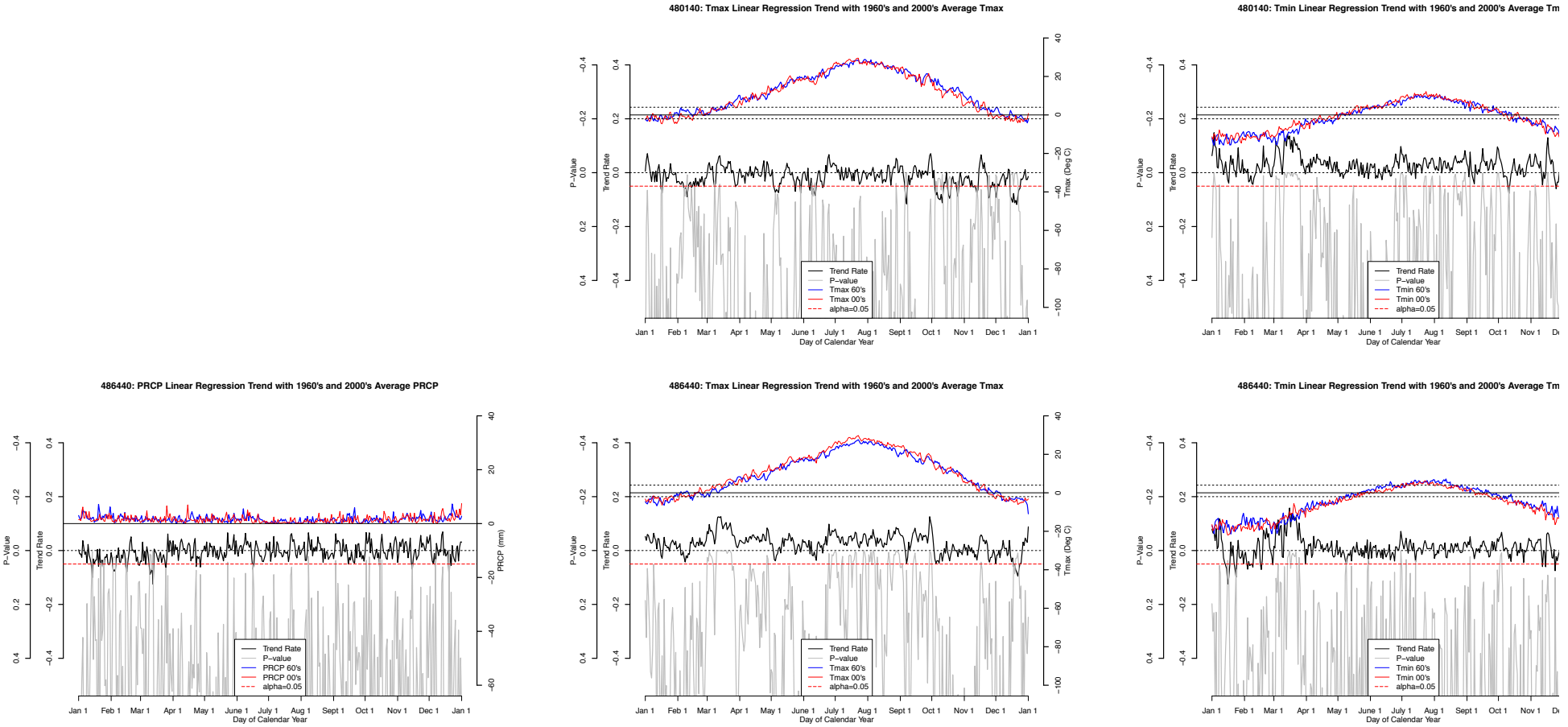

Figure B-13. Daily significant increases and decreases in precipitation, maximum temperature and minimum temperature along with 1960's and 2000's mean precipitation and temperatures. Trend rate units are log(mm)/year for precipitation and Deg C/year for temperatures. Temperature plots have dotted lines at -2 and 4 degrees C representing the rain to snow transition zone.

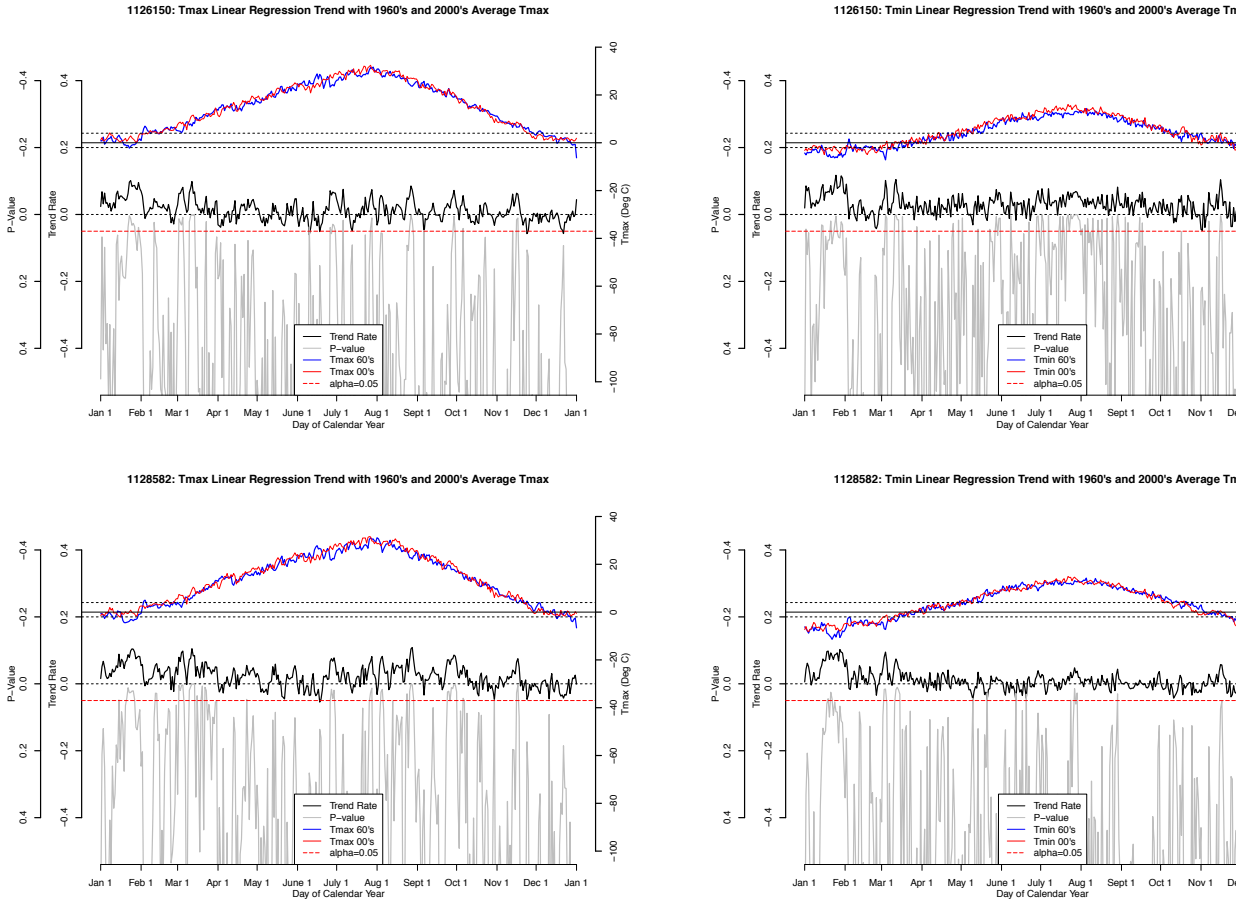

Figure B-14. Daily significant increases and decreases in precipitation, maximum temperature and minimum temperature along with 1960's and 2000's mean precipitation and temperatures. Trend rate units are log(mm)/year for precipitation and Deg C/year for temperatures. Temperature plots have dotted lines at -2 and 4 degrees C representing the rain to snow transition zone.

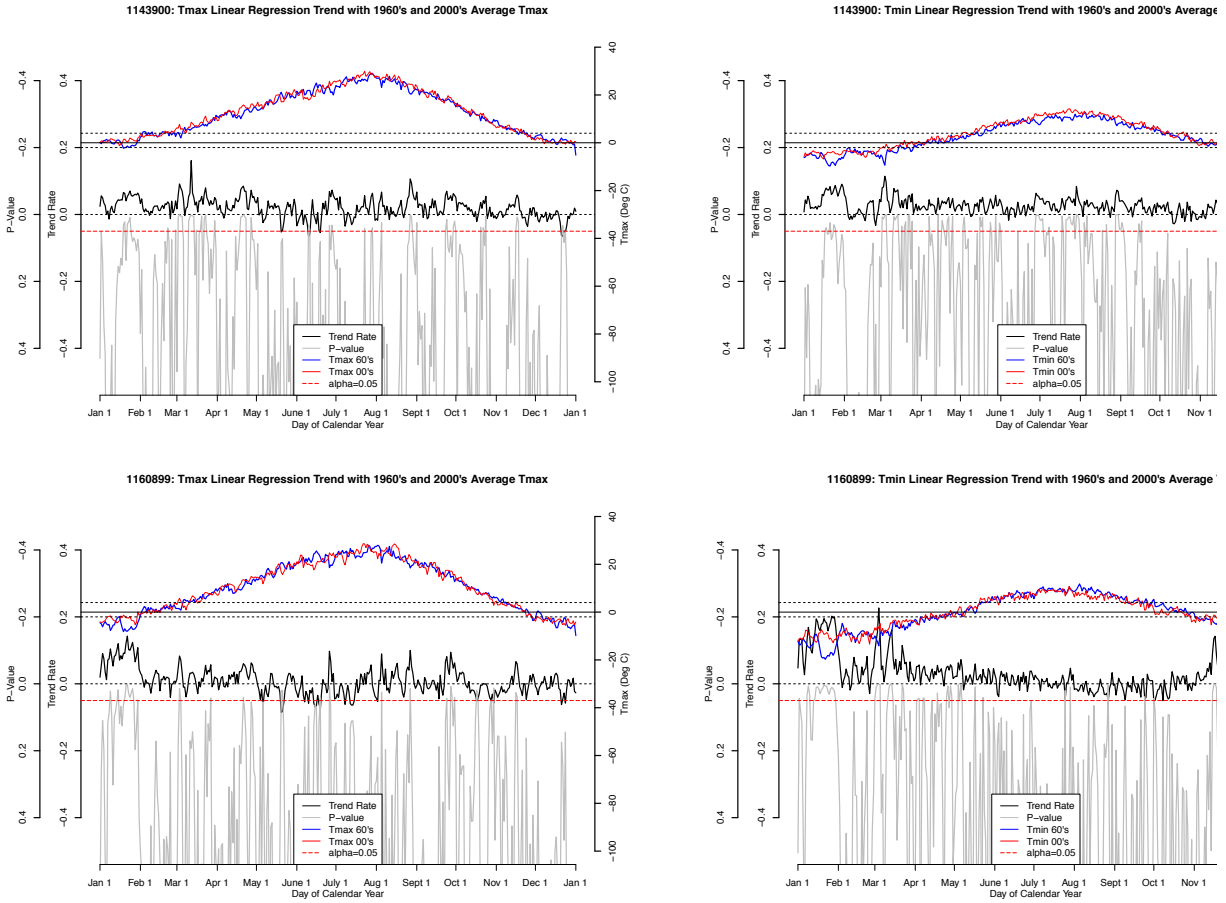

Figure B-15. Daily significant increases and decreases in precipitation, maximum temperature and minimum temperature along with 1960's and 2000's mean precipitation and temperatures. Trend rate units are log(mm)/year for precipitation and Deg C/year for temperatures. Temperature plots have dotted lines at -2 and 4 degrees C representing the rain to snow transition zone.

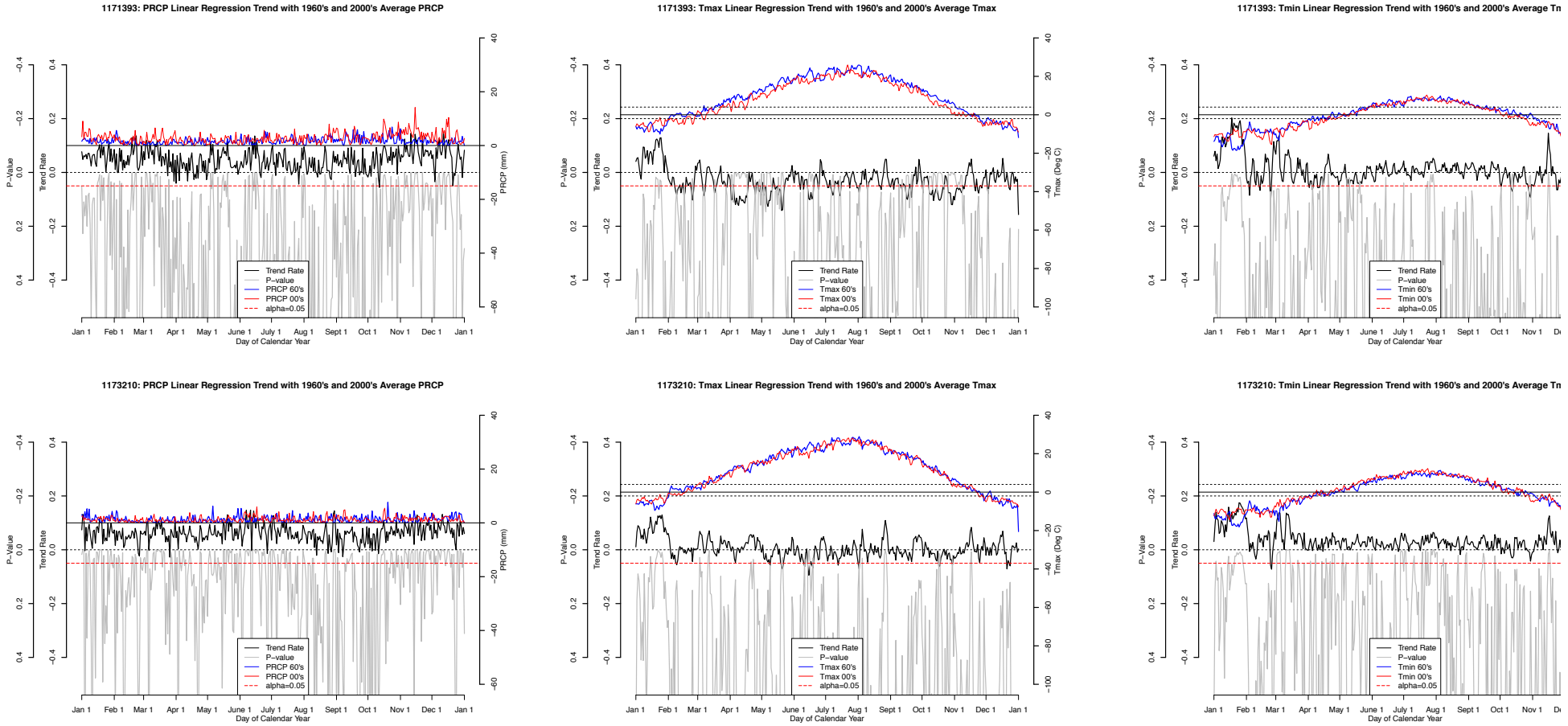

Figure B-16. Daily significant increases and decreases in precipitation, maximum temperature and minimum temperature along with 1960's and 2000's mean precipitation and temperatures. Trend rate units are log(mm)/year for precipitation and Deg C/year for temperatures. Temperature plots have dotted lines at -2 and 4 degrees C representing the rain to snow transition zone.

Streamflow

Results from individual streamflow gauges for the variables of discharge in cubic meters per second both above (figures B-17 to B-25) and below dams (B-26 to B-32) are displayed. In general, the magnitude of trend below dams is greater than that above dams in the Columbia River Basin. All below dam records include a maximum of four years of record prior to dam completion lowering the influence of dam construction on trend results.

Within the Boise sub-basin, both above dam gauges USGS 13185000 and 13186000 display significant increases in middle of March daily discharge as well as significant daily decreases in daily discharge in June and October flows. Additionally, the USGS 13186000 record displays significant decreases in December, January, February, June and July flows. The USGS 13190500 below dam record shows many days in March, April, May, August, and October with significant increases and significant decreases in June and late December flows. Anderson Ranch Dam above USGS 13190500 is managed for irrigation, flood control, recreation and hydropower. The USGS 13202000 below dam record displays mainly strong increases in flow from mid October to the beginning of February as well as a few days in the middle of March. Decreases of lower magnitude occurred during late July and early August flows. Lucky Peak Dam above USGS 13202000 is managed for flood control, irrigation and recreation. Lucky peak dam is also below the Anderson Ranch Dam system and thus receives the management signal from this dam.

In the Clearwater sub-basin above dam gauge USGS 12332000 displays significant increases in several middle of March daily flows as well as a few days in the

beginning of January and at the end of February with significant decreases in several days in June and July. The below dam USGS 12340500 shows decreases in September and October daily flows with a few scattered days with decreases in February, March, June, August, November and December flows, all with lesser magnitude than those seen in the Boise sub-basin. Milltown dam above USGS 12340500 is managed for hydropower.

The Clark Fork sub-basin above dam USGS 13340600 shows a few days with low magnitude significant decreasing flows in mid May and late September flows. The below dam USGS 13341050 shows greater magnitude significant increases in July to September daily flows with scattered decreases in flows during the winter months. Dworshak Dam above USGS 13341050 is managed for hydropower, flood control, and recreation.

The Coeur D'Alene sub-basin above dam USGS 12413000 shows significant increases in mid March daily flows and decreases in mid May and September and October flows with USGS 12414900 showing parallel increase and decreases. Above dam USGS 12414500 only displays a few days of decrease in September flows while below dam USGS 12419000 show many decreases in May flows with increases in July through October flows. Post Falls dam above USGS 12419000 is managed for irrigation and hydropower.

The Deschutes sub-basin above dam USGS 14095500 displays many low magnitude significant decreases in summer, fall and winter flows with below dam USGS 14097100 showing only significant decreases in a few daily December flows. Warm Springs Dam above USGS 14097100 is managed for hydropower. Above dam USGS 14050500 shows many decreases in daily flows from January to August and December flows while below dam 14054000 shows only significant decreases in late May flows.

Craine Prairie Dam above USGS 14054000 is managed for irrigation and recreation. Above dam 14091500 displays a near absence of trend while below dam USGS 14092500 shows low magnitude increases in late October flows.

The Flathead sub-basin above dam USGS 1237000 displays small increases in late March flows with decreases in May, June, September, October and December flows. Below dam USGS 12372000 shows a period of daily increases from mid to late August with scattered decreases in January, February, May and October flows. Kerr Dam above USGS 12372000 is managed for hydropower and recreation.

The Kootenay sub-basin above dam WSC 08NF001 show strong increases in late January to mid May flows with scattered low magnitude decreases from mid May to August and again in October. Below dam USGS 12301933 shows high magnitude May to August and December increases and high magnitude decreases in September to November and January daily flows. Libby Dam above USGS 12301933 is managed for hydropower, flood control and recreation. Above dam WSC 08NH119 displays significant decreases in summer flows while below dam WSC 08NH118 shows increases in mid March to mid April flows with greater magnitude decreases in mid May to September and mid December flows. An increase in mid April above dam flows is shown, but is not significant at the alpha 0.05 level. Duncan Dam above WSC 08NH118 is managed for flood control and regulated flow for hydropower downstream.

In the Lake Chelan sub-basin, above dam USGS 1245100 displays increases in mid March flows as well as decreases in June to mid October flows while below dam USGS 12452500 shows greater magnitude decreases in mid March flows, increases in

mid April to June and October flows, and decreases in July to mid September flows. Chelan Dam above USGS 12452500 is managed for hydropower and recreation.

The Sandy sub-basin above dam USGS 14138800 displays increases in mid April flows and decreases in mid May, late summer and winter flows. Below dam USGS 14140000 shows mainly higher magnitude decreases in spring and summer flows. Bull Run Dam Two above USGS 1414000 is managed for Portland, Oregon's municipal water supply. Above dam USGS 14141500 displays scattered low magnitude decreases throughout the year while below dam USGS 14142500 shows a near parallel pattern. USGS 14142500 is also below the Bull Run Dam's managing Portland, Oregon's municipal water supply.

The Snake Headwaters sub-basin above dam USGS 13011500 displays many strong daily increases in April with decreases in late summer months. Below dam USGS 13011000 displays strong increases in October through March flows and mid April through mid June with decreases in July and August flows. Jackson Lake Dam above USGS 13011000 is managed for irrigation, flood control and recreation. Above dam USGS 13022500 displays only small decline in late July flows and increases in late September flows while below dam USGS 13032500 shows small increases in late September flows and scattered decreases in winter month flows as well as mid June flows. Palisades Dam above USGS 13032500 is managed for irrigation, flood control, hydropower and recreation.

In the Upper Columbia sub-basin, above dam WRS 08NM174 displays a strong significant increase in mid April flows along with strong decreases in daily August and September flows. Below dam WRS 08NM050 shows decreases in mid October through

January daily flows. Okanagan Lake Dam above WRS 08NM050 is managed for flood control, recreation and municipal water supply. Above dam WRS 08NC004 displays only weak decreases in August and September daily flows. There is also a non-significant increase in late April daily flows at alpha equals 0.05. BC Hydro Mica Dam outflow displays increases in early May and November through December daily flows with decreases in mid June through July flows. Mica Dam is managed for flood control and hydropower.

The Upper Snake sub-basin above dam USGS 13147900 displays decreases in early February and September flows while below dam USGS 13148500 shows strong decreases in October through February flows and smaller decreases during the summer months. Little Wood River Dam above USGS 13148500 is managed for irrigation, recreation and flood control. Above dam USGS 13078000 displays decreases in February daily flows as well as decreases from mid July to Mid December while below dam USGS 13081500 shows decreases in February through April flows and late October through December flows with weak increases in beginning of October daily flows.

The Willamette sub-basin contained the most gauge pairs of any sub-basin included in this study. Above dam USGS 14161500 displays small significant decreases in daily flows at the beginning of February, beginning of May, and from mid August to the end of October. Below dam USGS 14162200 shows strong decreases in February and July to September daily flows as well as strong increases in September to November and early January flows. Blue River Dam above USGS 14162200 is managed for flood control and recreation. Above dam USGS 14179000 displays daily decreases in early February and October flows. Below dam USGS 14181500 shows similar decreases in

February flows as well as increases in September and October flows. Detroit Dam above USGS 14181500 is managed for hydropower, flood control, and recreation. Above dam USGS 14159200 displays small increases in a few daily January and April flows and decreases in October flows. Below dam USGS 14159500 shows decreases in February and March flows and increases in July to November flows. Cougar Dam above USGS 14159500 is managed for hydropower and flood control. Above dam USGS 14158500 displays small declines in October daily flows. Below dam USGS 14158850 shows no significant linear trends in discharge. Trail Bridge Dam above USGS 14158850 is managed for hydropower. Above dam USGS 14152500 displays strong declines in January and February flows. Below dam USGS 14153500 shows a few decreases in January and February flows, strong increases in June and October flows, and strong decreases in August daily flows. Cottage Grove Dam above USGS 14153500 is managed for flood control, irrigation and recreation.

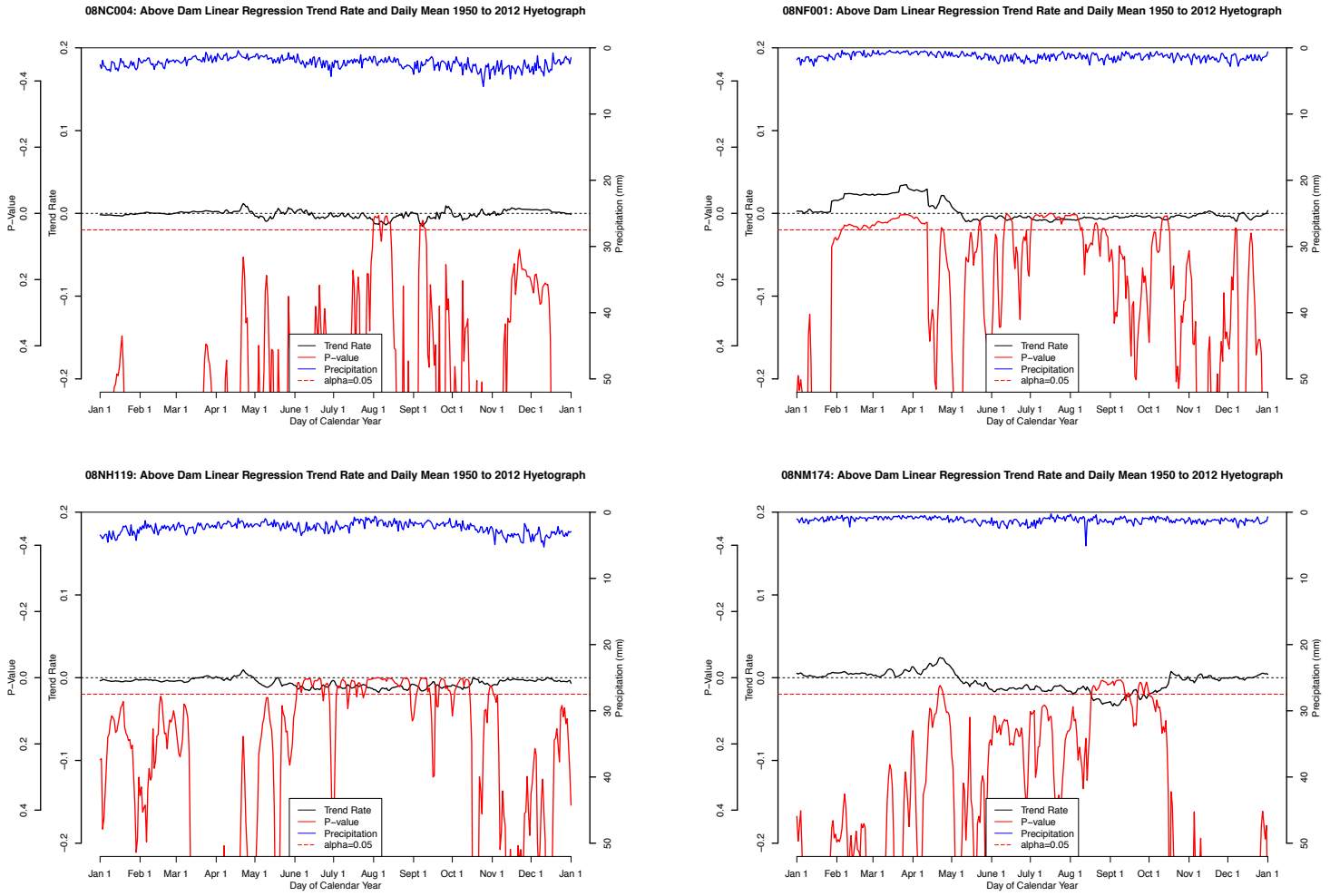

Figure B-17. Above dam daily significant increases and decreases in streamflow along with precipitation timing by study site. Trend rate units are ln(cms)/year.

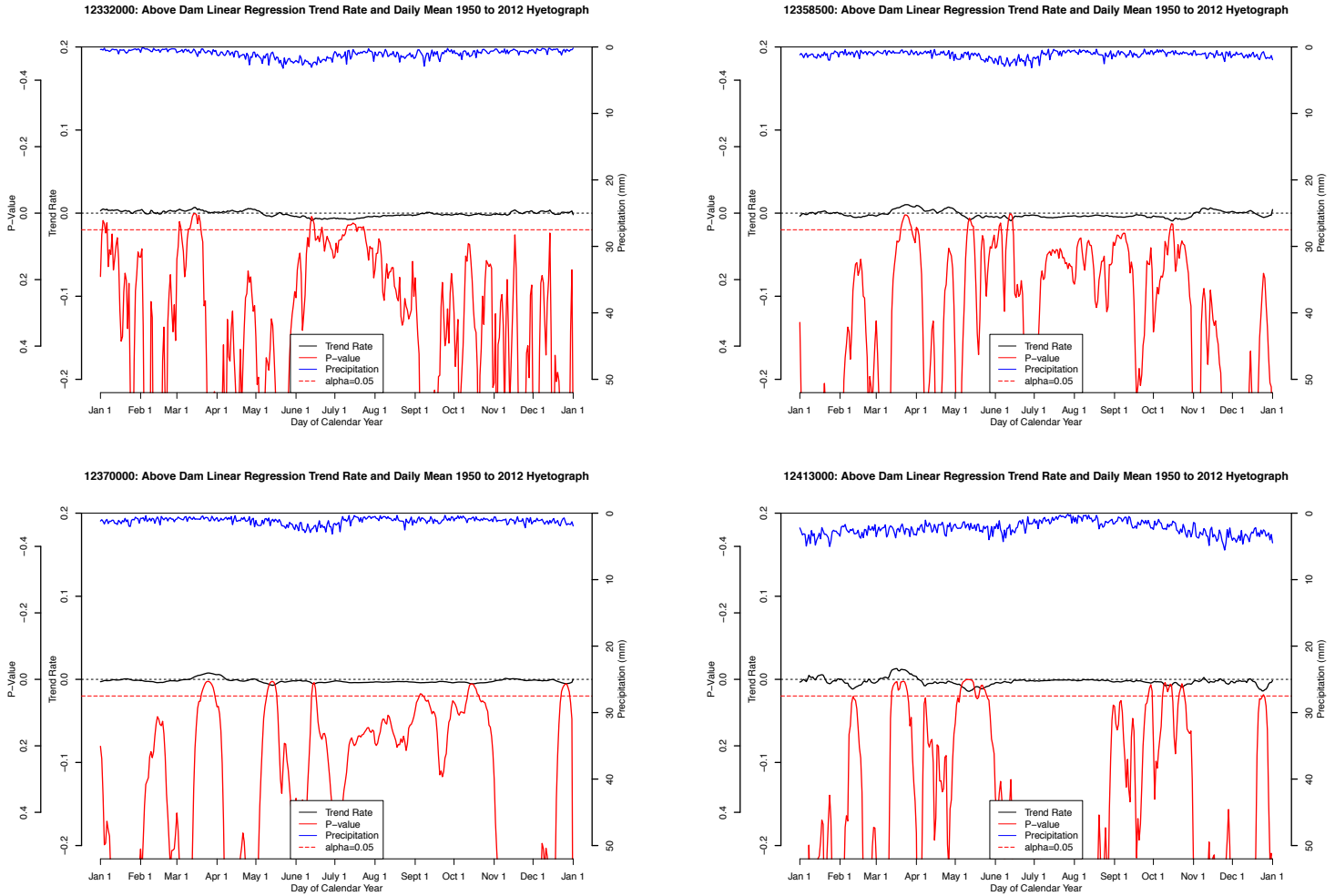

Figure B-18. Above dam daily significant increases and decreases in streamflow along with precipitation timing by study site. Trend rate units are ln(cms)/year.

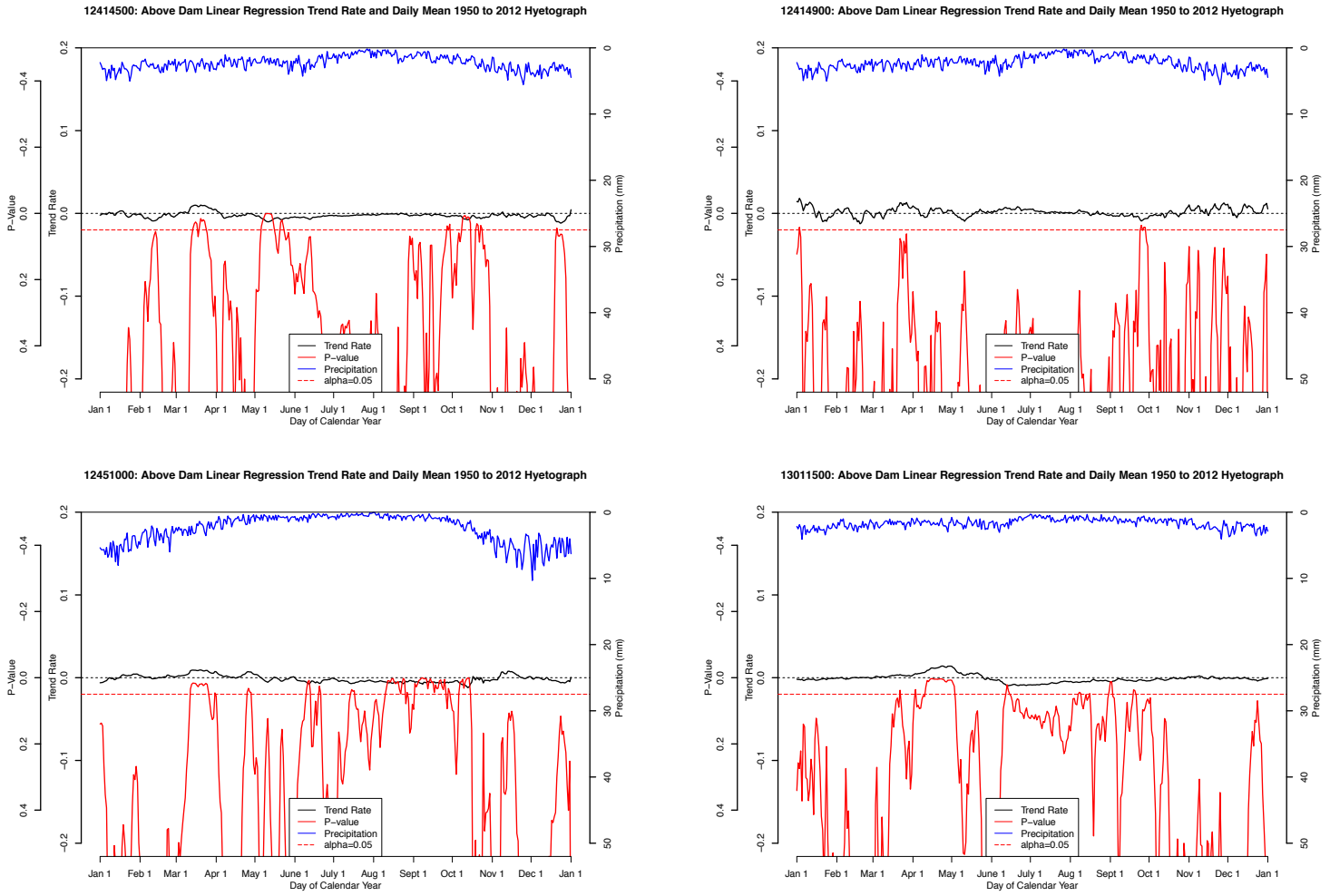

Figure B-19. Above dam daily significant increases and decreases in streamflow along with precipitation timing by study site. Trend rate units are ln(cms)/year.

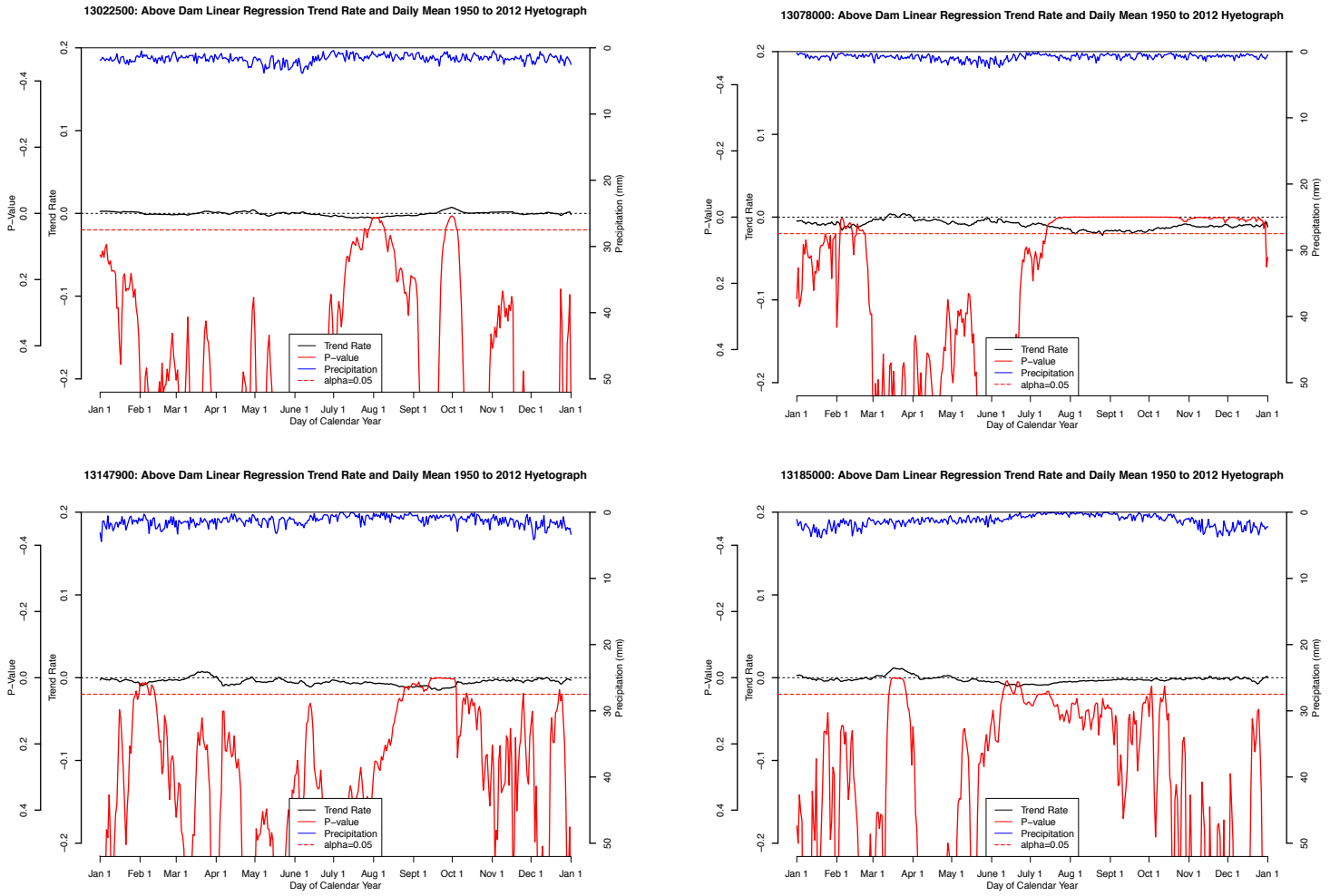

Figure B-20. Above dam daily significant increases and decreases in streamflow along with precipitation timing by study site. Trend rate units are ln(cms)/year.

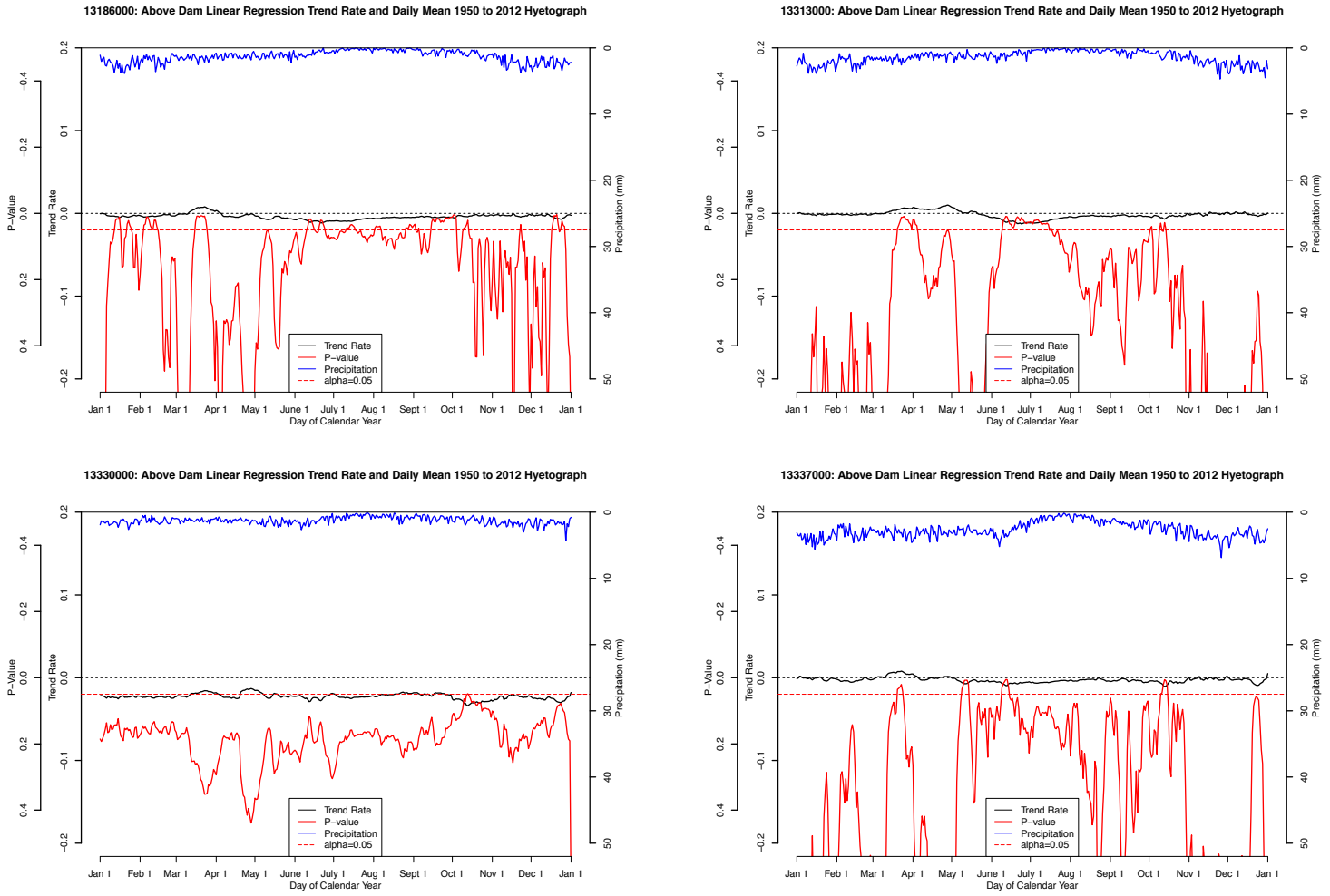

Figure B-21. Above dam daily significant increases and decreases in streamflow along with precipitation timing by study site. Trend rate units are ln(cms)/year.

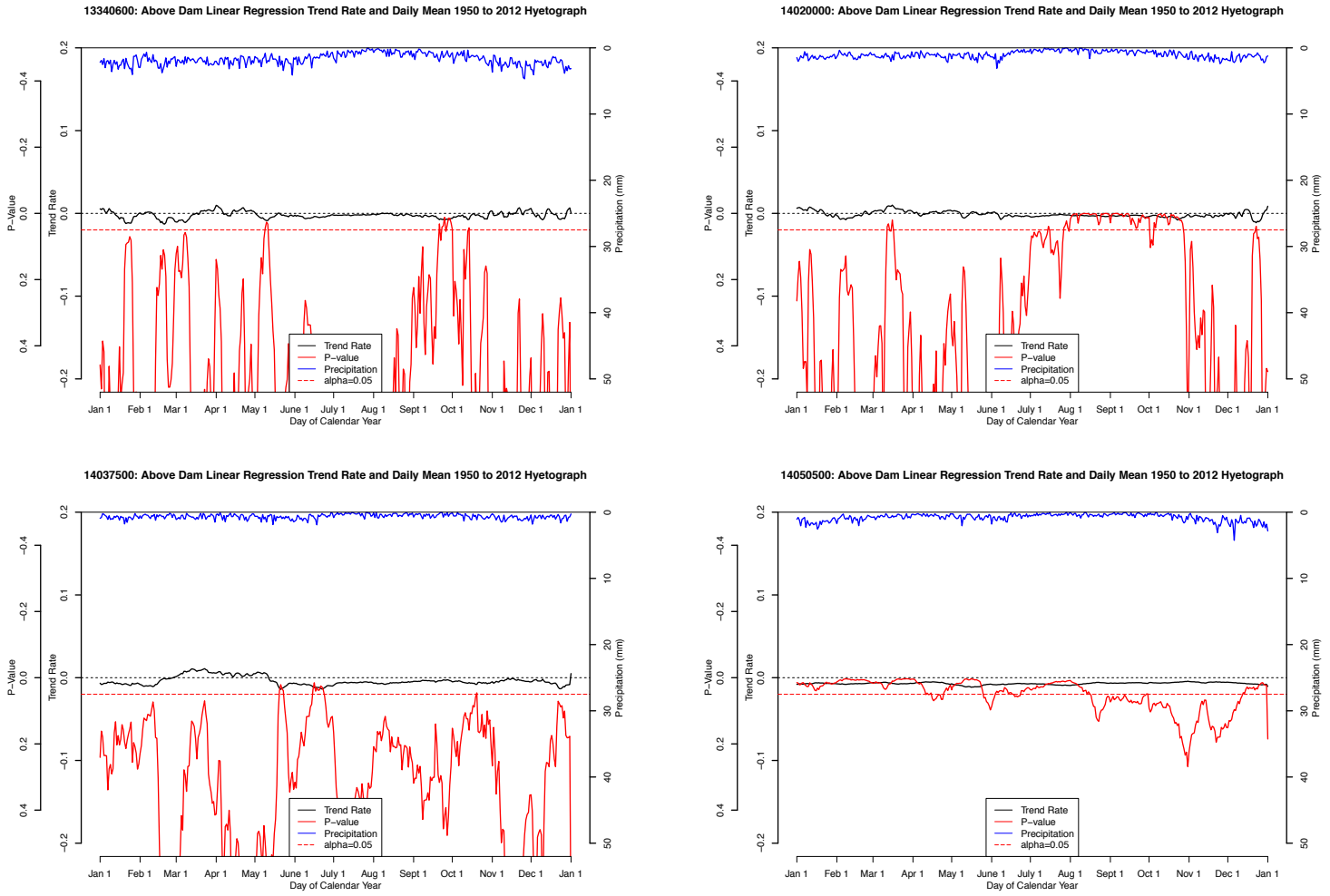

Figure B-22. Above dam daily significant increases and decreases in streamflow along with precipitation timing by study site. Trend rate units are ln(cms)/year.

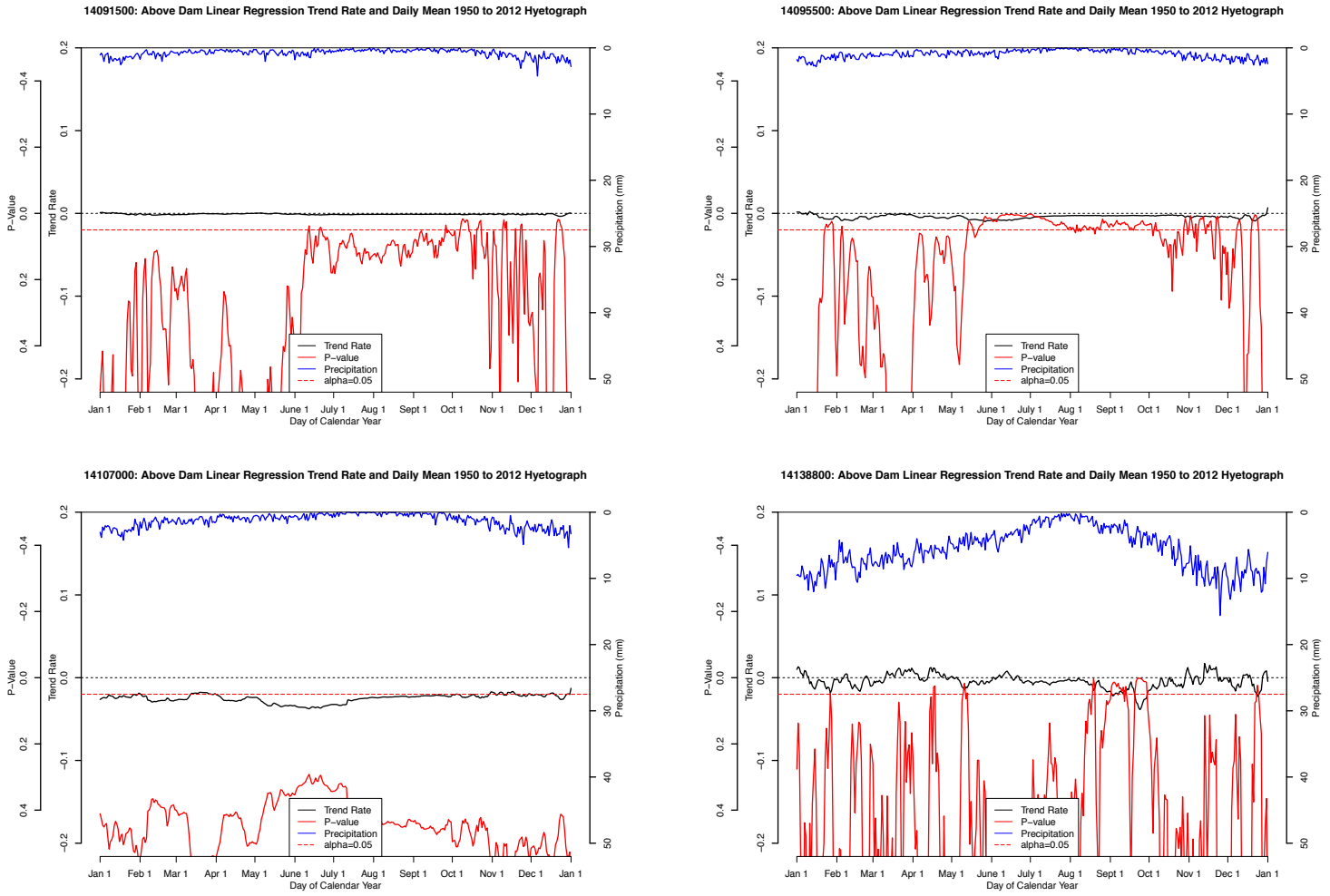

Figure B-23. Above dam daily significant increases and decreases in streamflow along with precipitation timing by study site. Trend rate units are ln(cms)/year.

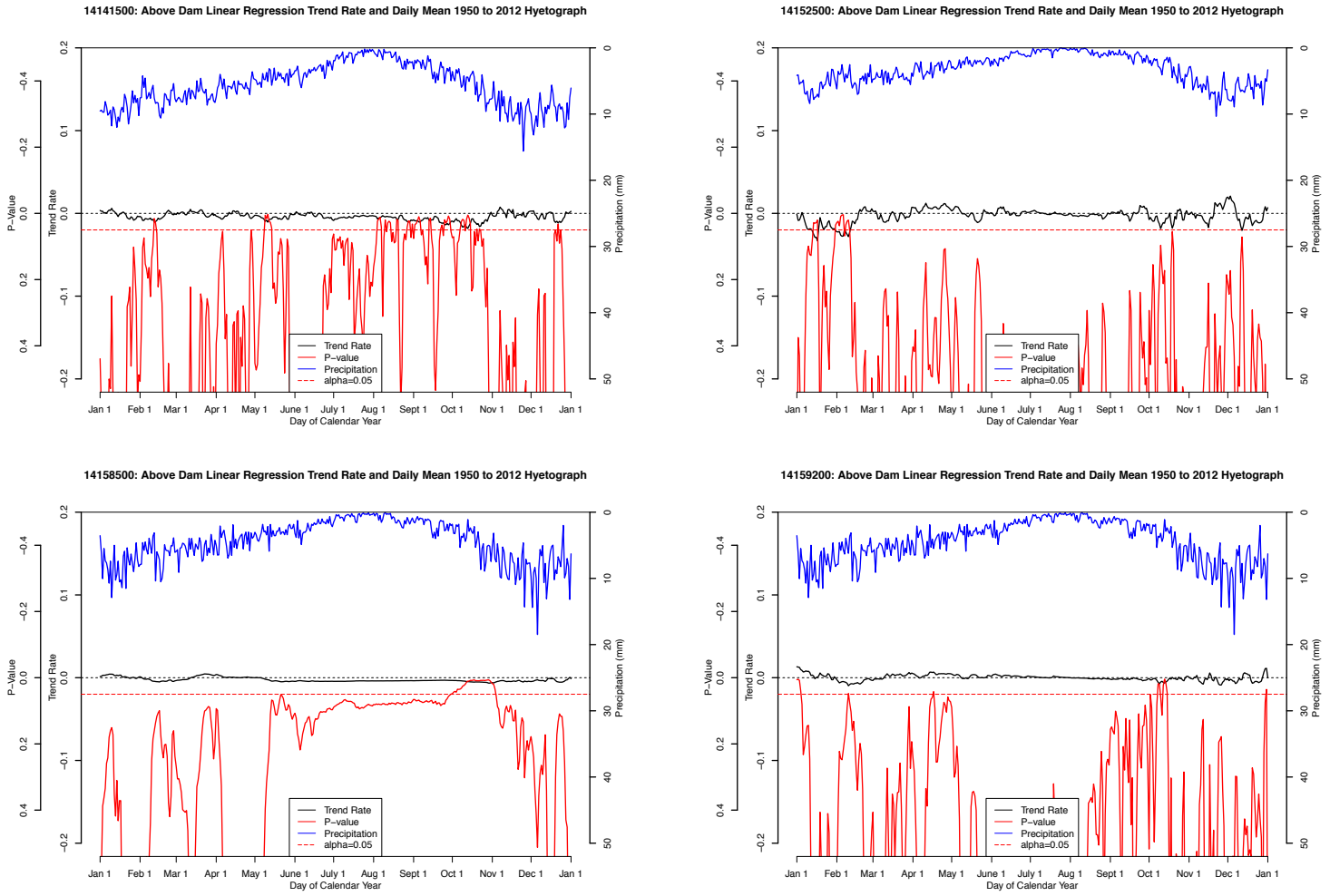

Figure B-24. Above dam daily significant increases and decreases in streamflow along with precipitation timing by study site. Trend rate units are ln(cms)/year.

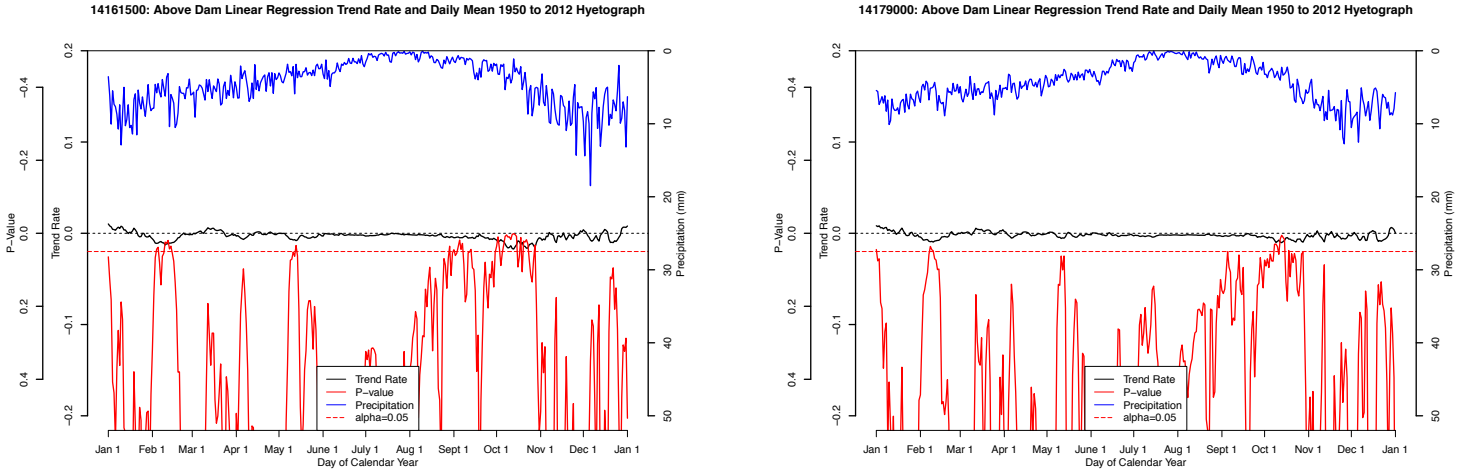

Figure B-25. Above dam daily significant increases and decreases in streamflow along with precipitation timing by study site. Trend rate units are ln(cms)/year.

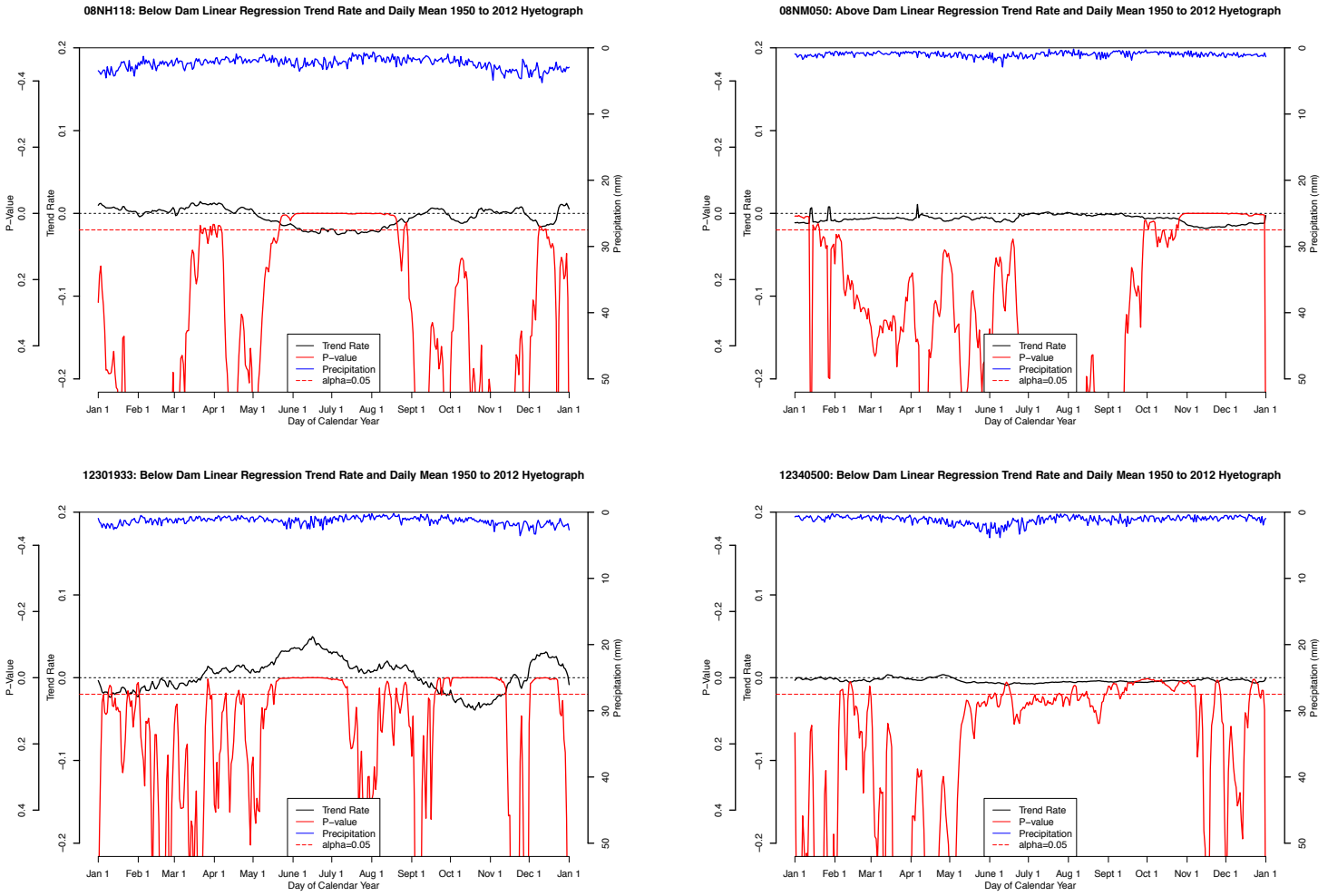

Figure B-26. Below dam daily significant increases and decreases in streamflow along with precipitation timing by study site. Trend rate units are ln(cms)/year.

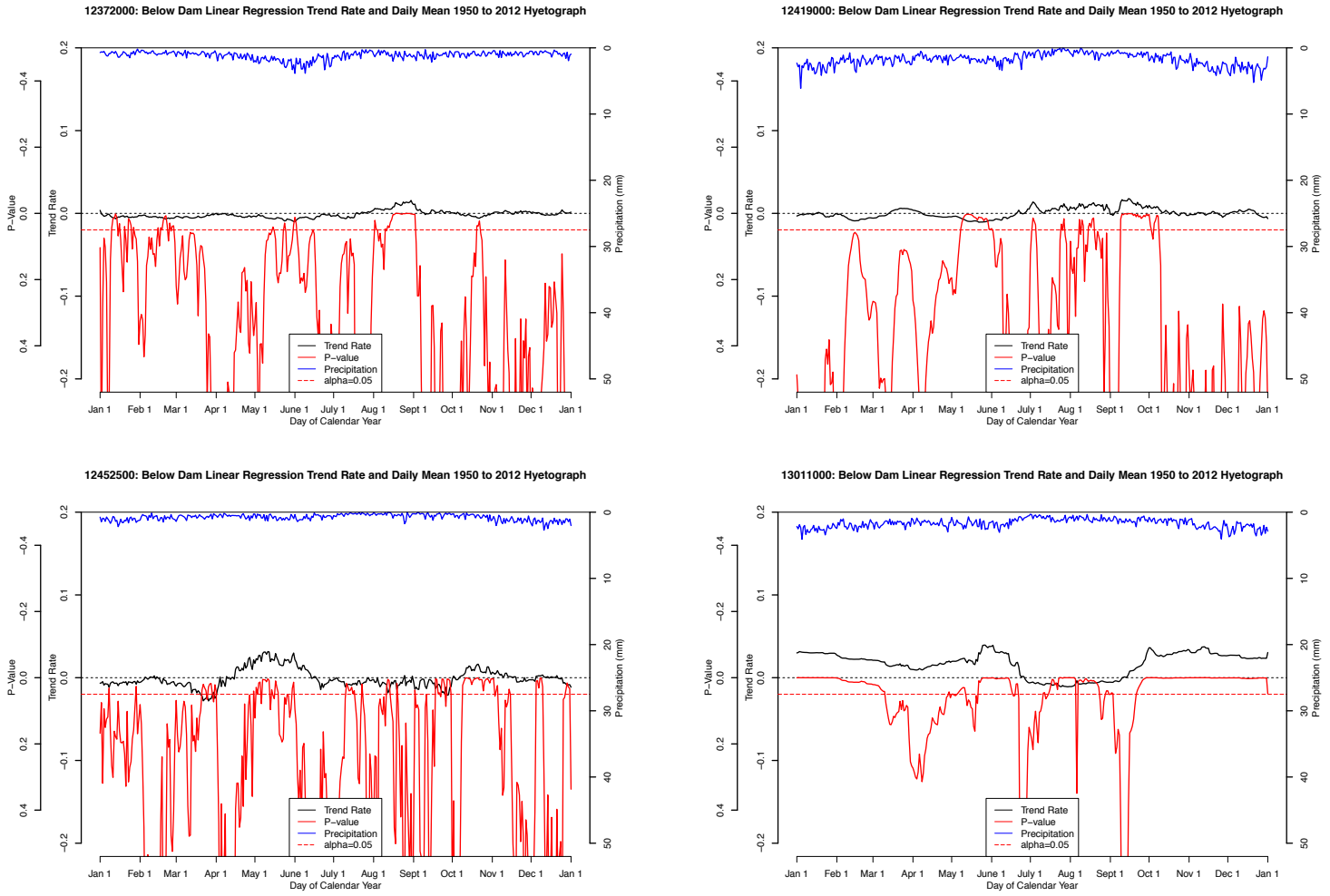

Figure B-27. Below dam daily significant increases and decreases in streamflow along with precipitation timing by study site. Trend rate units are ln(cms)/year.

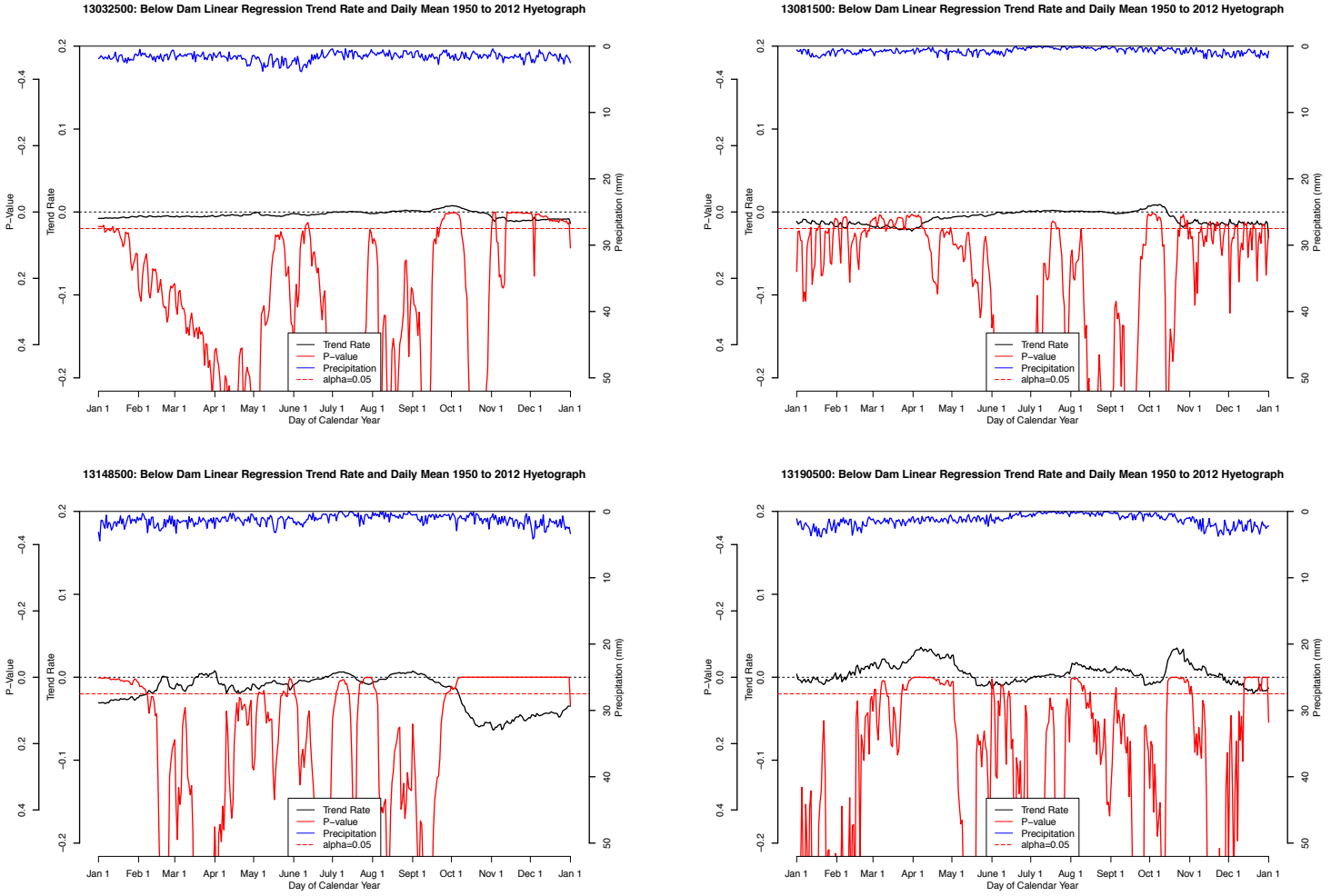

Figure B-28. Below dam daily significant increases and decreases in streamflow along with precipitation timing by study site. Trend rate units are ln(cms)/year.

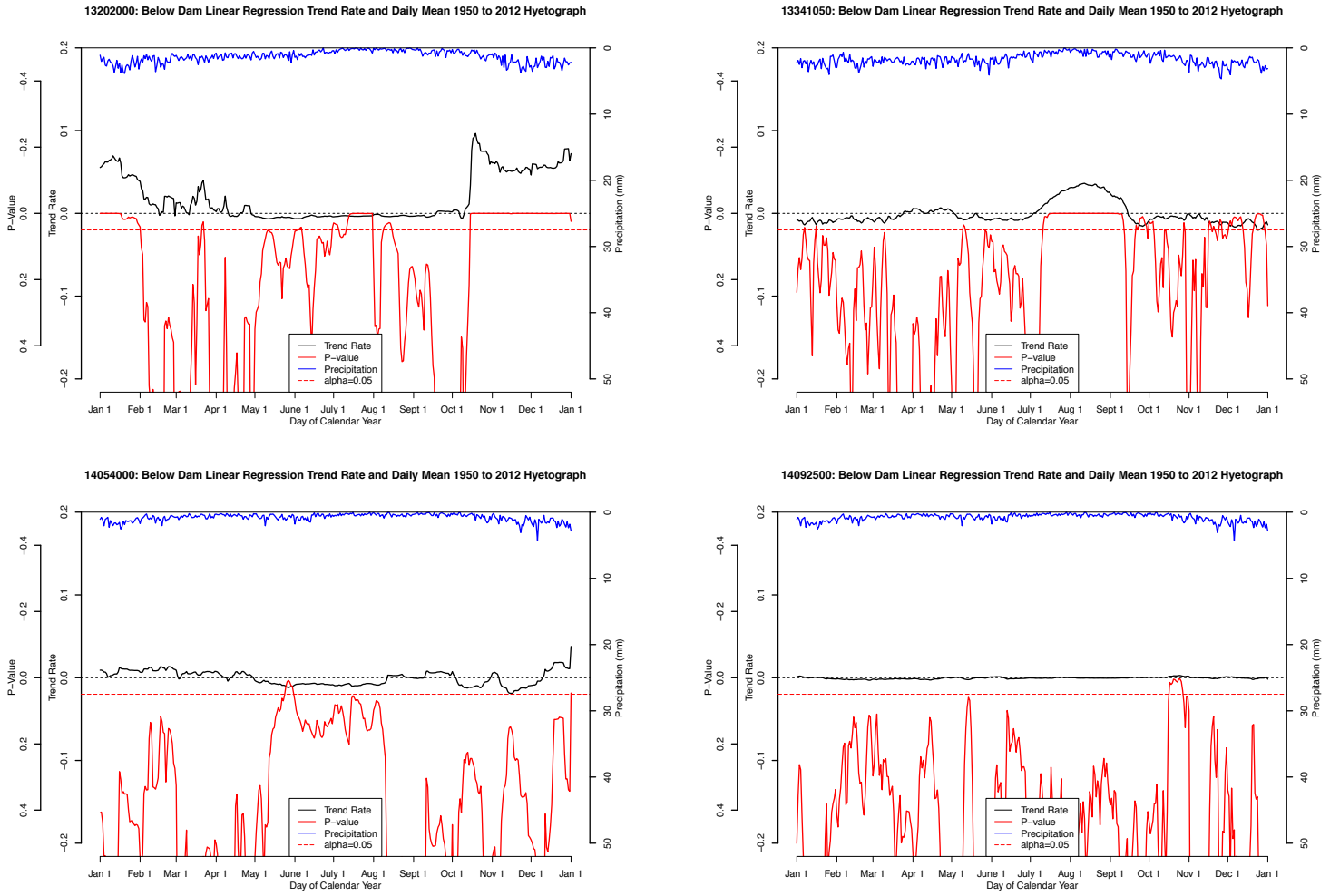

Figure B-29. Below dam daily significant increases and decreases in streamflow along with precipitation timing by study site. Trend rate units are ln(cms)/year.

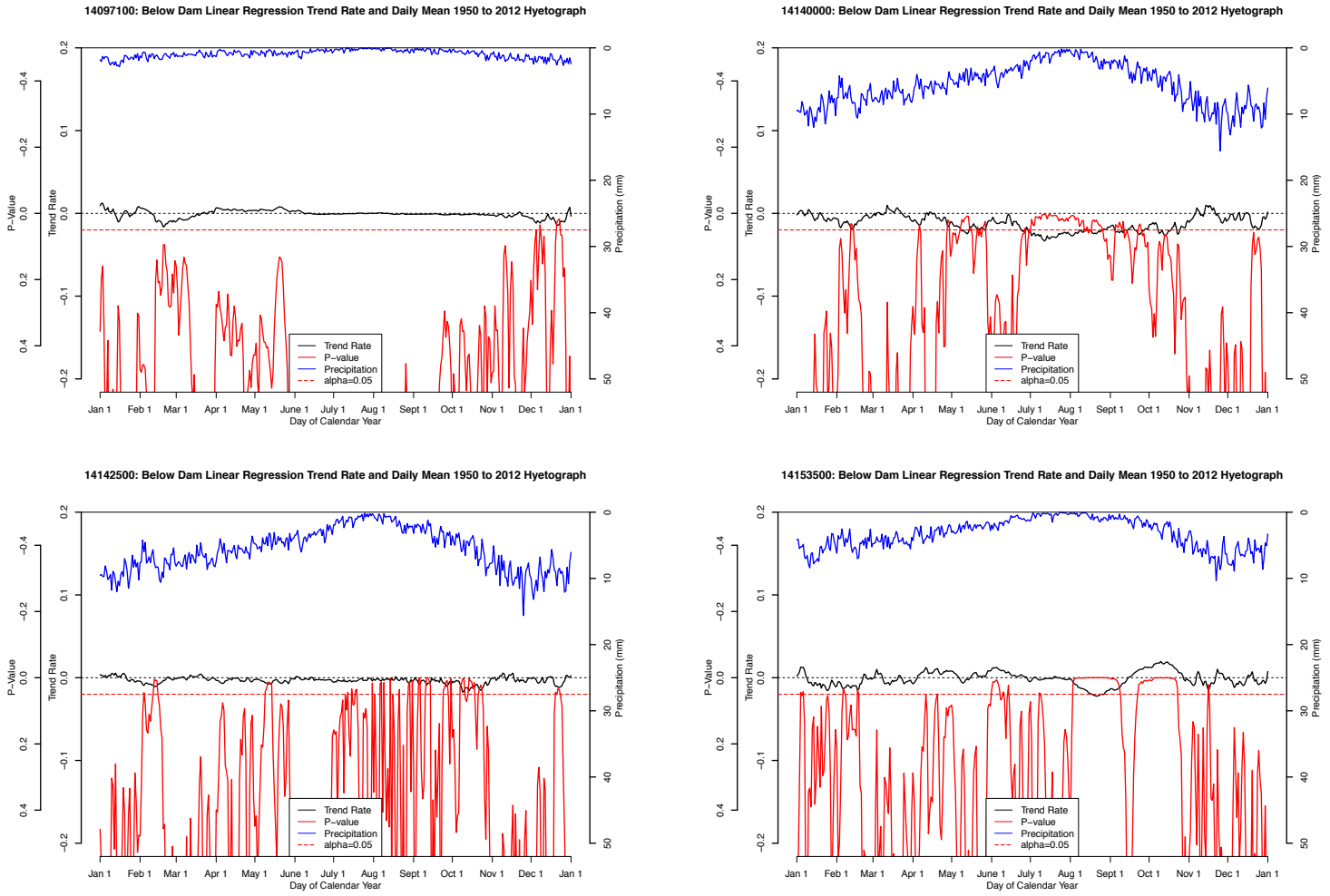

Figure B-30. Below dam daily significant increases and decreases in streamflow along with precipitation timing by study site. Trend rate units are ln(cms)/year.

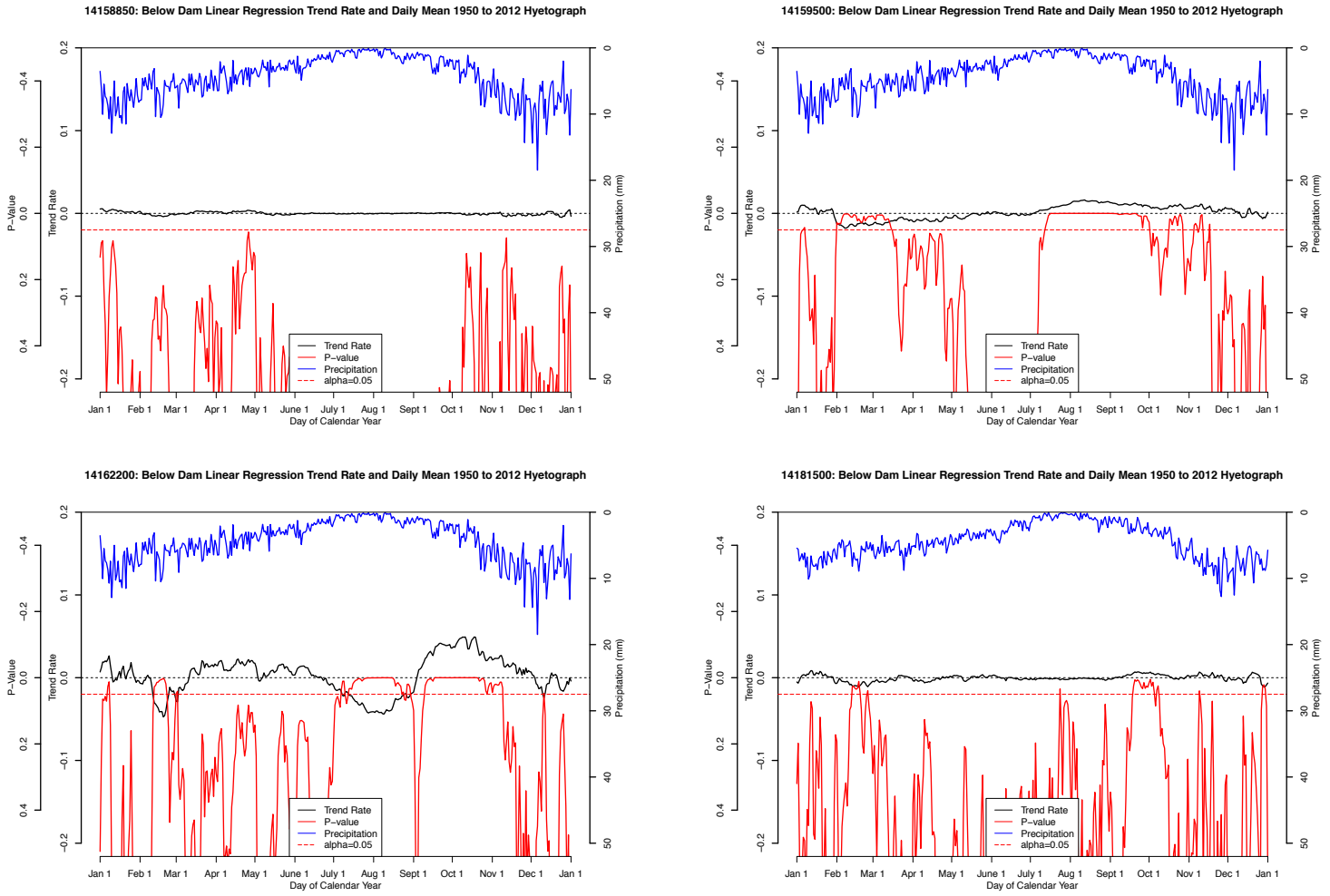

Figure B-31. Below dam daily significant increases and decreases in streamflow along with precipitation timing by study site. Trend rate units are ln(cms)/year.

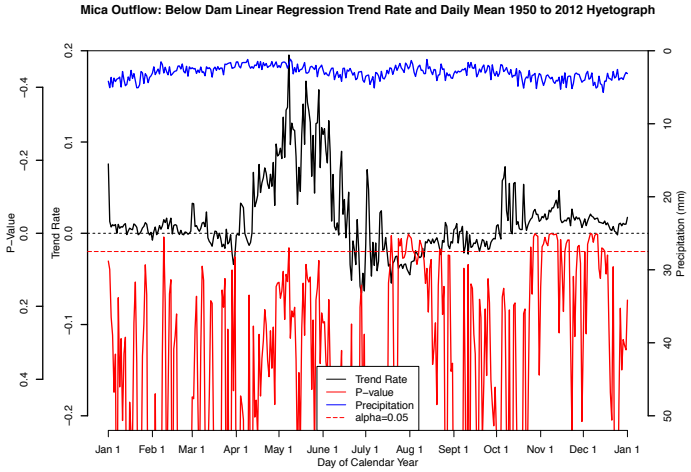

Figure B-32. Below dam daily significant increases and decreases in streamflow along with precipitation timing by study site. Trend rate units are ln(cms)/year.

Appendix C

Edge results by individual streamflow gauge

Representative streamflow gauges in the same sub-basins as used in results section 4.1.1.2 were chosen to display changes in cyclical behavior and edges in streamfow across the CRB. For the seven sites described in section 4.1.1.2 wavelet plots and plots of power at specified periods of 15 days, 90 days, and an average of three years are provided both for above dam and below dam gauges (figures Q through W).

Above dam wavelet power at the 15 day period averages lower values in the Willamette, Boise and Flathead sites when compared with the rest, but all sites display stochastic patterns with neither increasing or decreasing trends through time. Above dam wavelet power at the 90 day period also does not exhibit trends though time, instead increasing and decreasing throughout each gauge record. Above dam wavelet power at the average three year period exhibit different patterns of maximum and minimum power depending on the site that seem to differ more between sites that the power at the 15 and 90 day periods.

Below dam wavelet power at the 15 day period is shown to decrease throughout time at four of the seven sites chosen. The Sandy, Willamette and Kootenay above dam wavelet plots do not show this decline. This decline in 15 day power is likely attributable to the management of dams, which in many cases reduces the hydrograph signal of storms that typically have a duration between several hours and a couple of weeks.

Below dam wavelet power at the 90 day period at the Boise, Snake Headwaters and Upper Columbia gauges shows declines throughout the record of the gauges. Each of the three dams above these gauges is managed for flood control. The reduction of flows during fall and

winter months following dam construction likely accounts for this reduction in power though the record.

Below dam wavelet power at the average three year period exhibits somewhat cyclical behavior in maximum and minimum wavelet power at the Flathead, Sandy and Upper Columbia sites that is absent at the rest of these sites.

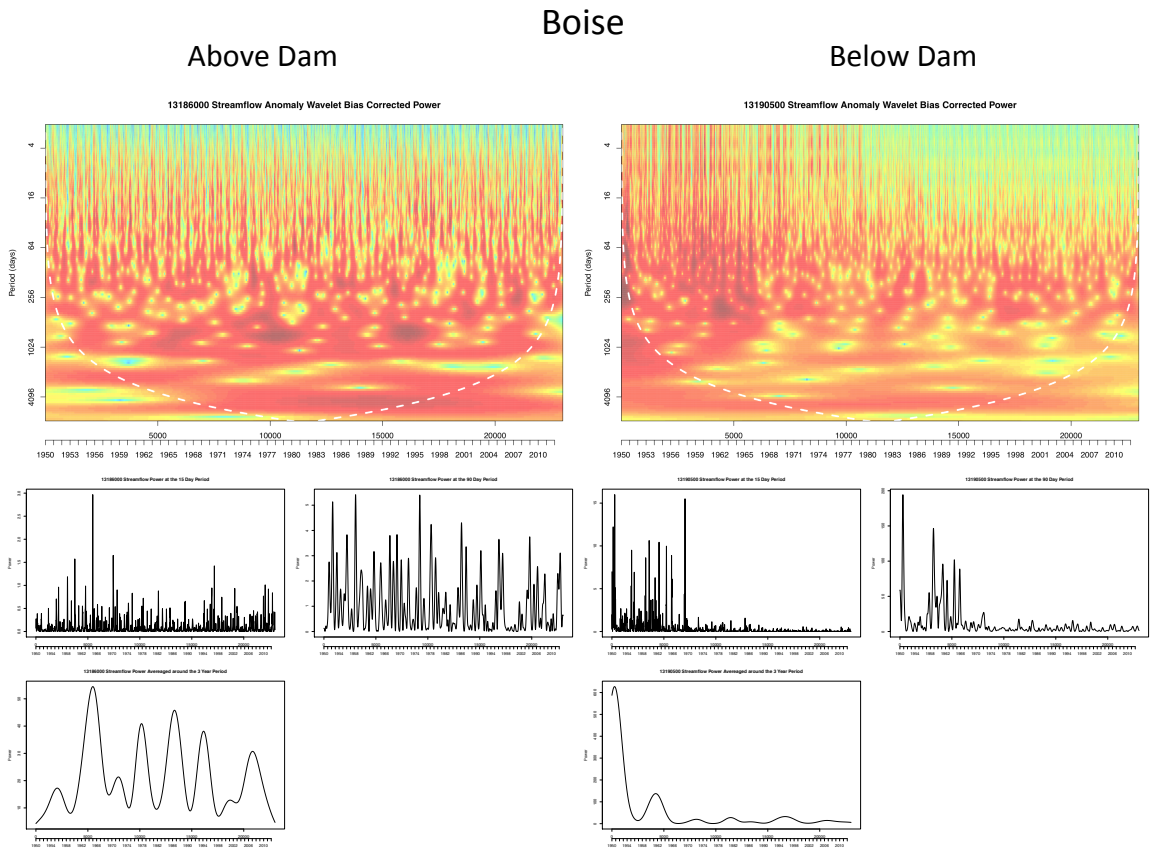

Figure C-8. Boise above and below dam streamflow figures with additional plots of bias corrected power at the 15 day, 90 day and average three year periods.

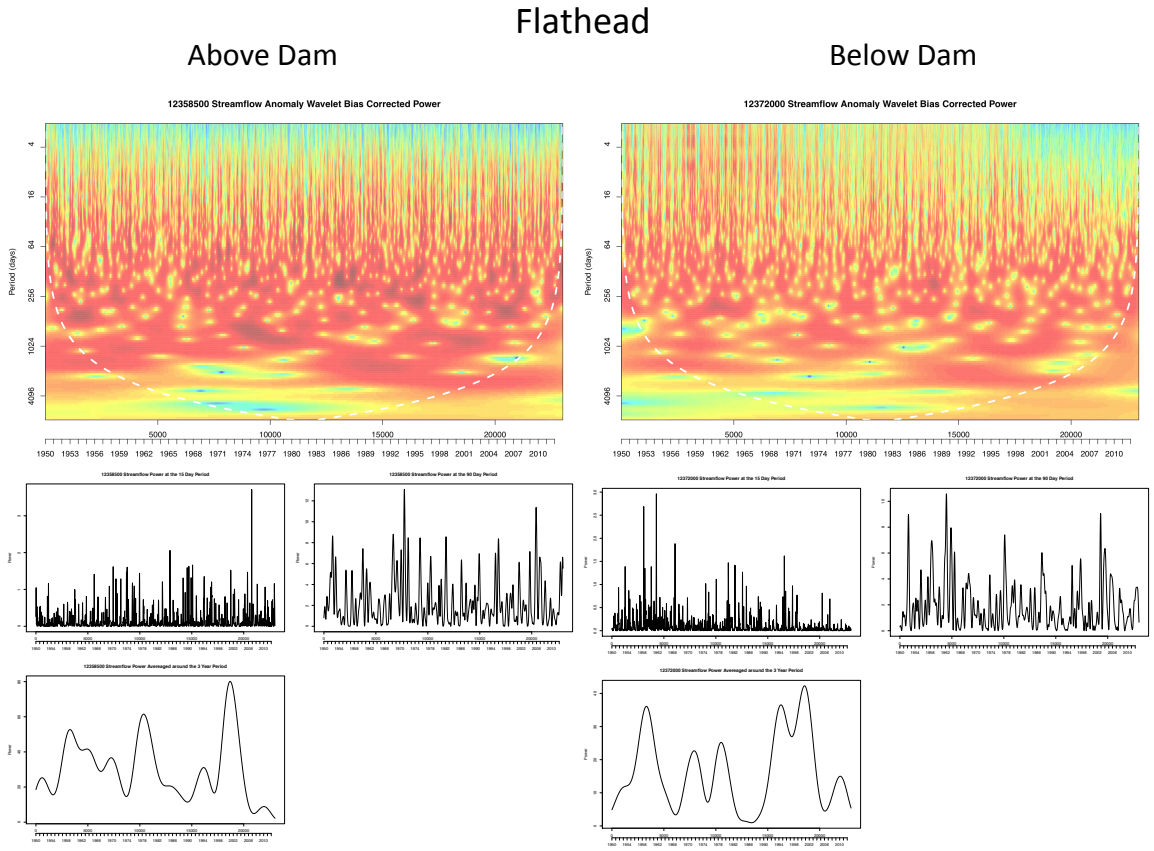

Figure C-9. Flathead above and below dam streamflow figures with additional plots of bias corrected power at the 15 day, 90 day and average three year periods.

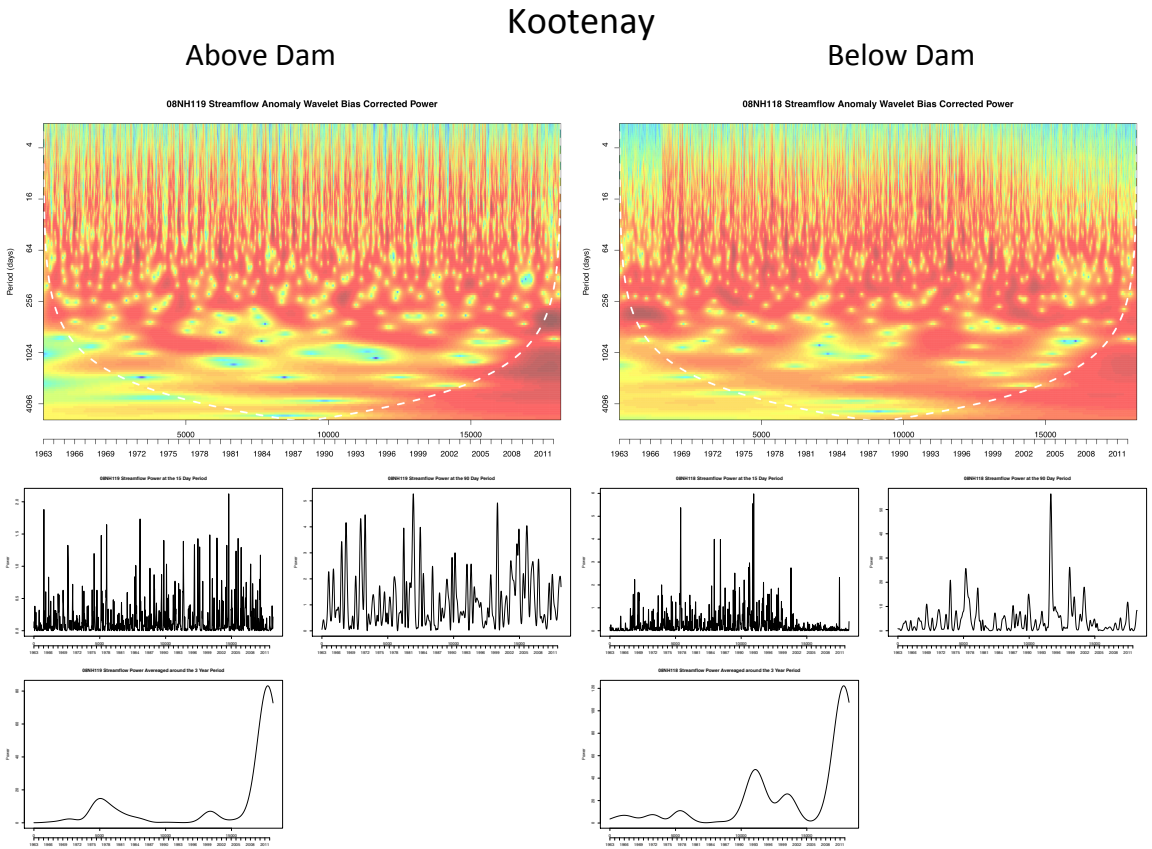

Figure C-10. Kootenay above and below dam streamflow figures with additional plots of bias corrected power at the 15 day, 90 day and average three year periods.

Sandy

Above Dam

Below Dam

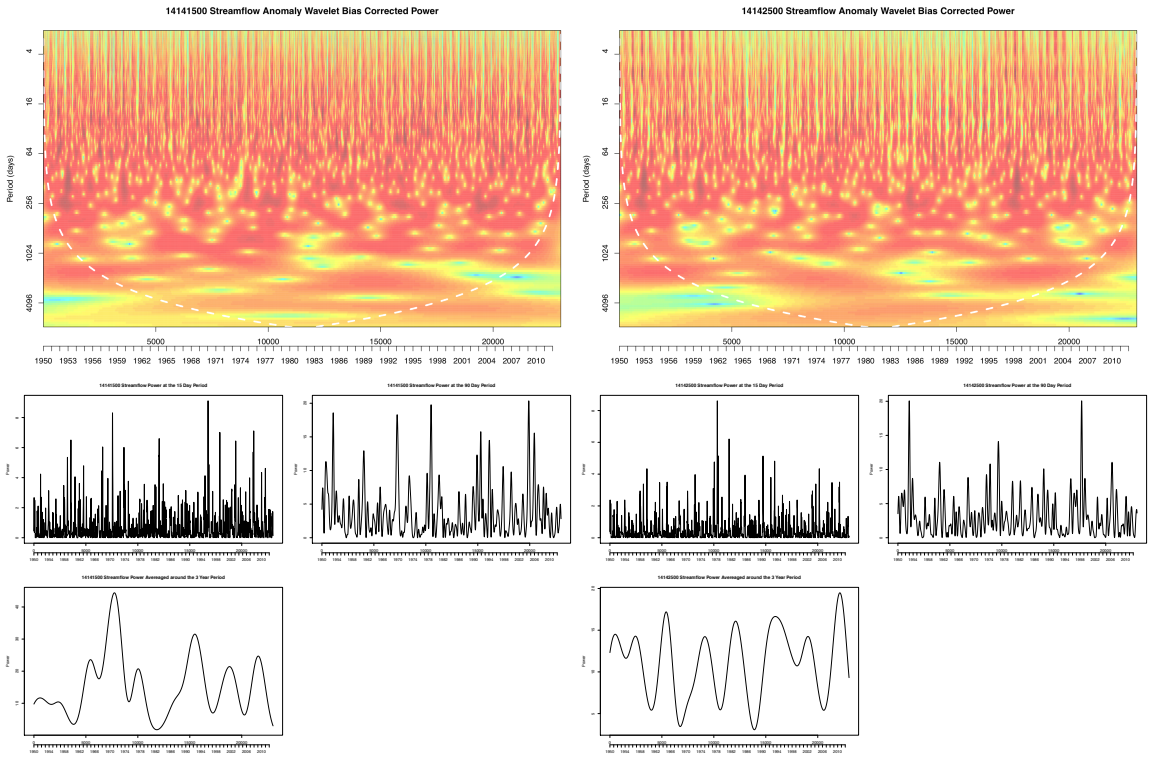

Figure C-11. Sandy above and below dam streamflow figures with additional plots of bias corrected power at the 15 day, 90 day and average three year periods.

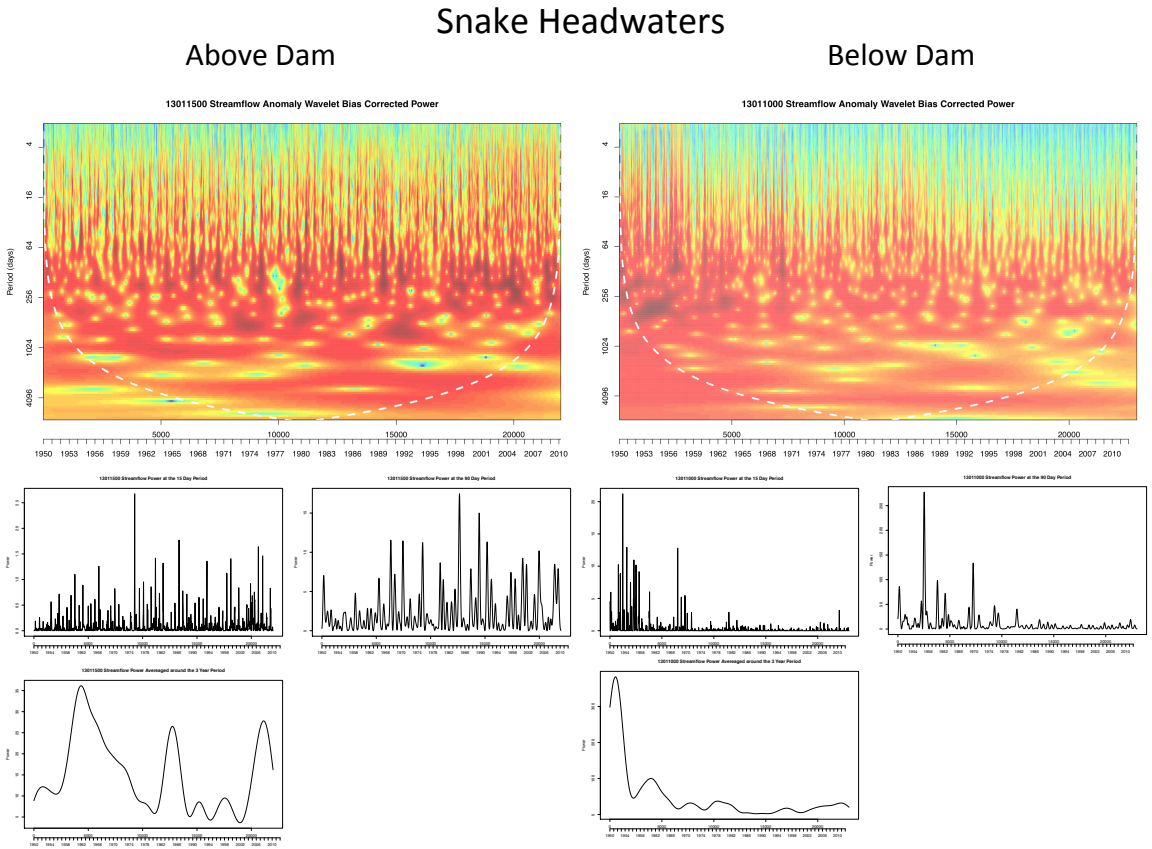

Figure C-12. Snake Headwaters above and below dam streamflow figures with additional plots of bias corrected power at the 15 day, 90 day and average three year periods.

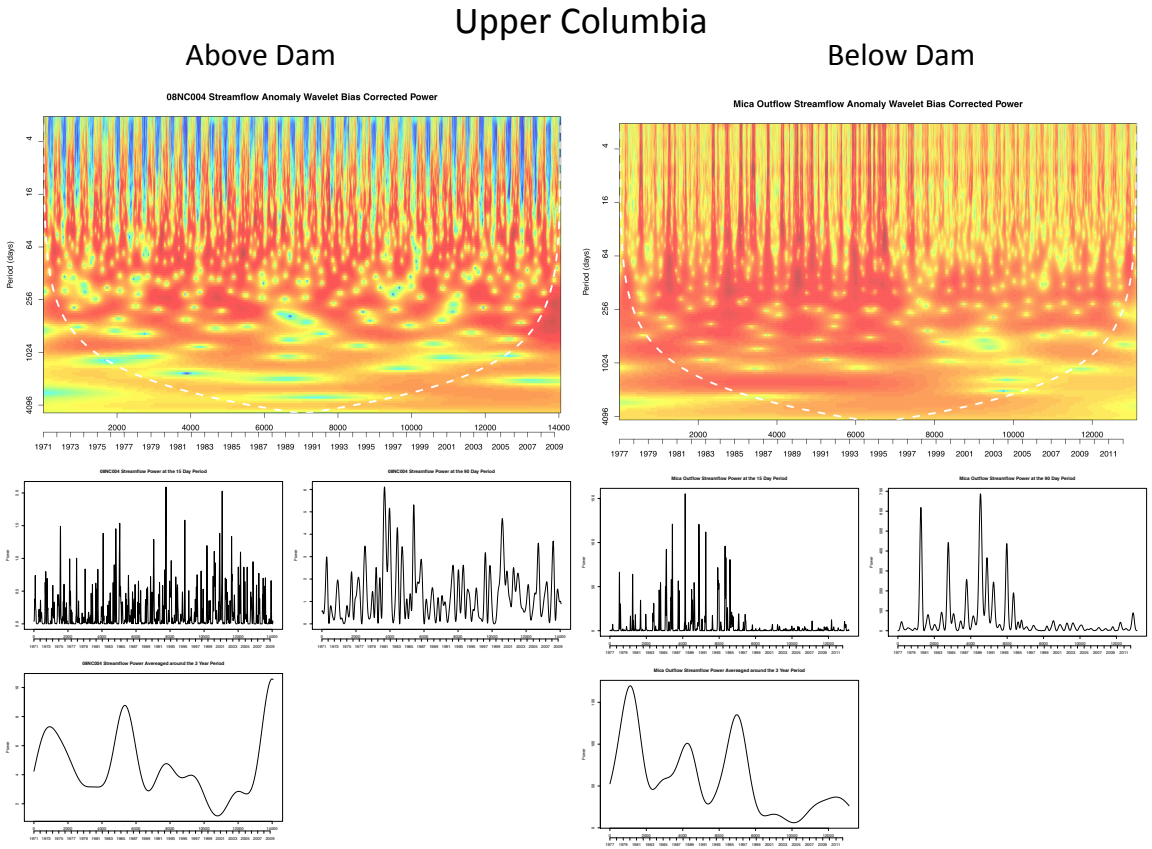

Figure C-13. Upper Columbia above and below dam streamflow figures with additional plots of bias corrected power at the 15 day, 90 day and average three year periods.

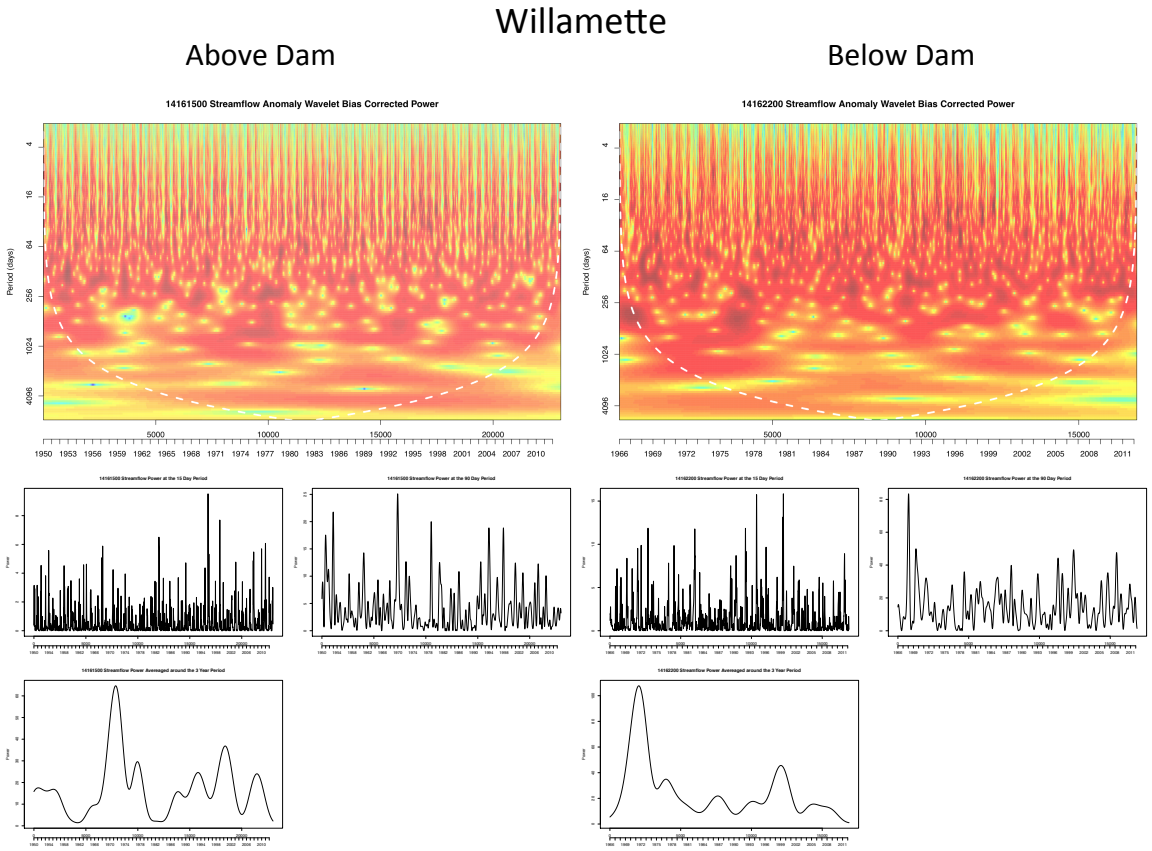

Figure C-14. Willamette above and below dam streamflow figures with additional plots of bias corrected power at the 15 day, 90 day and average three year periods.

Appendix D

Linear trend results by sub-basin

Climate

Linear trends in precipitation (figures D-1 to D-5) by day of year across the Columbia River Basin for the most part seem to have not changed at the stations analyzed in this study. However, Boise and John Day sub-basins are dominated by negative daily trends in precipitation on several days throughout the year. Even more noticeably, in the Kootenay and Upper Columbia sub-basins there are many more days displaying significant increases in precipitation throughout the calendar year.

Many sub-basins in this study including the Boise, Kootenay, Lake Chelan, Lower Columbia, Lower Snake and Salmon show more daily significant increases than decreases in maximum surface air temperature (figures D-6 to D-10). These daily increases and decreases in maximum surface daily air temperature do not display obvious timing patterns between sub-basins.

In contrast to precipitation and maximum air temperature results, there is near uniform increases in daily minimum surface air temperatures in many of the sub-basins included in this study (figures D-11 to D-15). These significant linear increases are spread throughout the year and throughout the basin as a whole.

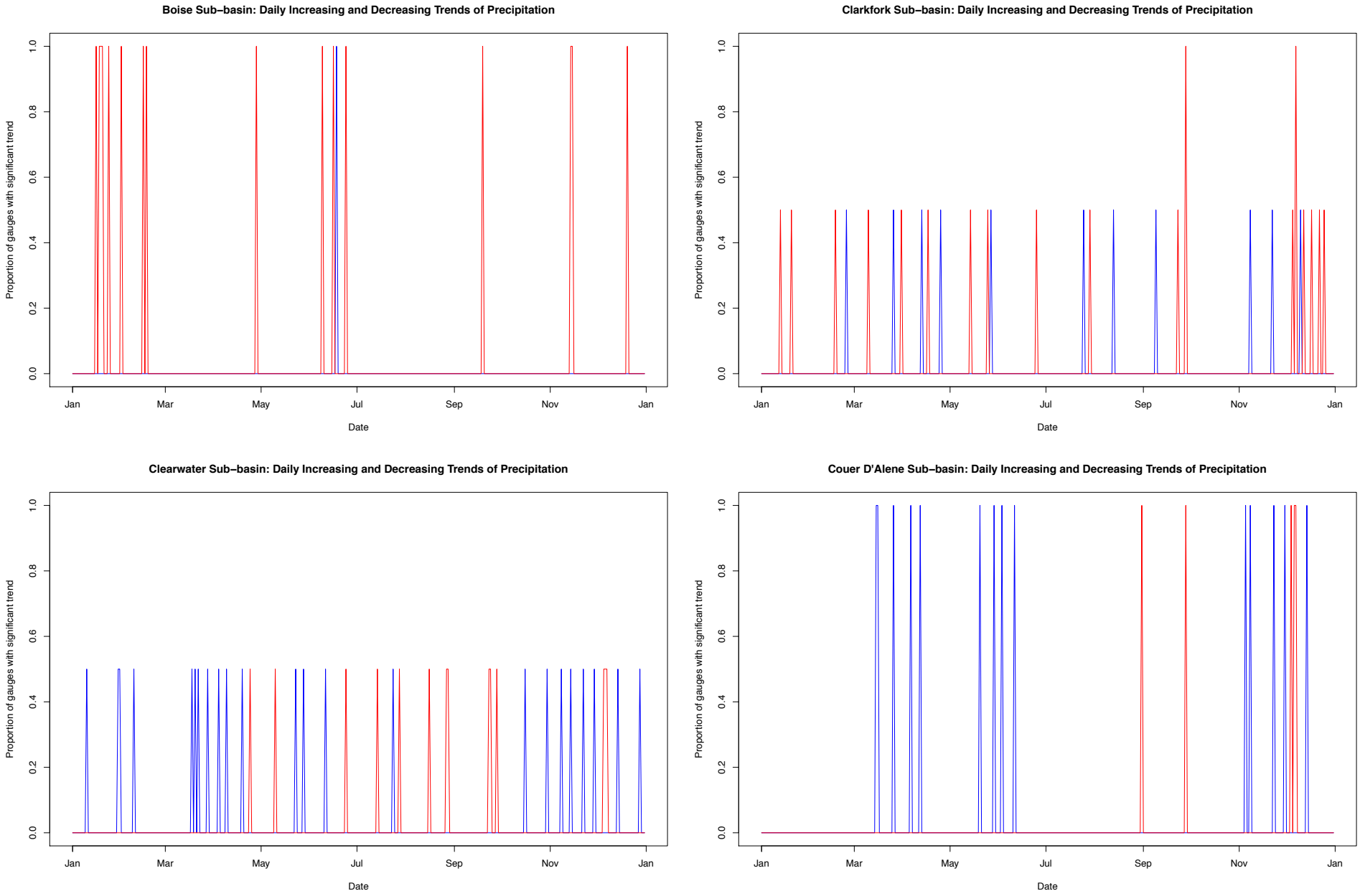

Figure D-1. Daily significant increases and decreases in precipitation by sub-basin.

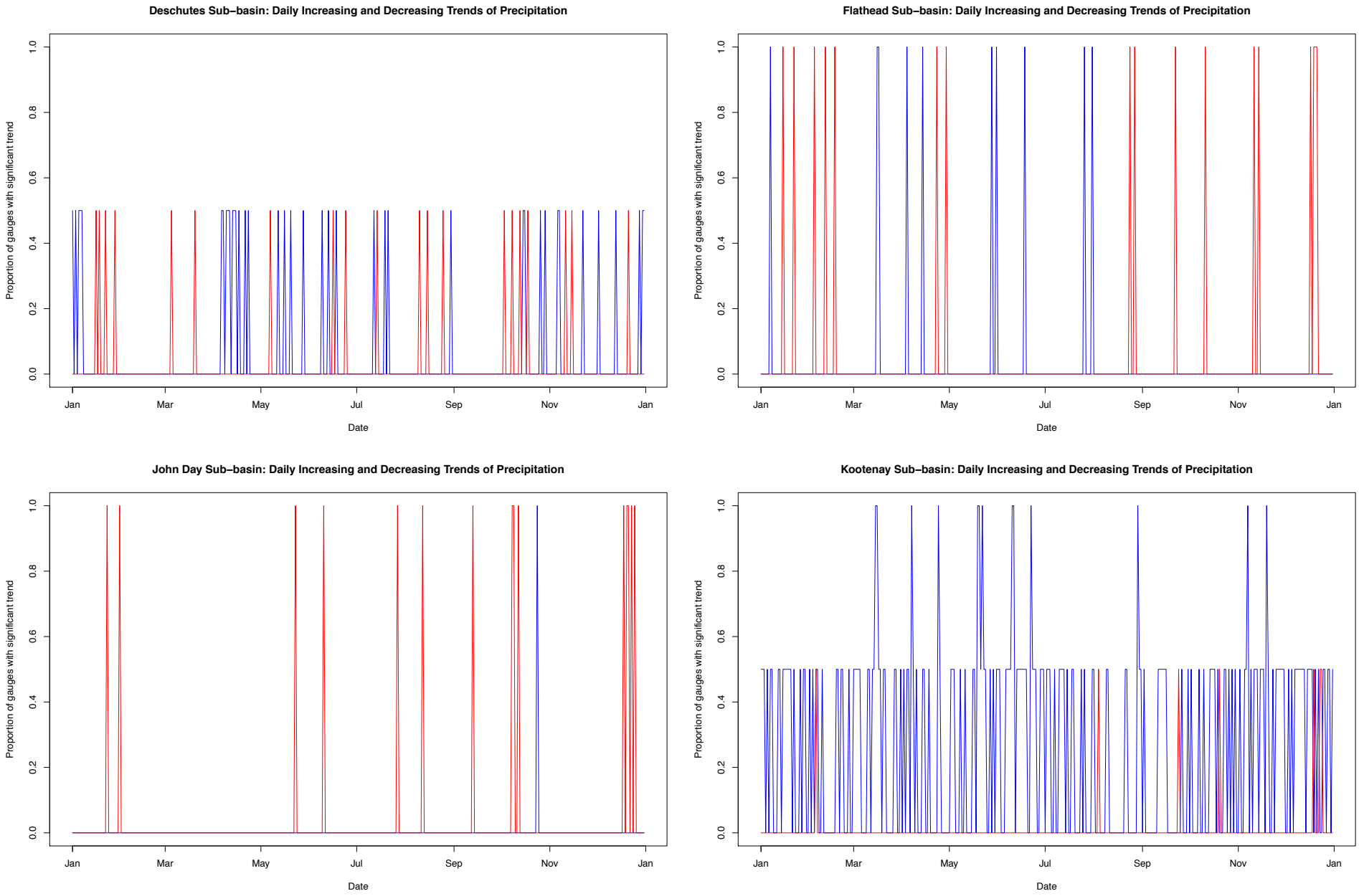

Figure D-2. Daily significant increases and decreases in precipitation by sub-basin.

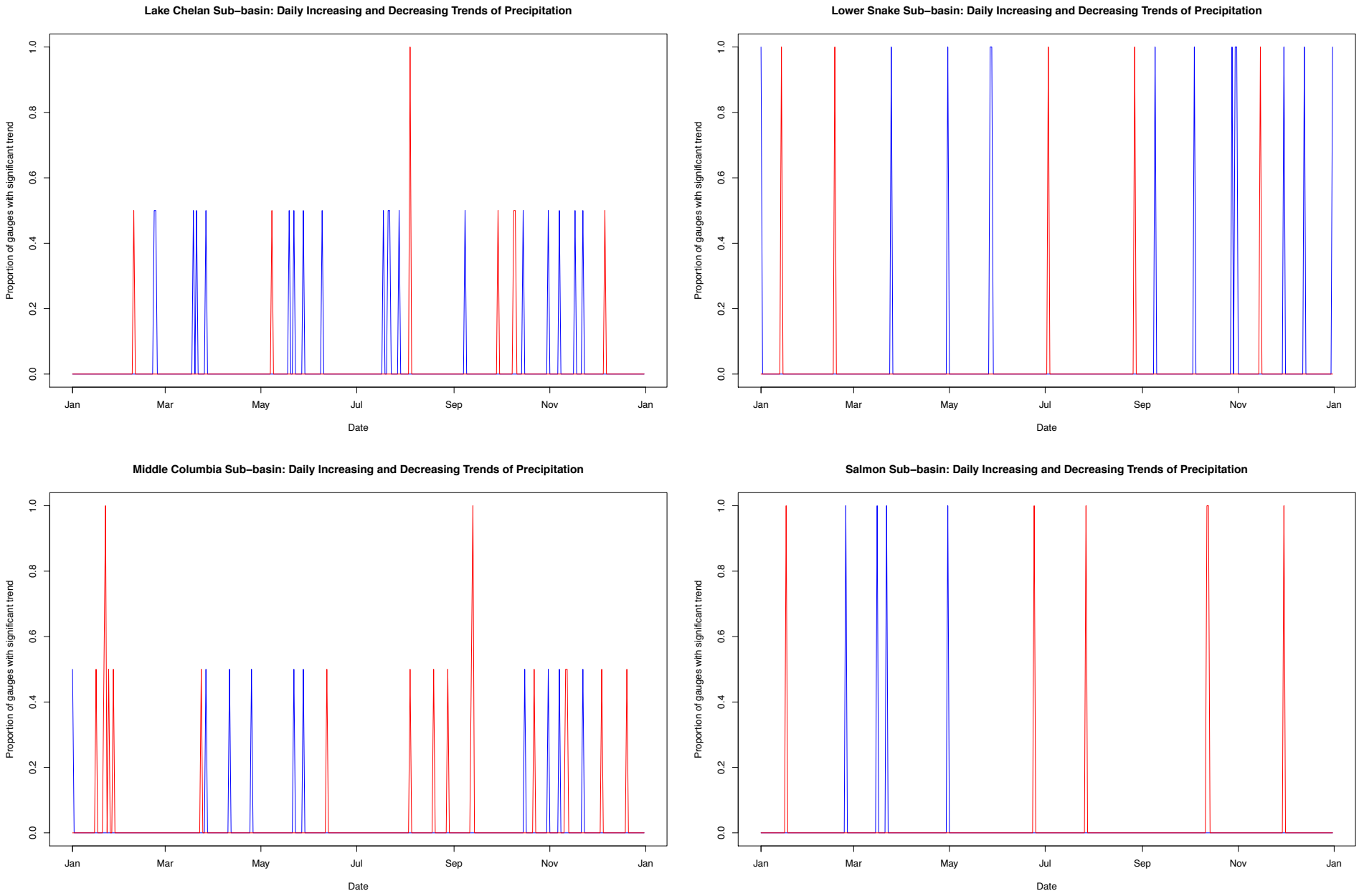

Figure D-3. Daily significant increases and decreases in precipitation by sub-basin.

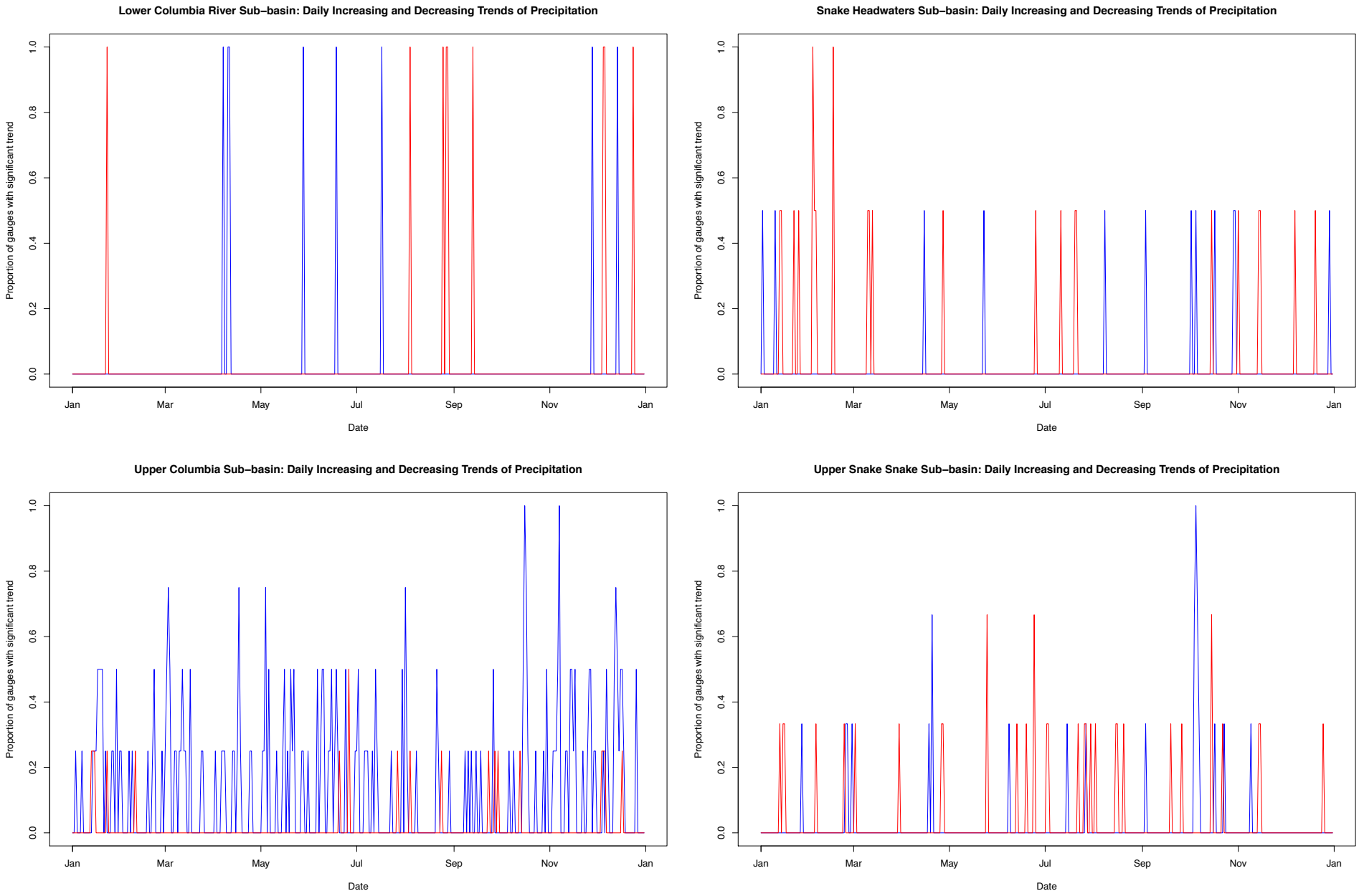

Figure D-4. Daily significant increases and decreases in precipitation by sub-basin.

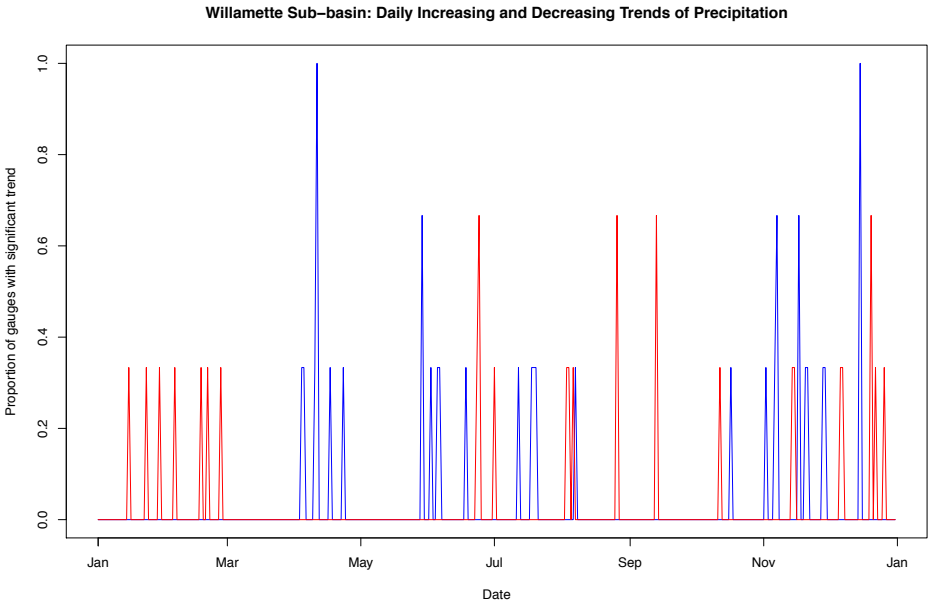

Figure D-5. Daily significant increases and decreases in precipitation by sub-basin.

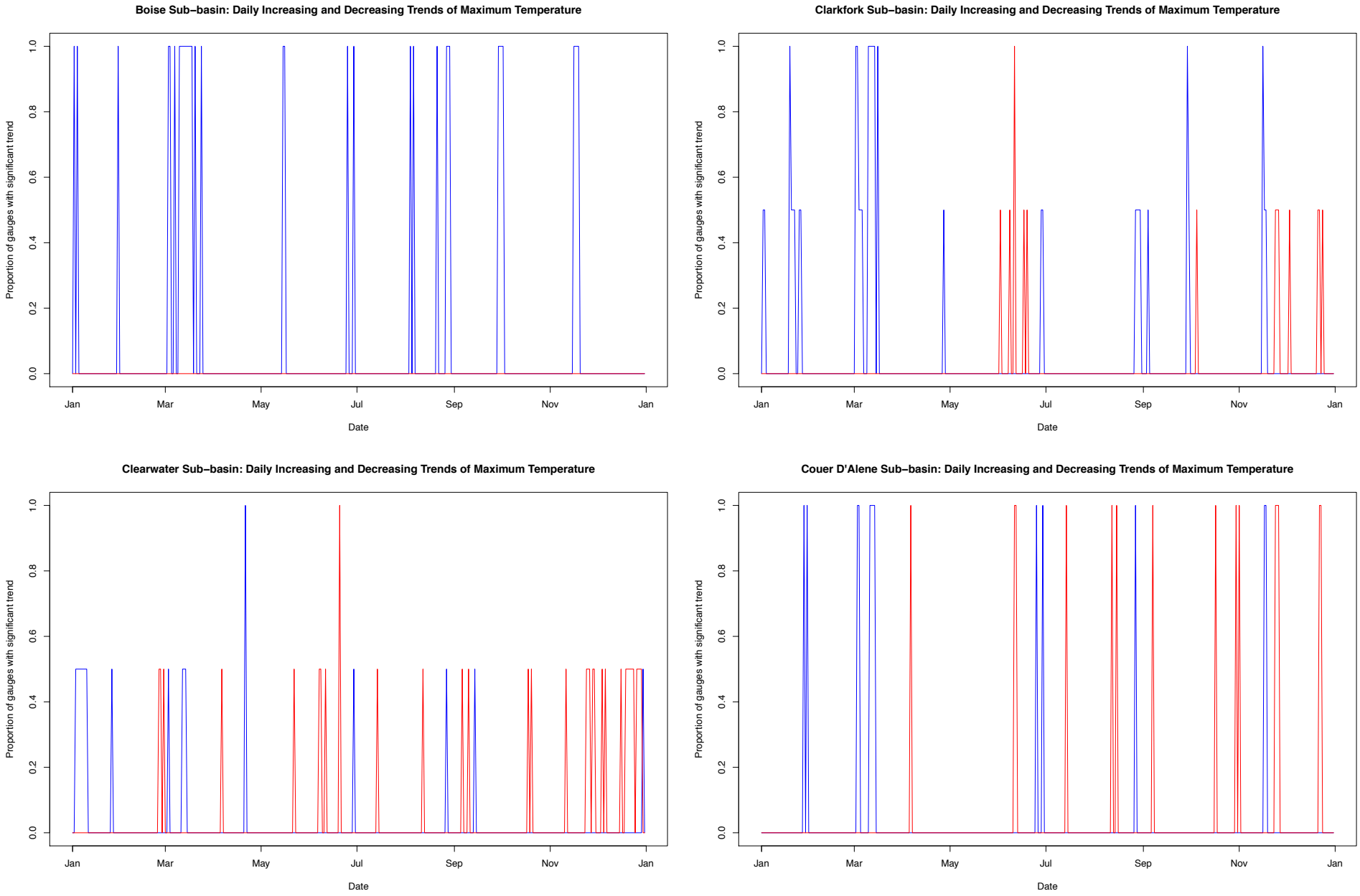

Figure D-6. Daily significant increases and decreases in maximum surface air temperature by sub-basin.

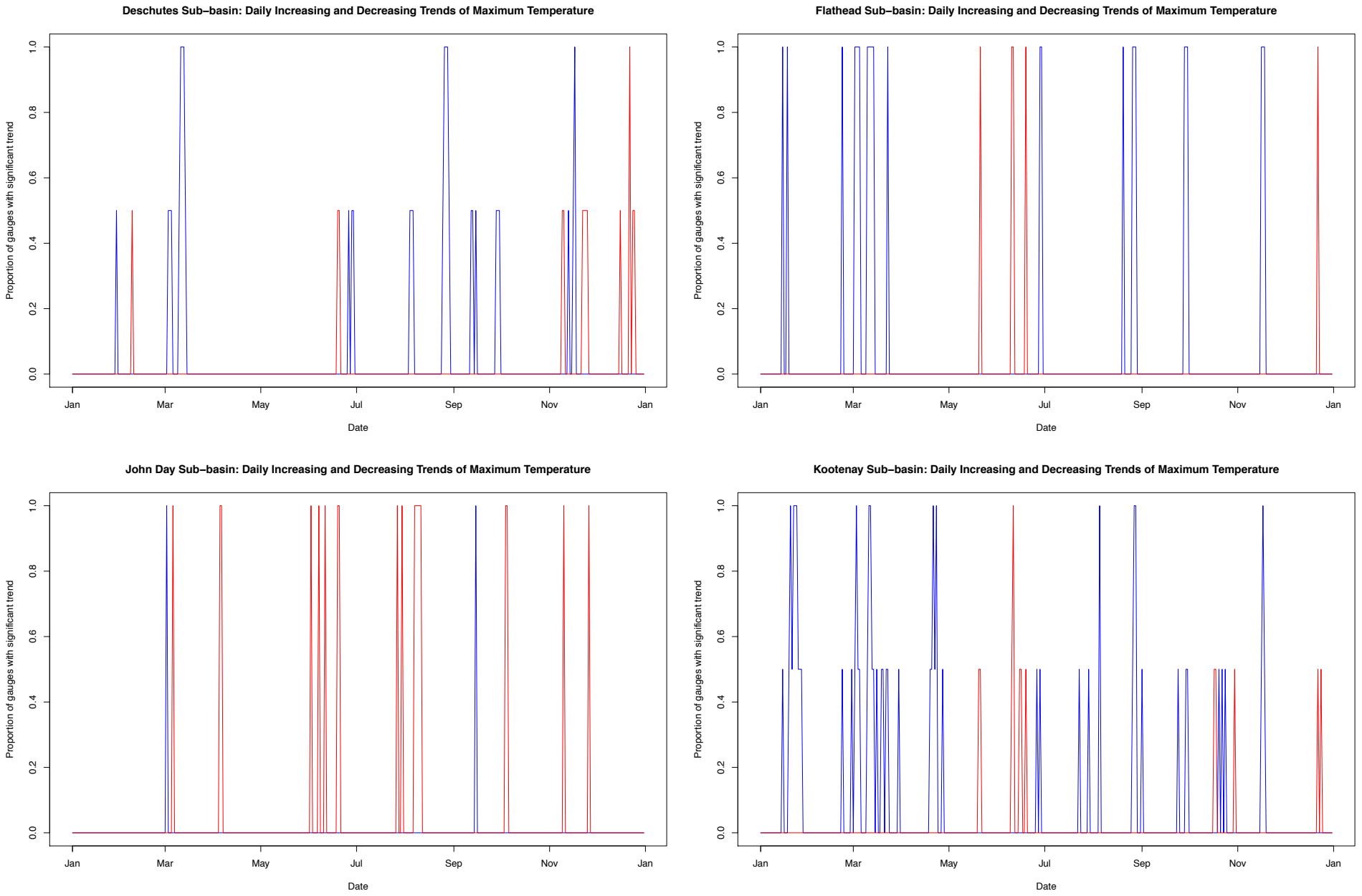

Figure D-7. Daily significant increases and decreases in maximum surface air temperature by sub-basin.

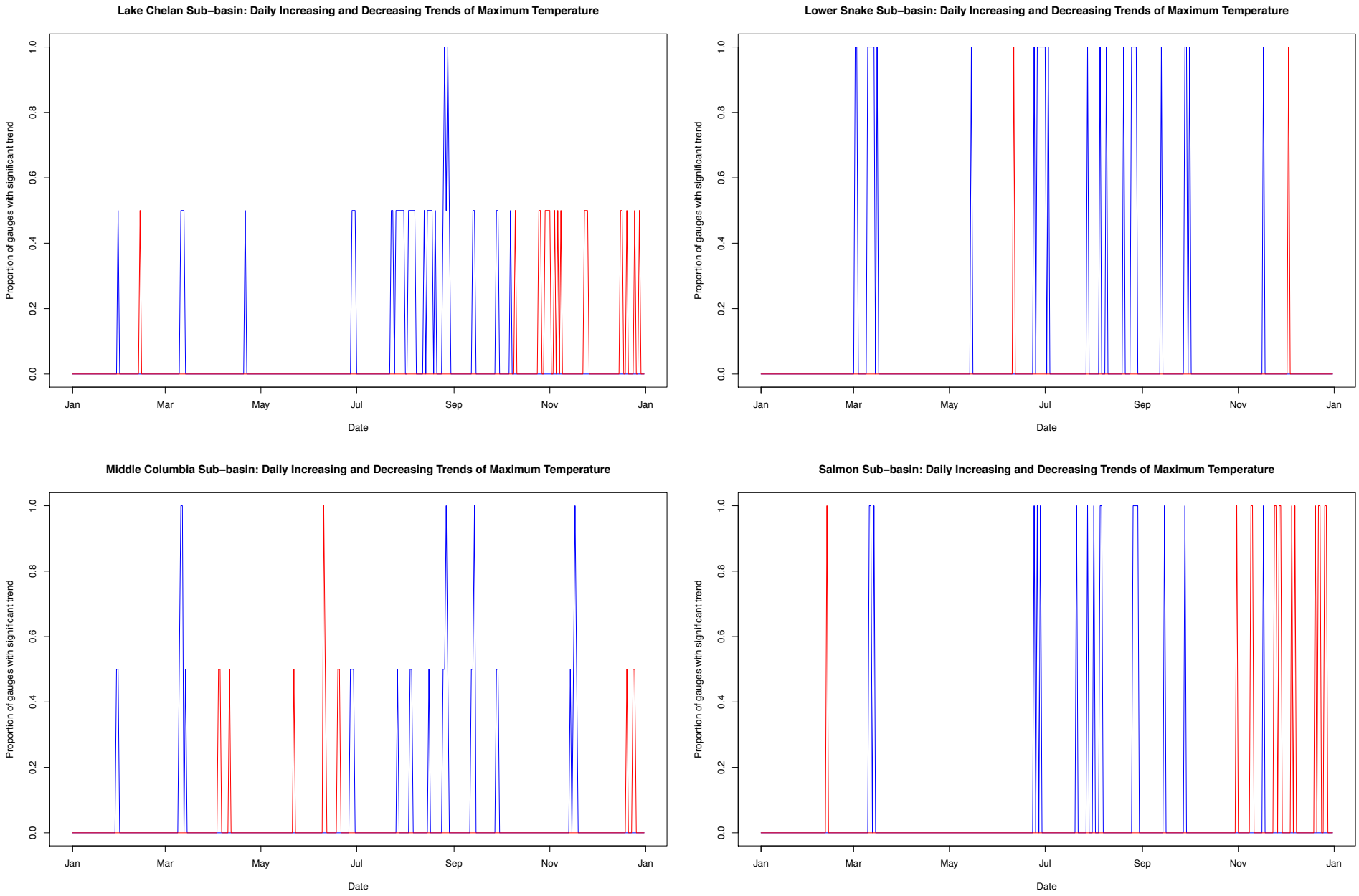

Figure D-8. Daily significant increases and decreases in maximum surface air temperature by sub-basin.

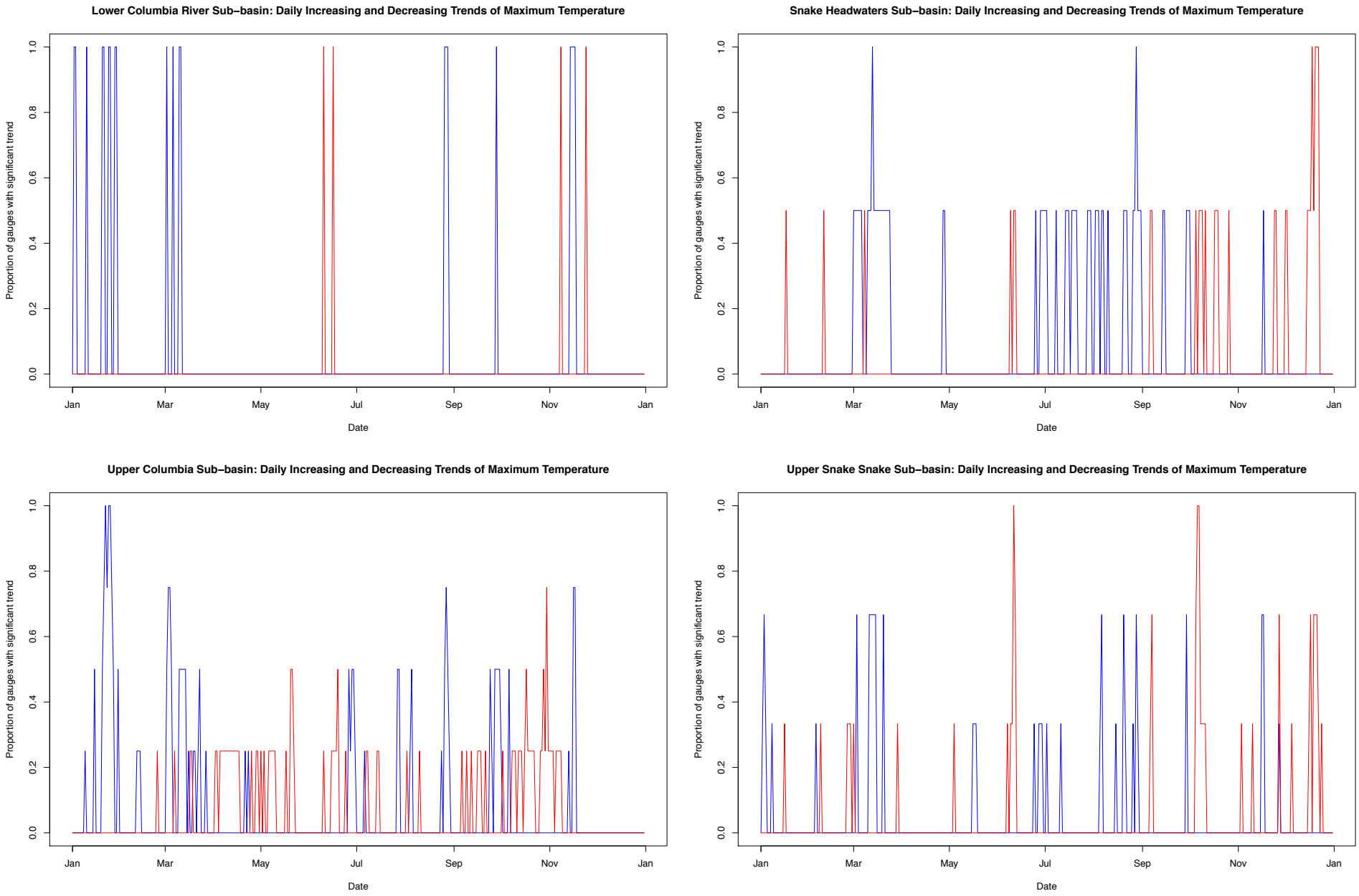

Figure D-9. Daily significant increases and decreases in maximum surface air temperature by sub-basin.

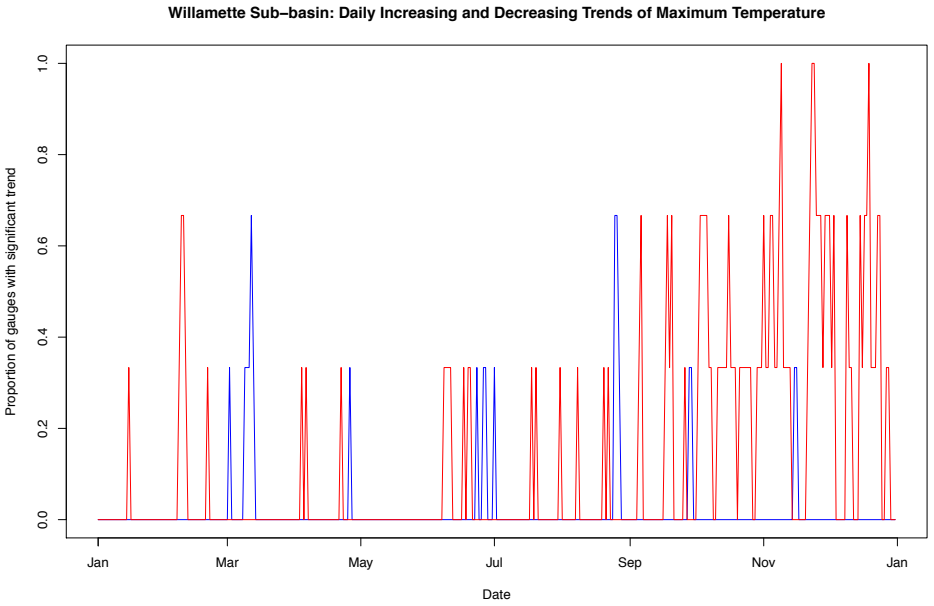

Figure D-10. Daily significant increases and decreases in maximum surface air temperature by sub-basin.

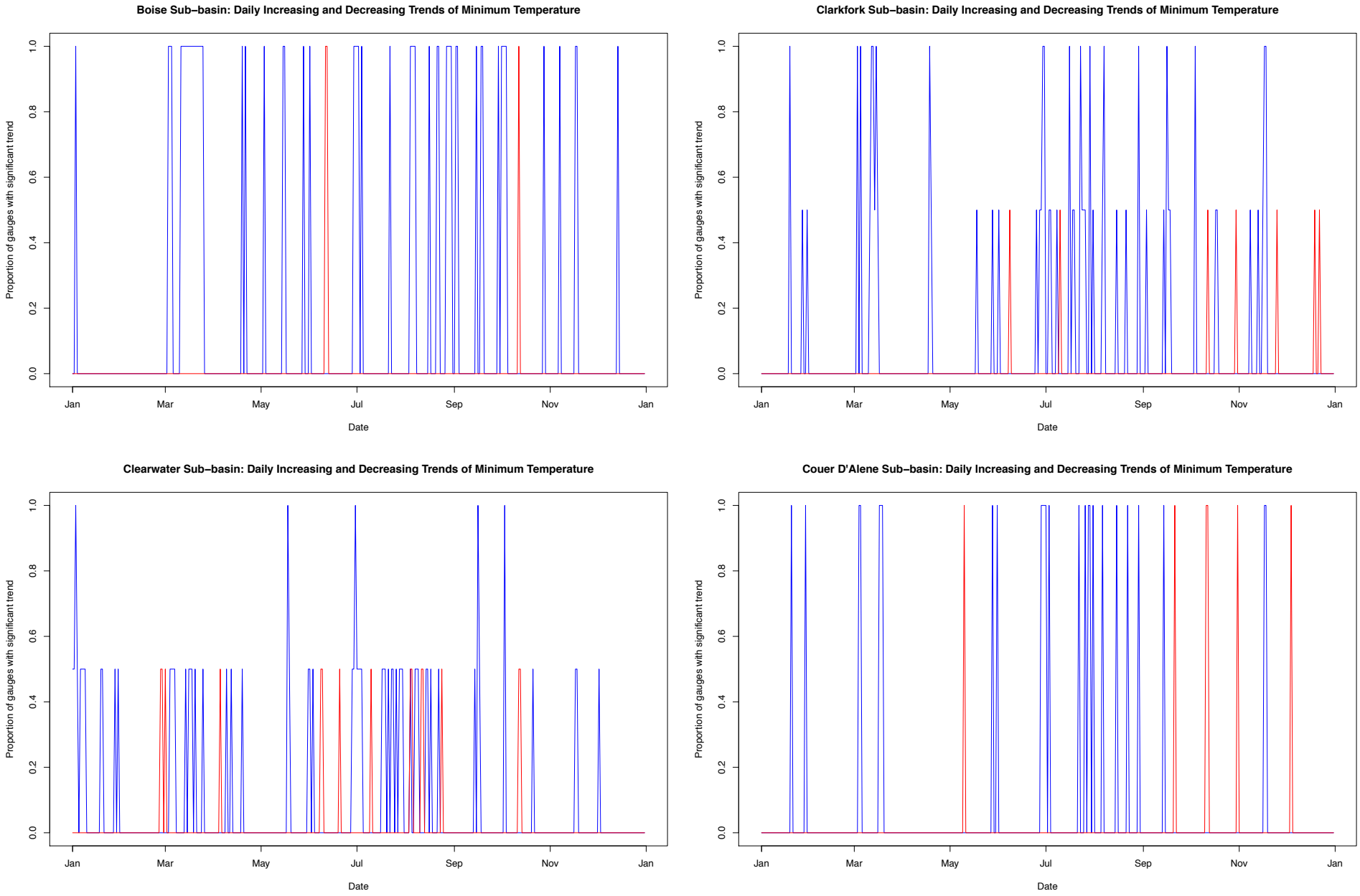

Figure D-11. Daily significant increases and decreases in minimum surface air temperature by sub-basin.

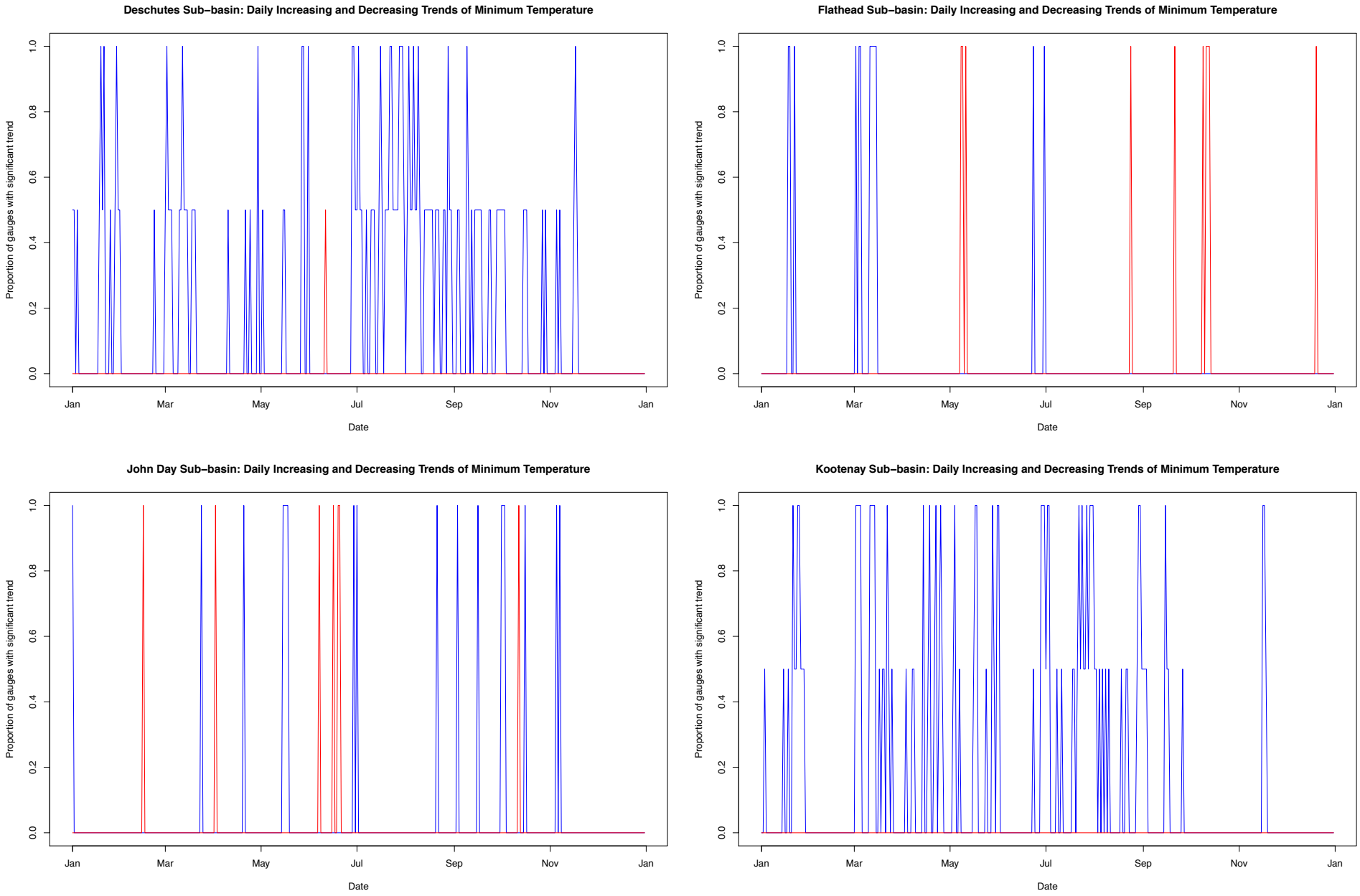

Figure D-12. Daily significant increases and decreases in minimum surface air temperature by sub-basin.

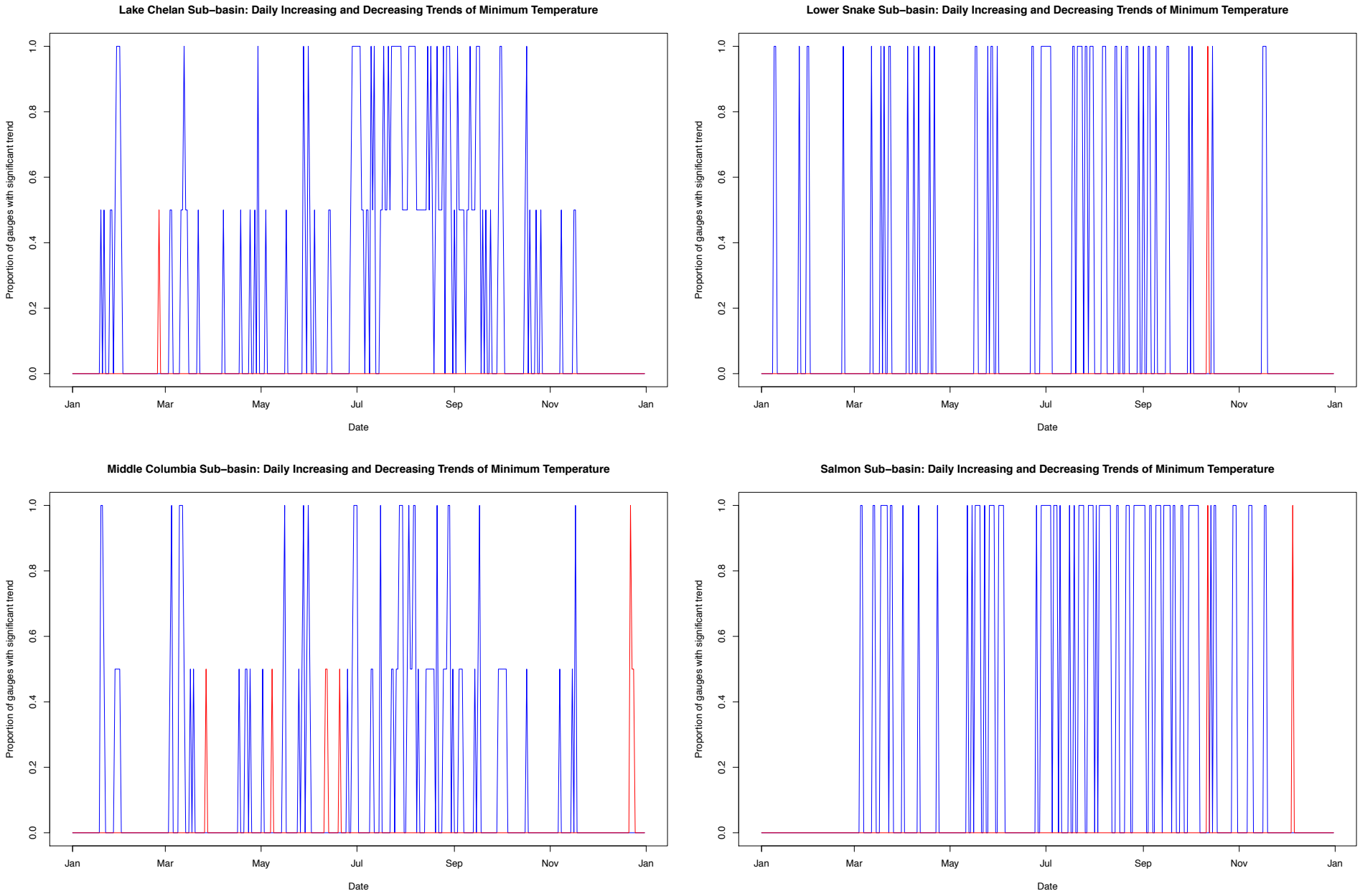

Figure D-13. Daily significant increases and decreases in minimum surface air temperature by sub-basin.

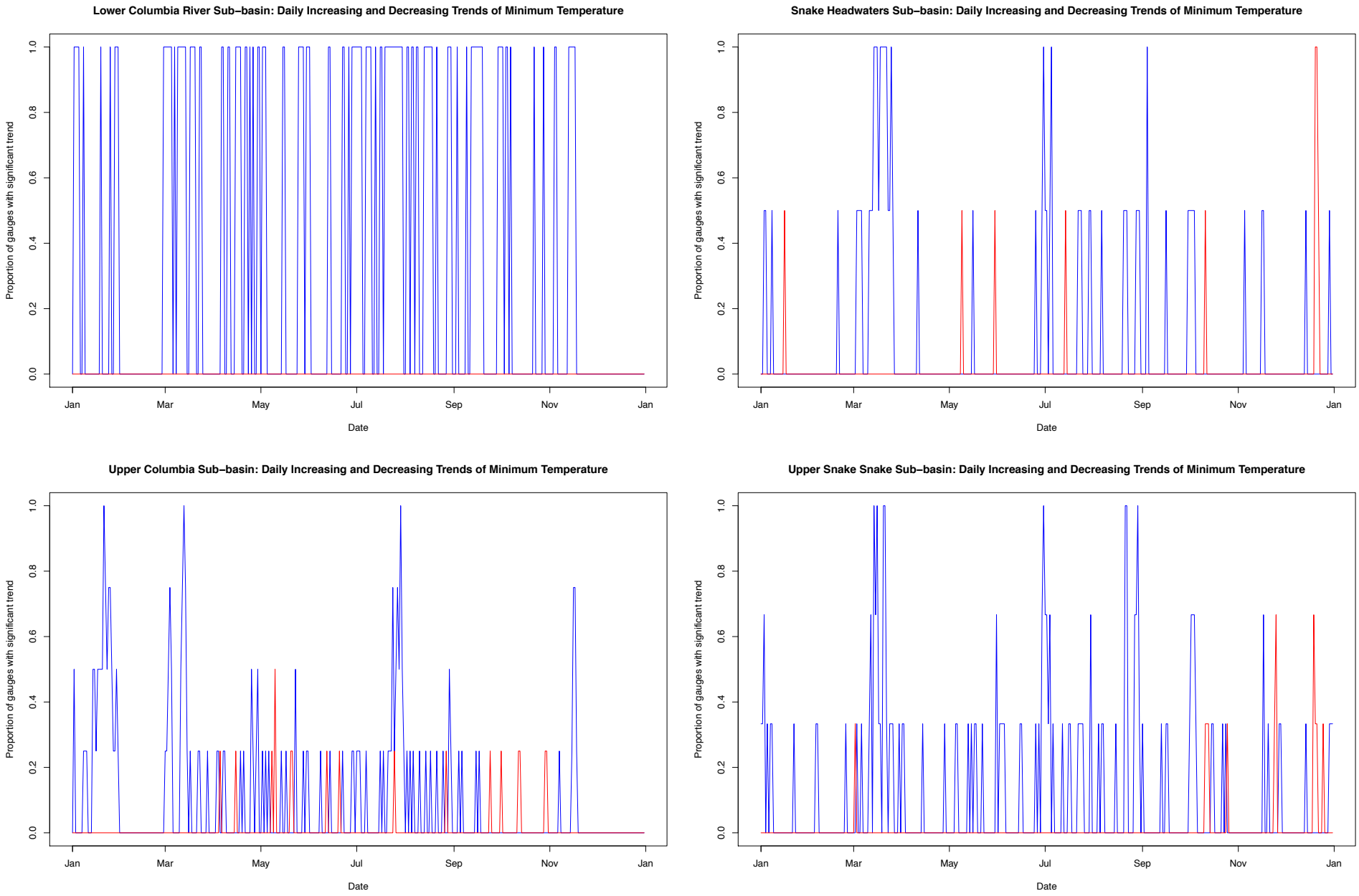

Figure D-14. Daily significant increases and decreases in minimum surface air temperature by sub-basin.

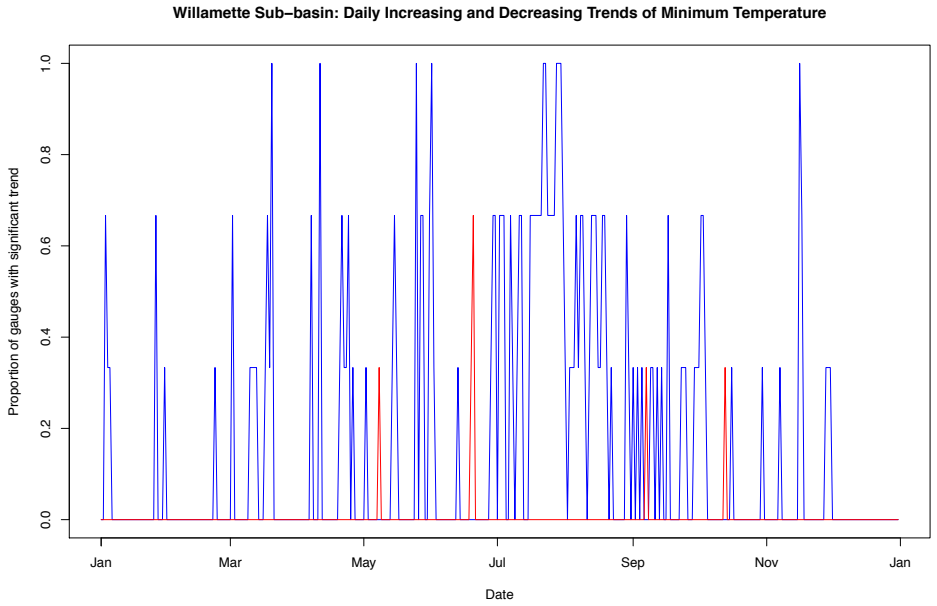

Figure D-15. Daily significant increases and decreases in minimum surface air temperature by sub-basin.

Streamflow

Above dams (figures D-16 to D-20), sub-basins of the Columbia have experienced both significant increases and decreases in daily streamflow partially associated with changes in precipitation, maximum and minimum temperatures. The Boise, Clark Fork, Clearwater, Couer D'Alene, Flathead, Kootenay, Lake Chelan, Middle Columbia, Salmon, Lower Columbia, Snake Headwaters, Upper Columbia, and Willamette sub-basins all display significant increases in March or April daily flows depending on the timing of the sub-basin's snowmelt freshet. Additionally, the Boise, Clark Fork, Clearwater, Couer D'Alene, Deschutes, Flathead, Kootenay, Lake Chelan, John Day, Middle Columbia, Salmon, Lower Columbia, Snake Headwaters, Upper Snake, Upper Columbia and Willamette basins all display significant reductions in summer daily flows at some point during the summer months.

Below dams (figures D-20 to D-24), the Clark Fork and Lower Columbia sub-basins are dominated by decreases in flows throughout the year. Boise and Clearwater sub-basins display increases in below dam flows during April, July and August flows with decreases during much of the rest of the year. Below dam flows in the Upper Snake sub-basin seem to closely follow dam management for irrigation. Increases in flows during summer months with decreases during fall and winter months when precipitation falls seem to suggest that water is being saved and delivered to agricultural users. In the Willamette and Kootenay sub-basins, there are periods of increases below dams during April and May with decreases in summer and winter flows. The Willamette sub-basin additionally displays increases in October and November flows at some gauges.

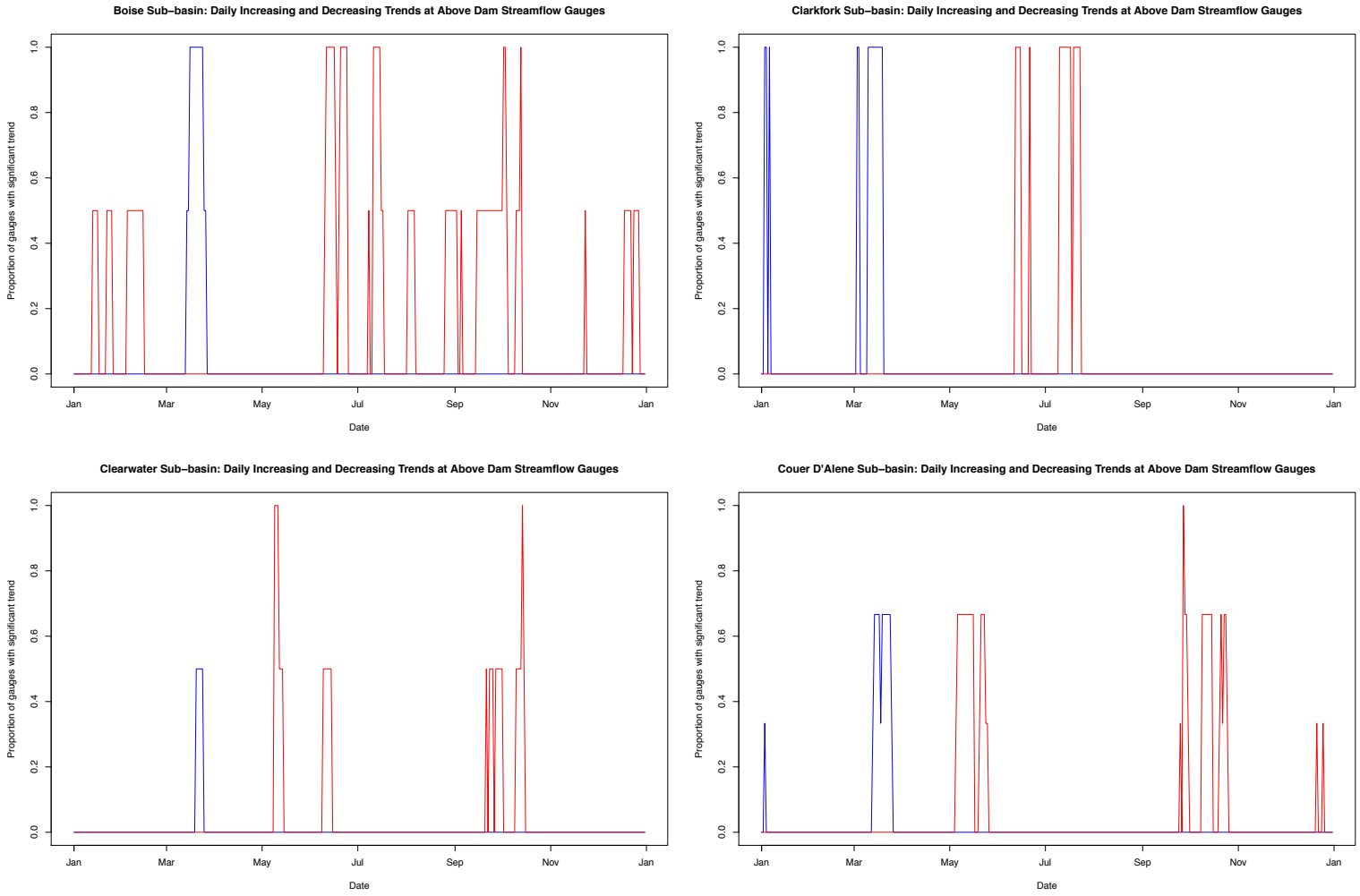

Figure D-16. Daily significant increases and decreases in above dam streamflow by sub-basin.

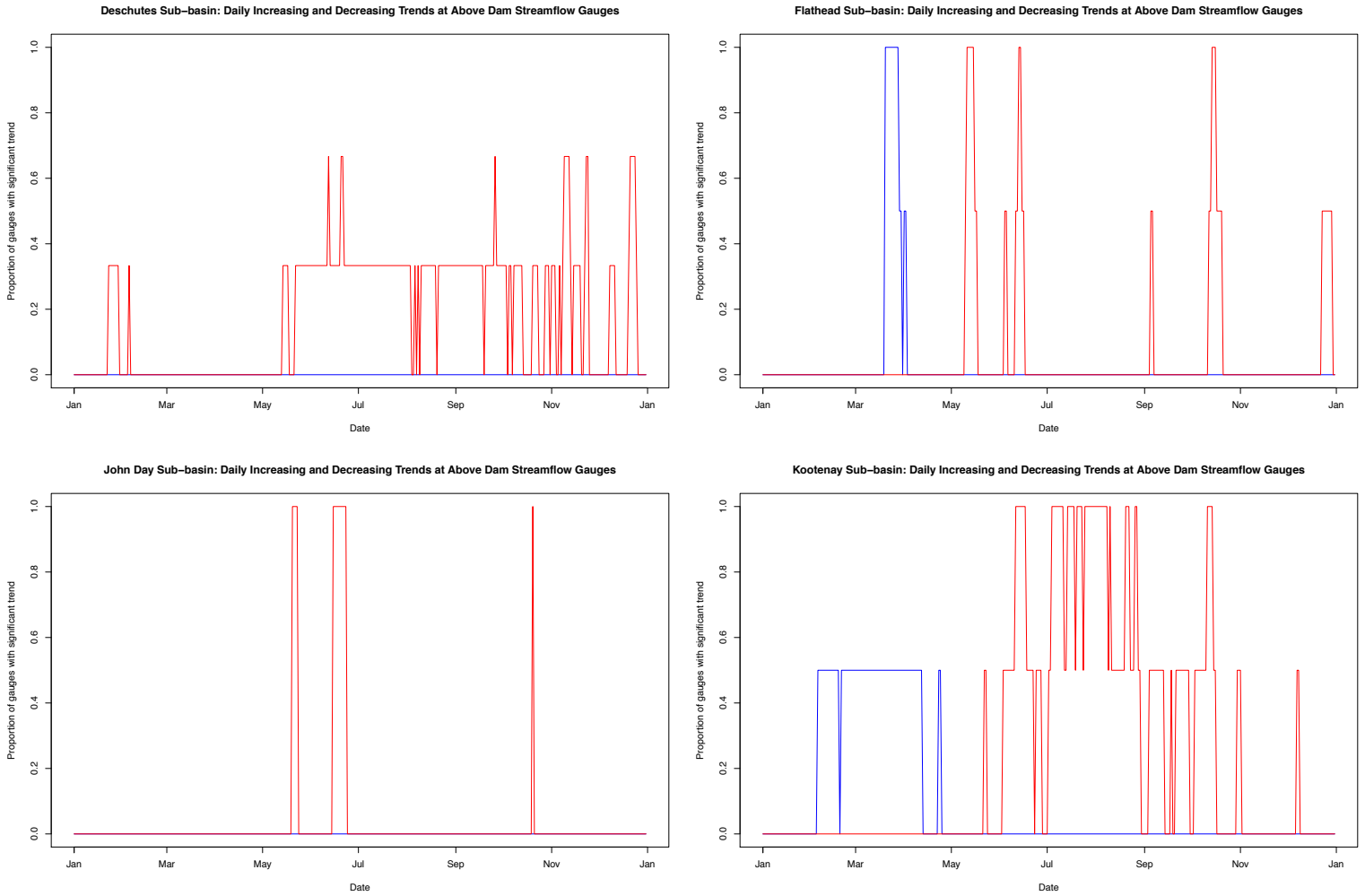

Figure D-17. Daily significant increases and decreases in above dam streamflow by sub-basin.

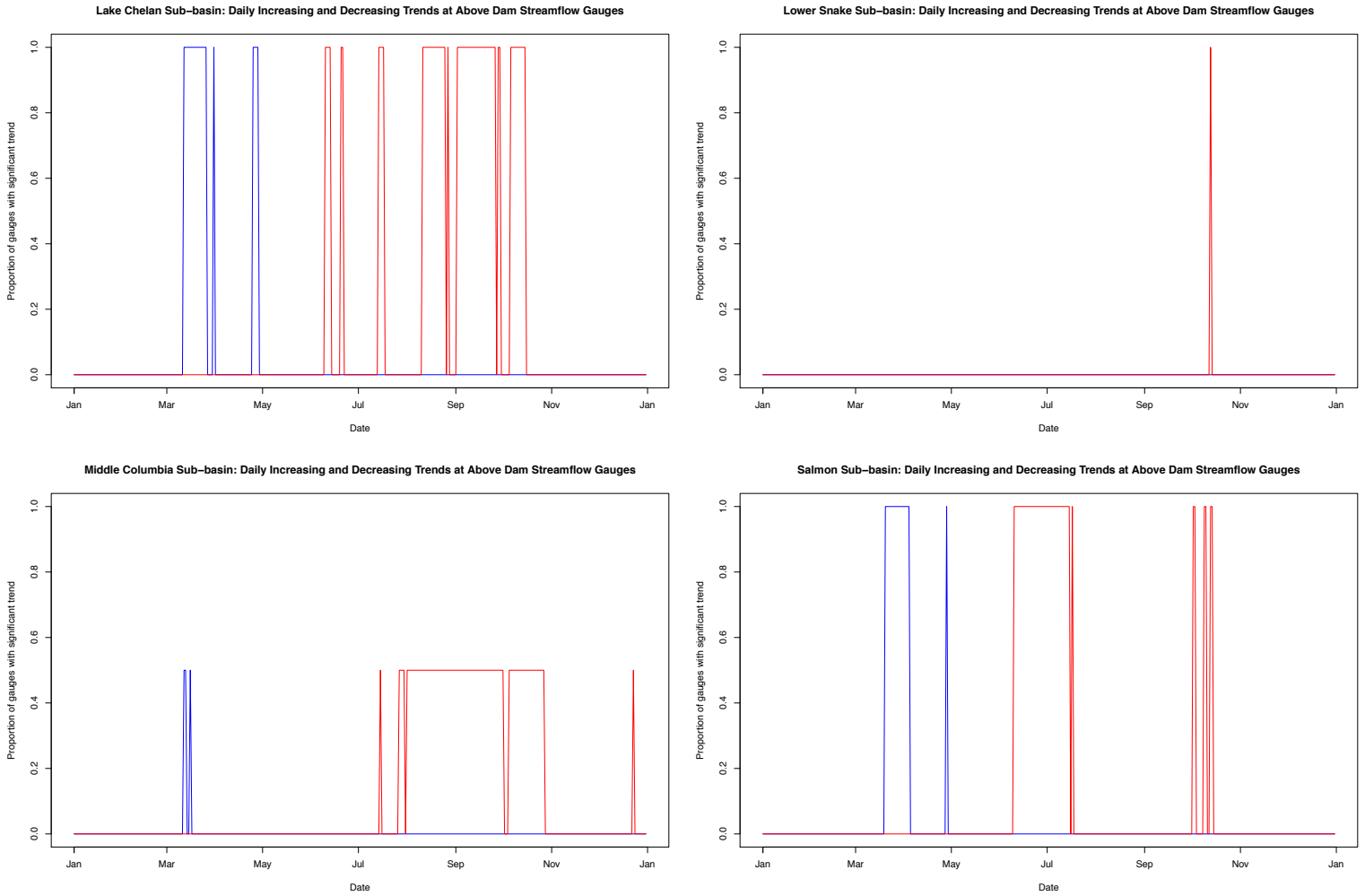

Figure D-18. Daily significant increases and decreases in above dam streamflow by sub-basin.

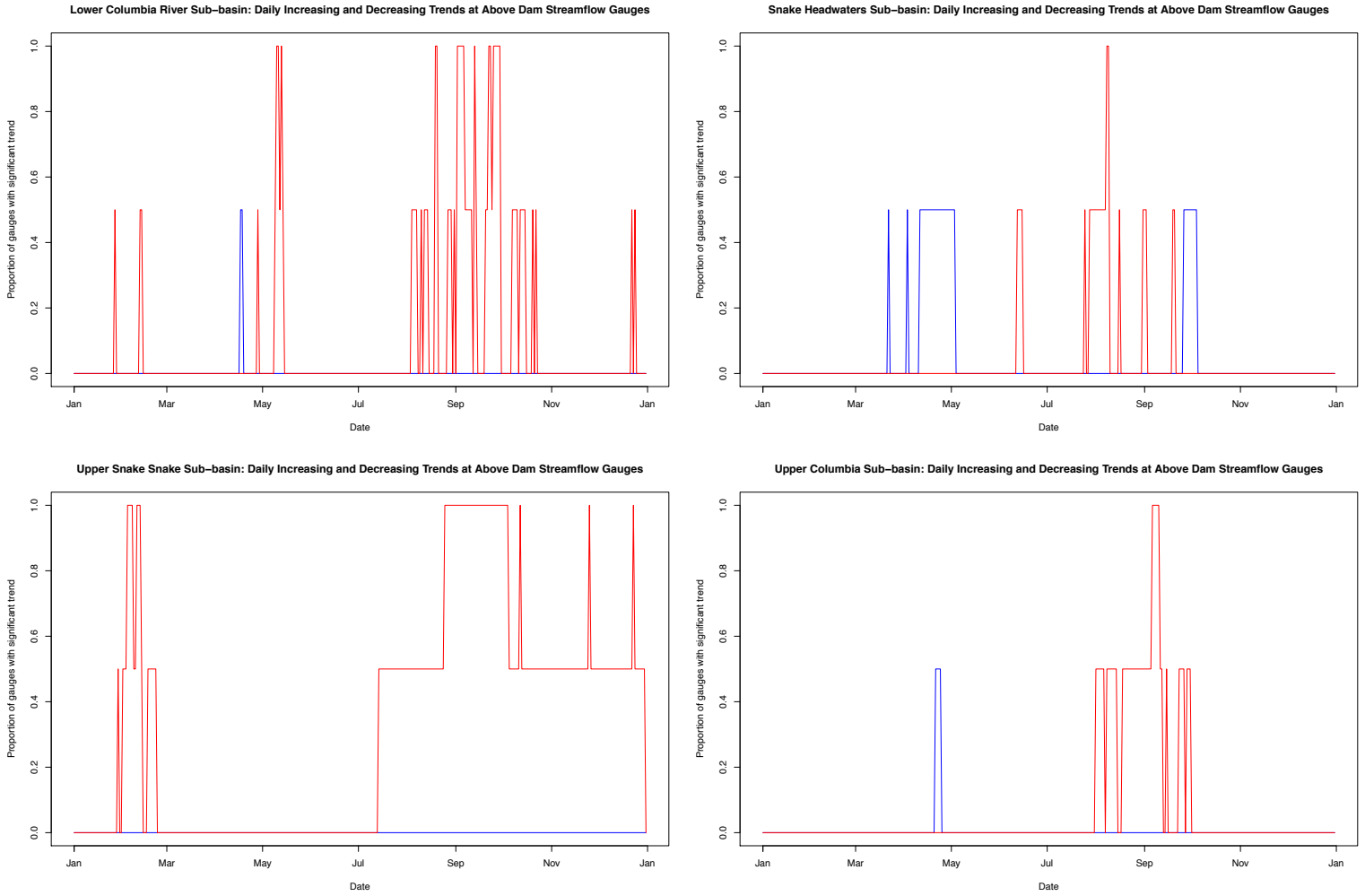

Figure D-19. Daily significant increases and decreases in above dam streamflow by sub-basin.

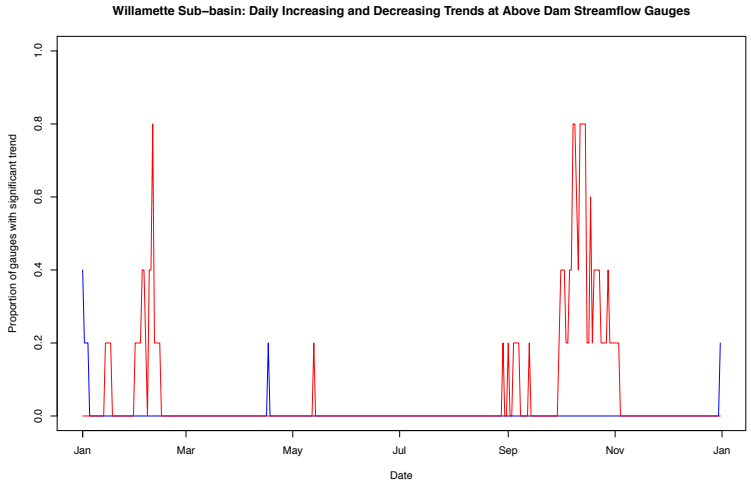

Figure D-20. Daily significant increases and decreases in above dam streamflow by sub-basin.

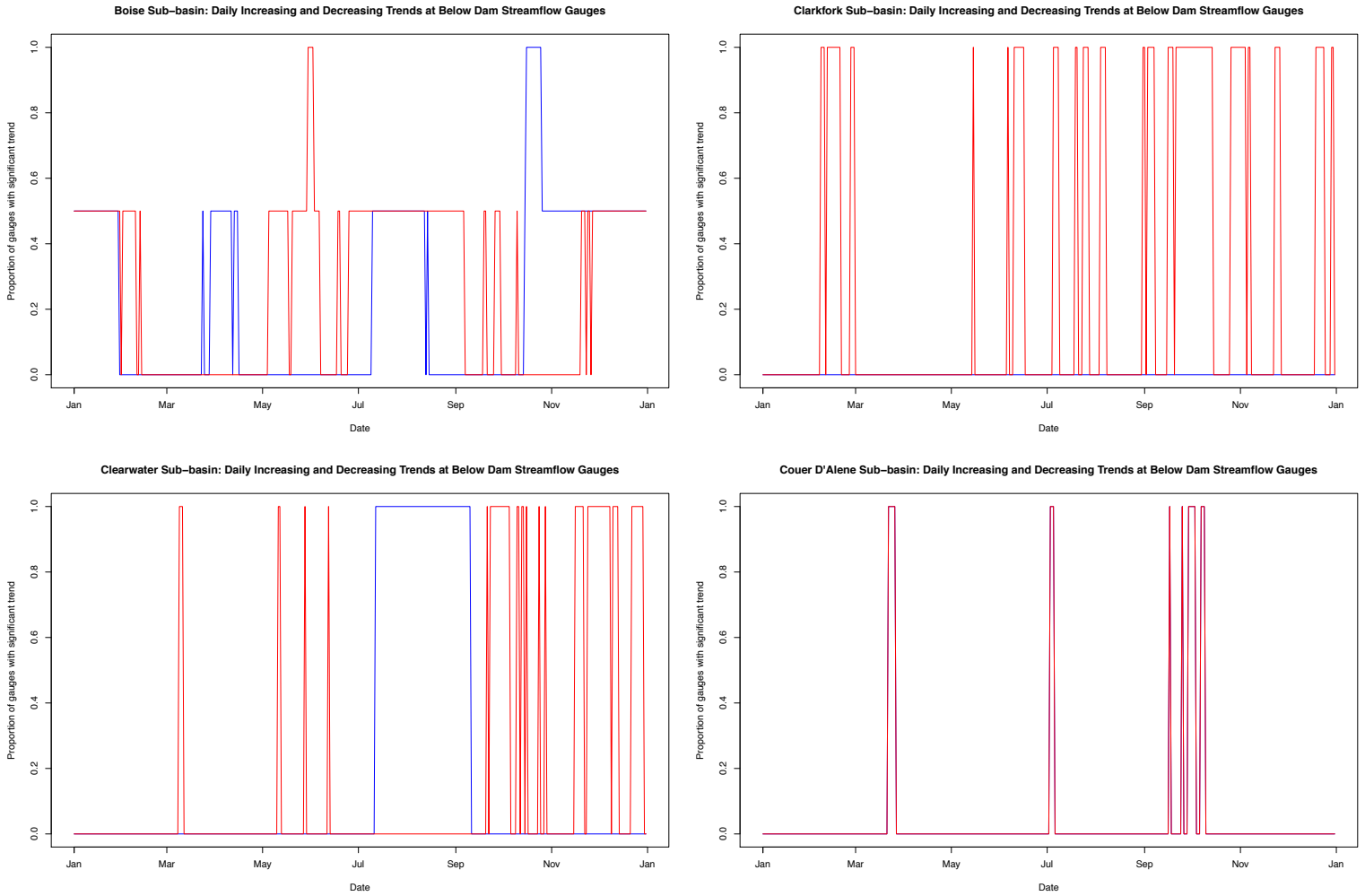

Figure D-21. Daily significant increases and decreases in below dam streamflow by sub-basin.

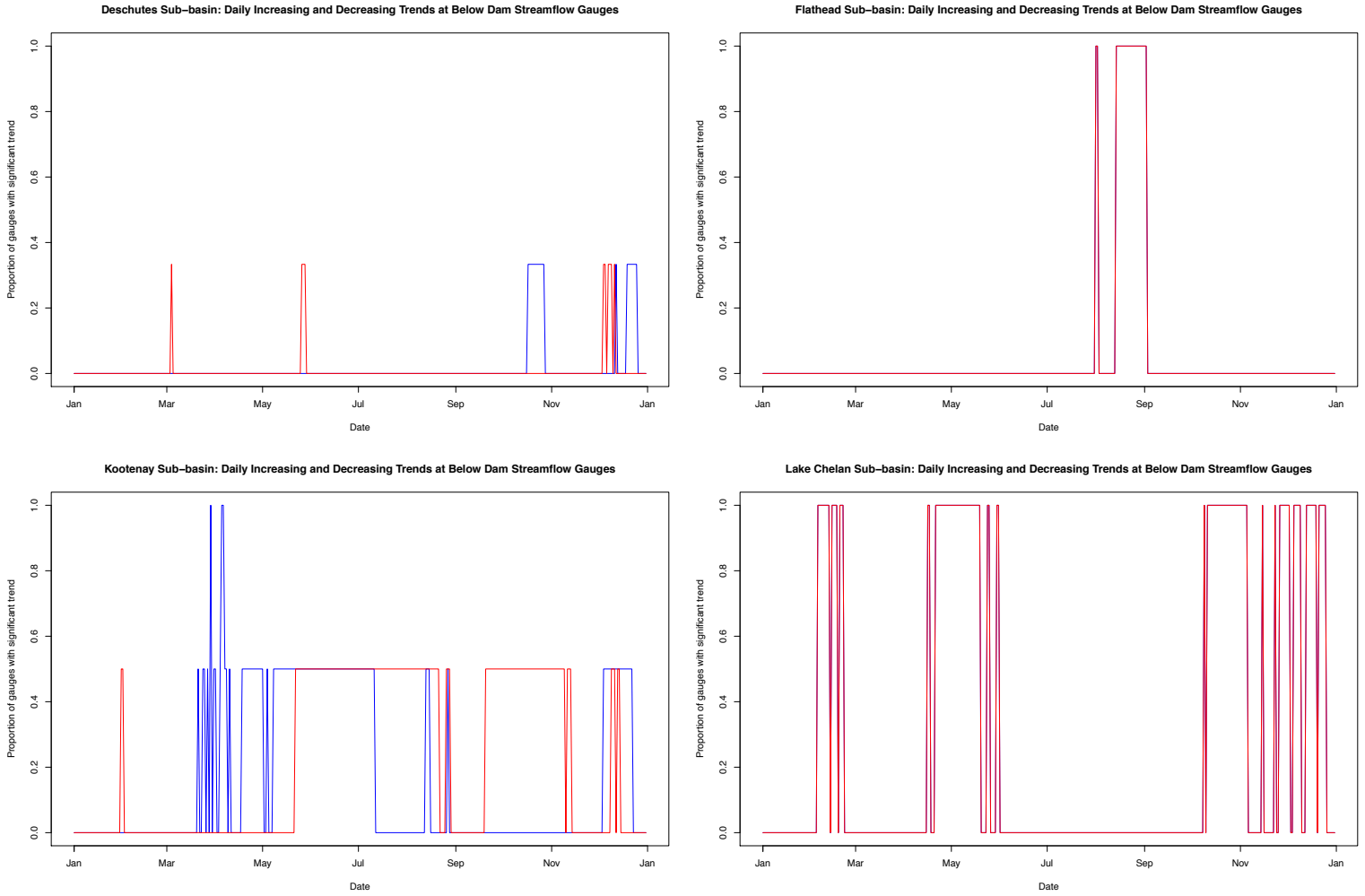

Figure D-22. Daily significant increases and decreases in below dam streamflow by sub-basin.

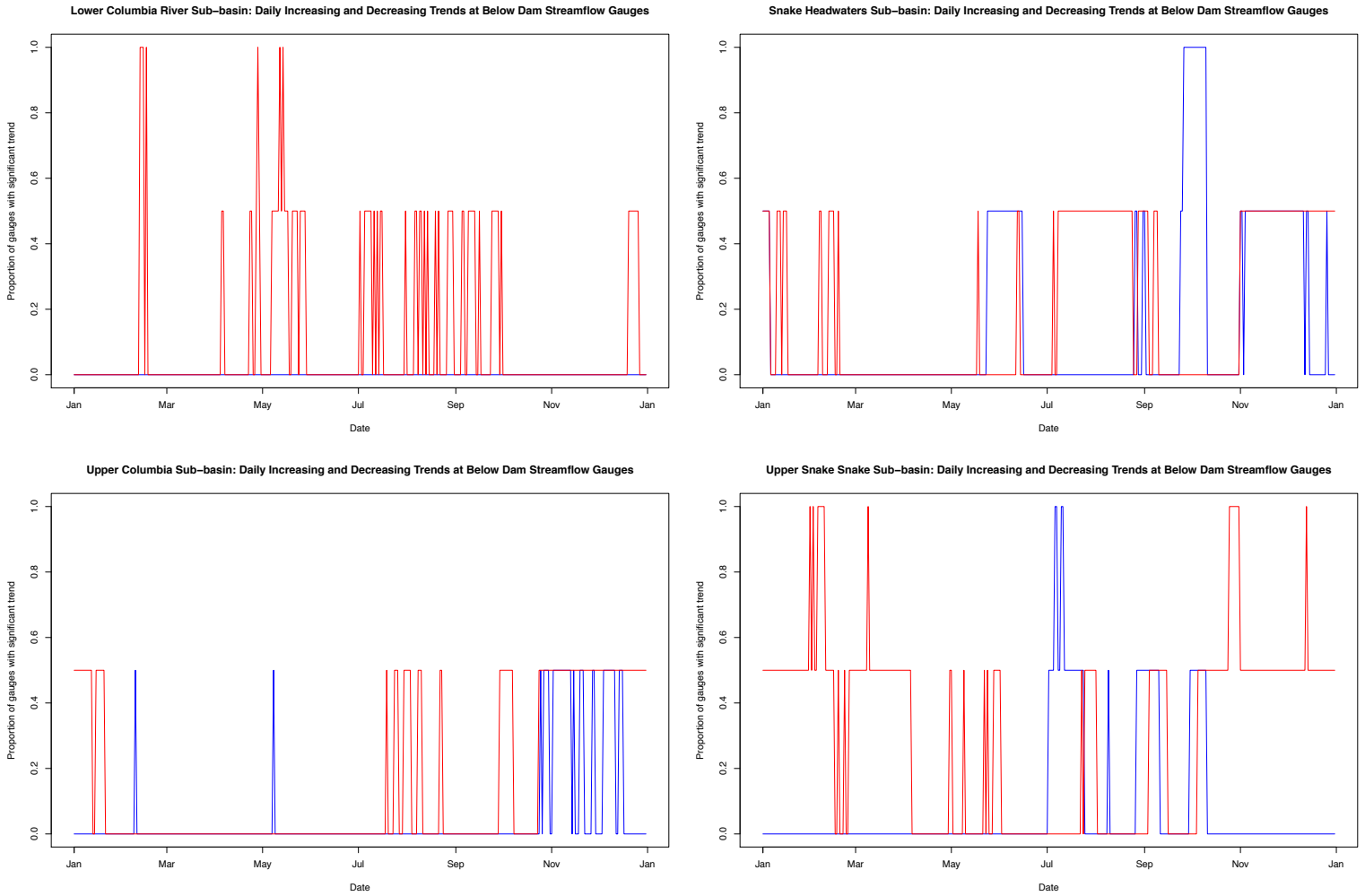

Figure D-23. Daily significant increases and decreases in below dam streamflow by sub-basin.

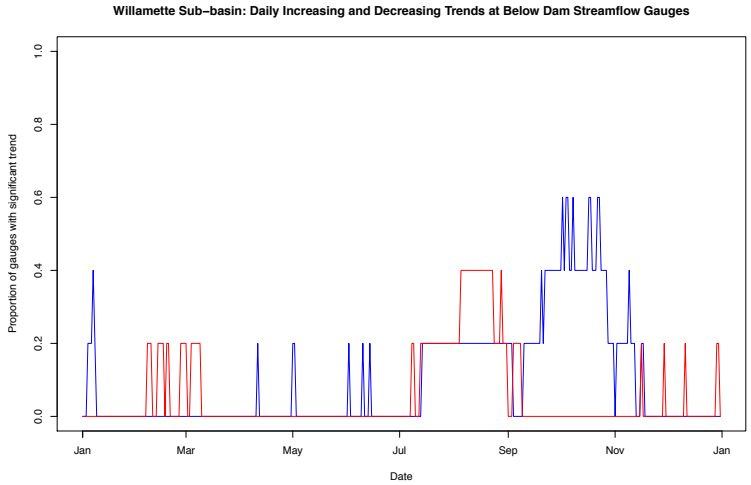

Figure D-24. Daily significant increases and decreases in below dam streamflow by sub-basin.

Appendix E

Linear trend results for the full CRB

Climate

As noted in study site and sub-basin sections of the results, there seems to be a near uniform increase in minimum temperature across the Columbia River Basin from 1950 to 2012. This increase in minimum surface air temperature is present throughout the year, though this analysis counting trends at the alpha equals 0.05 level found few increasing trends in February and December minimum temperatures.

Maximum daily surface air temperatures across the basin show both increasing and decreasing trends throughout the records of the climate station used in this study. Increases seem to dominate, but not to the same degree as present in minimum surface air temperature results.

There do not seem to be any coherent trends in increasing or decreasing precipitation at the basin scale. The balance between whether there are more increasing or decreasing trends on each day of year switches many times throughout the year without any mechanistic explanation.

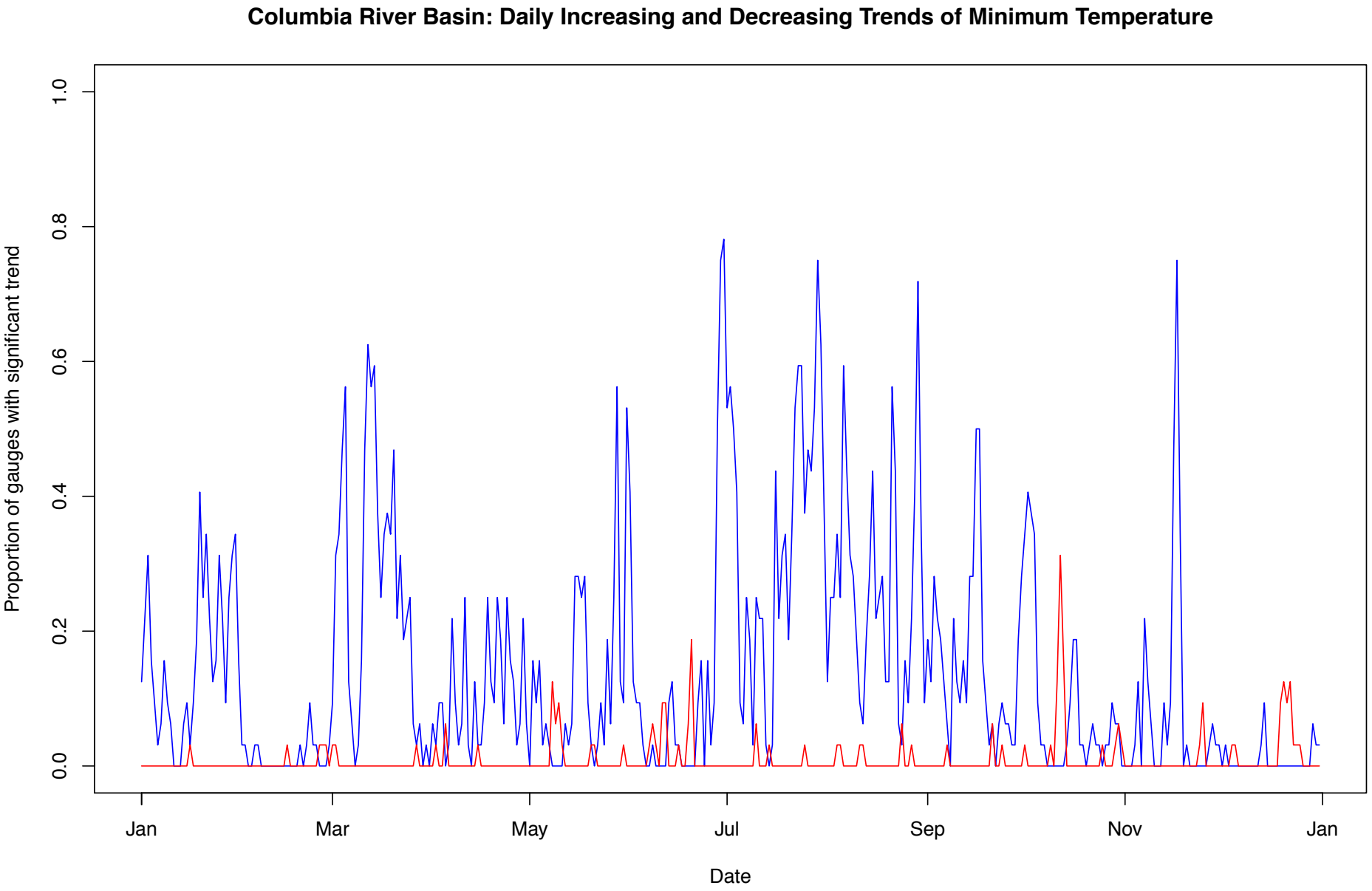
Columbia River Basin: Daily Increasing and Decreasing Trends of Minimum Temperature
Proportion of gauges with significant trend
0.0
0.2
0.4
0.6
0.8
1.0
Jan
Mar
May
Jul
Sep
Nov
Jan
Date

Figure E-1. Significant increasing and decreasing trends in minimum surface air temperature.

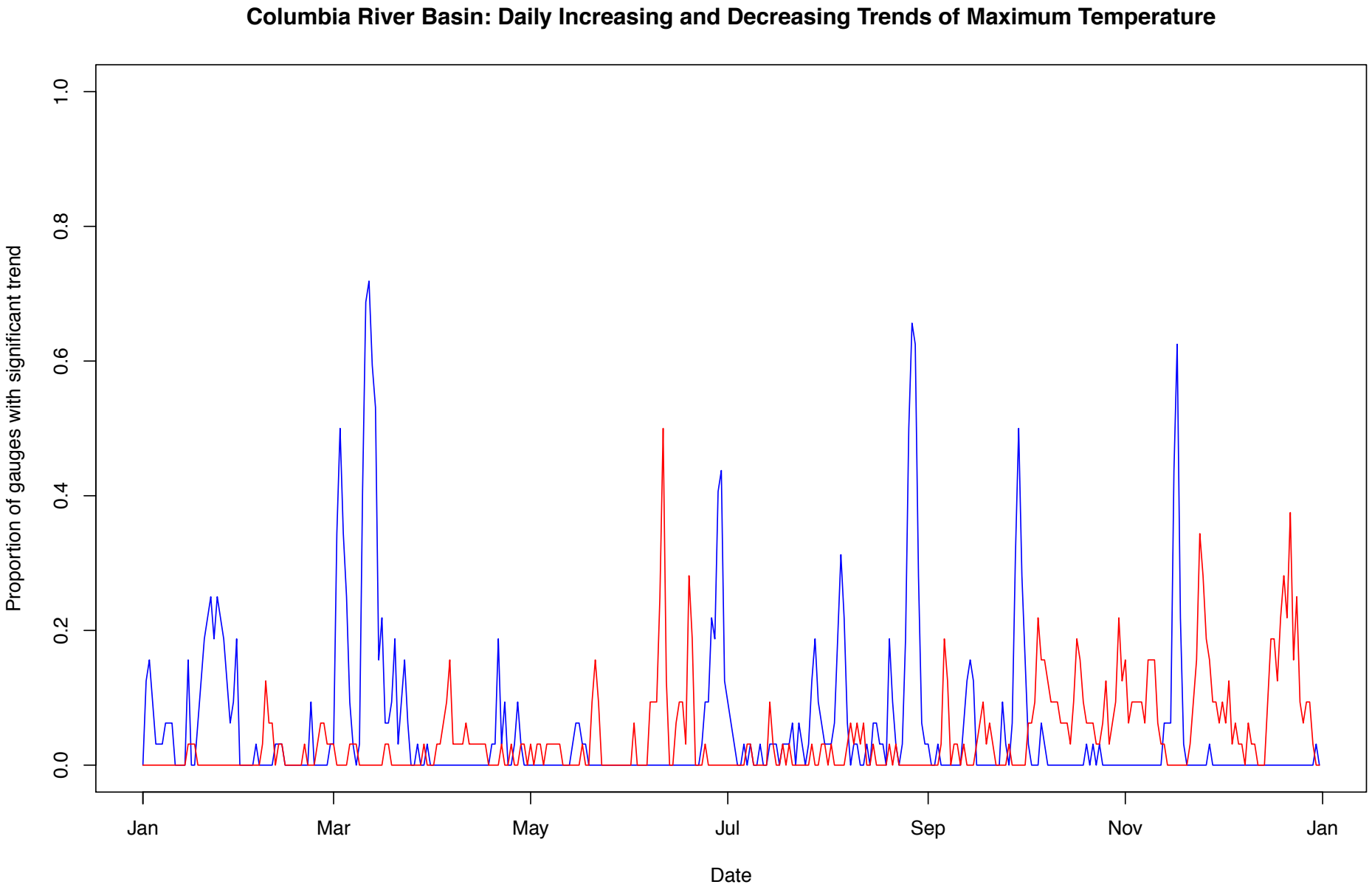

Figure E-2. Significant increasing and decreasing trends in maximum surface air temperature.

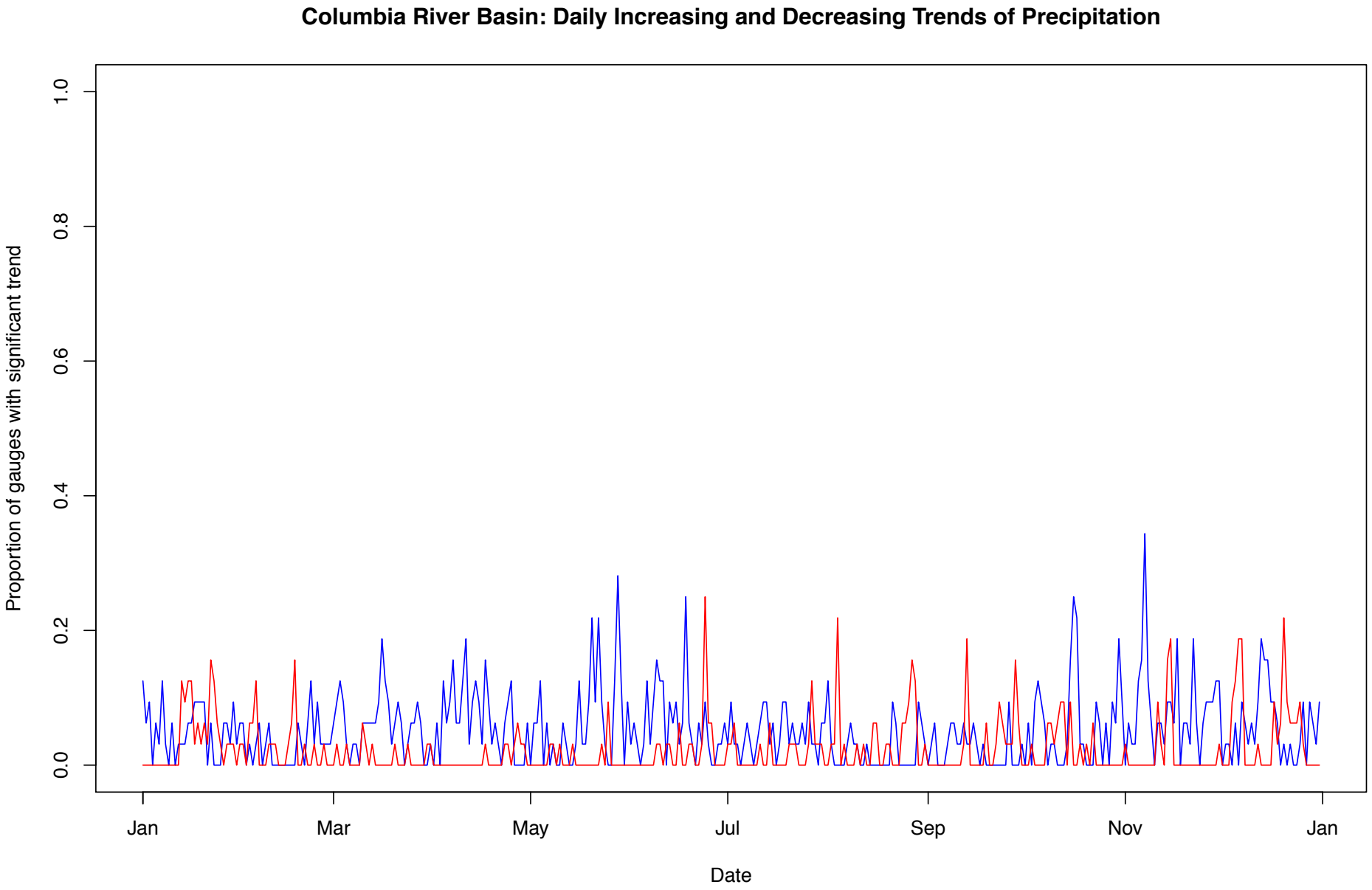

Figure E-3. Significant increasing and decreasing trends in precipitation.

Streamflow

Across the CRB, there have been most markedly increasing daily trends in mid March to the beginning of May, and corresponding decreasing trends from the middle of May to the middle of October. The broad peak of increases in flows from March to May corresponds with the large variety in latitude across these sites, which influences the arrival of the snowmelt freshet in these systems. These results of the proportion of gauges showing a significant increasing or decreasing trend by day of year come from a total of 34 above dam streamflow gauges.

Basin wide below dam results are complicated by the fact that below dam flows are the result of above dam flows as well as reservoir and dam management. Management values are diverse and include flood control, hydropower, irrigation, water supply, and recreation that all exert different changes on the above dam hydrographs. Results of the proportion of gauges showing a significant increasing or decreasing trend by day of year come from a total of 25 below dam streamflow gauges. Parsing below dam gauges by dam and reservoir management goals removes some of the noise present in the following figure.

Below dams that are managed for flood control there are decreases in flows between July and the middle of September. This is also true for dams that are managed for hydropower during the month of September. Significant decreases above dams overlap with below dam decreases during these periods and thus it is possible that the climate signal from above dams in propagating below several dams that are managed for hydropower and flood control across the basin.

Above dams, March monthly flows display significant increases at a fraction of the headwater gauges used in this study. A total of nine gauges show these increases with an

additional station in the Deschutes sub basin showing a significant decrease. A total of sixteen gauges show significant declines in September monthly flows at the alpha equals 0.1 level. Part of the reason that there may be a greater fraction of above dam gauges showing significant decreases in September flows is that across the basin, this is the month the furthest removed from the fall, winter and spring rains and snows deposited in the mountain systems. March flows on the other hand may be illustrative changes toward earlier flows in the southern sub-basins of the CRB, but northern sub-basins have snowmelt freshets arriving in April or even early May. Differences between the results in this study and those from Heejun Chang's 2012 publication are due to differences in methodology and gauge selections, with each study utilizing gauges that matched their research questions. Below dams, trends in March and September flows are mixed and do not readily seem to fit a pattern.

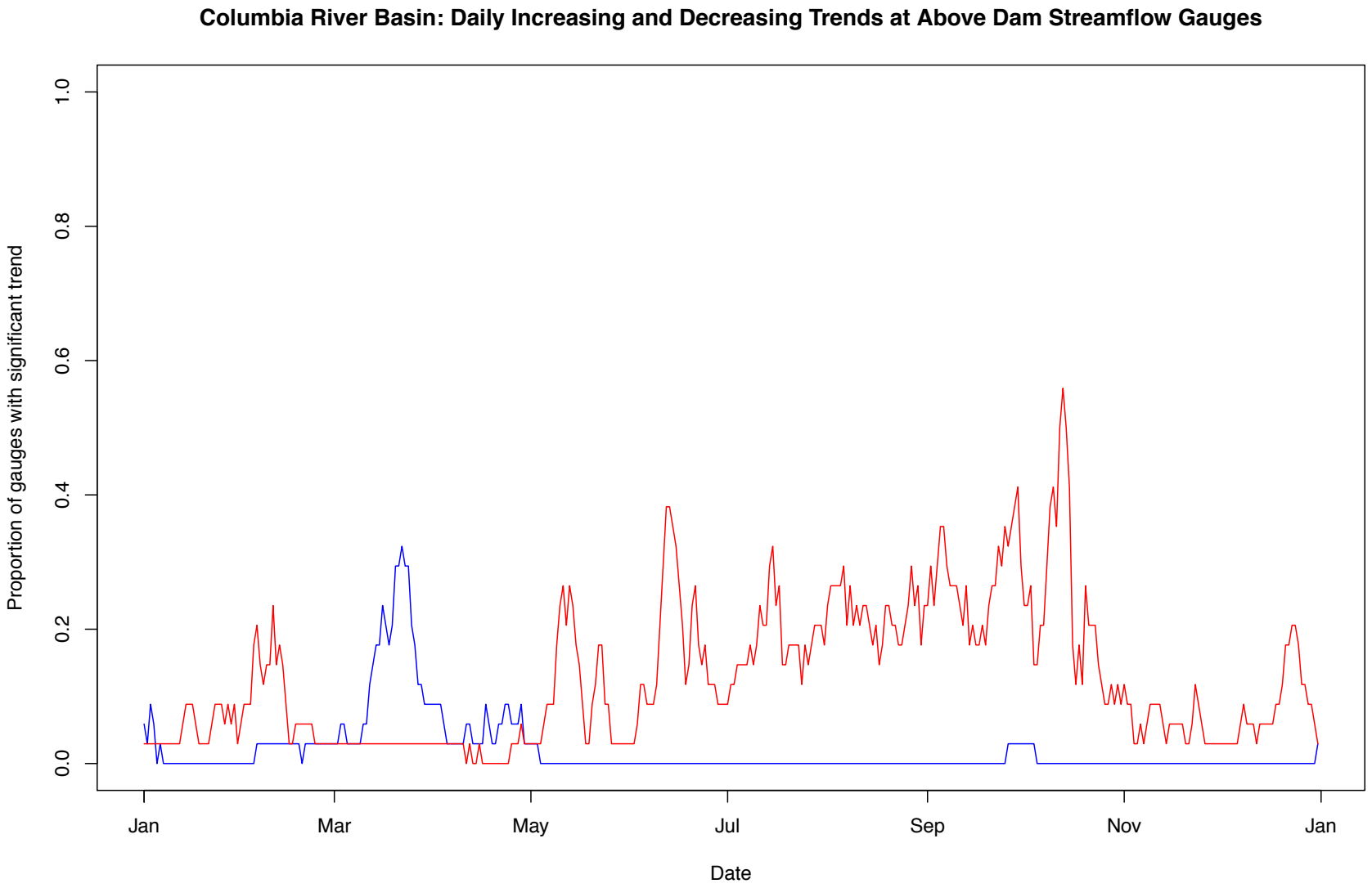

Figure E-4. Significant increasing and decreasing trends in streamflow above dams.

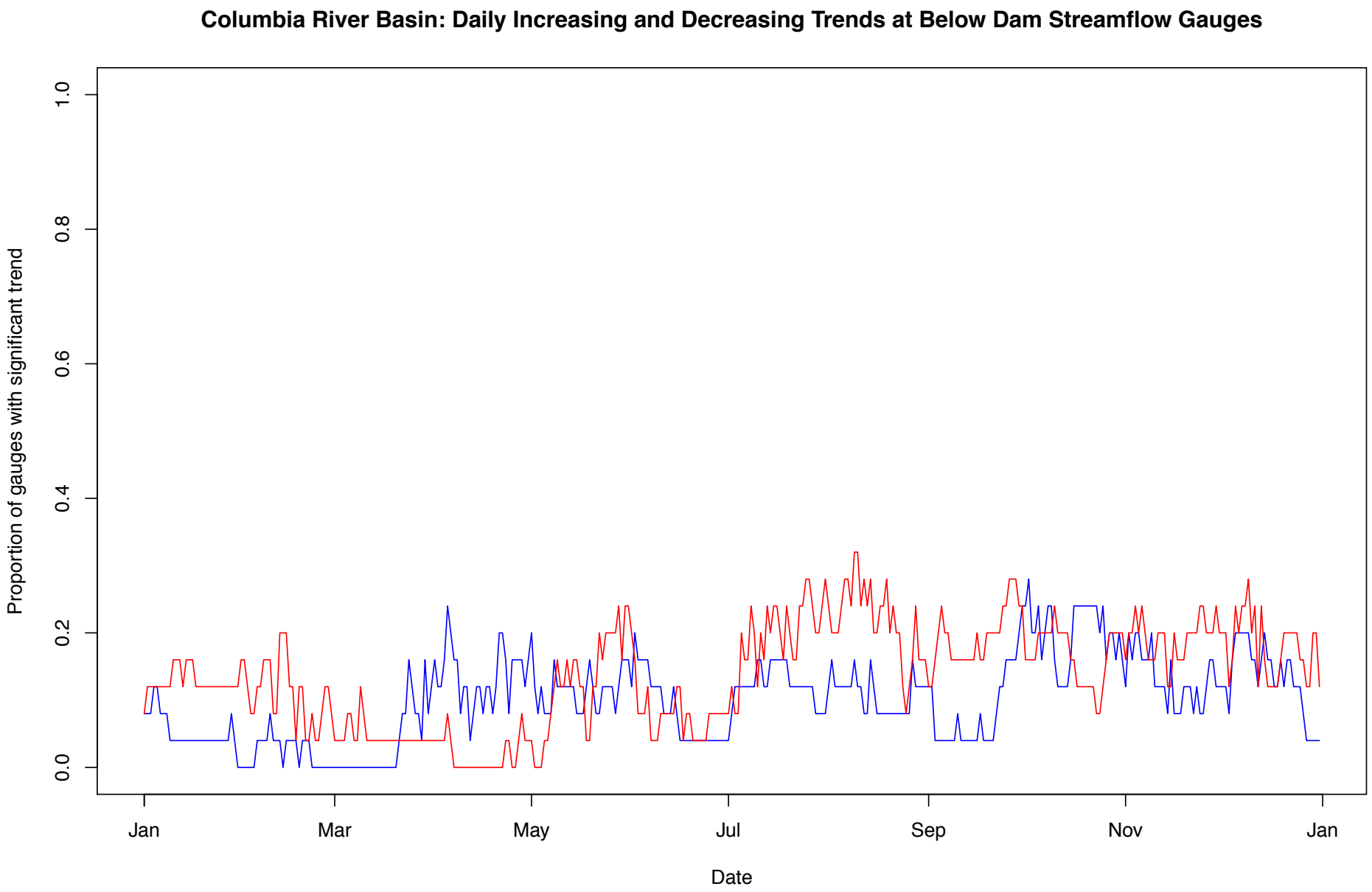

Figure E-5. Significant increasing and decreasing trends in streamflow below dams.

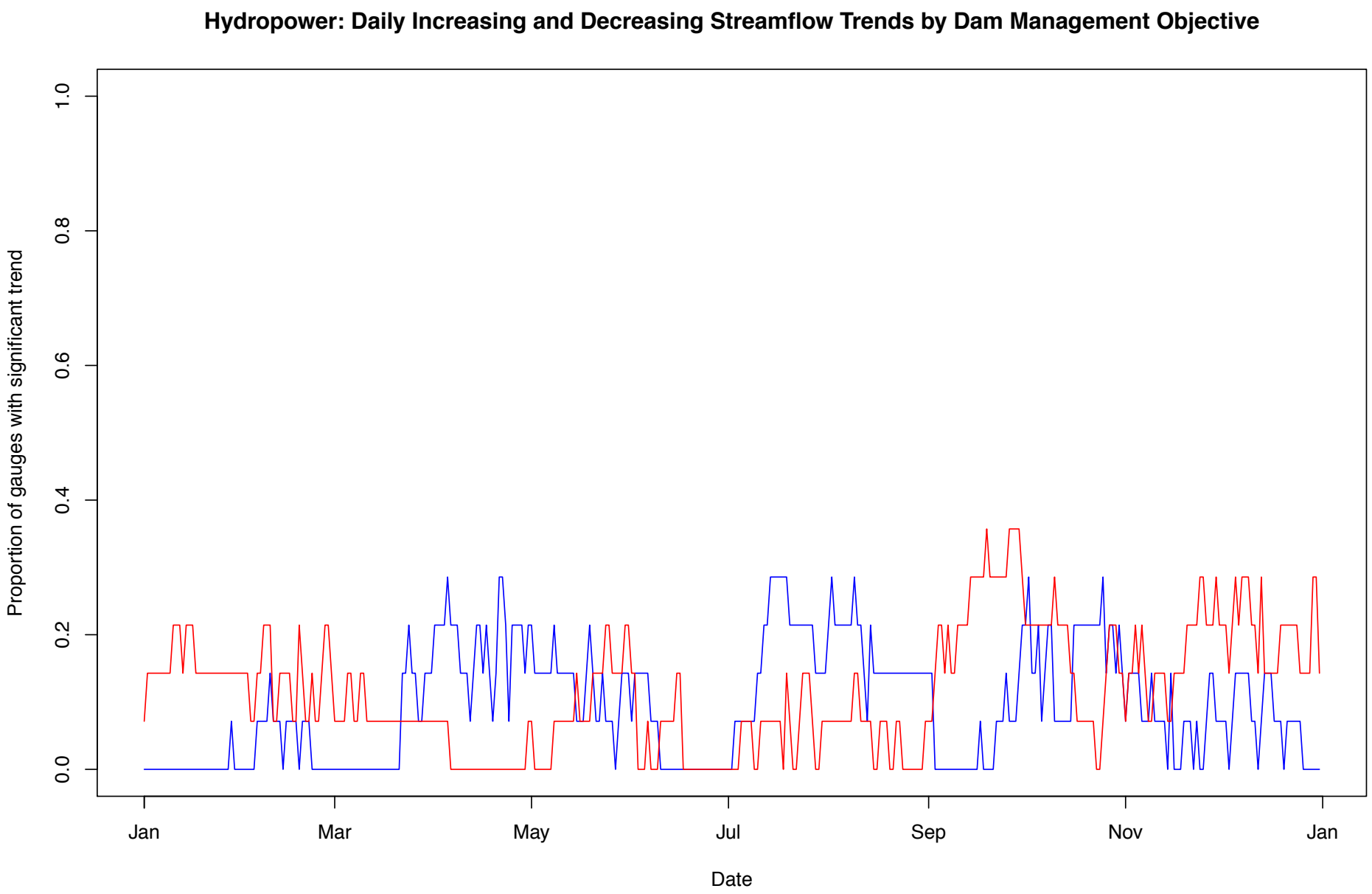

Figure E-6. Significant increasing and decreasing trends in streamflow below dams managed for hydropower.

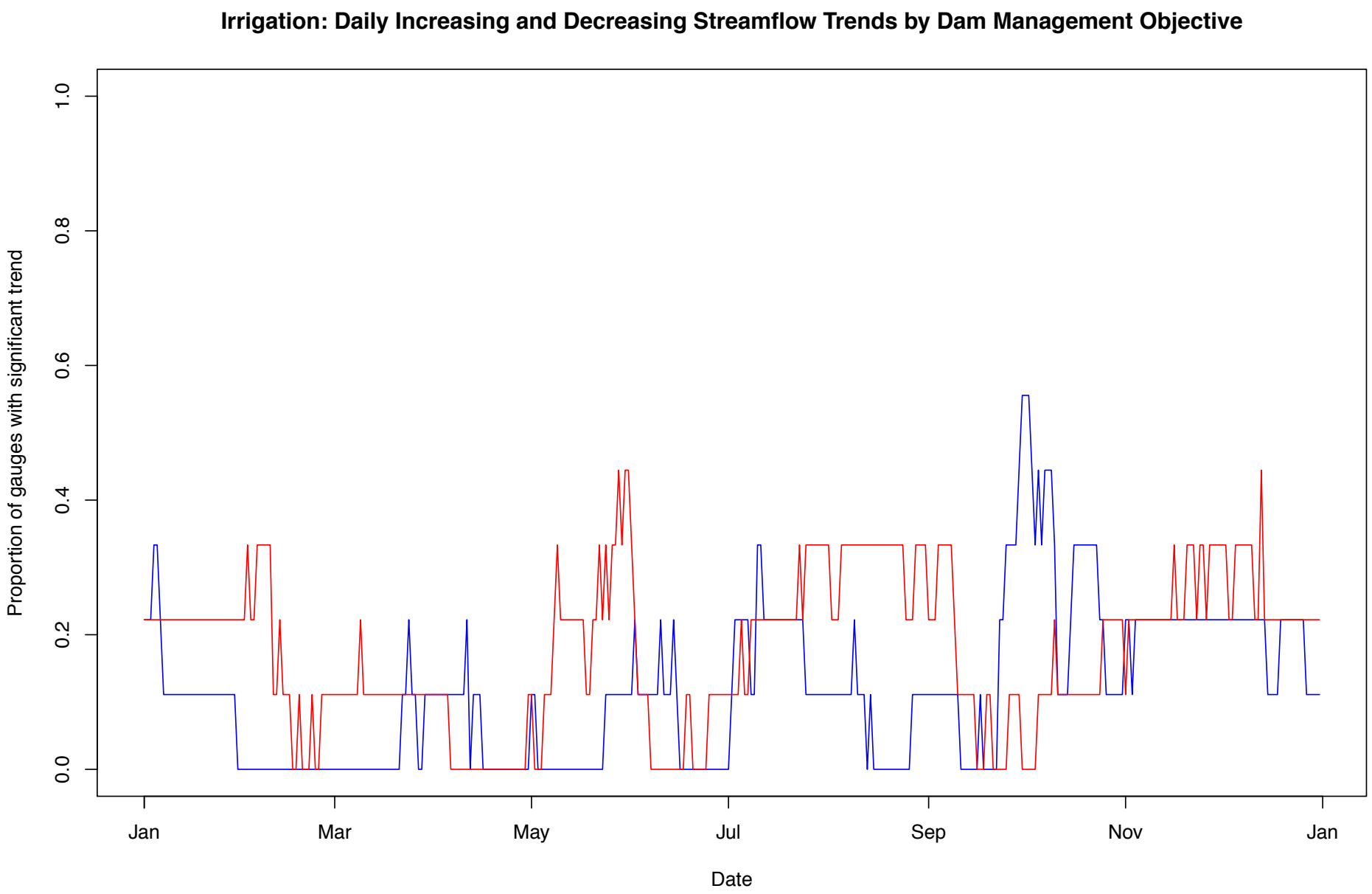

Figure E-7. Significant increasing and decreasing trends in streamflow below dams managed for irrigation.

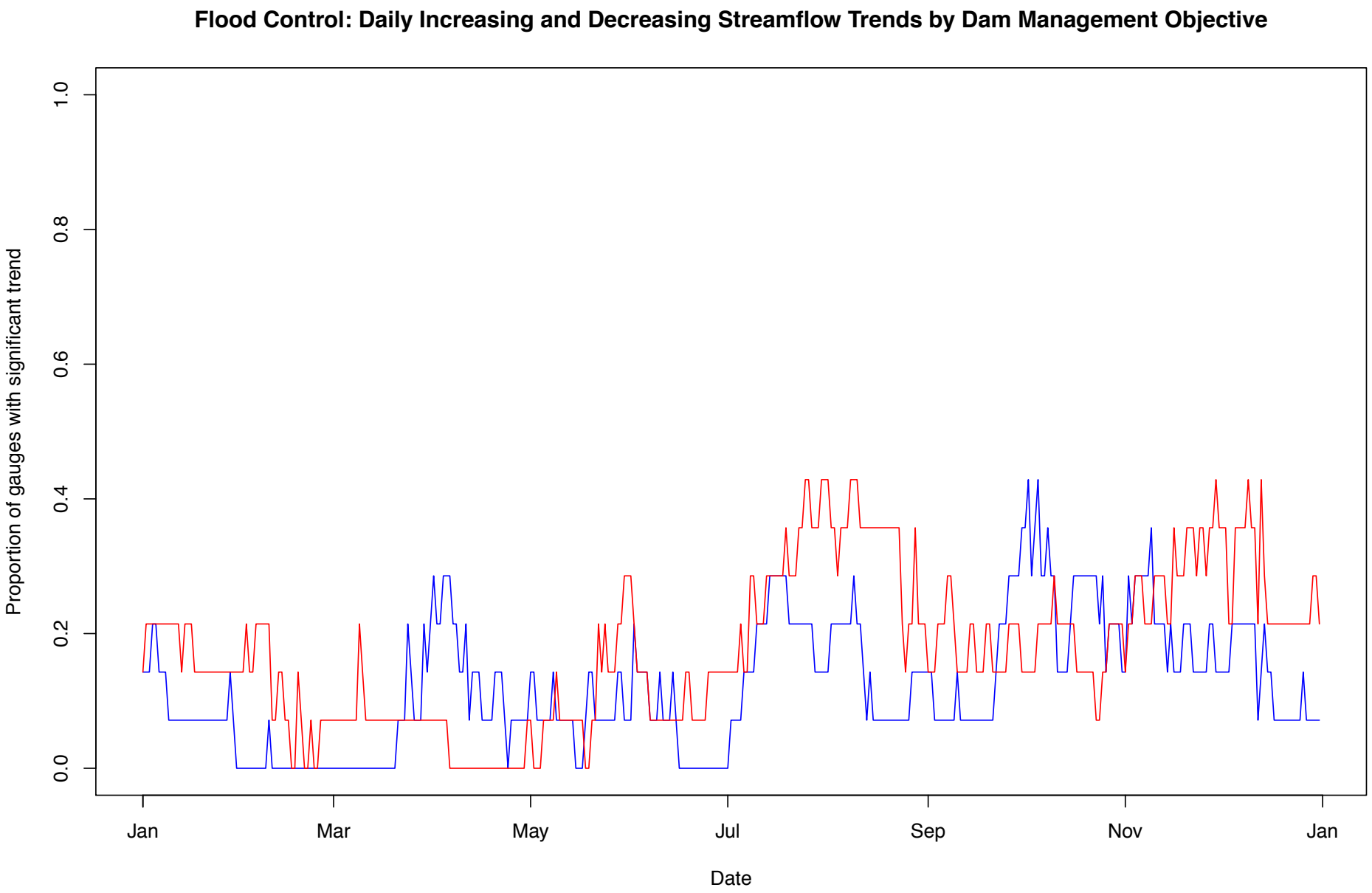

Figure E-8. Significant increasing and decreasing trends in streamflow below dams managed for flood control.

Appendix F

Precipitation and streamflow changes in mm, and trend result differences between Mann-Kendall and linear regression analyses

Total annual precipitation from 1950 to 2012 for each climate station

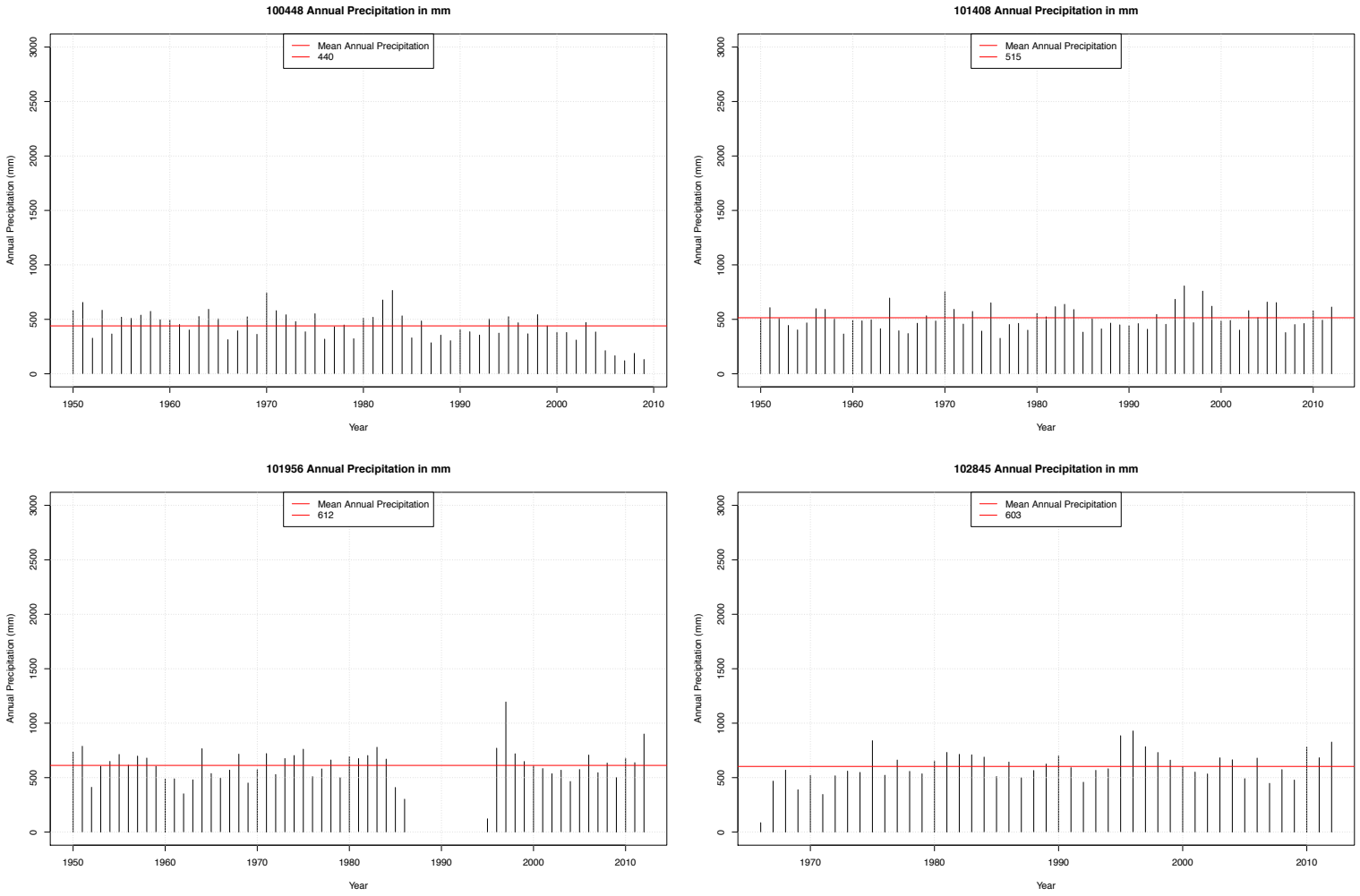

Figure F-1. Total annual precipitation and mean annual precipitation.

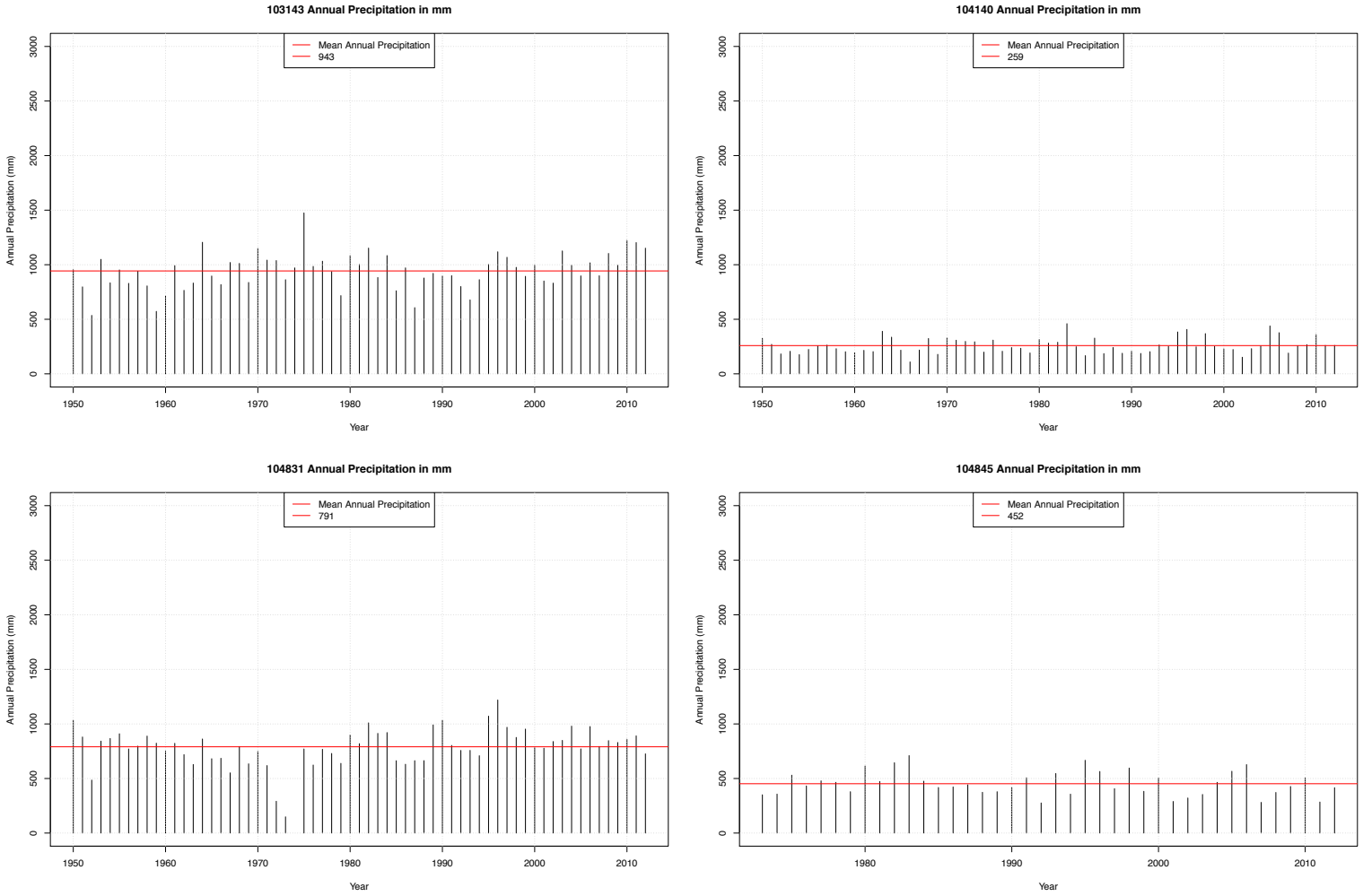

Figure F-2. Total annual precipitation and mean annual precipitation.

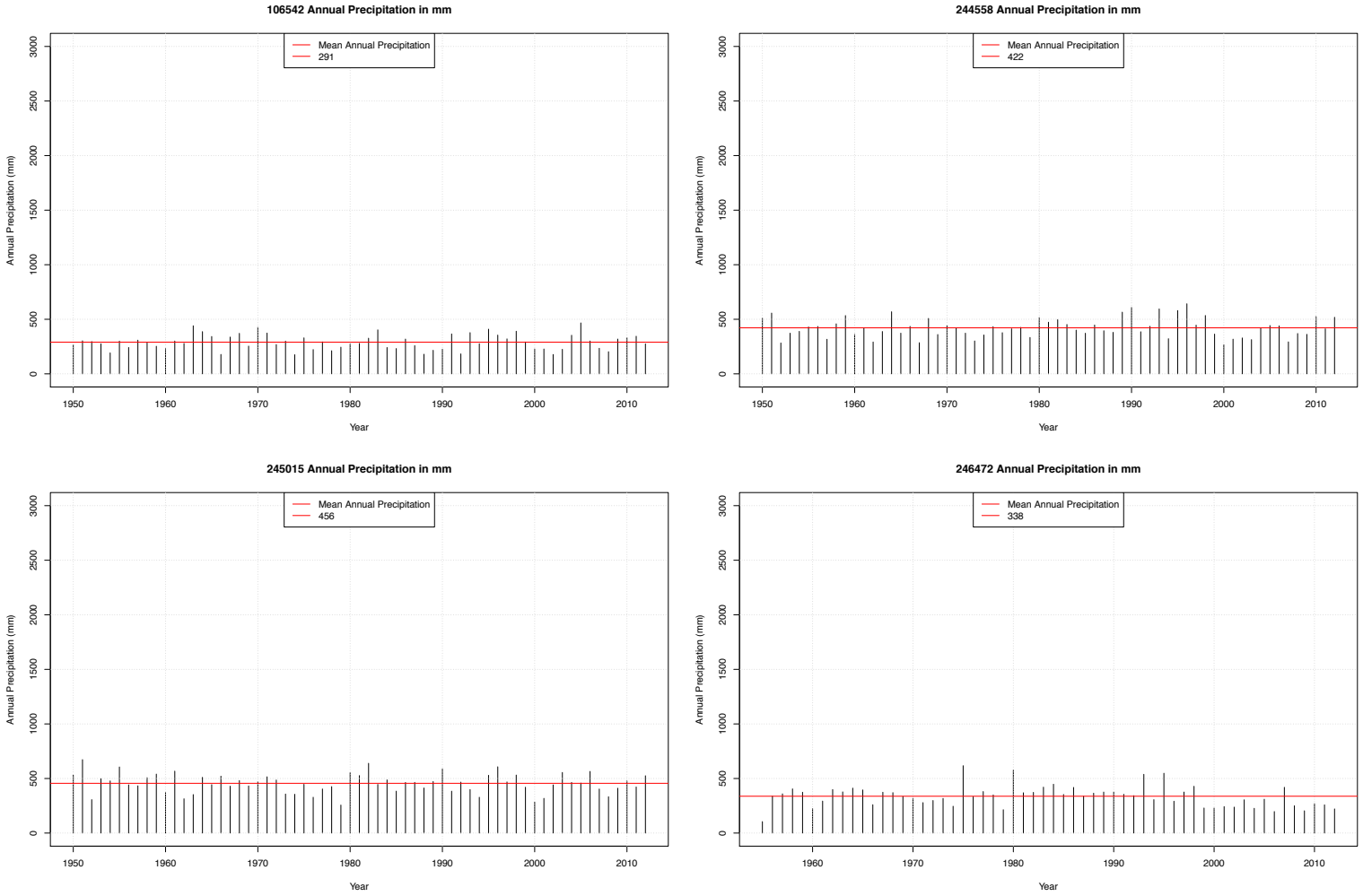

Figure F-3. Total annual precipitation and mean annual precipitation.

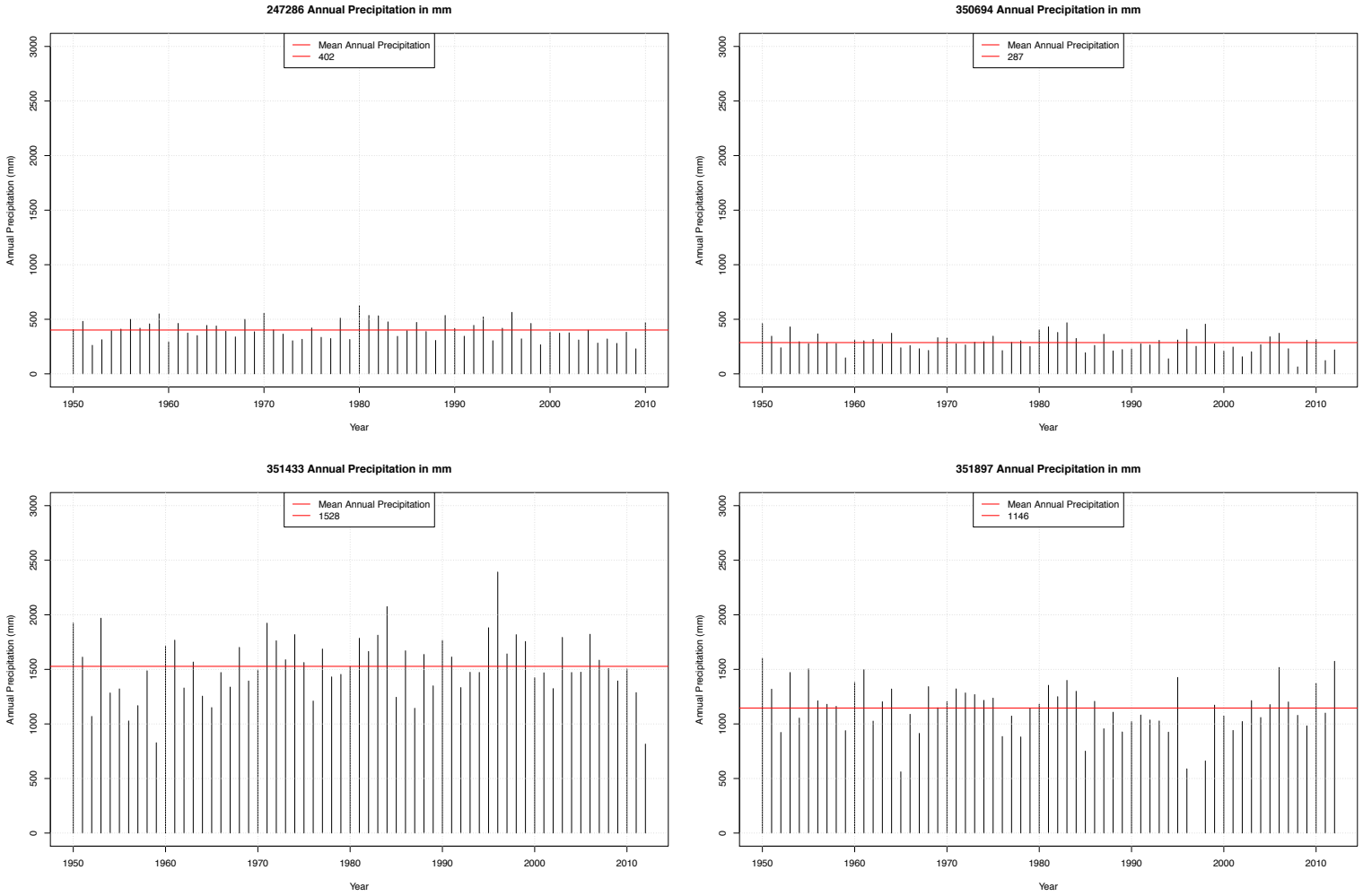

Figure F-4. Total annual precipitation and mean annual precipitation.

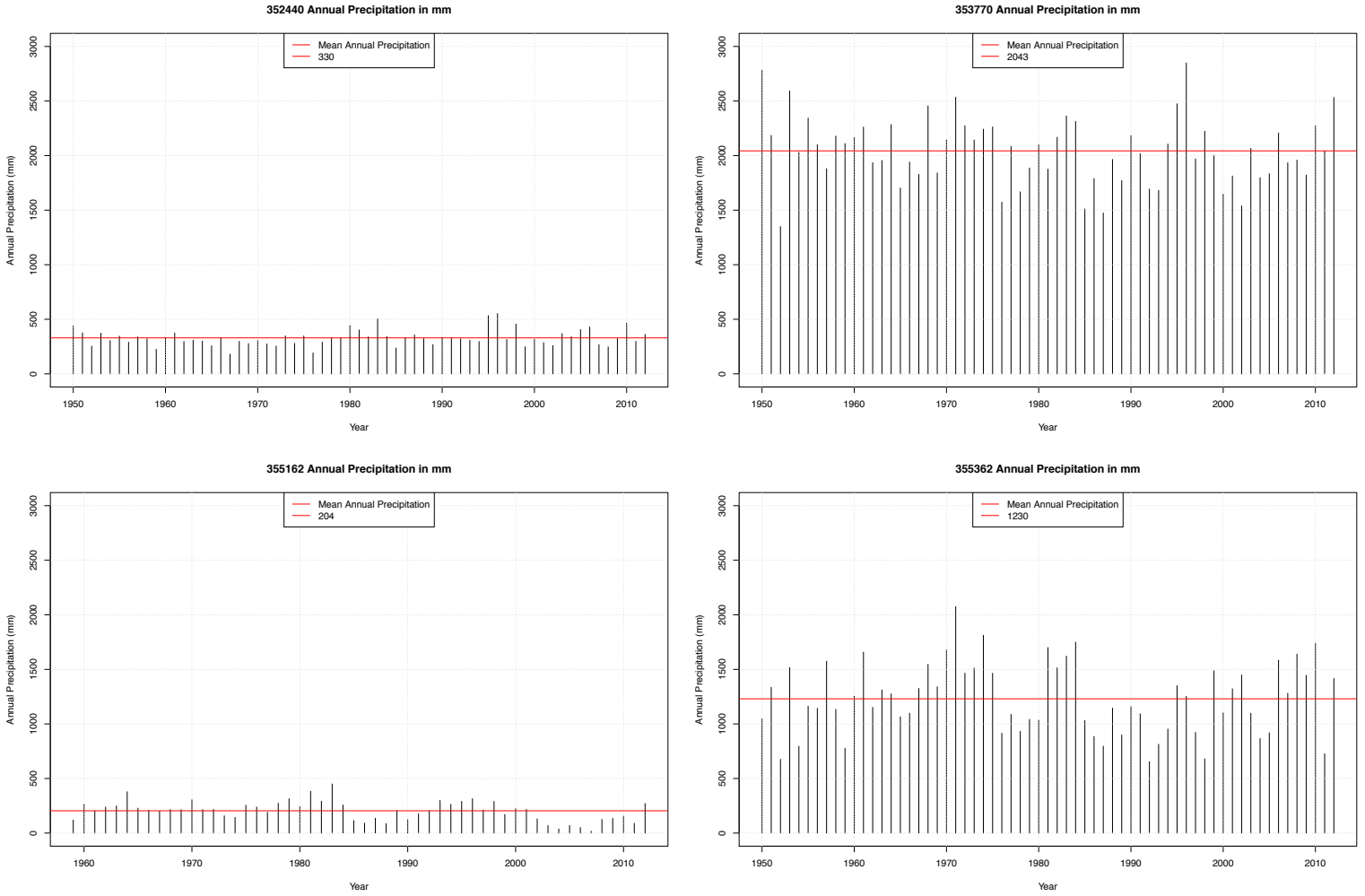

Figure F-5. Total annual precipitation and mean annual precipitation.

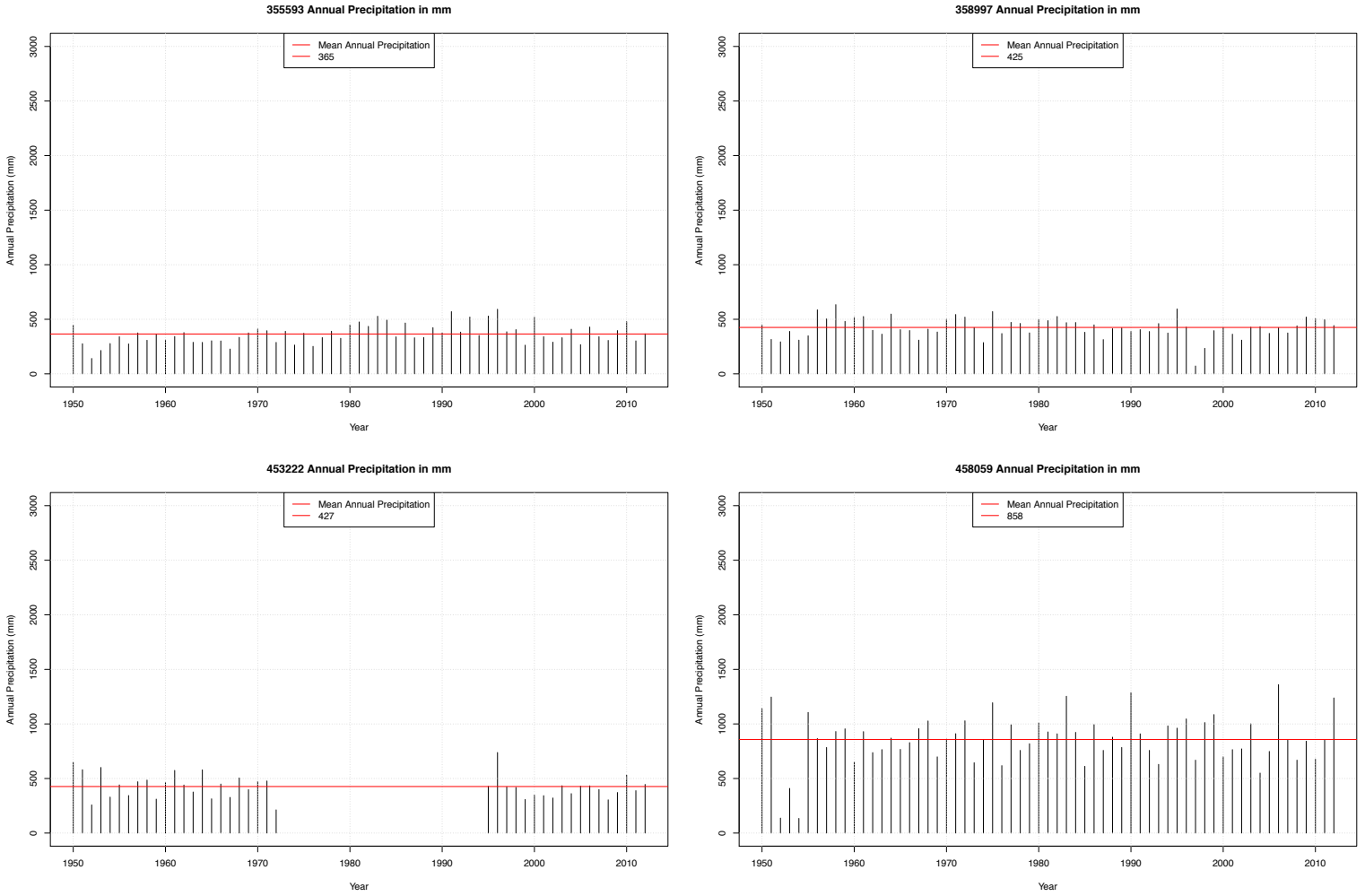

Figure F-6. Total annual precipitation and mean annual precipitation.

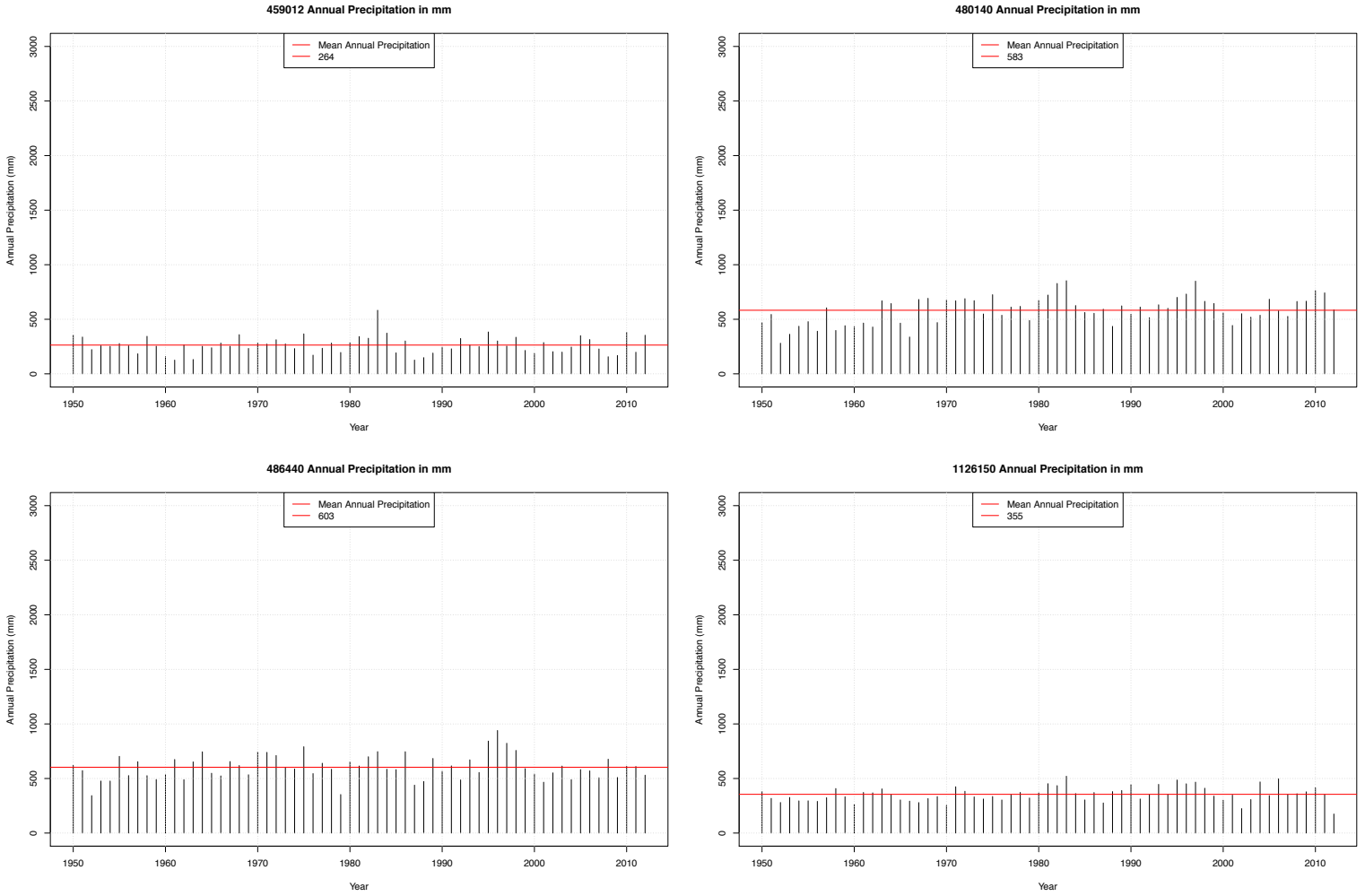

Figure F-7. Total annual precipitation and mean annual precipitation.

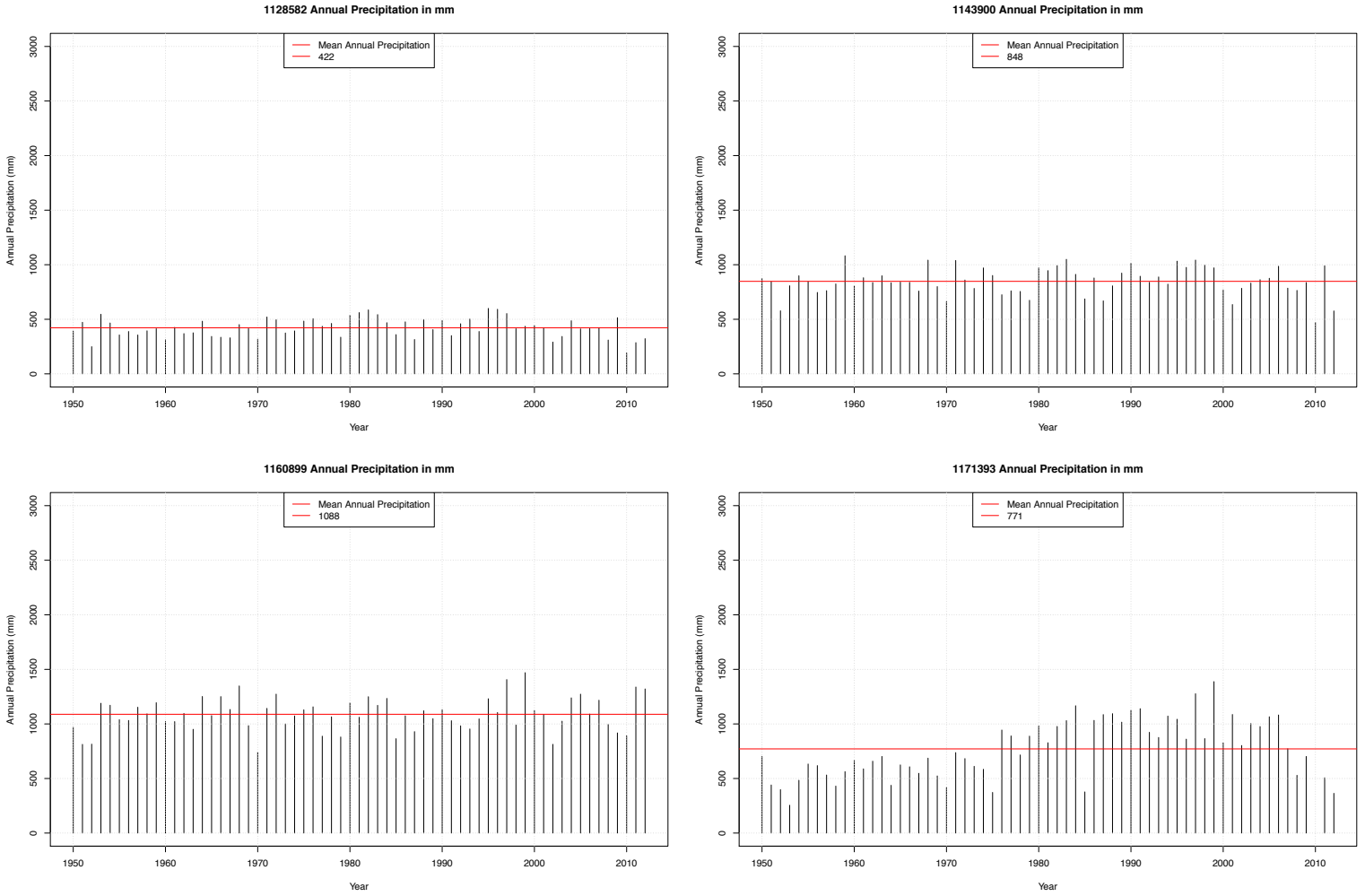

Figure F-8. Total annual precipitation and mean annual precipitation.

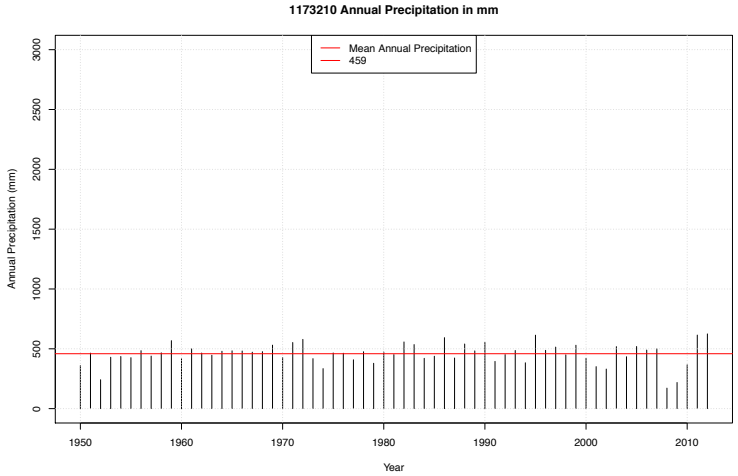

Figure F-9. Total annual precipitation and mean annual precipitation.

Total above dam summer decreases from May 1 to November 1 by gauge.

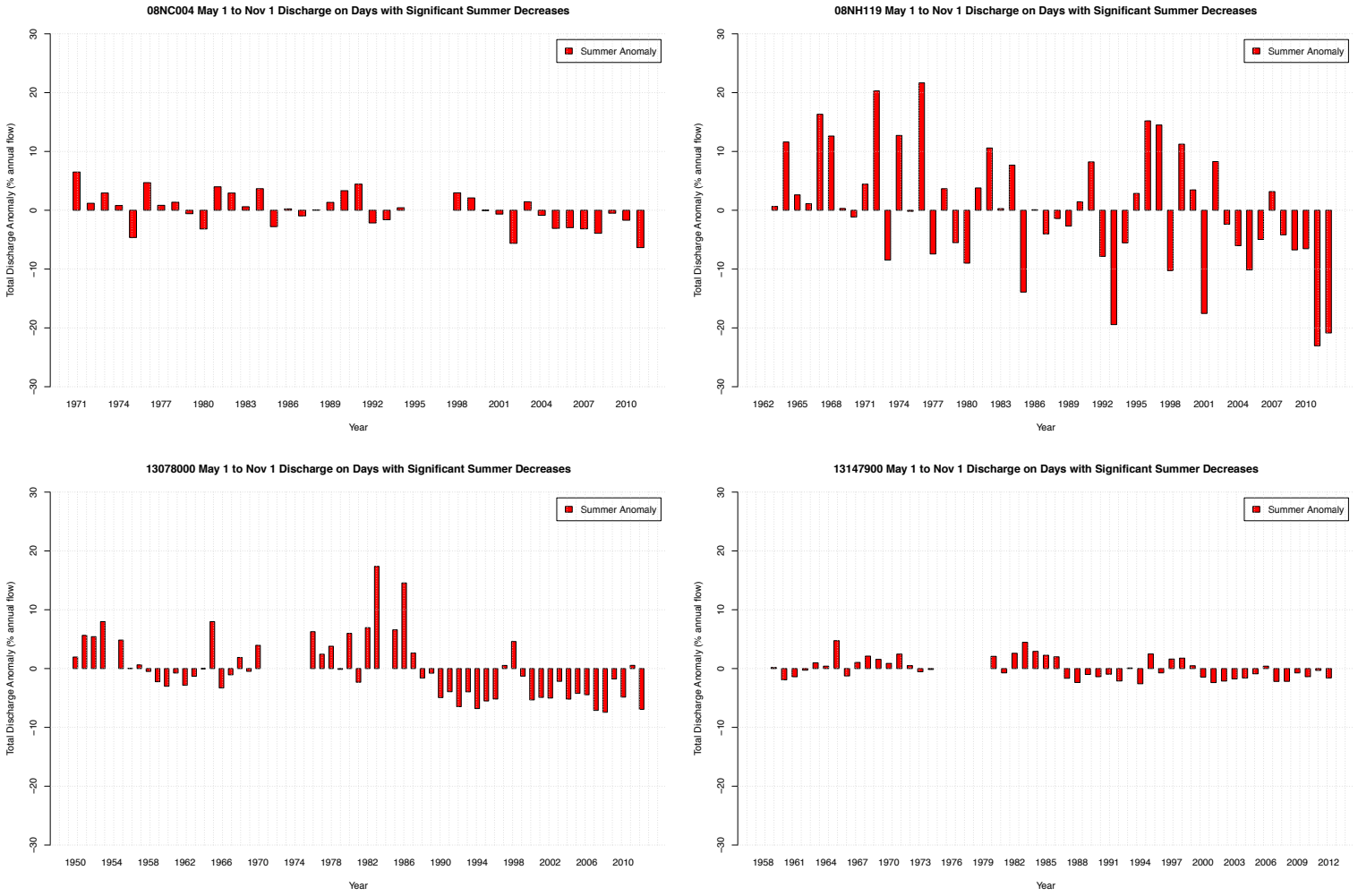

Figure F-10. Sum of above-dam anomalous daily flows over the period from May 1 to November 1 (summer) expressed as percent of annual flow

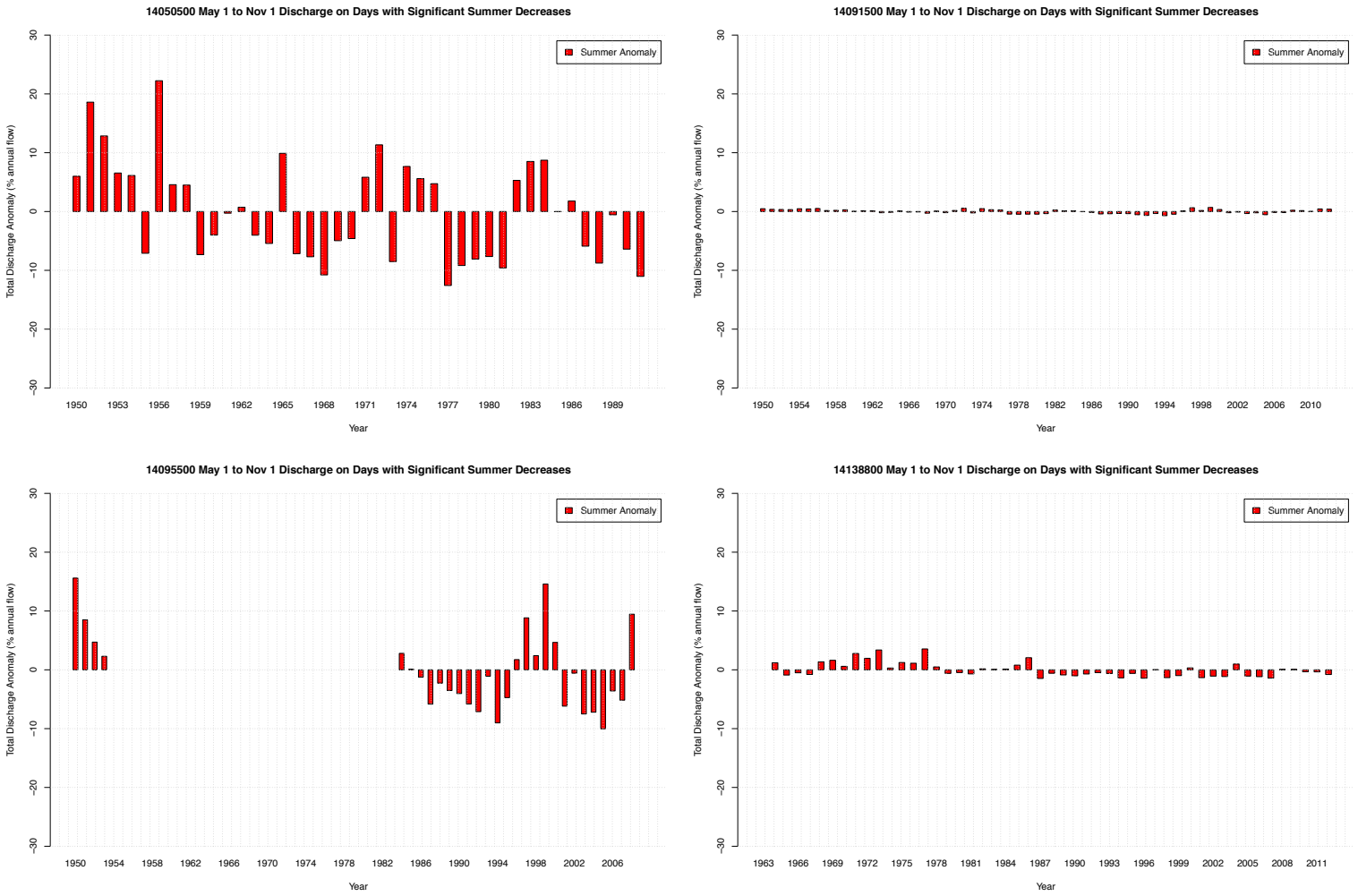

Figure F-11. Sum of above-dam anomalous daily flows over the period from May 1 to November 1 (summer) expressed as percent of annual flow

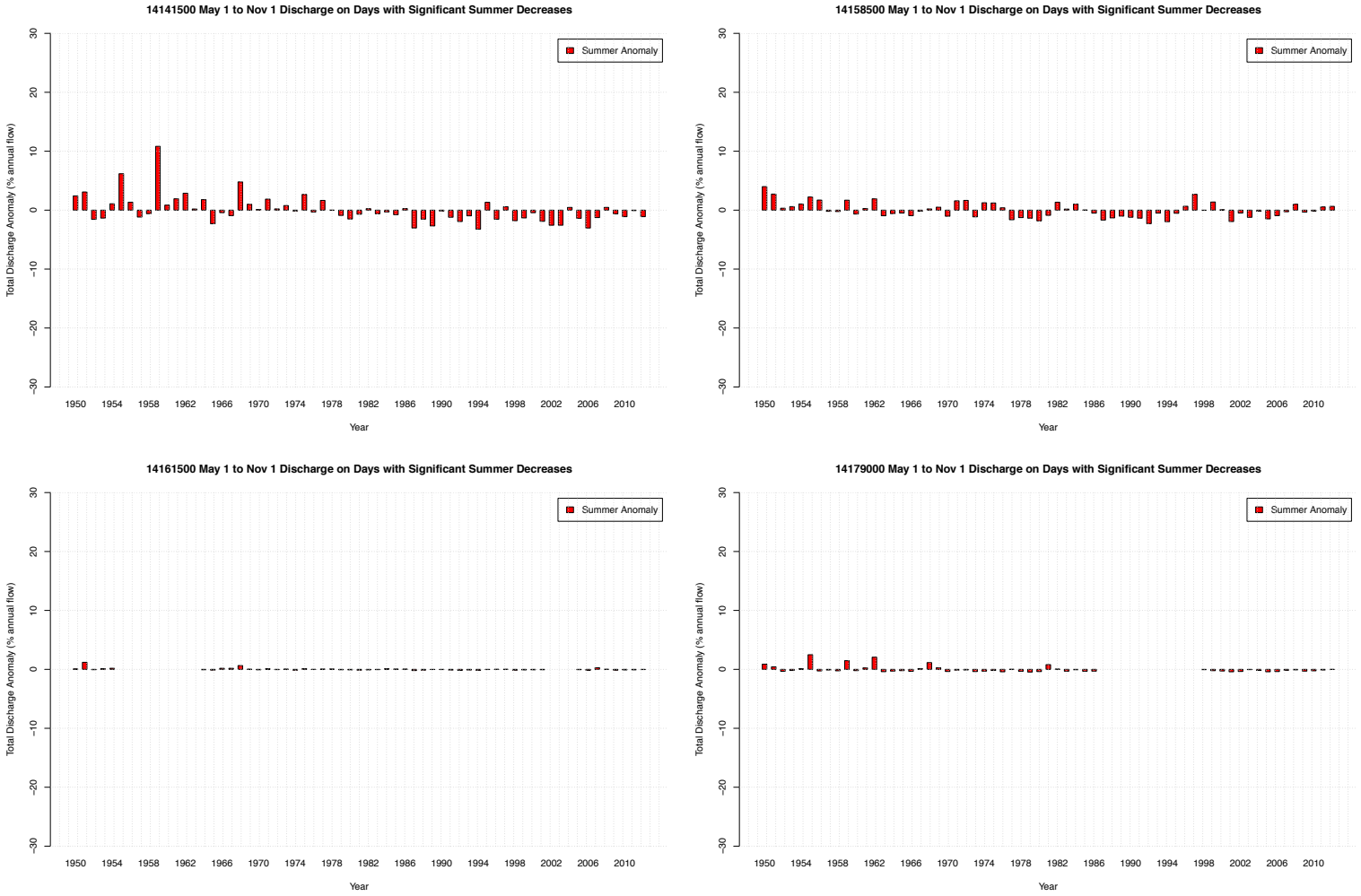

Figure F-12. Sum of above-dam anomalous daily flows over the period from May 1 to November 1 (summer) expressed as percent of annual flow

Total above dam and below dam increases from March 1 to May 1 and summer decreases from May 1 to November 1 by gauge.

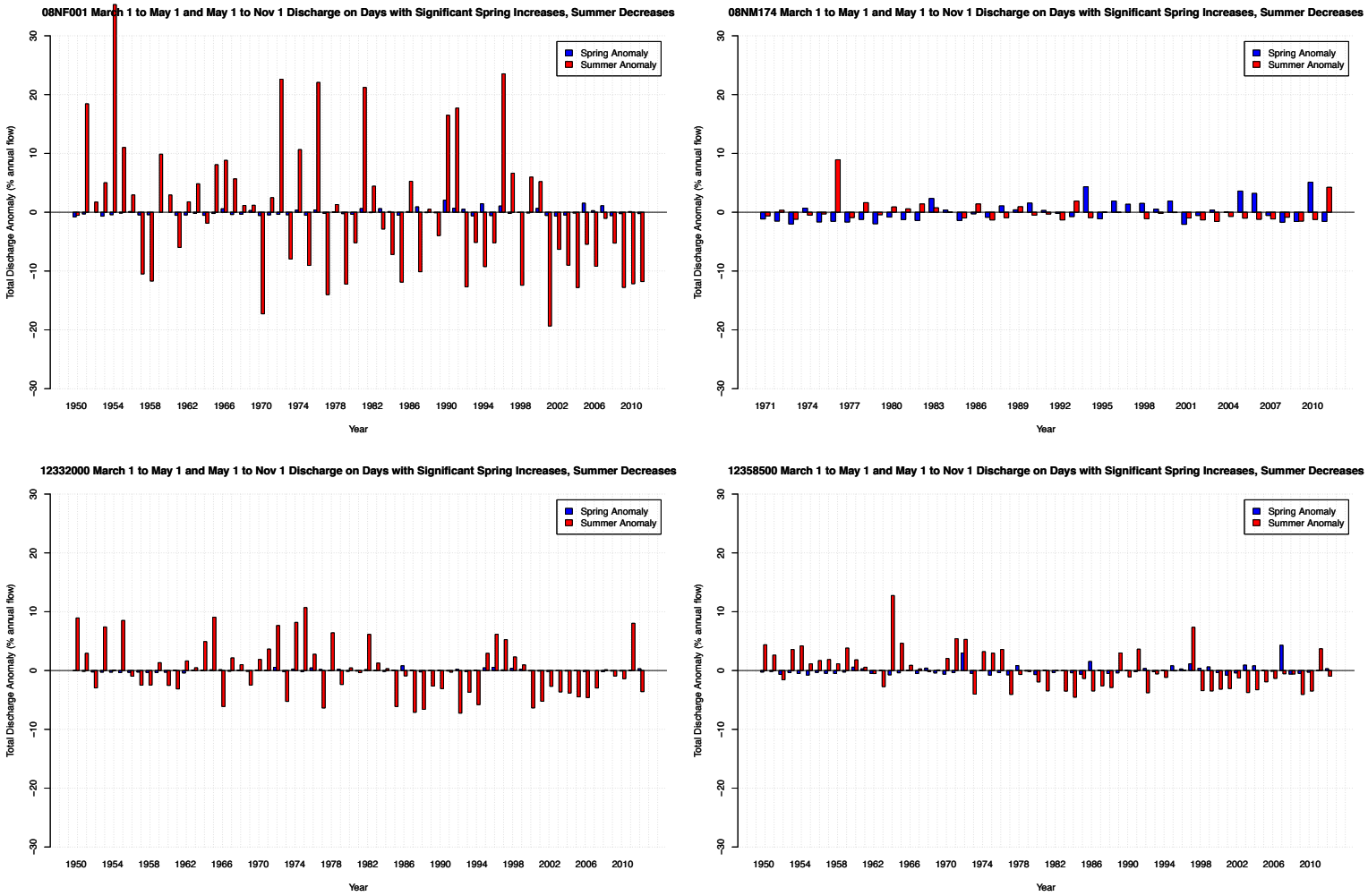

Figure F-13. Sum of above-dam anomalous daily flows over the period from March 1 to May 1 (spring) and May 1 to November 1 (summer) expressed as percent of annual flow

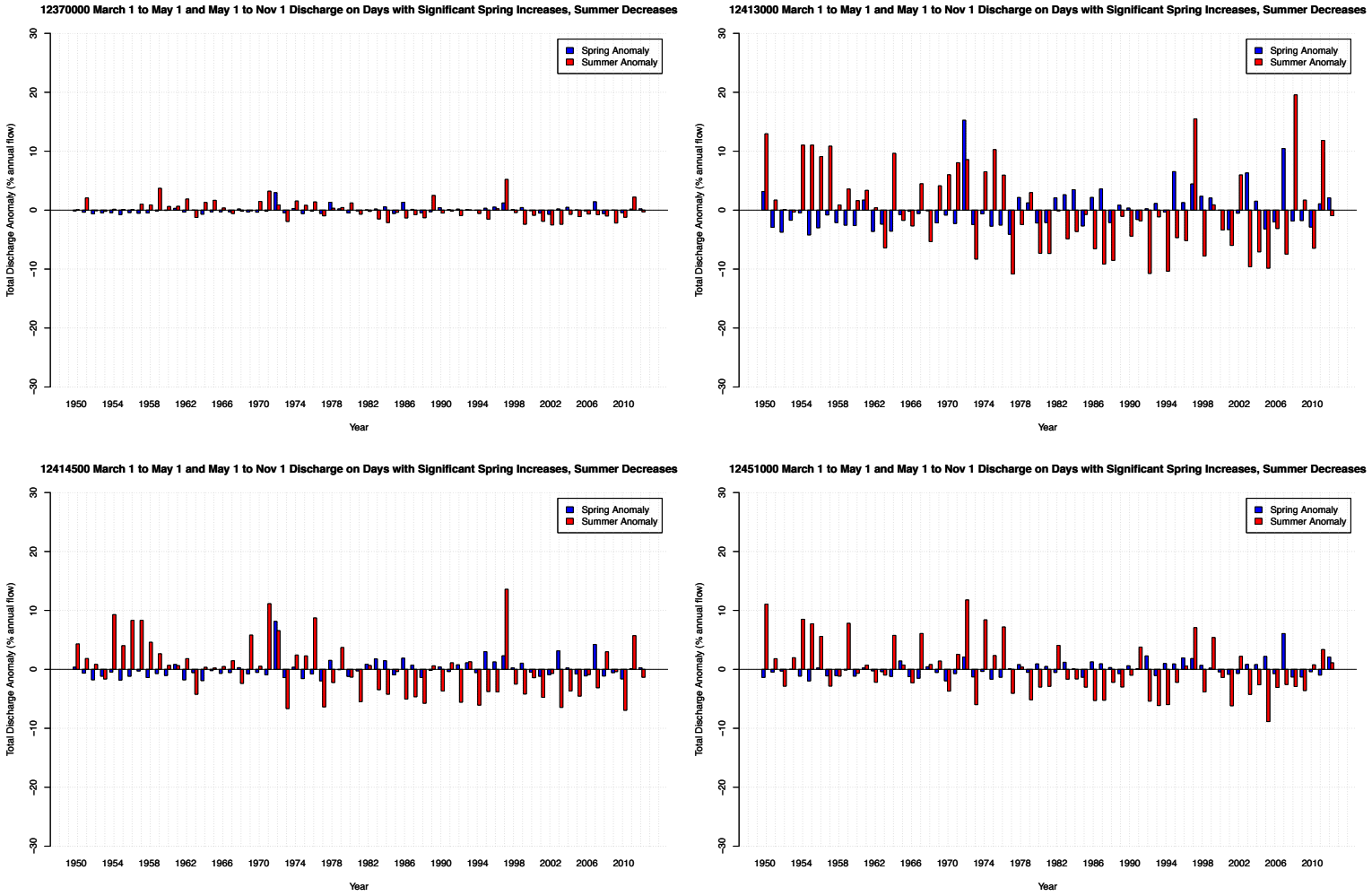

Figure F-14. Sum of above-dam anomalous daily flows over the period from March 1 to May 1 (spring) and May 1 to November 1 (summer) expressed as percent of annual flow

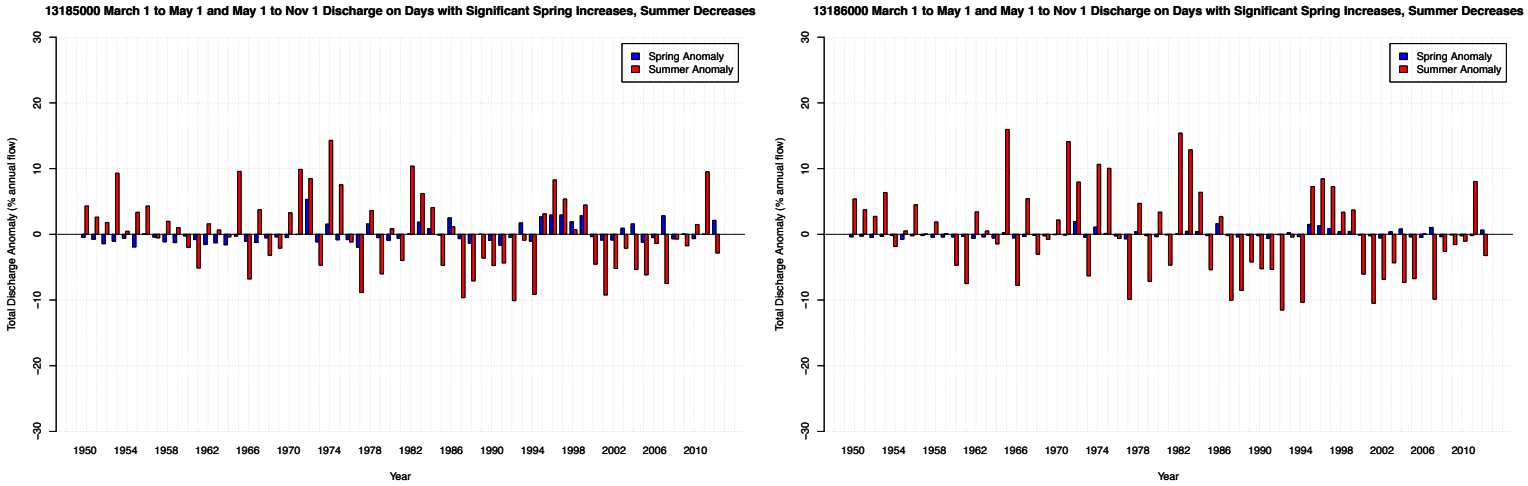

Figure F-15. Sum of above-dam anomalous daily flows over the period from March 1 to May 1 (spring) and May 1 to November 1 (summer) expressed as percent of annual flow

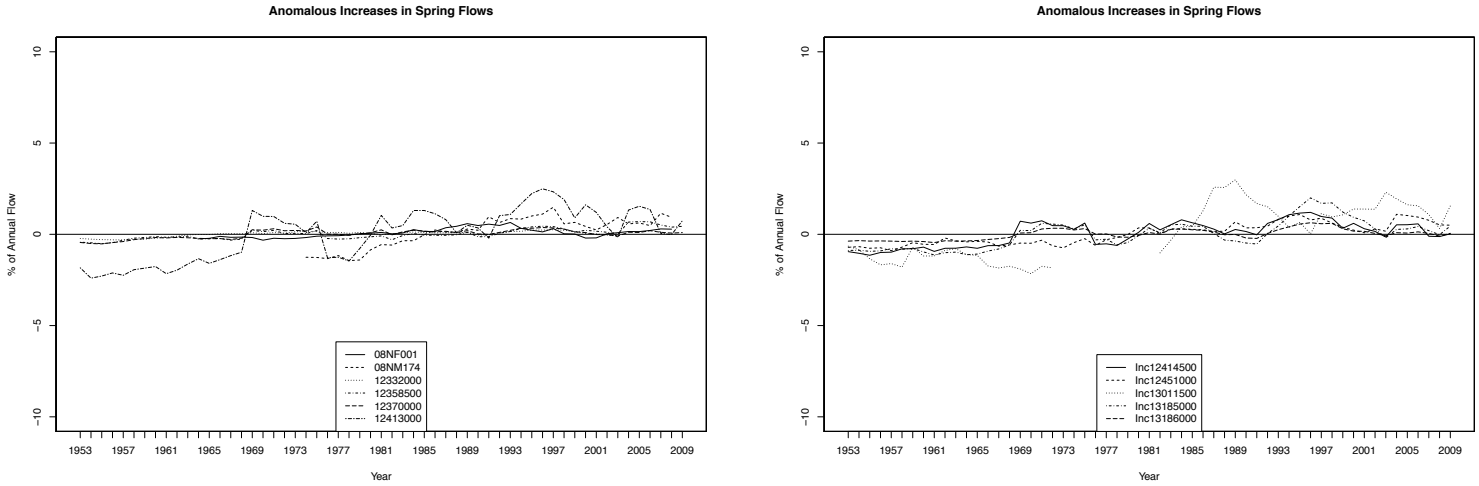

Figure F-16. Seven-year moving average percent annual flow above dam spring increase.

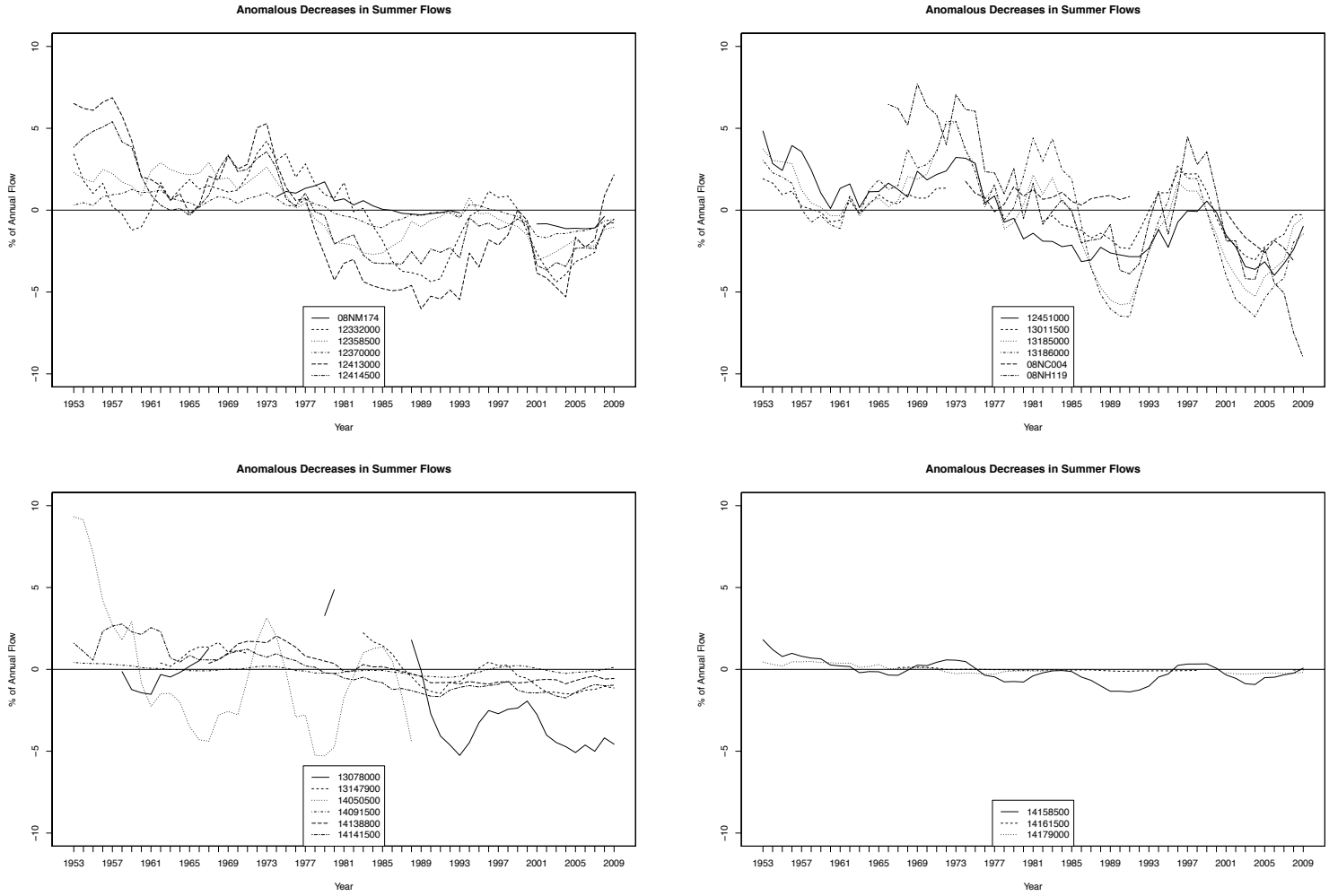

Figure F-17. Seven-year moving average percent annual flow above dam summer decrease.

Comparison between Mann-Kendall and linear regression trend results by gauge.

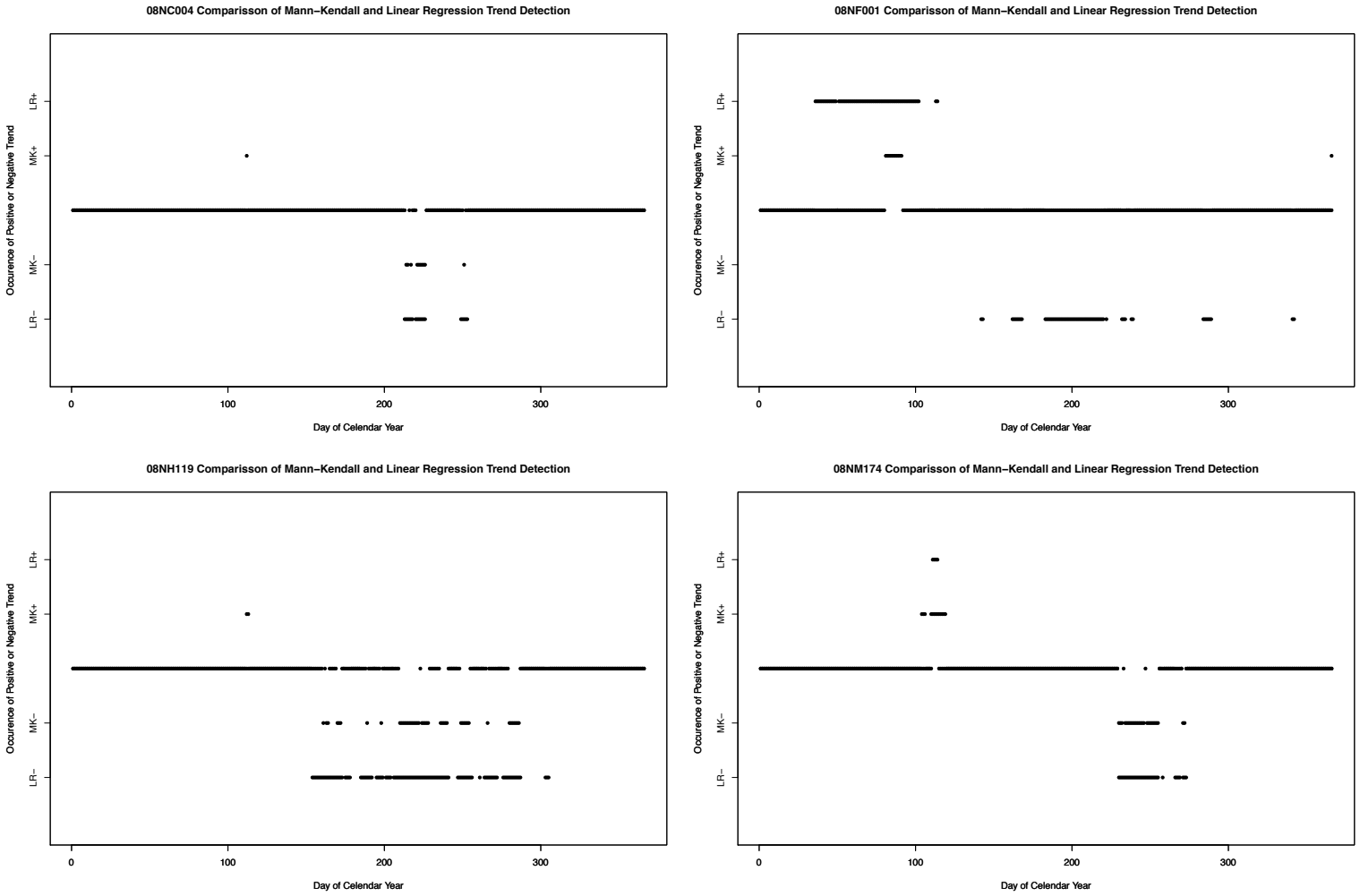

Figure F-22. Above Dam Mann-Kendall vs Linear Regression Results.

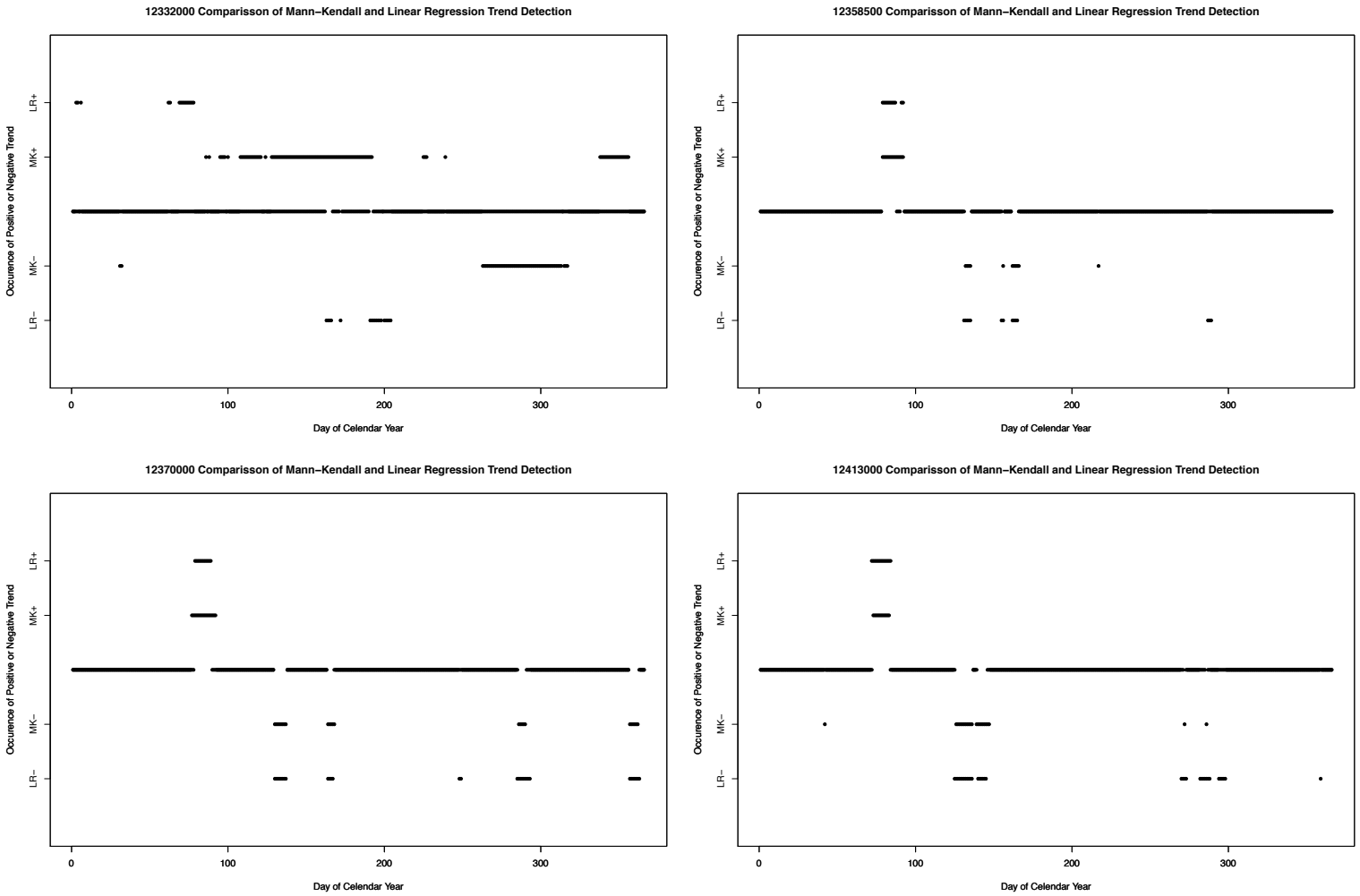

Figure F-23. Above Dam Mann-Kendall vs Linear Regression Results.

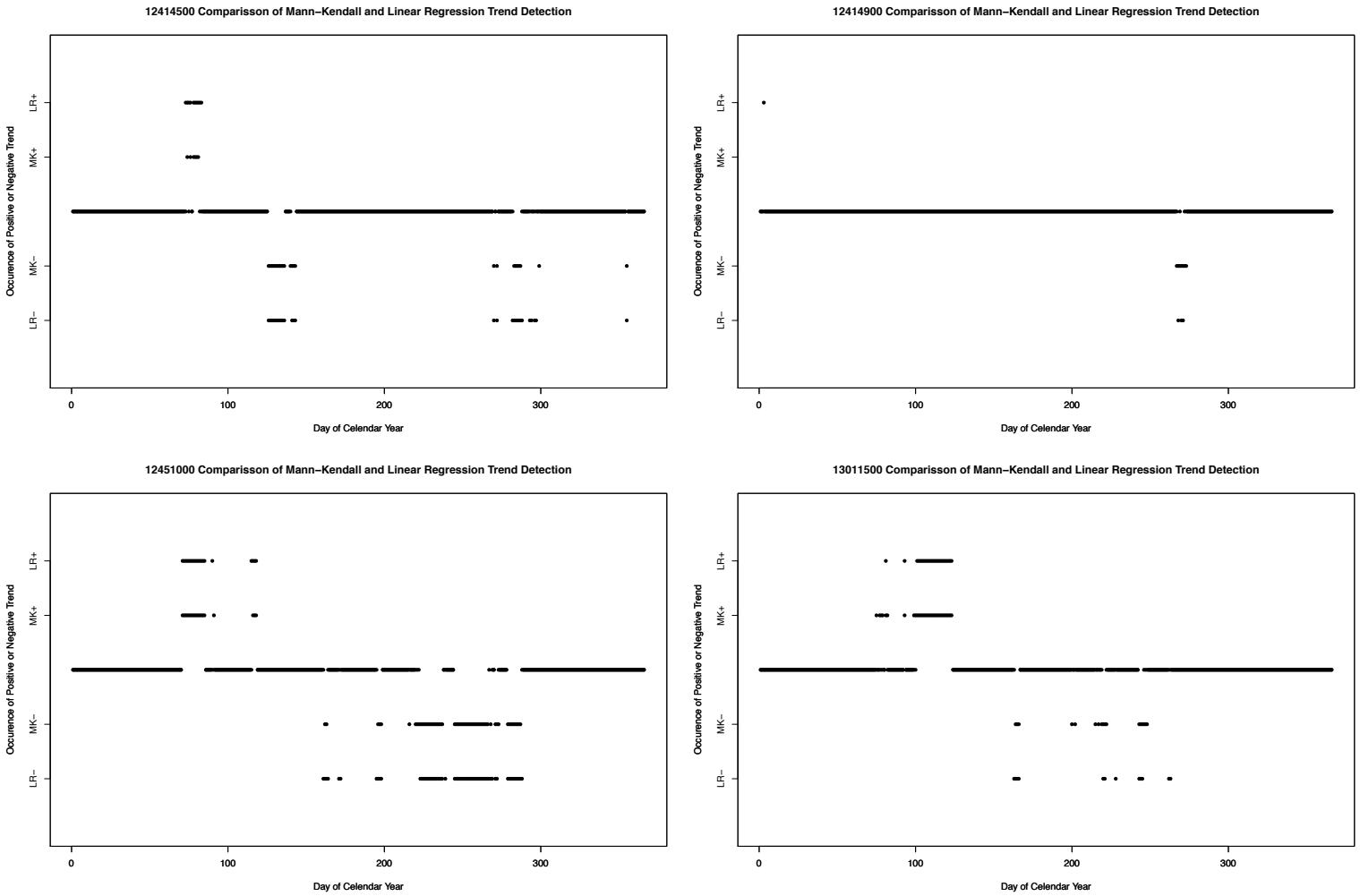

Figure F-24. Above Dam Mann-Kendall vs Linear Regression Results.

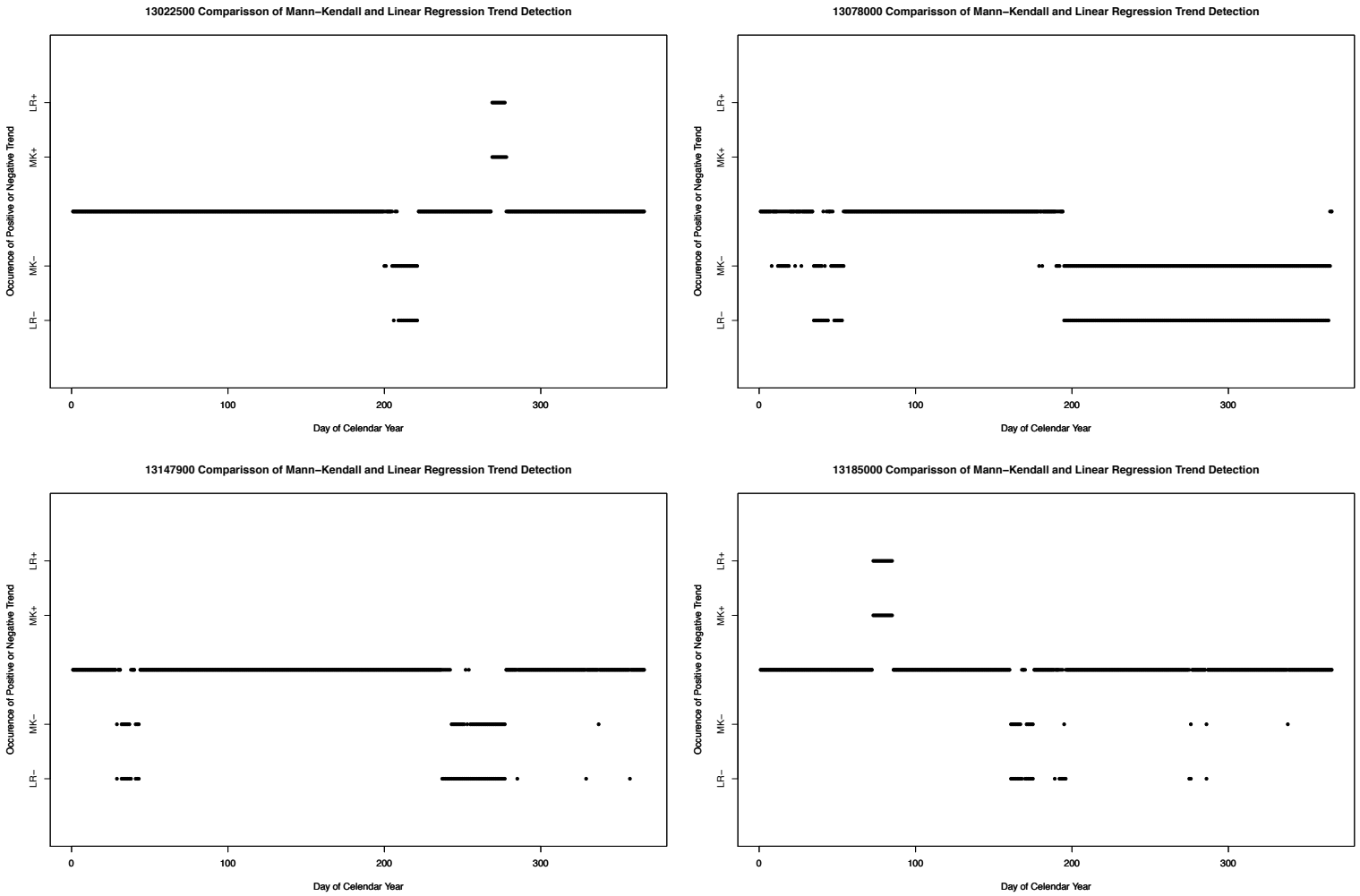

Figure F-24. Above Dam Mann-Kendall vs Linear Regression Results.

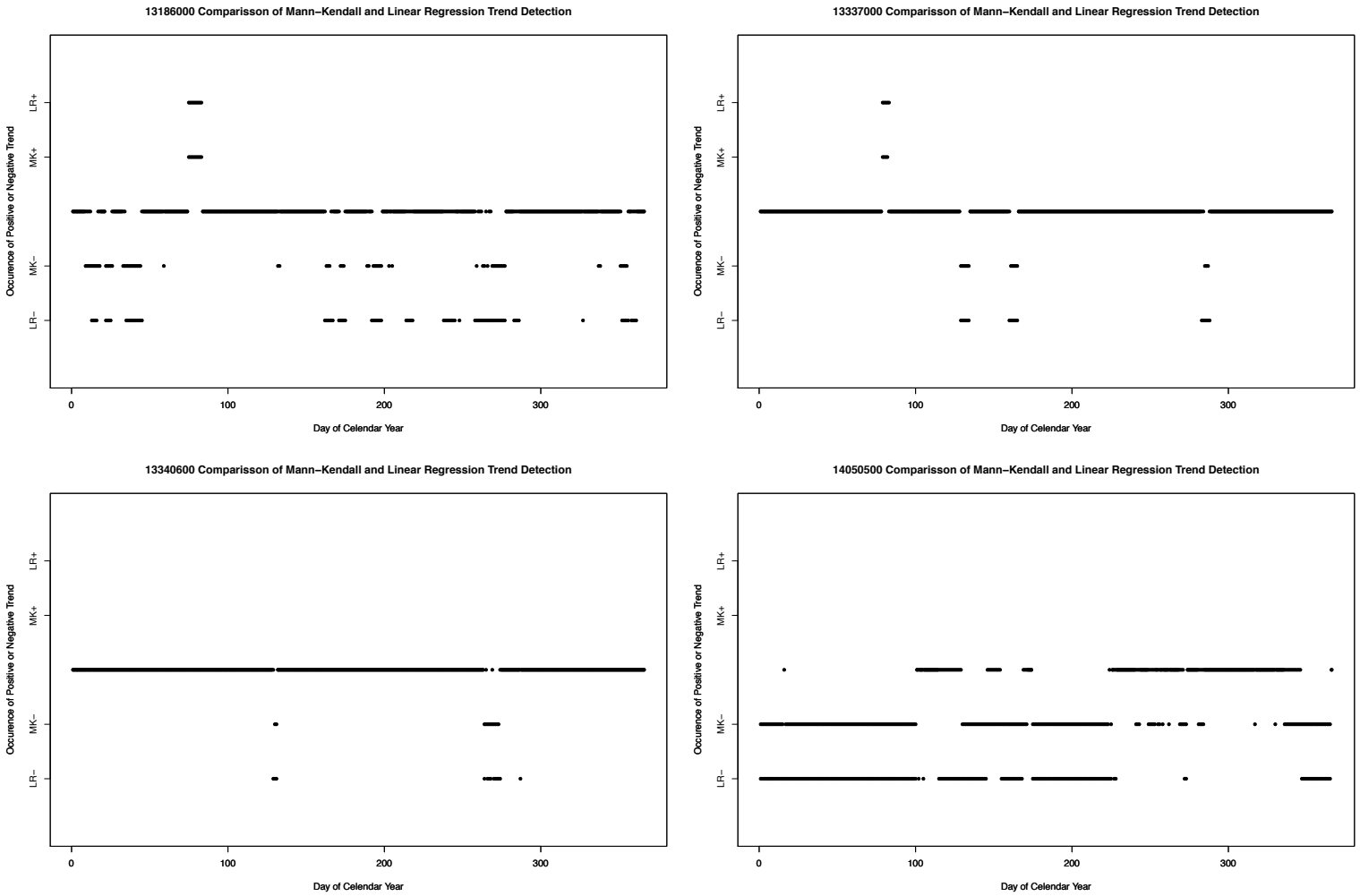

Figure F-24. Above Dam Mann-Kendall vs Linear Regression Results.

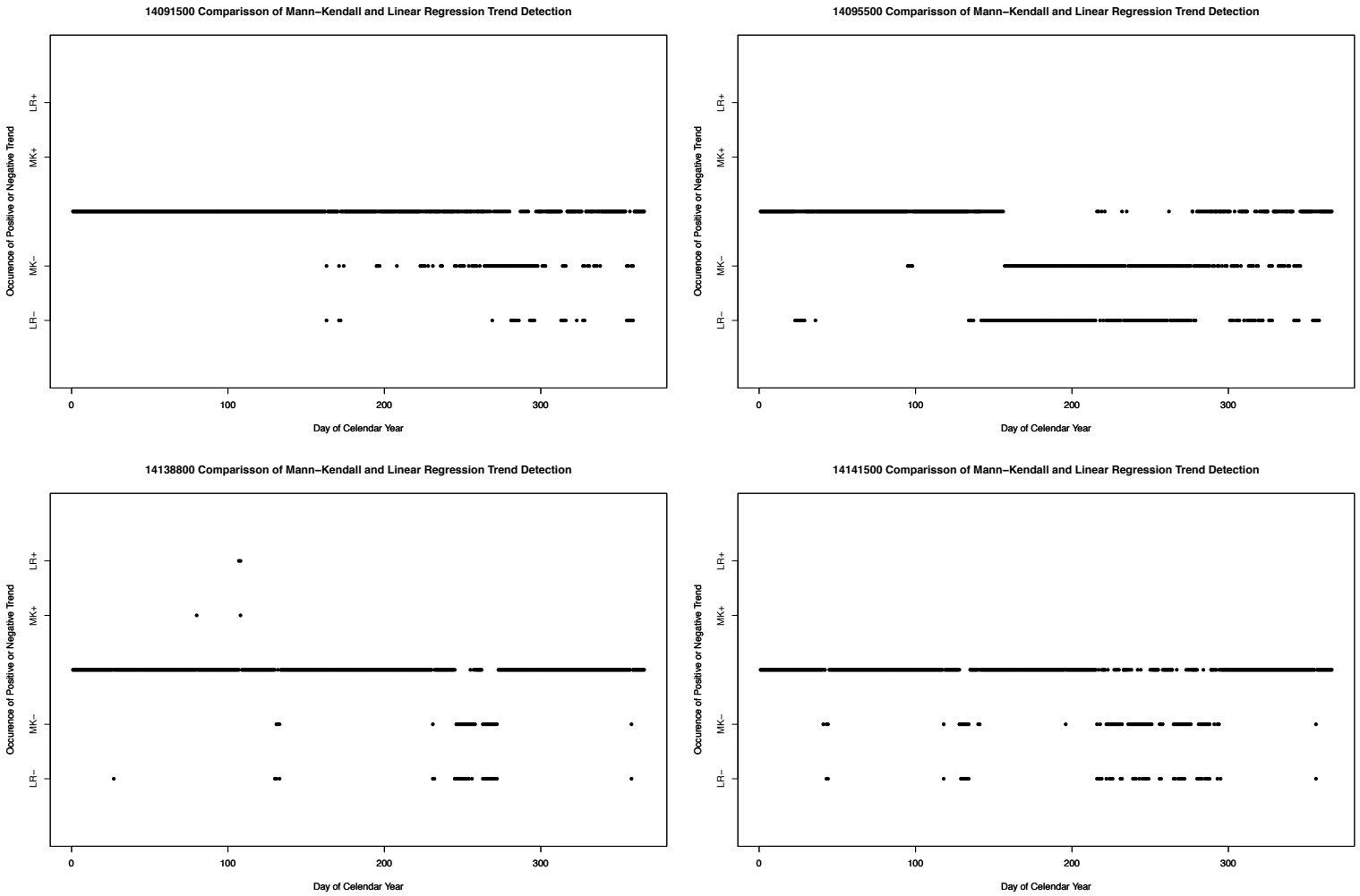

Figure F-24. Above Dam Mann-Kendall vs Linear Regression Results.

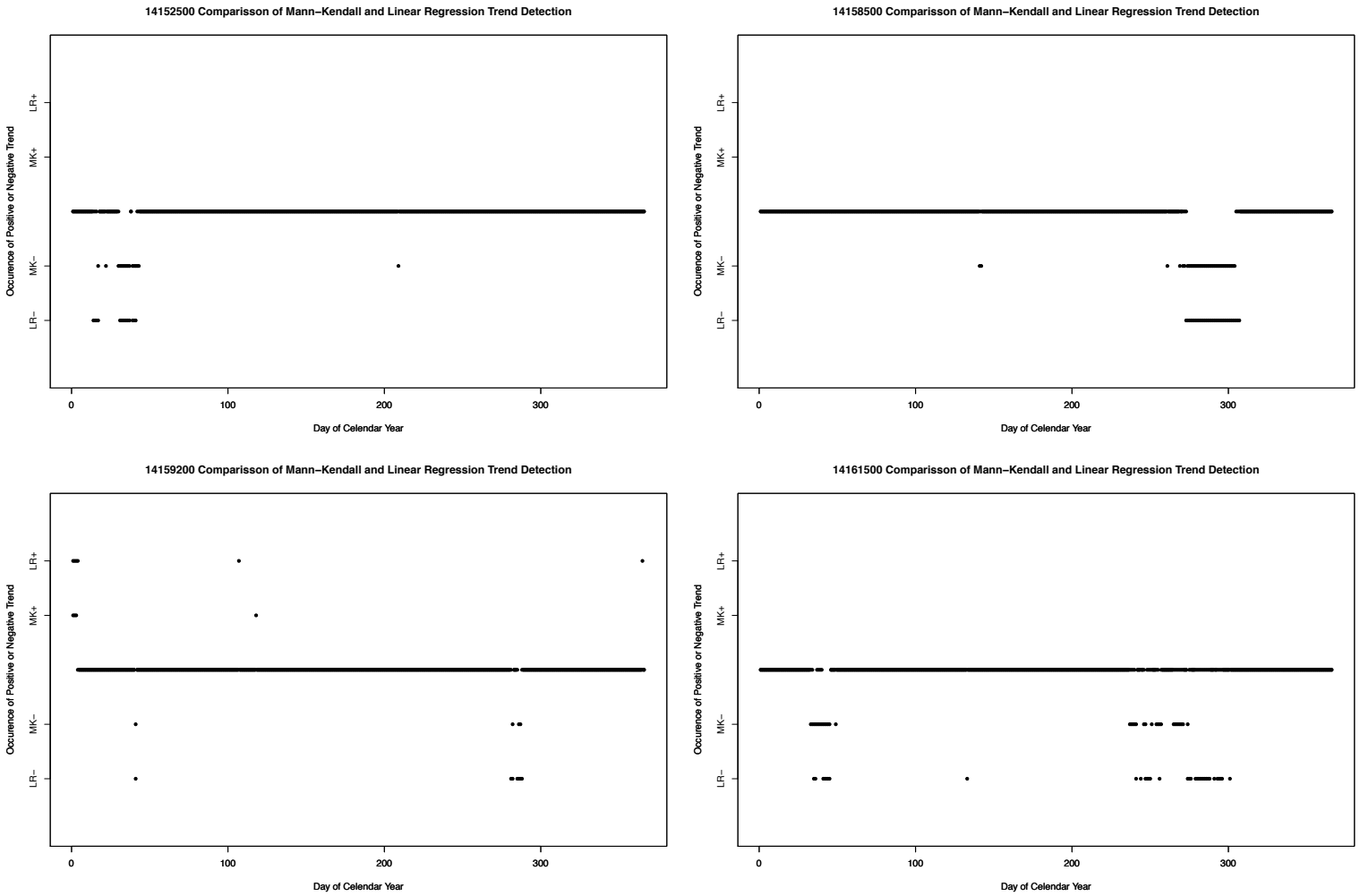

Figure F-24. Above Dam Mann-Kendall vs Linear Regression Results.

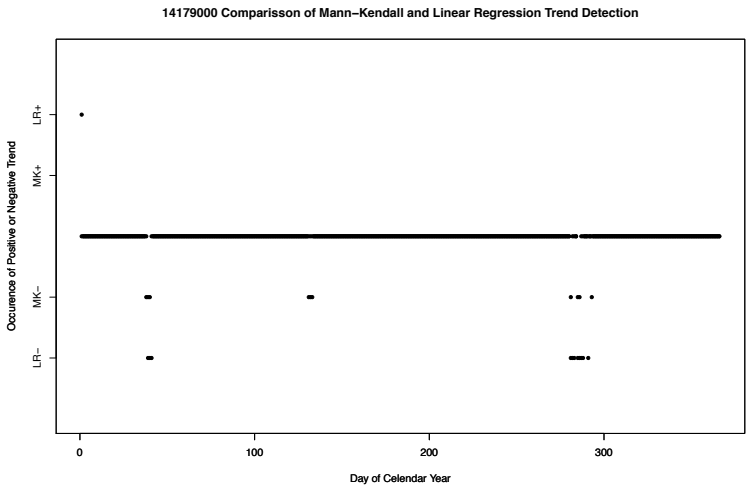

Figure F-24. Above Dam Mann-Kendall vs Linear Regression Results.

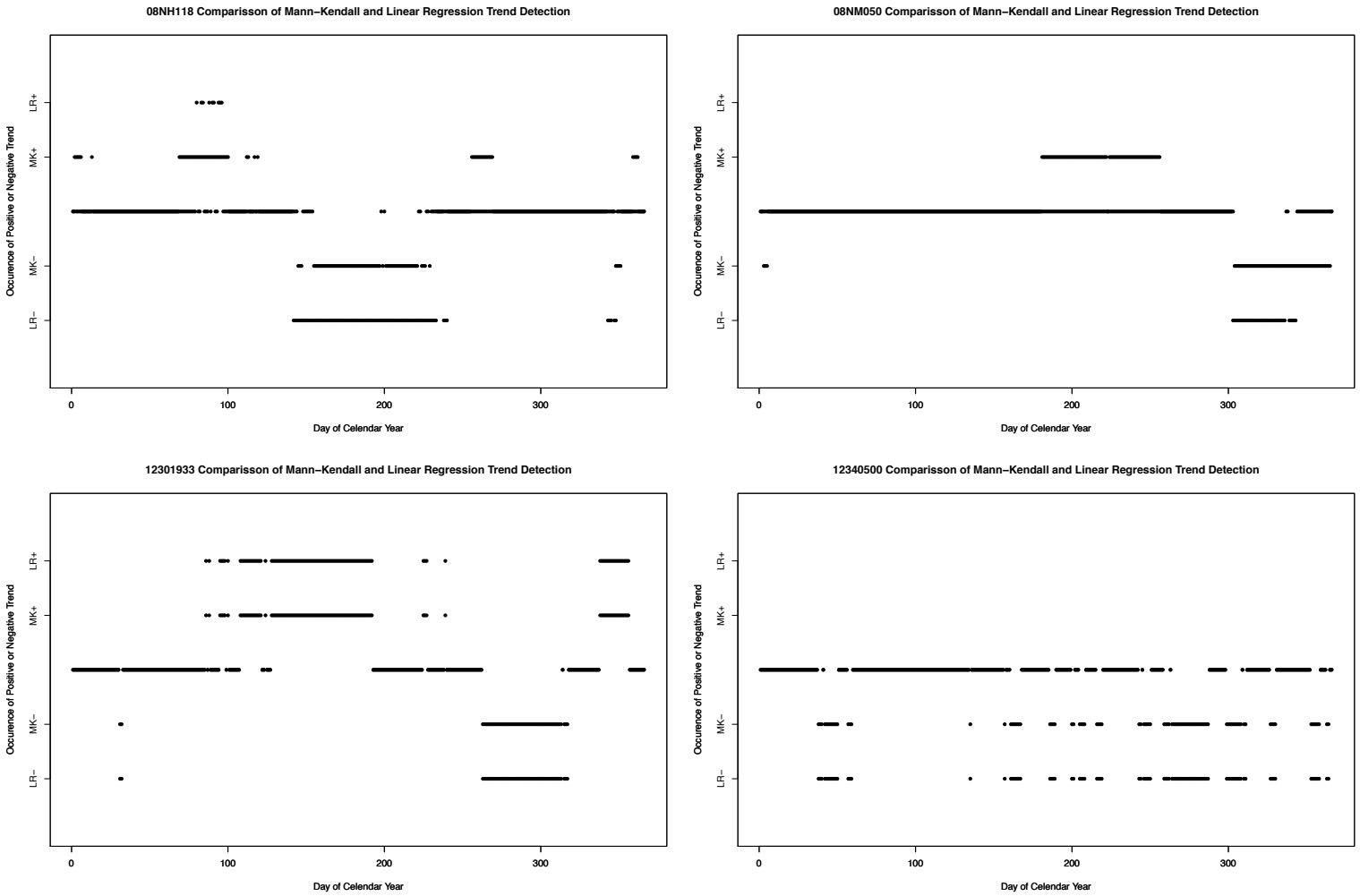

Figure F-25. Below Dam Mann-Kendall vs Linear Regression Results.

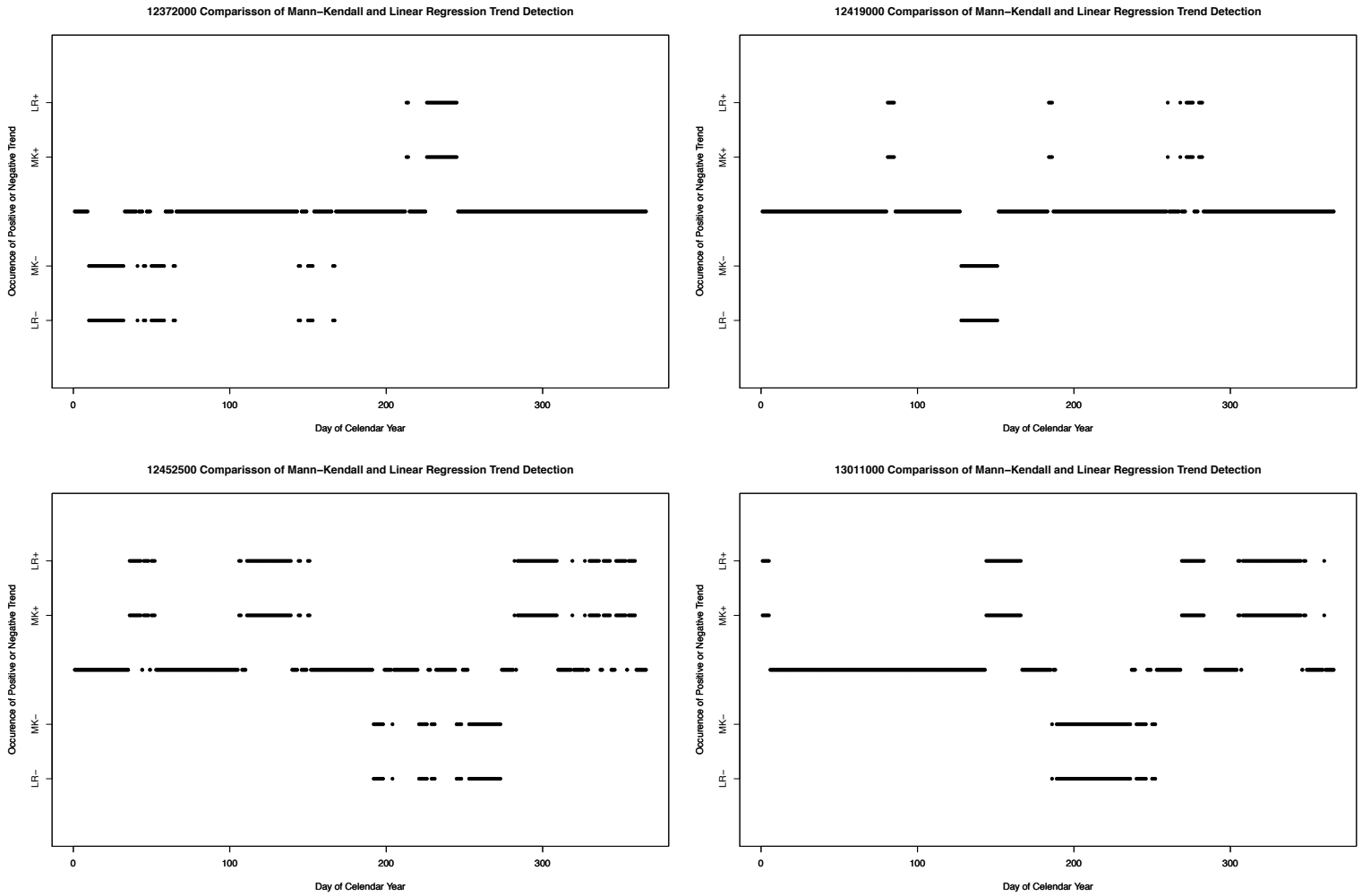

Figure F-26. Below Dam Mann-Kendall vs Linear Regression Results.

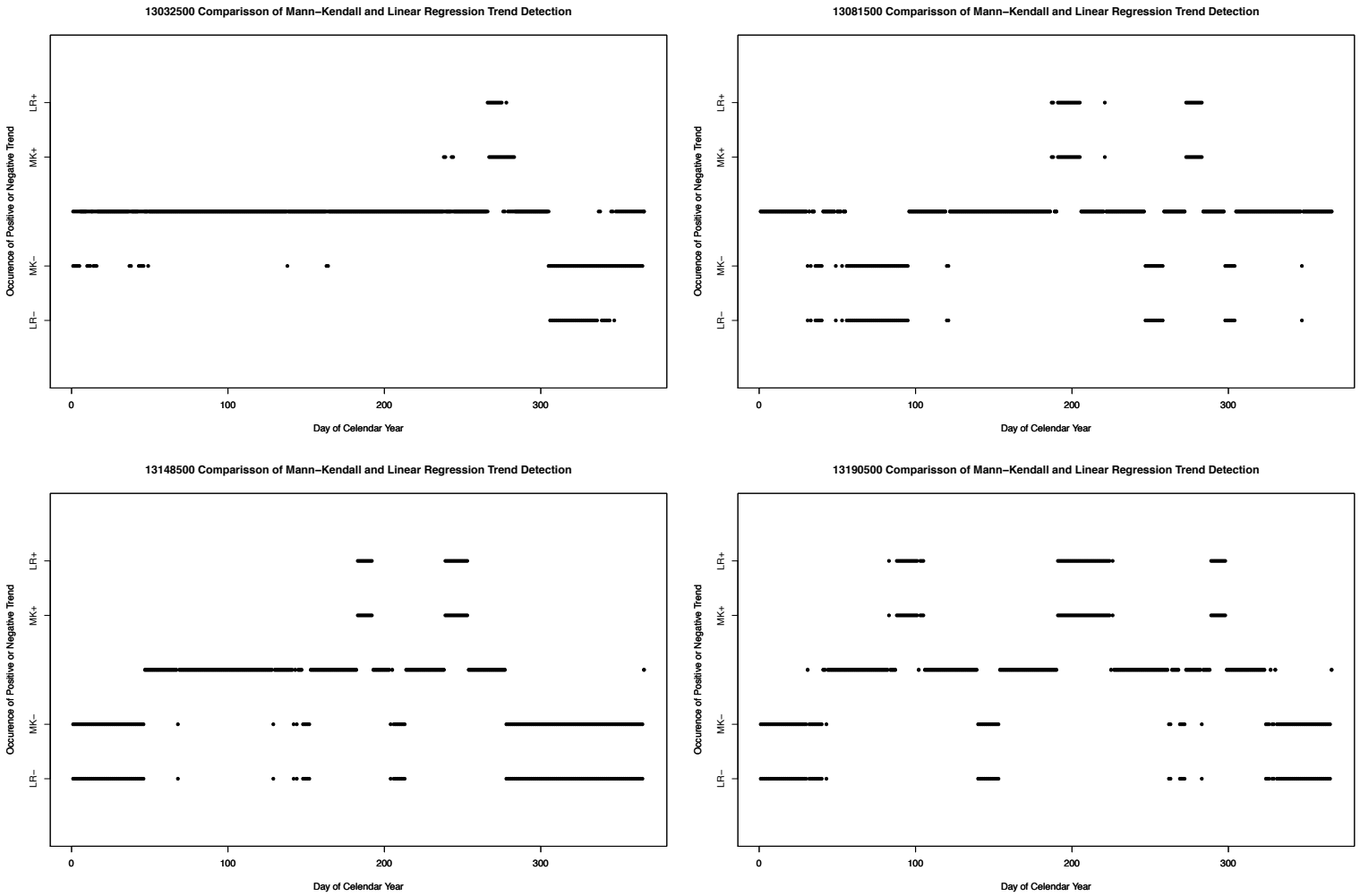

Figure F-27. Below Dam Mann-Kendall vs Linear Regression Results.

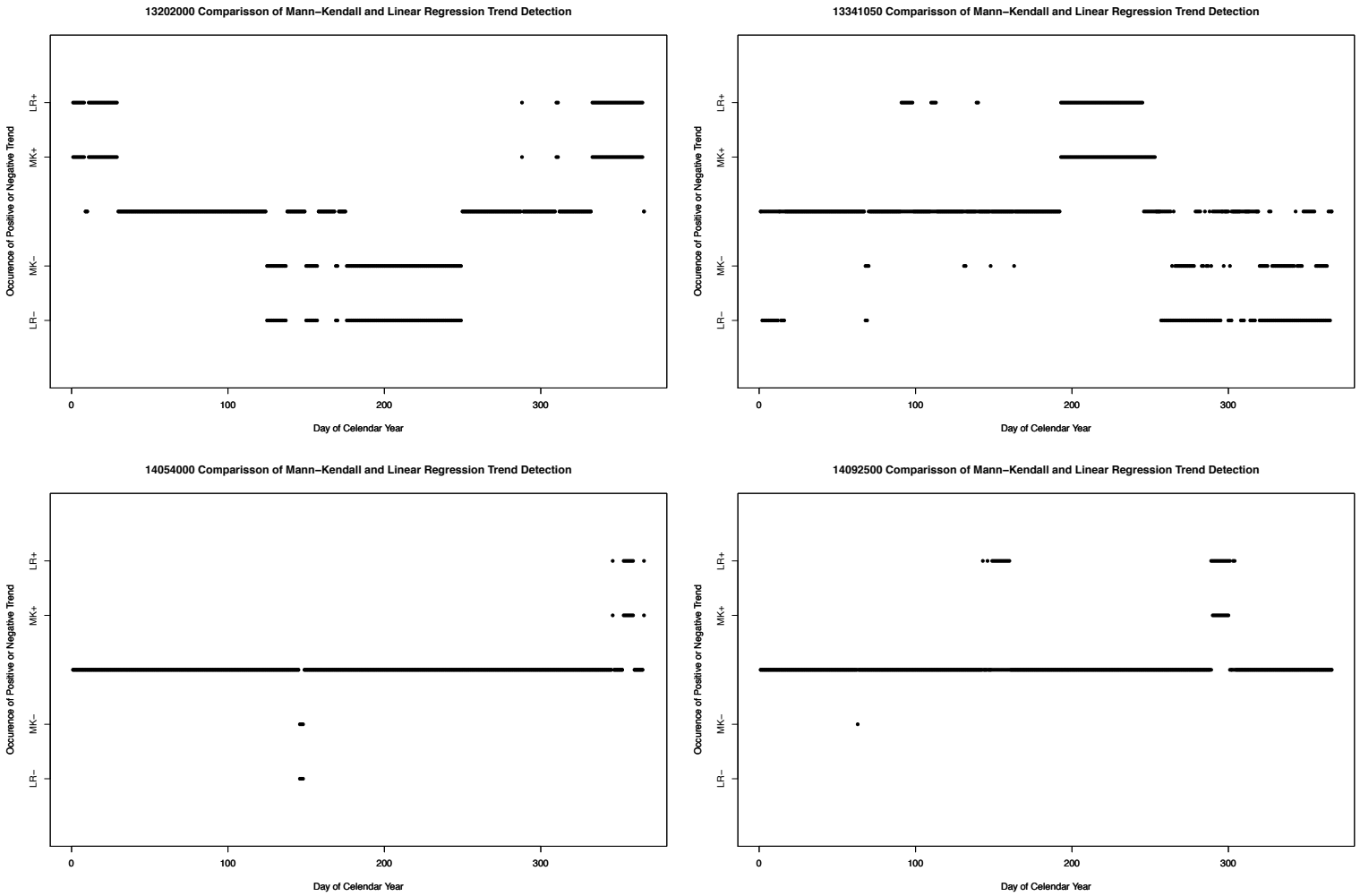

Figure F-28. Below Dam Mann-Kendall vs Linear Regression Results.

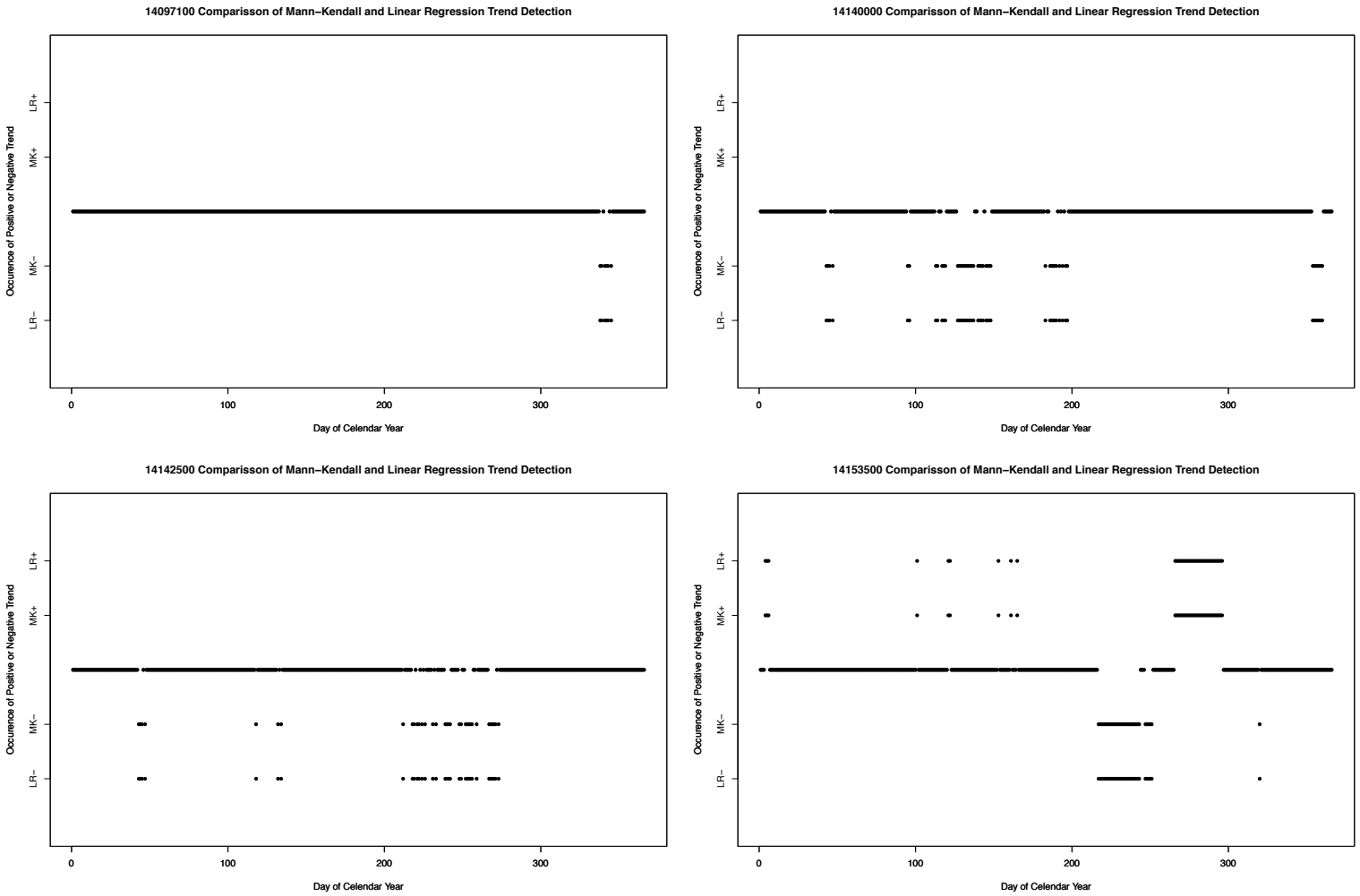

Figure F-29. Below Dam Mann-Kendall vs Linear Regression Results.

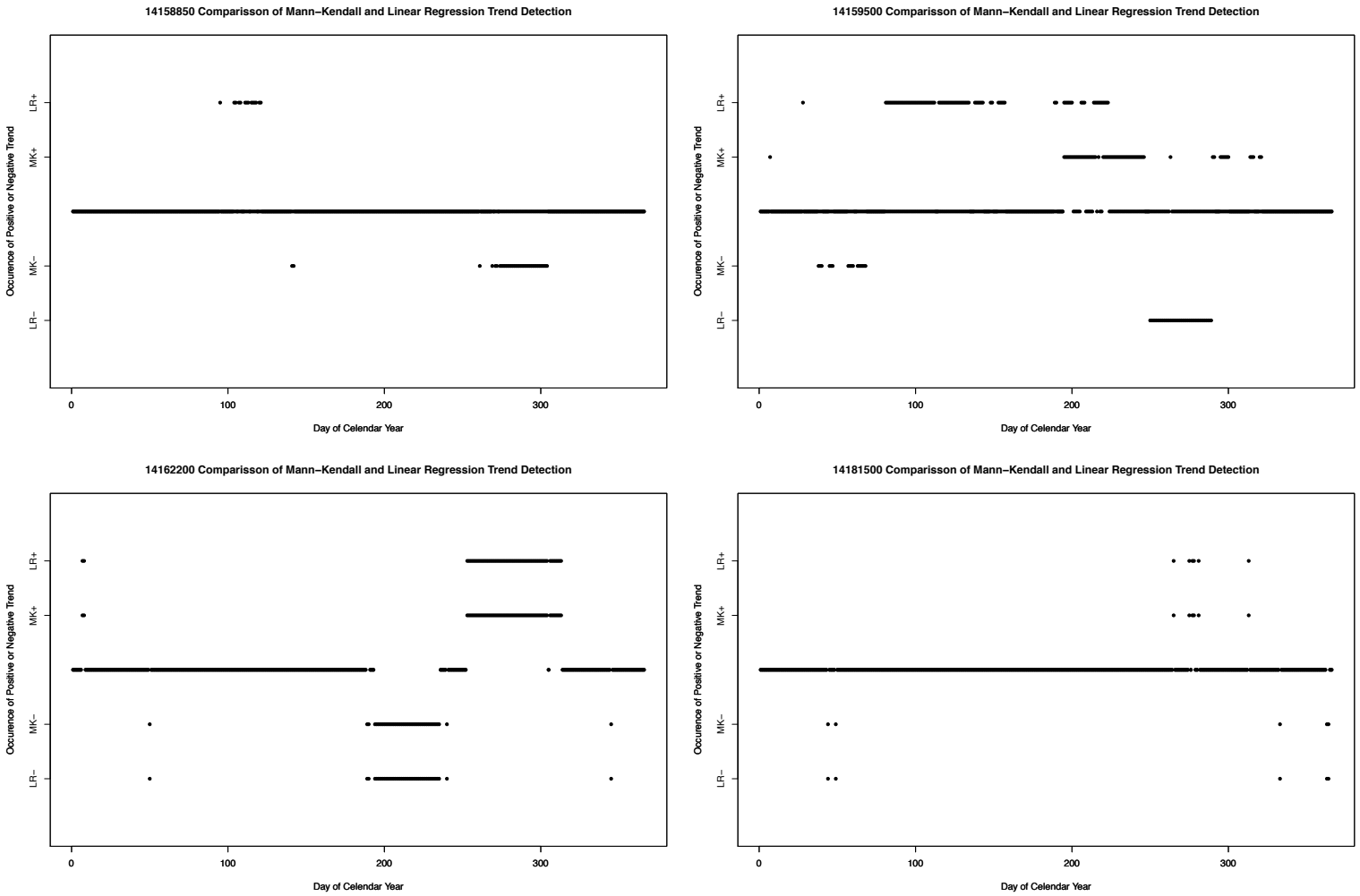

Figure F-30. Below Dam Mann-Kendall vs Linear Regression Results.

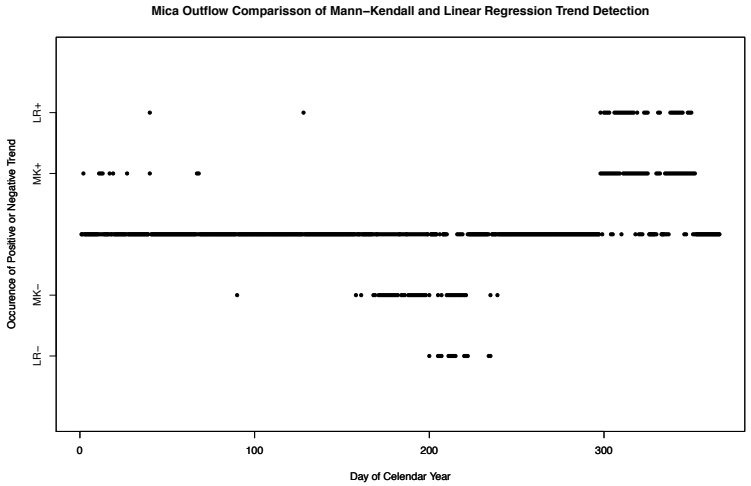

Figure F-31. Below Dam Mann-Kendall vs Linear Regression Results.

Appendix H

R codes

Linear Regression and Mann-Kendall Tests:

```
library(ggplot2)
library(lubridate)
library(reshape)
library(plyr)
library(Kendall)
# Change the below to chnage the working directory
setwd("/Users/johnhammondplease/Desktop/Experimenting_on_data/Final_Streamflow_Data_cubic_meters_per_second")
# Load file(s) txt
`sf` <-
read.delim("~/Desktop/Experimenting_on_data/Final_Streamflow_Data_cubic_meters_per_second/g14161500corf.txt")
# Change the below to chnage the working directory
setwd("/Users/johnhammondplease/Desktop/Experimenting_on_data/final_ushcn_c_mm")
# Load file(s) csv climate data
`clim` <-
read.csv("~/Desktop/Experimenting_on_data/final_ushcn_c_mm/c355362_formated.csv")
# Make proper date column for streamflow
sf$postime <- as.POSIXlt(sf$date, format = "%Y/%m/%d")
# Make proper date column for climate
clim$postime <- as.POSIXlt(clim$Date, format = "%Y/%m/%d")
# check distribution to see spread / skew
hist(sf$discharge)
hist(clim$PRCP)
# Preparing for Linear Regression
# Make log column for streamflow
sf$discharge[sf$discharge == 0] <- 0.0001
sf$logsf <- log(sf$discharge)
# Make log column for precipitation
clim$PRCP[clim$PRCP == 0] <- 0.0001
clim$logprcp <- log(clim$PRCP)
# Make New Dataframes for each variable containing columns of interest (date in POSIX format and variable(sf, prcp, tmax, tmin))
sflow <- sf[c(6,7)]
# Subset for only the dates that I am interested in (1950-01-01 to 2012-12-31): Taken care of in data parsing
sflowsub <- subset(sflow, as.Date(postime) >= '1950-01-01' & as.Date(postime) <= '2012-12-31')
```

```
sflowsub$year <- year(sflowsub$postime)
sflowsub$yday <- yday(sflowsub$postime)
sflowlinreg <- cast(sflowsub, year ~ yday, value = "logsf")
climprcp <- clim[c(6,7)]
climprcpsub <- subset(climprcp, as.Date(postime) >= '1970-01-01' & as.Date(postime)
<= '2012-12-31')
climprcpsub$year <- year(climprcpsub$postime)
climprcpsub$yday <- yday(climprcpsub$postime)
climprcplinreg <- cast(climprcpsub, year ~ yday, value = "logprcp")
climtmax <- clim[c(6,3)]
climtmaxsub <- subset(climtmax, as.Date(postime) >= '1970-01-01' & as.Date(postime)
<= '2012-12-31')
climtmaxsub$year <- year(climtmaxsub$postime)
climtmaxsub$yday <- yday(climtmaxsub$postime)
climtmaxlinreg <- cast(climtmaxsub, year ~ yday, value = "TMAX")
climtmin <- clim[c(6,4)]
climtminsub <- subset(climtmin, as.Date(postime) >= '1970-01-01' & as.Date(postime)
<= '2012-12-31')
climtminsub$year <- year(climtminsub$postime)
climtminsub$yday <- yday(climtminsub$postime)
climtminlinreg <- cast(climtminsub, year ~ yday, value = "TMIN")
# Now that data is formatted correctly, calculate daily anomalies, anomaly for that day of
the year (value - dayofyear mean)
sflowlinreganom <- apply(sflowlinreg[2:367] , 2, FUN = scale, scale=FALSE,
center=TRUE)
colnames(sflowlinreganom) <- c(1:366)
rownames(sflowlinreganom) <- c(1950:2012)
climprcplinreganom <- apply(climprcplinreg[2:367] , 2, FUN = scale, scale=FALSE,
center=TRUE)
colnames(climprcplinreganom) <- c(1:366)
rownames(climprcplinreganom) <- c(1970:2012)
climtmaxlinreganom <- apply(climtmaxlinreg[2:367] , 2, FUN = scale, scale=FALSE,
center=TRUE)
colnames(climtmaxlinreganom) <- c(1:366)
rownames(climtmaxlinreganom) <- c(1970:2012)
climtminlinreganom <- apply(climtminlinreg[2:367] , 2, FUN = scale, scale=FALSE,
center=TRUE)
colnames(climtminlinreganom) <- c(1:366)
rownames(climtminlinreganom) <- c(1970:2012)
#########################################################################
# Perform Linear Regression on the daily anomalies (log transform has already occured)
setwd("/Users/johnhammondplease/Desktop/Experimenting_on_data/linregfig")
# Streamflow
# years1 <- 1966:2012
years <- 1971:2012
lmsf <- alply(sflowlinreganom, 2, function(x){
```

```
  lm(x ~ years)
})
lmsf.info <- ldply(lmsf, function(fit){
  data.frame(slope = coef(fit)[2], pval = summary(fit)$coefficients[2, 4])
})
pdf('sflinreg_12301933.pdf', width = 12, height = 8)
qplot(data = lmsf.info, x = X1, y = slope, col = ifelse(pval < 0.05,'significant at a=0.05',
'not significant'), main = "Linear Regression Slope of Streamflow by Day of Year", xlab
= "Day of Year", ylab = "Slope of Regression") + opts(legend.position = "none") +
scale_x_discrete(breaks = c(1,32,60,91,121,152,182,213,244,274,305,335), labels=c("Jan
1","Feb 1","Mar 1","Apr 1","May 1", "June 1", "July 1", "Aug 1", "Sept 1", "Oct 1",
"Nov 1", "Dec 1"))
dev.off()
# Precipitation
lmprcp <- alply(climprcplinreganom, 2, function(x){
  lm(x ~ years)
})

lmprcp.info <- ldply(lmprcp, function(fit1){
  data.frame(slope = coef(fit1)[2], pval = summary(fit1)$coefficients[2, 4])
})
pdf('prcplinreg_Lookout.pdf', width = 12, height = 8)
qplot(data = lmprcp.info, x = X1, y = slope, col = ifelse(pval < 0.05,'significant at
a=0.05', 'not significant'), main = "Linear Regression Slope of Precipitation by Day of
Year", xlab = "Day of Year", ylab = "Slope of Regression") + opts(legend.position =
"none") + scale_x_discrete(breaks = c(1,32,60,91,121,152,182,213,244,274,305,335),
labels=c("Jan 1","Feb 1","Mar 1","Apr 1","May 1", "June 1", "July 1", "Aug 1", "Sept 1",
"Oct 1", "Nov 1", "Dec 1"))
dev.off()
# TMAX
lmtmax <- alply(climtmaxlinreganom, 2, function(x){
  lm(x ~ years)
})
lmtmax.info <- ldply(lmtmax, function(fit2){
  data.frame(slope = coef(fit2)[2], pval = summary(fit2)$coefficients[2, 4])
})
pdf('tmaxlinreg_Lookout.pdf', width = 12, height = 8)
qplot(data = lmtmax.info, x = X1, y = slope, col = ifelse(pval < 0.05,'significant at
a=0.05', 'not significant'), main = "Linear Regression Slope of Maximum Temperature by
Day of Year", xlab = "Day of Year", ylab = "Slope of Regression") +
opts(legend.position = "none") + scale_x_discrete(breaks =
c(1,32,60,91,121,152,182,213,244,274,305,335), labels=c("Jan 1","Feb 1","Mar 1","Apr
1","May 1", "June 1", "July 1", "Aug 1", "Sept 1", "Oct 1", "Nov 1", "Dec 1"))
dev.off()
# TMIN
lmtmin <- alply(climtminlinreganom, 2, function(x){
```

```
  lm(x ~ years)
})
lmtmin.info <- ldply(lmtmin, function(fit3){
  data.frame(slope = coef(fit3)[2], pval = summary(fit3)$coefficients[2, 4])
})
pdf('tminlinreg_Lookout.pdf', width = 12, height = 8)
qplot(data = lmtmin.info, x = X1, y = slope, col = ifelse(pval < 0.05,'significant at
a=0.05', 'not significant'), main = "Linear Regression Slope of Minimum Temperature by
Day of Year", xlab = "Day of Year", ylab = "Slope of Regression") +
opts(legend.position = "none") + scale_x_discrete(breaks =
c(1,32,60,91,121,152,182,213,244,274,305,335), labels=c("Jan 1","Feb 1","Mar 1","Apr
1","May 1", "June 1", "July 1", "Aug 1", "Sept 1", "Oct 1", "Nov 1", "Dec 1"))
dev.off()
##############################################
write.csv(lmsf.info, file = "lmsf12301933.csv")
write.csv(lmprcp.info, file = "lmprcpLookout.csv")
write.csv(lmtmax.info, file = "lmtmaxLookout.csv")
write.csv(lmtmin.info, file = "lmtminLookout.csv")
# Move this file and make a wavelet with the anomalies
# Take anomalies and make them back into a time series for plotting
sfanomaly <- melt(sflowlinreganom, id=c("day","year"), measured=c("discharge"))
names(sfanomaly)[1]<-paste("year")
names(sfanomaly)[2]<-paste("yday")
names(sfanomaly)[3]<-paste("discharge")
sfanomaly1 <- sfanomaly[order(sfanomaly$year),]
#######
sfanomaly1$monday <- format(strptime(sfanomaly1$yday, format="%j"), format="%m-
%d")
sfanomaly1$date <- paste(sfanomaly1$year, sfanomaly1$monday,sep="-")
sfanomaly1$date <- as.Date(sfanomaly1$date)
sfanomaly1$postime <- as.POSIXlt(sfanomaly1$date, format = "%Y/%m/%d")
setwd("/Users/johnhammondplease/Desktop/Experimenting_on_data/anomaly")
pdf('sfanom_13011000.pdf', width = 12, height = 8)
ggplot(sfanomaly1) + ggtitle("13011000 Discharge Anomaly") + xlab("Date") +
ylab("Log Discharge Anomaly") + geom_line(aes(postime, discharge), color = "black") +
xlim(as.POSIXlt(c("1950-01-01 00:00:00", "2012-12-31 00:00:00")))
dev.off()
######
prcpanomaly <- melt(climprcplinreganom, id=c("day","year"), measured=c("PRCP"))
names(prcpanomaly)[1]<-paste("year")
names(prcpanomaly)[2]<-paste("yday")
names(prcpanomaly)[3]<-paste("PRCP")
prcpanomaly1 <- prcpanomaly[order(prcpanomaly$year),]
#######
prcpanomaly1$monday <- format(strptime(prcpanomaly1$yday, format="%j"),
format="%m-%d")
```

```
prcpanomaly1$date <- paste(prcpanomaly1$year, prcpanomaly1$monday,sep="-")
prcpanomaly1$date <- as.Date(prcpanomaly1$date)
prcpanomaly1$postime <- as.POSIXlt(prcpanomaly1$date, format = "%Y/%m/%d")
setwd("/Users/johnhammondplease/Desktop/Experimenting_on_data/anomaly")
tmaxanomaly <- melt(climtmaxlinreganom, id=c("day","year"), measured=c("TMAX"))
names(tmaxanomaly)[1]<-paste("year")
names(tmaxanomaly)[2]<-paste("yday")
names(tmaxanomaly)[3]<-paste("TMAX")
tmaxanomaly1 <- tmaxanomaly[order(tmaxanomaly$year),]
#######
tmaxanomaly1$monday <- format(strptime(tmaxanomaly1$yday, format="%j"),
format="%m-%d")
tmaxanomaly1$date <- paste(tmaxanomaly1$year, tmaxanomaly1$monday,sep="-")
tmaxanomaly1$date <- as.Date(tmaxanomaly1$date)
tmaxanomaly1$postime <- as.POSIXlt(tmaxanomaly1$date, format = "%Y/%m/%d")
setwd("/Users/johnhammondplease/Desktop/Experimenting_on_data/anomaly")
pdf('tmaxanom_13011000.pdf', width = 12, height = 8)
ggplot(tmaxanomaly1) + ggtitle("13011000 Tmax Anomaly") + xlab("Date") +
ylab("Tmax Anomaly") + geom_line(aes(postime, TMAX), color = "black") +
xlim(as.POSIXlt(c("1950-01-01 00:00:00", "2012-12-31 00:00:00")))
dev.off()
######
tminanomaly <- melt(climtminlinreganom, id=c("day","year"), measured=c("TMIN"))
names(tminanomaly)[1]<-paste("year")
names(tminanomaly)[2]<-paste("yday")
names(tminanomaly)[3]<-paste("TMIN")
tminanomaly1 <- tminanomaly[order(tminanomaly$year),]
#######
tminanomaly1$monday <- format(strptime(tminanomaly1$yday, format="%j"),
format="%m-%d")
tminanomaly1$date <- paste(tminanomaly1$year, tminanomaly1$monday,sep="-")
tminanomaly1$date <- as.Date(tminanomaly1$date)
tminanomaly1$postime <- as.POSIXlt(tminanomaly1$date, format = "%Y/%m/%d")
setwd("/Users/johnhammondplease/Desktop/Experimenting_on_data/anomaly")
pdf('tminanom_13011000.pdf', width = 12, height = 8)
ggplot(tminanomaly1) + ggtitle("13011000 Tmin Anomaly") + xlab("Date") +
ylab("Tmin Anomaly") + geom_line(aes(postime, TMIN), color = "black") +
xlim(as.POSIXlt(c("1950-01-01 00:00:00", "2012-12-31 00:00:00")))
dev.off()
############################
write.csv(sfanomaly1, file = "a14161500corsfanom.csv")
write.csv(prcpanomaly1, file = "aLookoutprcpanom.csv")
write.csv(tmaxanomaly1, file = "aLookouttmaxanom.csv")
write.csv(tminanomaly1, file = "aLookouttminanom.csv")
# Mann-Kendall just needs data reformatted, does not need transformation or anomaly
calculation
```

```
sflowmann <- sf[c(6,4)]
sflowmann$year <- year(sflowmann$postime)
sflowmann$yday <- yday(sflowmann$postime)
sflowmannkenn <- cast(sflowmann, year ~ yday, value = "discharge")
climprcpmann <- clim[c(6,2)]
climprcpmann$year <- year(climprcpmann$postime)
climprcpmann$yday <- yday(climprcpmann$postime)
climprcpmannkenn <- cast(climprcpmann, year ~ yday, value = "PRCP")
climtmaxmann <- clim[c(6,3)]
climtmaxmann$year <- year(climtmaxmann$postime)
climtmaxmann$yday <- yday(climtmaxmann$postime)
climtmaxmannkenn <- cast(climtmaxmann, year ~ yday, value = "TMAX")
climtminmann <- clim[c(6,4)]
climtminmann$year <- year(climtminmann$postime)
climtminmann$yday <- yday(climtminmann$postime)
climtminmannkenn <- cast(climtminmann, year ~ yday, value = "TMIN")
################################################
# Mann-Kendall Analysis
mansf.mat <- data.matrix(sflowmannkenn)
manprcp.mat <- data.matrix(climprcpmannkenn)
mantmax.mat <- data.matrix(climtmaxmannkenn)
mantmin.mat <- data.matrix(climtminmannkenn)
######################################################
setwd("/Users/johnhammondplease/Desktop/Experimenting_on_data/mannkennfig")
sfmanken <- alply(mansf.mat, 2, function(x){
  MannKendall(x)
})
sfmanken.info <- ldply(sfmanken, function(fit4){
  data.frame(tau = (fit4)$tau, pval = (fit4)$sl)
})
sfmanken.info <- sfmanken.info[-1,]
pdf('sfmannkenn_12301933.pdf', width = 12, height = 8)
qplot(data = sfmanken.info, x = X1, y = tau, col = ifelse(pval < 0.05,'significant at
a=0.05', 'not significant'), main = "Mann-Kendall Tau of Streamflow by Day of Year",
xlab = "Day of Year", ylab = "Kendall's Tau") + opts(legend.position = "none") +
scale_x_discrete(breaks = c(1,32,60,91,121,152,182,213,244,274,305,335), labels=c("Jan
1","Feb 1","Mar 1","Apr 1","May 1", "June 1", "July 1", "Aug 1", "Sept 1", "Oct 1",
"Nov 1", "Dec 1"))
dev.off()
################################################
prcpmanken <- alply(manprcp.mat, 2, function(x){
  MannKendall(x)
})
prcpmanken.info <- ldply(prcpmanken, function(fit4){
  data.frame(tau = (fit4)$tau, pval = (fit4)$sl)
})
```

```
prcpmanken.info <- prcpmanken.info[-1,]
pdf('prcpmannkenn_Lookout.pdf', width = 12, height = 8)
qplot(data = prcpmanken.info, x = X1, y = tau, col = ifelse(pval < 0.05,'significant at
a=0.05', 'not significant'), main = "Mann-Kendall Tau of Precipitation by Day of Year",
xlab = "Day of Year", ylab = "Kendall's Tau") + opts(legend.position = "none") +
scale_x_discrete(breaks = c(1,32,60,91,121,152,182,213,244,274,305,335), labels=c("Jan
1","Feb 1","Mar 1","Apr 1","May 1", "June 1", "July 1", "Aug 1", "Sept 1", "Oct 1",
"Nov 1", "Dec 1"))
dev.off()
#####################################################
tmaxmanken <- alply(mantmax.mat, 2, function(x){
  MannKendall(x)
})
tmaxmanken.info <- ldply(tmaxmanken, function(fit4){
  data.frame(tau = (fit4)$tau, pval = (fit4)$sl)
})
tmaxmanken.info <- tmaxmanken.info[-1,]
pdf('tmaxmannkenn_Lookout.pdf', width = 12, height = 8)
qplot(data = tmaxmanken.info, x = X1, y = tau, col = ifelse(pval < 0.05,'significant at
a=0.05', 'not significant'), main = "Mann-Kendall Tau of Tmax by Day of Year", xlab =
"Day of Year", ylab = "Kendall's Tau") + opts(legend.position = "none") +
scale_x_discrete(breaks = c(1,32,60,91,121,152,182,213,244,274,305,335), labels=c("Jan
1","Feb 1","Mar 1","Apr 1","May 1", "June 1", "July 1", "Aug 1", "Sept 1", "Oct 1",
"Nov 1", "Dec 1"))
dev.off()
#####################################################
tminmanken <- alply(mantmin.mat, 2, function(x){
  MannKendall(x)
})
tminmanken.info <- ldply(tminmanken, function(fit4){
  data.frame(tau = (fit4)$tau, pval = (fit4)$sl)
})
tminmanken.info <- tminmanken.info[-1,]
pdf('tminmannkenn_Lookout.pdf', width = 12, height = 8)
qplot(data = tminmanken.info, x = X1, y = tau, col = ifelse(pval < 0.05,'significant at
a=0.05', 'not significant'), main = "Mann-Kendall Tau of Tmin by Day of Year", xlab =
"Day of Year", ylab = "Kendall's Tau") + opts(legend.position = "none") +
scale_x_discrete(breaks = c(1,32,60,91,121,152,182,213,244,274,305,335), labels=c("Jan
1","Feb 1","Mar 1","Apr 1","May 1", "June 1", "July 1", "Aug 1", "Sept 1", "Oct 1",
"Nov 1", "Dec 1"))
dev.off()
#################################################
write.csv(sfmanken.info, file = "mankensf12301933.csv")
write.csv(prcpmanken.info, file = "mankenprcpLookout.csv")
write.csv(tmaxmanken.info, file = "mankentmaxLookout.csv")
write.csv(tminmanken.info, file = "mankentminLookout.csv")
```

Wavelet plotting:

```
library(ggplot2)
library(timeDate)
library(lubridate)
library(fields)
library(biwavelet)
library(timeSeries)
setwd("/Users/johnhammondplease/Desktop/Experimenting_on_data/anomaly")
`sfanom` <-
read.csv("~/Desktop/Experimenting_on_data/anomaly/a14161500corsfanom.csv")
`prcpanom` <-
read.csv("~/Desktop/Experimenting_on_data/anomaly/aLookoutprcpanom.csv")
`tmaxanom` <-
read.csv("~/Desktop/Experimenting_on_data/anomaly/aLookouttmaxanom.csv")
`tminanom` <-
read.csv("~/Desktop/Experimenting_on_data/anomaly/aLookouttminanom.csv")
sfanom1 <- sfanom[c(7,4)]
sfanom_nona <- subset(sfanom1, !is.na(sfanom1$discharge))
wt.sfanom <- wt(cbind(1:23011, sfanom_nona$discharge), mother = "morlet")
options(max.contour.segments = 100000)
setwd("/Users/johnhammondplease/Desktop/Experimenting_on_data/final_anom_wavele
t_figures")
pdf('streamflow_anom_wavelet_14161500.pdf', width = 12, height = 8)
plot(wt.sfanom, axes=F, plot.cb = FALSE, type= "power.corr", plot.sig = TRUE, main =
"14161500 Streamflow Anomaly Wavelet Bias Corrected Power", xlab = "", ylab =
"Period (days)")
axis(1, at=seq(1, 23011, by= 365.25), labels=seq(1950,2012, by = 1), line=2)
dev.off()
# precipitation wavelet
prcpanom1 <- prcpanom[c(7,4)]
prcpanom_nona <- subset(prcpanom1, !is.na(prcpanom1$PRCP))
wt.prcpanom <- wt(cbind(1:18818, prcpanom_nona$PRCP), mother = "morlet")
pdf('precipitation_anom_wavelet_14161500.pdf', width = 12, height = 8)
plot(wt.prcpanom, plot.cb = FALSE, axes=F, type= "power.corr", plot.sig = TRUE, main
= "14161500 Precipitation Anomaly Wavelet Bias Corrected Power", xlab = "", ylab =
"Period (days)")
axis(1, at=seq(1, 23011, by= 365.25), labels=seq(1950,2012, by = 1), line=2)
dev.off()
# temperature wavelet TMAX
tmaxanom1 <- tmaxanom[c(7,4)]
tmaxanom_nona <- subset(tmaxanom1, !is.na(tmaxanom1$TMAX))
wt.tmaxanom <- wt(cbind(1:18761, tmaxanom_nona$TMAX), mother = "morlet")
pdf('tmax_anom_wavelet_14161500.pdf', width = 12, height = 8)
```

```
plot(wt.sfanom, plot.cb = FALSE, axes=F, type= "power.corr", plot.sig = TRUE, main =
"14161500 Tmax Anomaly Wavelet Bias Corrected Power", xlab = "", ylab = "Period
(days)")
axis(1, at=seq(1, 23011, by= 365.25), labels=seq(1950,2012, by = 1), line=2)
dev.off()
# Cross-wavelet of streamflow and precipitation
sfanom_nona$julian <- as.numeric(as.Date(sfanom_nona$postime))
prcpanom_nona$julian <- as.numeric(as.Date(prcpanom_nona$postime))
towxt <- merge(sfanom_nona, prcpanom_nona, by = "julian")
toxwtsf <- towxt[c(2,3)]
toxwtpr <- towxt[c(4,5)]
xwt.1 <- xwt(cbind(1:18998, toxwtsf$discharge), cbind(1:18998, toxwtpr$PRCP))
pdf('anom_cross_wavelet_14161500.pdf', width = 12, height = 8)
plot(xwt.1, plot.cb=FALSE, plot.sig=TRUE, axes=F, type= "power.corr", main =
"14161500 Streamflow-Preicipitation Anomaly Cross Wavelet Bias Corrected Power",
xlab = "", ylab = "Period (days)", legend.horiz=TRUE)
axis(1, at=seq(1, 23011, by= 365.25), labels=seq(1950,2012, by = 1), line=2)
dev.off()
##########################################
# Extract power for one period of interest for each wavelet
# 15 days is [36], 90 days is [67],365 days is [90],4 years(1460 days) is [115]
# Streamflow Wavelet Power at Period of Interest
summary(wt.sfanom)
wt.sfperiod <- wt.sfanom$period
wt.sfperiod
wt.sfpower <- t(wt.sfanom$power)
wt.sfpower15 <- wt.sfpower[,36]
dates <- seq(as.Date("01/01/1950", format = "%d/%m/%Y"), by = "days", length =
length(wt.sfpower365))
pdf('sfpower_15day_14161500.pdf', width = 12, height = 8)
plot(dates, wt.sfpower15, axes=F, xlab = "", ylab = "Power", type= "power.corr", main =
"14161500 Streamflow Power at the 15 Day Period", type = "l")
axis(1, at=seq(1, 23011, by= 365.25), labels=seq(1950,2012, by = 1), line=2)
dev.off()
summary(wt.sfanom)
wt.sfperiod <- wt.sfanom$period
wt.sfperiod
wt.sfpower <- t(wt.sfanom$power)
wt.sfpower90 <- wt.sfpower[,67]
dates <- seq(as.Date("01/01/1950", format = "%d/%m/%Y"), by = "days", length =
length(wt.sfpower365))
pdf('sfpower_90day_14161500.pdf', width = 12, height = 8)
plot(dates, wt.sfpower90, axes=F, xlab = "", ylab = "Power", type= "power.corr", main =
"14161500 Streamflow Power at the 90 Day Period", type = "l")
axis(1, at=seq(1, 23011, by= 365.25), labels=seq(1950,2012, by = 1), line=2)
dev.off()
```

```
summary(wt.sfanom)
wt.sfperiod <- wt.sfanom$period
wt.sfperiod
wt.sfpower <- t(wt.sfanom$power)
wt.sfpower1 <- wt.sfpower[,90]
dates <- seq(as.Date("01/01/1950", format = "%d/%m/%Y"), by = "days", length =
length(wt.sfpower365))
pdf('sfpower_1yr_14161500.pdf', width = 12, height = 8)
plot(dates, wt.sfpower1, axes=F, xlab = "", ylab = "Power", type= "power.corr", main =
"14161500 Streamflow Power at the 1 Year Period", type = "l")
axis(1, at=seq(1, 23011, by= 365.25), labels=seq(1950,2012, by = 1), line=2)
dev.off()
summary(wt.sfanom)
wt.sfperiod <- wt.sfanom$period
wt.sfperiod
wt.sfpower <- t(wt.sfanom$power)
wt.sfpower4 <- wt.sfpower[,115]
dates <- seq(as.Date("01/01/1950", format = "%d/%m/%Y"), by = "days", length =
length(wt.sfpower365))
pdf('sfpower_4yr_14161500.pdf', width = 12, height = 8)
plot(dates, wt.sfpower4, axes=F, xlab = "", ylab = "Power", type= "power.corr", main =
"14161500 Streamflow Power at the 4 Year Period", type = "l")
axis(1, at=seq(1, 23011, by= 365.25), labels=seq(1950,2012, by = 1), line=2)
dev.off()
```